

APOLLO

Final Report

(NASA-CR-136716) APOLLO: GUIDANCE AND
CONTROL SYSTEM 2 Final Report (Martin
Co.) 253 p

N74-71537

253p

00/99

Unclas
28852

Code SA

ER 12007-2 JUNE 1961

Guidance and Control System

CLASSIFICATION CHANGE
UNCLASSIFIED

Available to NASA Offices and
NASA Contractors

TO -

By authority of

Changed by

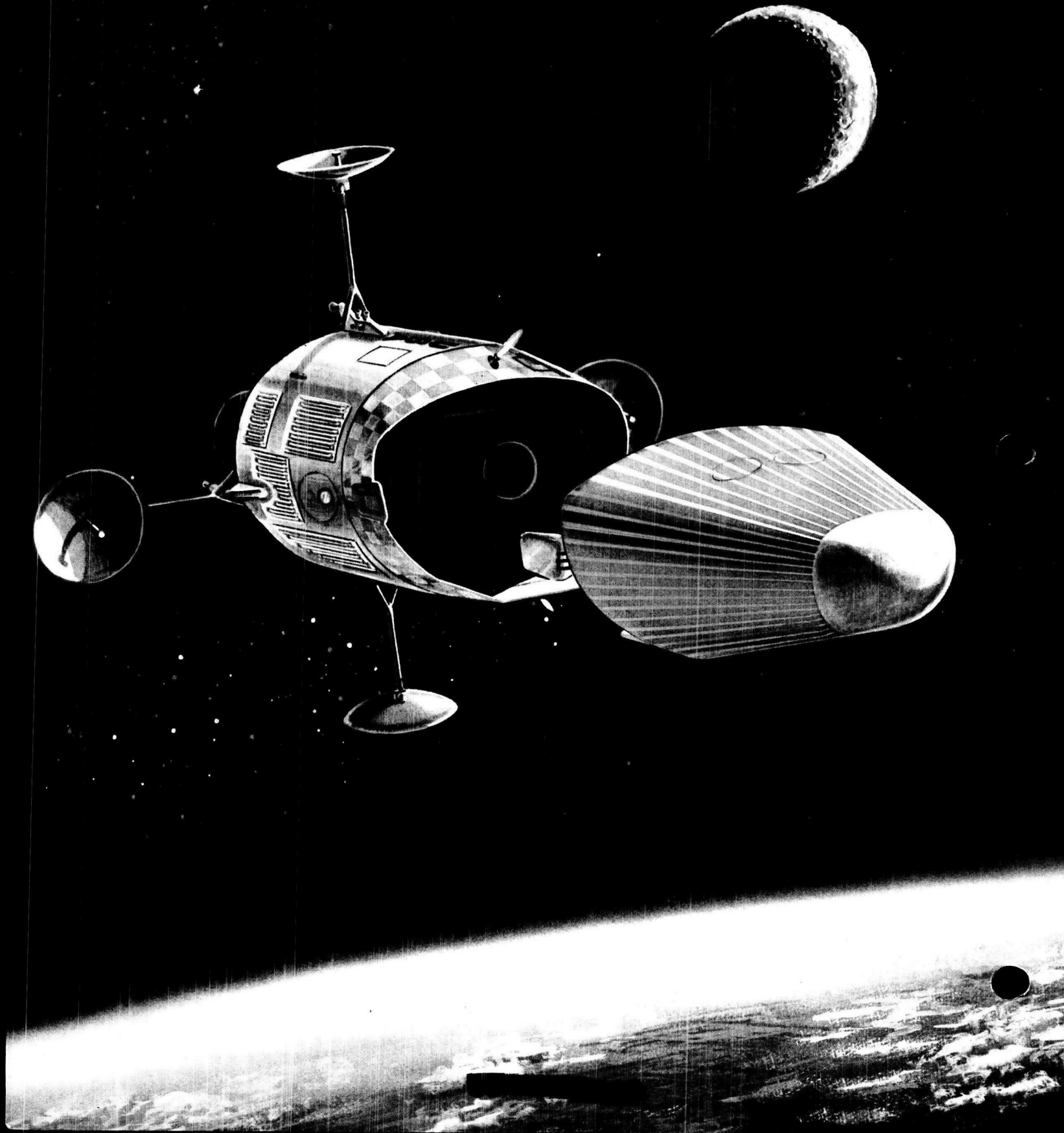
A. Shirley

E.O.

11652
to 11-30-73

MARTIN

COMET



APOLLO



Final Report

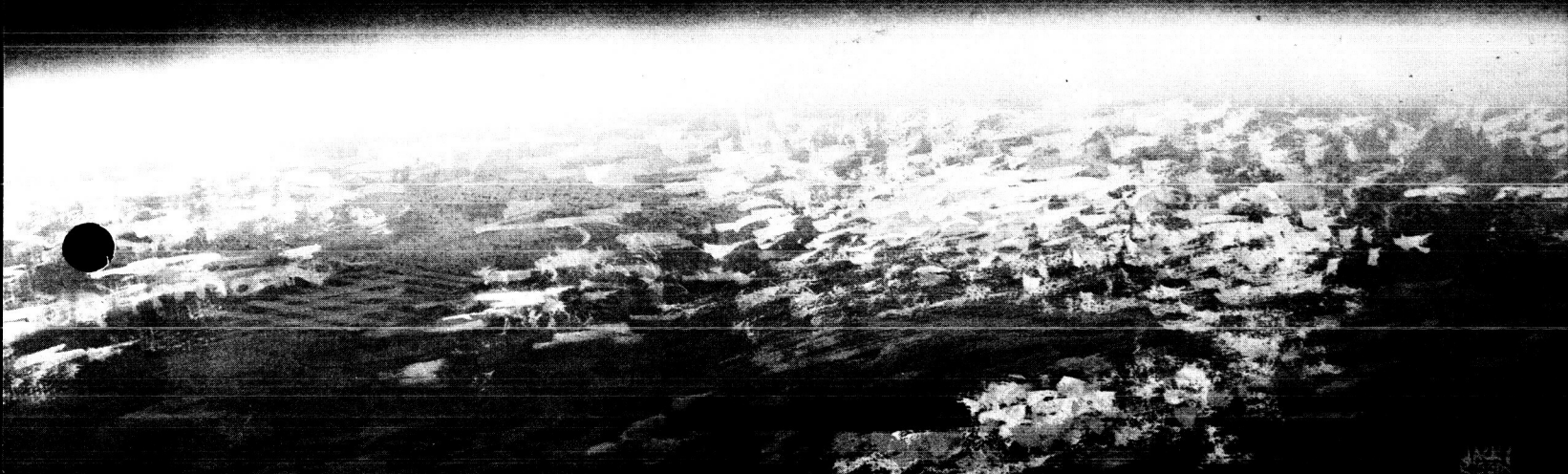
Submitted to: NASA Space Task Group.
Contract NAS 5-303, Exhibit A, Item 1.2

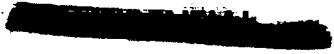
Guidance and Controls

II

ER 12007-2 JUNE 1961

MARTIN





MODEL 410 — THE SYSTEM AND ITS OPERATION

*A BRIEF DESCRIPTION**

Model 410 is the spacecraft system recommended by Martin for the Apollo mission. Its design satisfies the guidelines stated in NASA RFP-302, as well as a more detailed set of guidelines developed by Martin during the Apollo design feasibility study.

We conceive the ultimate Apollo mission to be a manned journey to the lunar surface, arrived at by the preliminary steps of earth orbit, circumlunar and lunar orbit flights. Operational procedures proved out in the early steps will be carried over into the advanced steps, thus establishing a high level of confidence in the success of the lunar flights. With the recommended system, manned lunar orbit missions can be made as early as 1966.

Operational Features

For a circumlunar flight when the moon is at its most southerly declination (Fig. p-1) the launch operation proceeds southeast from Cape Canaveral and down the Atlantic Missile Range. The Saturn C-2 third stage shuts down when orbital velocity is reached at an altitude of 650,000 feet. What follows is a coasting orbit passing over the southern tip of Africa, the Indian Ocean and up the Pacific Missile Range. In this interval the crew checks out all onboard equipment, which has just passed through the accelerations, noise and vibration of the boost phase. If the pilot-commander is satisfied that all systems are working properly, the third stage is restarted and the spacecraft is injected at parabolic velocity northwest of Hawaii. If the pilot-commander is dissatisfied with the condition of the vehicle or crew, he separates from the Saturn S-IV, starts the mission abort engine, re-enters at the point shown in Fig. p-1 and lands at Edwards AFB.

Continuing translunar flight from the point of injection, the trajectory trace swings down over the Caribbean and then west over South America. This particular trajectory passes within 240 naut mi of the moon, then turns back for a direct re-entry some six days after launch. Re-entry occurs southwest of Hawaii some 3300 naut mi from the Edwards AFB landing site.

Tracking. The range coverage provided by present and planned facilities is shown in Fig. p-1 for this trajectory and for a second return trace representing the case when the moon is at the most northerly declination. This second trajectory establishes the 10000-naut mi re-entry range requirement for Apollo to meet the guidelines of operation on every day of the lunar month and of operation into a single landing site.

*For more complete descriptions, see ER 12000 or ER 12001.

Abort. During the critical launch and checkout phase, abort will be possible at any time : at the crew's discretion, automatically or by ground command. Up to nine minutes after launch (from Canaveral), the abort landing is restricted to the AMR for a circumlunar flight. Beyond this point the pilot has the option of continuing to any point along the AMR, PMR or into Edwards AFB through the use of the mission abort propulsion system and the inherent downrange maneuverability of the Model-410.

The Selected Spacecraft

The Apollo space vehicle (Model 410 spacecraft plus launching vehicle) is shown in Fig. p-2. The spacecraft—that portion of the space vehicle which makes the flight to the moon—consists of these three modules:

- (1) Command module, housing the three crew members during all thrusting periods, e.g., launch from earth, any corrections to the flight path during flight in space, during re-entry and, ultimately, during landing and launch from the moon. It is the operating center from which all control of the flight is made.
- (2) Propulsion and equipment module, containing all the propulsion units which operate between the point of final booster separation and re-entry after the lunar flight. It is separated from the command module at 200 naut mi from the earth on the return trip. It is designed with tankage for lunar takeoff and will be offloaded for less ambitious missions.
- (3) Mission module—contained within the outer frame of the propulsion and equipment module—providing space during the lunar voyage for scientific observations and crew living functions.

Command Module

With its lifting capability, the Apollo command module represents a step forward in technology over ballistic vehicles, Mercury and (to the best of our knowledge the *Boctók* (*Vostok*)). The lift results from the capsule's shape—a blunted cone flattened on the top (see Fig. p-3).

Heating and radiation protection. The Model 410 is shaped conservatively for aerodynamic heating in addition to its relatively high L/D (0.77). By accepting the large convective heat load of a nose radius smaller than that of the Mercury type, the Model 410 shape tends to minimize radiative heat transfer which is less well understood and harder to protect against. The thermal protection system provides excellent protection for the crew from the large aerodynamic heat loads, from space radiation (including solar flares) and from meteorites.

The normal mission radiation dose will not exceed the five rem limit defined by NASA. If the crew should encounter a solar event as severe as that following the May 10, 1959 flare, they would receive a dose of only 67 rem—well within the 100 rem dose limit set by Martin as tolerable during an emergency.

Thermal protection for re-entry is provided by a composite shield of deep charring ablator (nylon phenolic) bonded to superalloy honeycomb panels which are set off and insulated from the water-cooled pressure shell. The control flaps are protected from the high initial heat rate by an ablator bonded directly to the flap. The long-time, lower heating rates are handled by re-radiation from the backside. The aft bulkhead is protected by a fiberglass phenolic honeycomb panel with a foamed polyurethane insulation.

Crew provisions. The crew has access to all electronic and electrical equipment in the command module for maintenance and replacement. Both pilots have two-axis sidestick and foot controllers as well as a manual guidance mode used with the computers inoperative for deep space and re-entry operations.

Cabin pressure is maintained at the equivalent of 5000 feet altitude ("shirt sleeve" environment). Protective suiting is donned only for launching and landing, but need not be inflated except in emergency.

Guidance. The guidance system consists of both automatic and manual star tracking equipment, as well as two inertial platforms and two general purpose digital computers. Two windows, with ablative heat shield covers, are provided for use with tracking instruments.

Flight control. Pitch and yaw attitude control within the atmosphere is provided by flaps driven by hot gas servos. Outside the atmosphere dual reaction controls are used. Roll is controlled at all times by a dual reaction system.

Communications. Communications equipment includes a K. band for re-entry, a C-band for the pre-reentry and both HF and VHF rescue beacons for landing and recovery.

Landing system. The landing system consists of a steerable parachute, retro-rocket combination, enabling the M-410 to avoid local obstacles, trim out wind drift and reduce sinking speed to a nominal three feet per second—low enough for safe landing on any kind of terrain or in very rough seas. In the event of retrorocket failure, accelerations on the crew will not exceed 20 G.

Launch escape propulsion system (LEPS). LEPS is a thrust-vector-controlled, solid rocket system which separates the command module from the rest of the space vehicle in the event of an emergency during launch pad operations or during boost through the atmosphere. In an off-the-pad abort, it lifts the command module to an altitude of more than 4000 feet. During a normal boost trajectory, LEPS is jettisoned at 300,000 feet.

Propulsion and Equipment Module

The propulsion and equipment module (shown in Fig. p-3) contains propulsion devices and equipment which are not necessary for re-entry. Its outer skin serves both as a load carrying structure and as a meteorite shield for the propellant tanks, mission module and other equipment.

Propulsion devices. The mission engine, used for trajectory correction and abort, is a high performance, modified LR-115 (Pratt & Whitney), developing 15,600 pounds of thrust. A total of 10,450 pounds of liquid hydrogen and liquid oxygen propellants may be carried, sufficient for lunar takeoff.

Four vernier engines, with 300 pounds of thrust each, are used for mid-course correction, ullage impulse to settle the mission engine propellants and for thrust vector control during operation of the mission engine. In addition there are two sets of six control jets which provide 30 pounds of thrust for roll, pitch and yaw control.

Power sources. Spacecraft equipment is powered by fuel cells (2 kw) which under normal conditions, use the boiloff from the mission propulsion system. A supply of independent reactants is provided for emergencies. Battery power is used during re-entry.

Communications. Four large antennas fold out to provide S-band communications and X-band radar altimeter information. VHF communications gear is also provided.

Mission Module

The mission module provides 400 cubic feet of living space during the lunar voyage. It serves as a midcourse work-rest area, providing freedom of movement and privacy. For operations on the lunar surface it will be a base of scientific investigations, and will serve as an airlock. The same "shirt sleeve" environment at 12.2 psi is maintained as in the command module.

The mission module provides the space and flexibility required for effective lunar reconnaissance and scientific experimentation. An Eastman-Kodak camera-telescope has been selected, for example, which has one-meter resolution at lunar orbit altitude of 50 naut mi.

MODEL 410 WEIGHT SUMMARY

MISSION	CIRCUMLUNAR	LUNAR ORBIT	LUNAR TAKEOFF
COMMAND MODULE	6954	6954	6954
PROPULSION AND EQUIPMENT MODULE	7372	13,192	15,618
LAUNCH ESCAPE PROPULSION SYSTEM	185	185	0
ADAPTER	489	489	0
EFFECTIVE LAUNCH WEIGHT	15,000	20,820	22,572

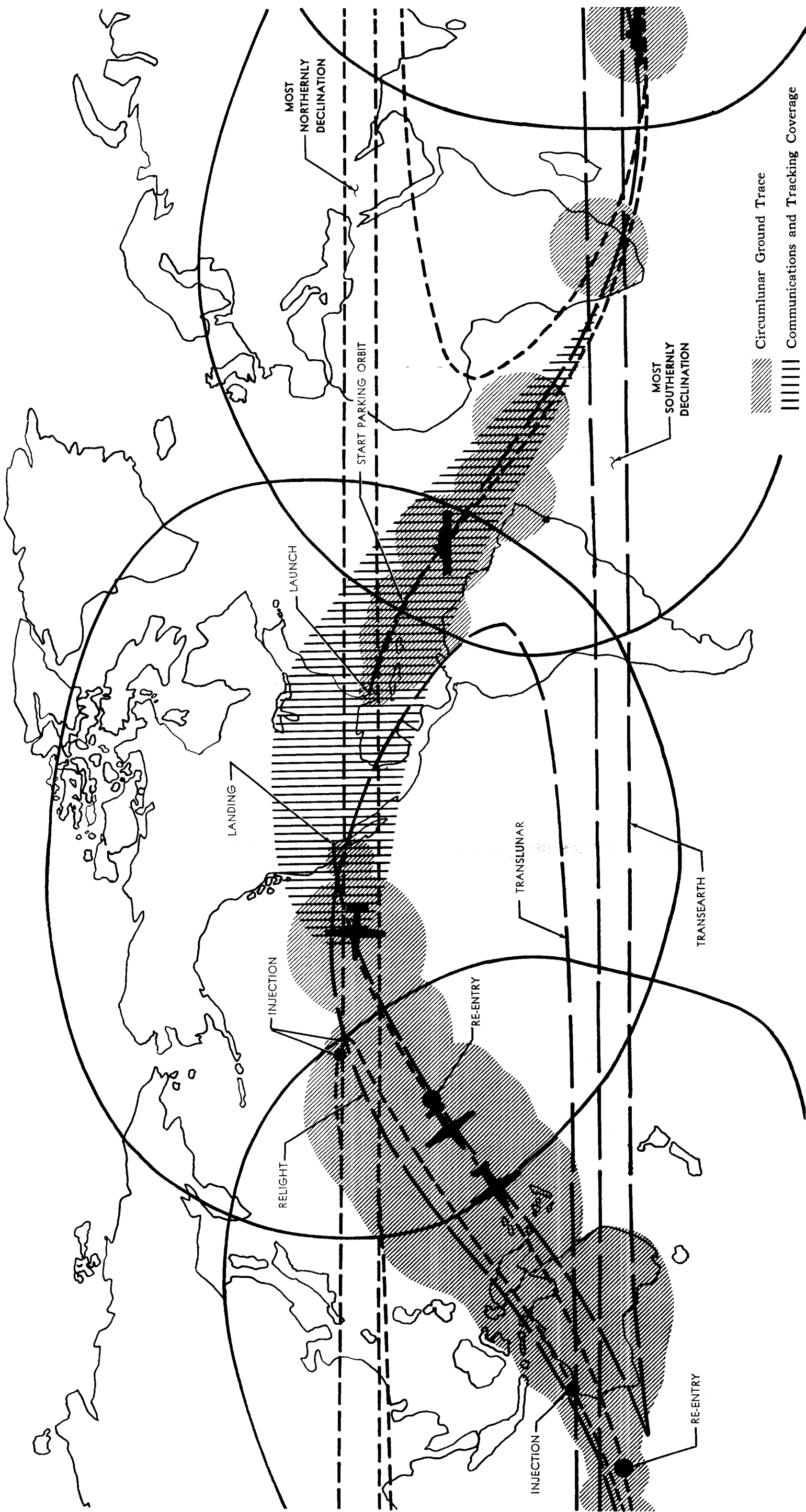
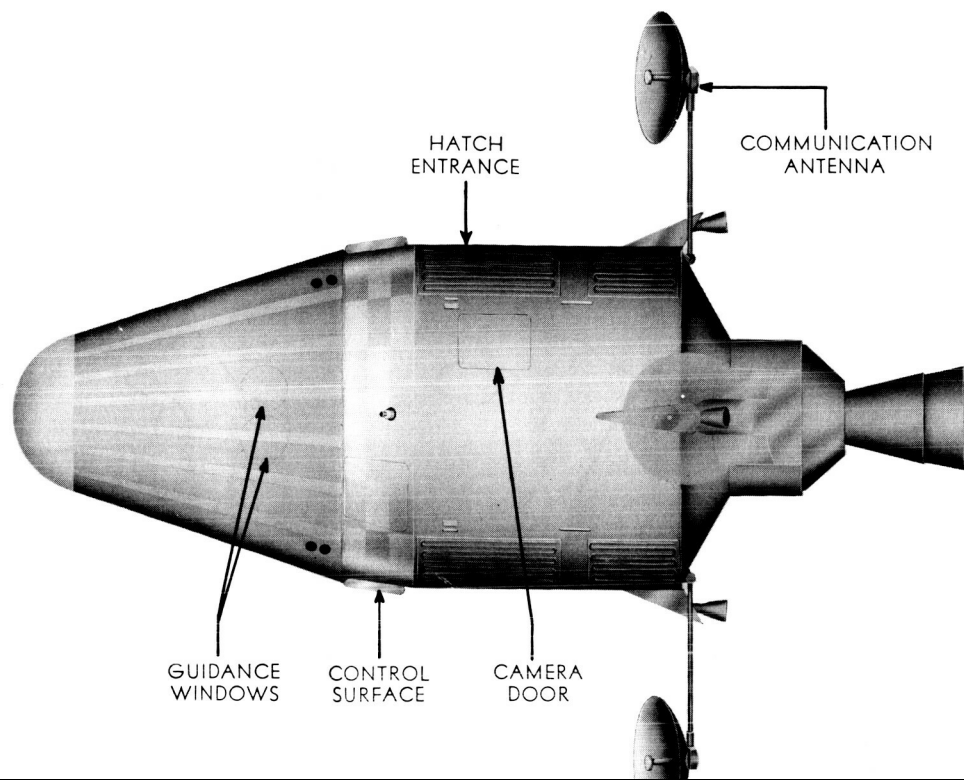
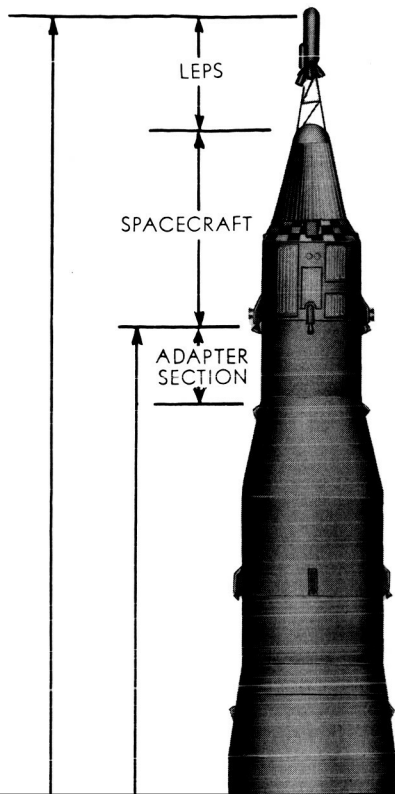


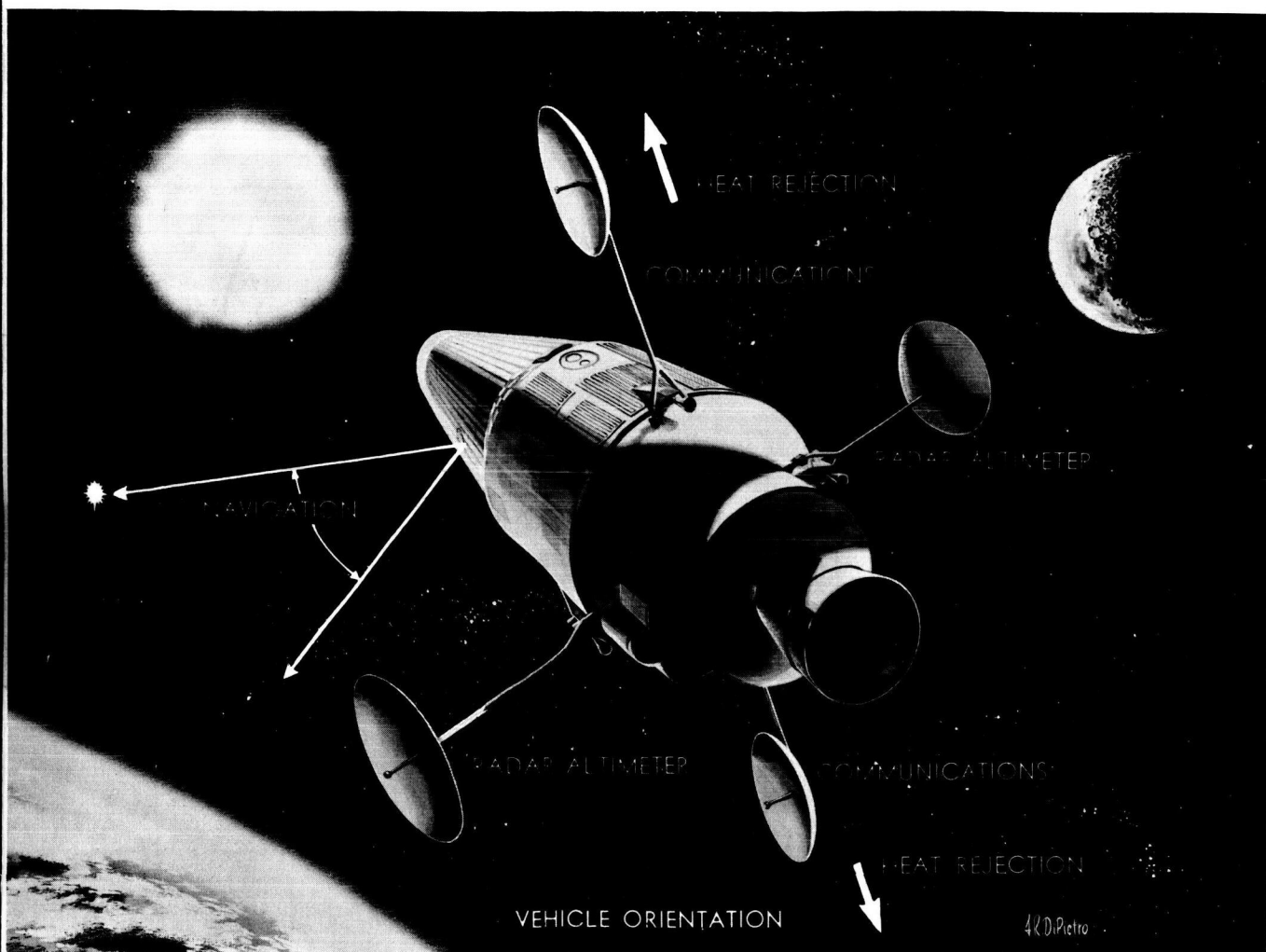
Fig. p-1 Model 410 Circumlunar Trajectory and Range Coverage



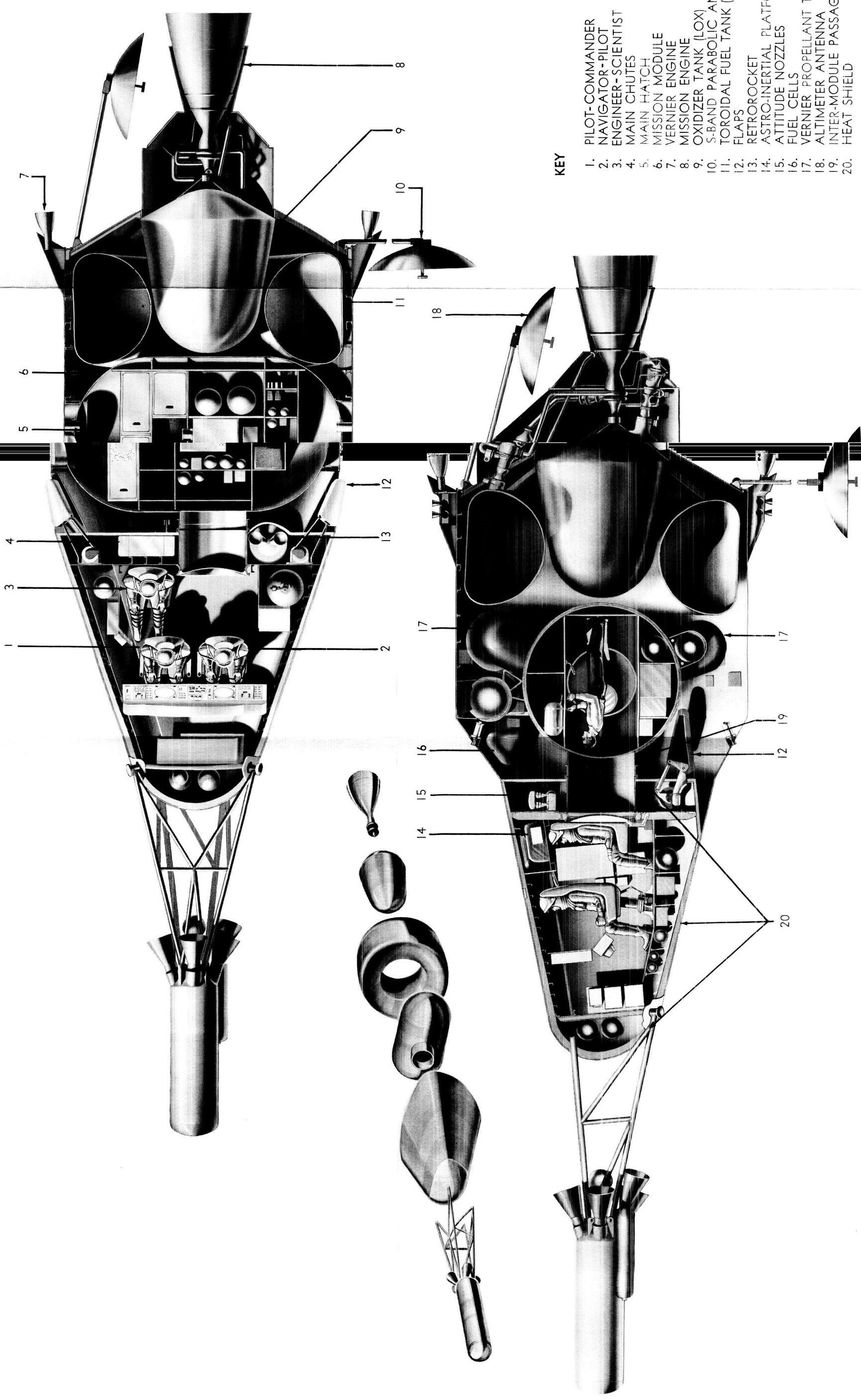
MISSION	EFFECTIVE GROSS WEIGHT (lb)	PROPULSION ΔV CAPABILITY (fps)		VOLUMES (cu ft)	
		MISSION	VERNIER	COMMAND MODULE	
CIRCUMLUNAR	15000	1830	525	COMMAND MODULE	350
LUNAR ORBIT	20820	6100	525	MISSION MODULE	400
LUNAR TAKEOFF	22572	8600	200	MISSION H ₂ TANK	400
				MISSION O ₂ TANK	122

PROPULSION SYSTEM DATA

PURPOSE	TYPE	ISP. (sec)	THRUST (lb)
MISSION (1)	H ₂ -O ₂ (ADV. LRI15)	427	15600
VERNIER (4)	N ₂ H ₄ /UDMH-N ₂ O ₄	315	300 EACH
ATTITUDE CONTROL (14+BACKUP)	N ₂ H ₄ /UDMH-N ₂ O ₄	250-315	15 TO 50



CONFIDENTIAL



KEY

- 1. PILOT-COMMANDER
- 2. NAVIGATOR-PILOT
- 3. ENGINEER-SCIENTIST
- 4. MAIN CHUTES
- 5. MAIN HATCH
- 6. MISSION MODULE
- 7. VERNIER ENGINE
- 8. MISSION ENGINE
- 9. OXIDIZER TANK (LOX)
- 10. S-BAND PARABOLIC ANTENNA
- 11. TOROIDAL FUEL TANK (LH)
- 12. FLAPS
- 13. RETOROCKET
- 14. ASTRO-INERTIAL PLATFORM
- 15. ATTITUDE NOZZLES
- 16. FUEL CELLS
- 17. VERNIER PROPELLANT TANK
- 18. ALTIMETER ANTENNA
- 19. INTER-MODULE PASSAGE
- 20. HEAT SHIELD

Fig. p-3. Model 410 Apollo Inboard Profile

CONFIDENTIAL

CONTENTS (cont)

VOLUME II

	Page
VI. Displays and Operator Controls	VI-1
A. Requirements	VI-1
B. Design	VI-1
C. Displays and Controls Subpanel Description . .	VI-19
D. Implementation	VI-27
VII. Error Analysis	VII-1
A. Introduction	VII-1
B. Summary of Results	VII-2
C. Analysis of Inertially Guided Phases	VII-4
D. Error Analysis of Midcourse Navigation System	VII-21
VIII. Vendor Studies	VIII-1
A. Method of Approach	VIII-1
B. System Vendors Contacted	VIII-1
C. Comparison of System Vendors	VIII-2
D. Definition of System Vendor Efforts	VIII-5
E. Component Vendor Efforts	VIII-6
F. Vendor Contributions	VIII-7
G. Utilization of Vendor Contributions	VIII-8
H. Summary	VIII-9

~~CONFIDENTIAL~~

CONTENTS (cont)

		Page
IX.	Reliability	IX-1
	A. Design Analysis	IX-1
	B. Failure Rate Data	IX-2
	C. Selected System	IX-2
	D. Additional Investigation	IX-5
	E. Calculations	IX-5
	F. Conclusions	IX-6
X.	Guidance Conclusions	X-1
XI.	Attitude Control System	XI-1
	A. Introduction	XI-1
	B. Abort Control System	XI-5
	1. System Requirements	XI-5
	2. System Selection	XI-6
	3. System Design	XI-6
	C. Midcourse Attitude Control	XI-7
	1. System Requirements	XI-7
	2. System Selection	XI-11
	3. System Design	XI-17
	4. Mechanization	XI-20
	5. Analog Program	XI-20
	D. Re-entry Attitude Control	XI-21
	1. Introduction	XI-21
	2. Reaction System Requirements	XI-21

CONTENTS (cont)

	Page
3. Reaction System Selection	XI-22
4. Reaction System Design	XI-22
5. Aerodynamic System Requirements	XI-23
6. Aerodynamic System Selection	XI-25
7. Aerodynamic System Design	XI-29
XII. Rendezvous Control System	XII-1
A. Introduction and Design Criteria	XII-1
1. Study Definition and Rendezvous Problem Description	XII-1
2. Manually Controlled Rendezvous System	XII-2
3. Analog Study	XII-3
B. Translation and Attitude Control Configurations	XII-10
1. Single Axis Translation Control	XII-10
2. Three Axis Translation Control, Plus Attitude Control	XII-11
3. Three Axis Translation Control, Combined with Attitude Control	XII-12
C. A Rendezvous System for Apollo	XII-13
1. Utilization of Onboard Equipment	XII-13
2. Maneuvering System	XII-14
3. Rendezvous Operation	XII-15
Illustrations	XII-18

VI DISPLAYS AND OPERATOR CONTROLS

A. REQUIREMENTS

Astronauts onboard the Apollo command the spacecraft. In this command function, the piloting, guidance, navigation and control, are closely interrelated, and are often characterized by complicated operational tasks. The extent to which these tasks can be successfully accomplished, indeed the success of the mission itself, depends in large part upon whether the design of the display and control system associated with guidance and control functions facilitates direct astronaut command-influence. Astronaut contribution is enhanced by providing accurate reliable data, and simple, readable, accessible controls for maneuvering the spacecraft and operating onboard equipment. This contribution is extended when system design offers maximum usefulness because it has been based upon detailed consideration of human-factor requirements. It is further enhanced when it intensifies man's capabilities which distinguish him from machines e.g. capabilities such as judgment, comparison, prediction, and task sharing. Achieving a design which fully accommodates these considerations during all mission phases, is regarded as a prime requirement underlying the design of the guidance and control display system for Apollo.

B. DESIGN

The design approach toward selecting the guidance and control display system for Apollo was to conduct a series of overlapping task studies which included:

- (1) Determination of preliminary guidance display and control system configuration.
- (2) Development of task analysis.
- (3) Determination of information and control requirements.
- (4) Cockpit layout and mockup studies.
- (5) Display system simulation.
- (6) Mechanization studies.

Early in these Apollo studies, it became clear that guidance and control display requirements would dominate the Apollo cabin design. The priority given to guidance requirements during the study is reflected by the panel arrangements and space allocations provided in the display system design. For overall display information, see ER 12008 and Ref IV-1.

The display and control system for guidance is provided on a unitized console in the Apollo command module. This console is illustrated in Fig. VI-1. The display components are arranged and selected to provide full guidance and control capability in any mission phase to either of two astronauts, identified as the pilot-commander (right side) and the navigator-pilot (left side), who are seated side-by-side in front of the console. The arrangement permits the two astronauts to aid one another in guidance tasks, to cross-check one another in critical operations and to command the spacecraft alone in an emergency. This capability is obtained by having the two astronauts share subpanels in the center of the console and by providing redundant displays and controls at both right and left sides when necessary or advantageous. Each major Apollo mission phase involves different guidance and control operations. To accommodate these different requirements a considerable flexibility has been incorporated into the display system design which permits much of the equipment to be used in different ways at different times with considerable savings in cabin panel space and spacecraft weight. Cathode ray tube displays for guidance data presentation especially contribute to this flexibility.

In the discussions which follow, the features of the display and control system associated with Apollo guidance are described in terms of display presentation and control panel function for the ascent guidance, midcourse guidance and re-entry guidance phases. While actual spacecraft command may shift from one seat position to the other during an Apollo mission, to simplify the discussions and at the same time illustrate the display and control system functions for unfavorable mission conditions (one-man control), the discussions treat guidance control from the navigator-pilot's (referred to also as navigator) position in all instances.

The displays and controls used by the navigator-pilot in guidance functions are shown in Fig. VI-2. Subpanels hatched out in the figure are elements not directly involved in the discussions. The subpanels on the right are shared with the pilot-commander. Numbers appearing in the text in parenthesis and in the figure help identify and locate the subpanels discussed. For completeness of this discussion, several elements not integral with the console are indicated. These include the control stick, toe pedals, abort handle and a remote guidance data panel.

As seen, the subpanels and controls include:

- | | | |
|-----|------------------------------|------|
| (1) | 7-in. Scope | (6) |
| (2) | 10-in. Scope | (24) |
| (3) | Scope display control | (33) |
| (4) | Slide projector and controls | (16) |
| (5) | Computer control | (23) |

~~CONFIDENTIAL~~

(6)	Attitude and vernier engine propulsion	(3)
(7)	Flight control display group	(14)
(8)	Automatic stabilization control system	(28)
(9)	Printer	(31)
(10)	Astro-inertial platform control	(7)
(11)	Miniature inertial platform control	(27)
(12)	Timer and sequence indicator	(15)
(13)	Communication control	(26)
(14)	Message command	(25)
(15)	Radar altimeter control	(39)
(16)	Spacecraft guidance command	(41)
(17)	Control stick	(46)
(18)	Toe pedals	(47)
(19)	Abort control (pilot)	(48)
(20)	Major system status	(1)
(21)	"Q" Meter	(11)
(22)	Pressure altimeter	(12)
(23)	Standby stability	(13)
(24)	Sequence lights and controls	(10)
(25)	Flap system display	(8)
(26)	Re-entry sequence lights and controls	(42)
(27)	Corrections path panel (engineer-scientist)	(40)

~~CONFIDENTIAL~~

Brief descriptions of each unit are given in the last part (part 3) of the guidance display section. Certain aspects of the guidance display and control system require a brief explanation.

The cathode ray tube (CRT) data display units (6 and 24) are used to display the primary data upon which navigation decisions are made. Control and selection of the data to be shown are obtained through use of the scope display control panel (33) which controls the transfer of data to the face of the CRT's. Alpha-numeric as well as analog data may be displayed on demand.

The slide projector and control panel (16) provides for presentation of data readily stored on film. This includes such data as:

- (1) Ephemeris.
- (2) Star tables.
- (3) Nominal trajectories.
- (4) Abort nominals.
- (5) Test procedures.
- (6) Maps.
- (7) Indexes of data.
- (8) Coordinate system pictorial.
- (9) Symbol lists.
- (10) Failure procedures.
- (11) Operating procedures.
- (12) Analog presentation of cislunar space.
- (13) Star charts.

The computer control (23) initiates specific guidance computer subroutines which program the computer to calculate upon demand, various data which may be needed by the navigator-pilot. Computer display data, once computed, is stored in the computer buffer storage unit after which time, display of the data does not interfere with computer operations.

The cathode ray tube data display units (6) and (24) offer tremendous flexibility with respect to data and format of data display. Examples follow. Unit (24) could be used for basic guidance data while unit (16) is used for abort

situation monitoring. Multiple data can be viewed simultaneously on either or both display units. The viewing surface can be split among several data if desired. Emergency data can be flashed into one sector of either data display unit. The display unit has wide usefulness whether the desired data are alphanumeric, TV monitor type, analog signal type, or map type. Finally, changes in guidance display parameters which may occur from mission to mission, as the Apollo program develops, can probably be accommodated with no or little change in the guidance and control display system.

1. Ascent Guidance Displays And Operator Controls

Ascent guidance displays commence to function prior to launch.

The launch countdown time is presented in numeric form on the elapsed time indicator on the timer and sequence panel (15).

At launch time, the navigator-pilot will observe the green ready light at the top left of the sequence lights and control panel (13) and if ready, he will press the "1st Stage Enable" button on that panel to ignite the Saturn first stage.

The monitoring of the Saturn booster during launch involves at least three separate areas of display on the forward console;

- (1) Light indicators on the system status panel (1) show the presence or absence of adequate tank pressures, engine chamber pressures, and gimbal system pressure.
- (2) Flight reference indicators of the flight control display groups (14) show vehicle attitude and angular acceleration.
- (3) The 10-in. scope displays information describing the thrust direction of each engine of the Saturn cluster in either analog or numerical form.

The 7-in. scope (6) is used during ascent to numerically display the x, y, and z trajectory errors as they develop. The scope is fed by data from the digital computer via a miniature printer (31) and a TV camera which scans the printer copy. (The ascent computer guidance program to generate this data will have been preset through the computer control panel (23). The display of the error data on the 7-in. scope will have been established by the scope display controls (33).)

The slide projector (16) will show (in color) a flow chart giving the key monitor, control and action alternating versus time for this portion of mission flight.

~~CONFIDENTIAL~~

As the Saturn stages burn, the navigator-pilot will monitor the flight profile as a function of time and altitude by referring periodically to the flight control display group (14), the pressure altimeter (12), the timer and sequence indicator (15), the standby stability indicator (13), and "Q" meter (11). One of the primary concerns will be to monitor for abort indications and to initiate abort procedure if necessary through use of the abort control (48). Ascent developments such as a large off-course trajectory, severe rocket engine malfunction, control system failure, and the sudden onset of high radiation are typical of developments that would provoke an abort decision. Indicator lights on the major system status panel (1), the parameter display panels already mentioned, and the two cathode ray tube displays (6) and (24) will signal abort type malfunctions as they occur. Although the navigator-pilot may receive additional data or warning from ground stations, he is in the best position to assess the data and take appropriate action. In the case of first stage burning, the AMR range safety officer will instruct the navigator-pilot to abort via both a voice message and an "ABORT" light indication on the major system status panel (1).

In a normal ascent, each launch sequence light of the sequence lights and controls panel (10) will illuminate green and remain on during the event, extinguishing at the termination of the event. For some of these events D-ring pull controls are provided which are used by the navigator-pilot to manually backup such operations as first stage separation, tower separation, second stage separation, third stage cutoff and third stage separation.

As the ascent flight progresses, the navigator-pilot will continually identify his choice of target areas in the event of an abort requirement. These choices are factored into the guidance system by means of the computer controls (23). Upon abort, this guidance system data automatically programs the abort engine to produce the required velocity.

During the parking orbit, a complete checkout of the Apollo subsystems will be accomplished. This will include checks on the communication, environmental, propulsion, re-entry system, electrical system, guidance system, and the display subsystem. The performance of each subsystem and the performance of the related display and control panels will be verified. Detail test procedures for these checks will be shown in the slide projector (16). The condition of both the equipment and the crew at this point in the flight (after initial launch acceleration) will enter into the navigator-pilot's decision whether to inject into the lunar mission or to return to Edwards AFB. The navigator will communicate his decision to the ground network via the communications control (26) and the message command (25) panels. As the time for third stage reignition approaches, the navigator-pilot will again orient the combined spacecraft-booster in the desired attitude by reference to the flight control display group (14) indicators. The guidance system will initiate the restart of the third stage booster and control the injection sequence. The navigator-pilot will monitor the injection sequence and provide manual backup for ignition of the booster engine.

~~CONFIDENTIAL~~

Primary injection monitor (termination of Saturn Stage 3) is exercised by the navigator-pilot through use of the 7-in. scope (6) and 10-in. scope (24) displays which are programmed to show position and velocity deviations from the nominal (phantom) injection trajectory. As the trajectory of the accelerating spacecraft approaches close coincidence with the nominal, the navigator-pilot will monitor the automatic sequence cutoff of the booster engine. The third stage cutoff is critical and must be manually operated should the automatic system fail to operate at the computer indicated time. Immediately after cutoff, the navigator will effect third stage separation.

Vernier injection monitor and control is accomplished by the navigator-pilot to obtain final shaping of the trajectory so that it lies as close as possible to the desired nominal. The spacecraft attitude propulsion system is activated using the controls on the attitude propulsion and vernier engine panel (3). The required attitude is obtained through control stick and yaw pedal operations and the vernier engine jet system selected via the selector switch on panel (3). Final velocity and position deviations as indicated by the trajectory data scope displays are nulled by supplying the required velocity increment via the vernier engine jets, to complete the trajectory injection vernier.

2. Midcourse Guidance Displays And Operator Controls

In the Apollo spacecraft, perhaps the principle command function during midcourse phases is the direction of the spacecraft along the desired trajectory. The guidance operations differ to some extent depending upon whether mission phase is translunar, lunar orbit injection, lunar orbit maneuvering, lunar orbit ejection, or transearth. However, the guidance display and control system functions are similar in all of these; and for this reason, a description of the display system and its function, restricted to cover the translunar midcourse phase only, is regarded as adequate.

To illustrate the functioning of the Apollo astronaut in the employment of the guidance and control display system in a mission translunar phase, the events of a sample guidance situation are outlined and the significant functions of the astronaut with respect to his use of the guidance and control display system are examined. In each case, reference is made to the display system arrangement given in Fig. VI-2 by the numbers in parenthesis on the extreme right.

The sample guidance situation taken in the translunar phase covers the operations immediately prior to, during, and immediately subsequent to a typical midcourse guidance correction.

For discussion purposes, the major events in this example are identified as follows:

- (1) Prior occurrences.

- 
- (2) Sensor measurements.
 - (3) Trajectory error determinations.
 - (4) Guidance data weighing and data selection.
 - (5) Evaluation of course correction alternates and selection of optimum CCA.
 - (6) ABLE correction.
 - (7) Post-ABLE correction sensor measurements and trajectory error determinations.

The operational sequences associated with the above listed events are described below.

a. Prior occurrences

The salient trajectory history relating to midcourse guidance includes:

- (1) By virtue of guidance control of the spacecraft injection operation, trajectory conformance to nominal path will have been assured.
- (2) Onboard use of optical equipment subsequent to insertion vernier, in the form of earth diameter measurements, earth landmark measurements, and star direction measurements has resulted in onboard confirmation that the trajectory is within the range of acceptable trajectories.
- (3) Prior trajectory analysis on the ground has determined that the optimum time for initiating trajectory correction (for the flight mode planned) is in the range three to eight hr from launch. The navigator, because no special problems have arisen, decides on the 4.0 hours ABLE time. (ABLE is the first of 2 separated corrective velocity impulses used to get back onto the desired trajectory.)
- (4) Deep space net data has been received at 2 hr giving the 2-hr estimate of trajectory parameters as well as course correction data in the form of angles and velocity values for course corrections at 3, 4, 5, 6, 7, and 8 hr exactly, toward a predetermined nominal future trajectory point.
- (5) Similar data have been received based on the radio guidance back-up system.

- (6) The spacecraft has been oriented with the nose to the sun.
- (7) Miscellaneous spacecraft operations have been accomplished in anticipation of commencing onboard trajectory measurements at a pre-planned time; i. e. , at 2 hr, 10 min. 0 sec.
- (8) Spacecraft has been attitude stabilized in limit cycle operation to planned attitude for 2.0 hr flight time.

b. Sensor measurements

Onboard instruments are used to obtain measurement data samples which are processed by an onboard digital computer to provide estimates of spacecraft trajectory.

The data from the instruments are entered as a series of numerical readings which are registered and operated upon by the computer arithmetic section. Typical input data would include:

- (1) Angle readouts from astro-tracker (azimuth and elevation)
- (2) Range readout from altimeter (when within range).
- (3) Angular diameter readout from telescope.
- (4) Occultation angles and time.

Also among data which may be acquired is radio guidance data from the earth.

Both manual control and automatic control of sensor measurements are obtained.

- (1) Typical automatic sequence operations relating to the use of the astro-tracker sensor system are listed below, starting at time 2 hours zero minutes.

<u>Time</u>			<u>Event</u>	<u>Display Subpanel</u>	
<u>Hr</u>	<u>Min</u>	<u>Sec</u>			
2	0	0	Astronaut commands computer to switch to automatic star search-acquisition routine.	(7)	(23)
		1	Shield removed from astro-tracker window		

~~CONFIDENTIAL~~

<u>Time</u>			<u>Event</u>	<u>Display Subpanel</u>
<u>Hr</u>	<u>Min</u>	<u>Sec</u>		
	1		Tracker scans commanded search area for star No. 1.	
	2		Tracker locks on star, angular readouts are registered, and appropriate torques are applied to platform.	
	3		Tracker searches for and locks on star No. 2.	
	4		Readout No. 2.	
	5		Star No. 1.	
	6		Readout No. 1.	(23) (14)
	7		Readout star No. 2.	(16)
	8		Readout star No. 1.	
	9		Readout star No. 2.	
	10		Platform completed alignment.	
	11		Platform checks alignment (ambiguity check on nearby star).	
2	12	0	Navigator instructs computer to identify spacecraft attitude angles for earth track routine, and observes angles on flight director. Navigator refers to slide showing approximate angles in current coordinate system.	(23) (14) (16)
	13		Navigator activates manual attitude control system, and with stick control and toe pedals, orients spacecraft to obtain nominal tracker sighting to earth.	(3) (14) (46) (47)
	14		Navigator controls astro-inertial platform to begin earth track routine. In general, only the east or west rim will be clearly seen (not both). Therefore, discrete points on the illuminated side will be scanned.	(7)

~~CONFIDENTIAL~~

<u>Time</u>			<u>Event</u>	<u>Display Subpanel</u>
<u>Hr</u>	<u>Min</u>	<u>Sec</u>		
			At least three points will be obtained for center and diameter.	
	15		West rim sight and readout point No. 1.	
	16		West rim sight and readout point No. 2.	
	17		West rim sight and readout point No. 3.	
	18 to 23		Same as events above for moon track.	Same as above.

(2) Typical manual sequence operations with the manual trackers, accomplished while auto-tracker operations proceed, are:

<u>Time</u>			<u>Operations</u>	<u>Display Subpanel</u>
<u>Hr</u>	<u>Min</u>	<u>Sec</u>	<u>(Stars)</u>	
2	0	0	Astronaut, assiting navigator with manual tracker telesextant, sights toward star No. 1. Navigator sets up computer and miniature platform controls.	(23) (27)
2	0	0	Astronaut presses keyboard on tracker to enter angular data into computer. Data also enters platform-computer axis orientation loop and results in partial alignment of miniature platform. Data could also have been conveyed verbally to navigator and inserted by him with computer controls. (23)	(23) (27)
			Astronaut sights toward star No. 2 and enters data to complete alignment of miniature platform.	
	11	0	Astronaut sights toward star No. 3 and enters data to check the alignment of miniature platform. Panel light shows miniature platform in alignment.	

<u>Time</u>			<u>Event</u>	<u>Display Subpanel</u>
<u>Hr</u>	<u>Min</u>	<u>Sec</u>	<u>(earth)</u>	
2	12	0	Astronaut assisting navigator sights with manual tracker telesextant toward earth rim. Since, in general, either the east or west edge will be dark, in this case, the north and south rims will be matched by a sextant to obtain the earth included angle. Other techniques would also be used during this time period; e.g., landmarks, edgepoints (with associated computer computation programs). Navigator sets up computer and manual tracker operations.	(23) (27)
			Navigator operates computer controls and scope display controls to obtain in numerical form a simultaneous display of automatic tracker and matching telesextant included angles to the earth, and navigator verified agreement.	(23) (6) (33)
			Navigator monitors auto-tracker operation.	(7)
2	17	0	Astronaut, with navigator at forward console controls, resumes manual sightings to accumulate onboard data.	

<u>Time</u>			<u>Event</u>	<u>Display Subpanel</u>
<u>Hr</u>	<u>Min</u>	<u>Sec</u>	<u>(moon)</u>	
2	18	0	Astronaut obtains center angle readings on moon using reticles and lines of position from telesextant in real and pseudo-occultation measurements (star on designated craters). Navigator use of display and control panels of forward console are same as those cited above.	(23) (27) (6) (23) (7)
2	24	0		

(3) Guidance data may be received at the spacecraft from the deep space net (DSN) radio guidance system or from the backup radio guidance system. The data from the DSN will be received through the communication system, controlled via communication control (26), on the Apollo in several forms:

~~CONFIDENTIAL~~

~~CONFIDENTIAL~~

- (a) As basic trajectory data in binary signal form. This data will channel directly into the computer store for radio guidance data and will consist of x, y, z position and velocity values in the prevailing coordinate system at a particular time thereby specifying completely the trajectory. This data entry into the computer store will be automatic.
- (b) As specific correction data in binary signal form. This data will channel directly to the computer as well as to a direct read-out on a backup data connection panel (not on forward console) which the navigator-pilot will be able to view by turning his head to the right. The data to the computer will be the time, spacecraft attitude (thrust direction angles), and velocity increment for the ABLE portion of midcourse correction at several specific elapsed flight times, toward particular nominal trajectories. One of these will be shown on the backup direct readout panel.
- (c) As specific correction data in voice signal form. The navigator will record these in permanent form on his voice recorder and perhaps with pencil and card. He will manipulate the computer controls (23) and scope display controls to obtain data translation and a numerical display on the 10-in. scope (24) which he can use to confirm the data received.

c. Trajectory error determinations

<u>Time</u>			<u>Event</u>	<u>Display Subpanel</u>
<u>Hr</u>	<u>Min</u>	<u>Sec</u>		
2	24	12	Navigator-pilot programs computer to determine trajectories based on available data. Separate computations are ordered, based on: <ul style="list-style-type: none"> A. Auto-system data B. Manually derived data C. Radio guidance data D. Radio backup data 	(23)
2	24	24	Navigator examines trajectory errors for a selected time in the near future in the prevailing coordinate system in terms of deviations from nominal, i. e. $\Delta x, \Delta y, \Delta z, \Delta t, \Delta \dot{x}, \Delta \dot{y}, \Delta \dot{z}$, as indicated by each system and	(23) (33) (24) (6) (16) (14)

~~CONFIDENTIAL~~

~~CONFIDENTIAL~~

<u>Time</u>			<u>Event</u>	<u>Display Subpanel</u>
<u>Hr</u>	<u>Min</u>	<u>Sec</u>		
			verifies that all are in substantial agreement. A typical 10-in. scope display is illustrated in Fig. VI-3. A typical analog display of trajectory deviation as presented on the 7-in. scope as shown in Fig. VI-4.	
			d. Guidance data weighing and data selection	
	25	12	Navigator programs computer to evaluate standard deviations corresponding to each trajectory determination (A, B, C, D)	(23)
2	25	24	Navigator examines on his displays:	
			(a) Normal data weighing arrangement for projected time of flight 3 hr, 0 min) (on slide projection (16). Figure VI-5 illustrates slide projection of normal data weighing.	(16)
			(b) Numerical ratio of standard deviations of each data group to expected deviation for data (on 10-in. scope from printer).	(23) (31) (24)
	25	30	Navigator considers factors which would change weighing arrangement; e. g., intermittent performance, insufficient samples, internal cabin conditions, crew performance.	(23) (31) (24) (16)
2	26	00	Navigator combines system data in various ways to obtain a "best" trajectory determination; i. e., arrangement which minimizes numerical ratio and selects a specific weighing arrangement to be used. (See typical 10-in. scope display in Fig. VI-6.)	(23) (31) (24) (16)
			e. Evaluation of course correction alternates	
2	27	00	Navigator-pilot programs computer to calculate by iterating the velocity correction solutions, using the previously determined	(23)

~~CONFIDENTIAL~~

<u>Time</u>			<u>Event</u>	<u>Display Subpanel</u>
<u>Hr</u>	<u>Min</u>	<u>Sec</u>		
			data as a basis. He will select:	
			(a) Nominal paths to test.	
			(b) Times for initial (ABLE) correction.	
			(c) Times for final (Baker) correction.	
	32	0	Navigator controls display system to present multiple solutions showing velocity impulses required to achieve trajectory correction. The principle variant is selected by the navigator (see display in Fig. VI-7).	(23) (24)
2	33	0	Navigator determines:	(6) (24) (16)
			(a) Whether to correct his trajectory or not.	
			(b) Which nominal to correct.	
			(c) Which timing is optimum.	
			(d) Whether an abort trajectory is required.	
			Using predetermined criteria:	
			(a) Relationship of minimum correction velocity required to current velocity uncertainty.	
			(b) Relationship of correction velocity required to that allocated.	
			(c) Which timing and nominal trajectory requires minimum fuel.	
2	34	0	Navigator decides upon one of the course correction alternates, typically, one commencing at 3.0 hr, 0 min, 0 sec.	(6) (24) (16) (14)

~~CONFIDENTIAL~~

<u>Time</u>			<u>Event</u>	<u>Display Subpanel</u>
<u>Hr</u>	<u>Min</u>	<u>Sec</u>		
f. ABLE correction				
2	34	6	Navigator controls display system to present the details of the correction alternate he has selected on the 7-in. scope. (See Fig. VI-8.)	(33) (23) (6)
	34	12	Navigator communicates essential data to the ground and requests confirmation of the computer solution by ground based computation.	(25) (26)
	40	0	Navigator checks onboard guidance and control subsystems for performance.	All
	46	0	Navigator receives confirmation of onboard trajectory solution. Navigator presses "normal command" button on spacecraft guidance command panel (41).	Voice and (23) (24) (33) (41)
	52	0	Navigator orders all crew stations to prepare for correction impulse at 3 hr 00 min, 00 sec.	Voice
2	52	12	Navigator commences to manually control the attitude toward that required for ΔV correction.	(14) (46) (47) (6)
	52	48	Spacecraft reaches ABLE attitude.	(6) (14)
	52	49	Navigator monitors time display.	(15)
2	58	0	Navigator through inputs into the computer control panel (23), establishes automatic thrust initiation; i.e., ignition of vernier engines by computer derived timing signal and automatic attitude control.	(23)
2	59	30	Navigator selects vernier engine arrangement (2 jets or 4) and arms system by use of controls on the attitude and vernier engine propulsion panel (3).	(3)
2	59	40	Navigator monitors time remaining and advises other crew members of impending impulse.	(15) (Voice)

~~CONFIDENTIAL~~

<u>Time</u>			<u>Event</u>	<u>Display Subpanel</u>
<u>Hr</u>	<u>Min</u>	<u>Sec</u>		
3	0	0	Navigator places fingers on button of stick control to backup vernier engine start. He monitors propulsion start and attitude control system operation, and prepares, if necessary, to assume manual attitude control with stick and toe controls.	(46) (47) (14) (3)
3	0	20	Navigator observes termination of ABLE impulse at proper time, providing backup control if necessary to obtain required	(14) (6)
3	1	0	Navigator checks operation of guidance equipment and orders checkout of all spacecraft systems.	All

g. Post-ABLE sensor measurements and trajectory error determination

3	4	20	Sequences essentially the same as those described in paragraphs b and c above, are undertaken to confirm the new trajectory while the 4 hr coast period ensues.	As noted before
---	---	----	---	-----------------

3. Re-entry Guidance Displays And Operator Controls

As the spacecraft approaches earth on the final leg of the transearth flight, a final pre-re-entry navigational fix will be obtained by the navigator-pilot through use of the onboard guidance equipment; i.e., the altimeter, telesexant, automatic astro-inertial platform, computers, computer controls, and display controls. The trajectory data thus obtained from onboard systems, in conjunction with earth tracking data, will be programmed on the computer to obtain the best estimate of the projected re-entry conditions; specifically, the vacuum perigee altitude, the predicted time of perigee, and the orbital inclination will be verified. The 10-in. scope (24) will display this data in an alpha-numeric format.

As a consequence of having established the re-entry conditions, the navigator will proceed to obtain, using the computer and scope displays:

- (1) A prediction of the position within the re-entry corridor.
- (2) A prediction of the probable mode of re-entry.

~~CONFIDENTIAL~~

- (3) An estimate of the landing area.
- (4) An estimate of the landing time.
- (5) The optimum vehicle attitude for commencing re-entry.

These are discussed verbally with the ground over the HF and VHF communication systems.

At approximately 10 minutes from re-entry, the spacecraft will be aligned to initial re-entry attitude ($C_{L_{max}}$). The hot gas aerodynamic flap system will be activated, the re-entry attitude propulsion system will be turned on and the propulsion and equipment module separated from the command module. To accomplish these operations, the navigator will use the flap system display (2), the re-entry attitude propulsion panel (3) and the re-entry sequence panel (39). Following separation of the modules, the control surfaces on the command module will be extended to their initial position and checked for operation.

At re-entry, defined as crossing 400,000 ft altitude, atmospheric conditions and range from the re-entry point to landing site are estimated. Ground station tracking information, if available, will be used to confirm the spacecraft's position and altitude in the re-entry corridor. Any attitude or trim corrections necessary are made with the command module control and stabilization jets. These jets will be used for maintaining vehicle attitude during the initial phase of re-entry. However, the dynamic pressure ("q") rises very rapidly and the aerodynamic control surfaces (flaps) will be used, once sufficient pressure as observed on the "q" meter (10) has developed. The transition period is less than a minute.

During re-entry, the inertial guidance system provides the navigation and steering logic. The guidance system seeks to solve simultaneously, if possible, three critical re-entry problems which are "g" loads, range-to-target limits (skip into Van Allen radiation) and ablator management.

The $C_{L_{max}}$ attitude is held until the altitude is approximately 300,000 ft. At 300,000 ft, the re-entry guidance system commences making re-entry path predictions on the basis of which the L/D and roll angle are commanded by the re-entry range prediction steering system (RERPS) for obtaining the range and heading to Edwards AFB. The fan type display from which the navigator determines L/D and roll angle estimates is presented on the 7-in. cathode ray tube (6) appearing as a "footprint" showing vehicle maneuver capability, predicted landing point and landing targets, relative to the maneuver capability, and the corresponding bank angles and L/D ratios required. (See Fig. VI-9.)

The load factor control limits are displayed to the navigator on the 10-in. scope display (29) in the form of near future "g's" (see Fig. VI-10.) Lift modulation will be used, if necessary, to restrict the maximum "g's" to 6.

~~CONFIDENTIAL~~

The navigator controls the command module heating during re-entry to stay within the limits of the available thermal protection material. Thermal protection management is accomplished by the navigator with the aid of three indicators in the flight control display group (14), illustrated in Fig. VI-11. One shows the temperature of the internal wall. A second shows the temperature of the metal radiator wall in relationship to the permissible limit (2,200°F). The third indicator shows in the lower, center, and upper portions, respectively, (1) the amount of thermal protection material (ablator) already expended, (2) the amount of additional ablator material that will be consumed in the remainder of re-entry flight for the re-entry trajectory being examined or flown, and (3) an index representing total ablator material available at start.

The navigator monitors these indicators for the re-entry path being considered to obtain a re-entry flight that is within the heating limit.

Vehicle attitude and rates are displayed to the navigator continuously during re-entry via a flight reference indicator (14A) illustrated in Fig. VI-12. Also presented on vertical axis indicators (14B) are present and demand values for L/D ratio and angle of attack. (See Fig. VI-13.)

During re-entry, the navigator observes the landing track pattern and continually confirms whether the vehicle has the capability of reaching the selected landing site (Edwards AFB) or whether an alternate landing site must be selected. He monitors the near future "g" display and changes his selection of re-entry paths as necessary to stay within a 6-g limit. He monitors the flight reference indicator and continuously maintains the required (demand) vehicle attitude through the autopilot by the use of his two-axis control stick (pitch and roll) and toe pedals (yaw). In addition, the navigator manages the flight to maintain spacecraft heating within the ablator limits. When acceleration and heating peaks have passed, the navigator will then concern himself with lateral and longitudinal maneuver requirements to approach the selected landing site, with insertion into his guidance system of any available ground tracking data to improve the accuracy of the final re-entry navigation. As the spacecraft reaches the predicted point for terminating re-entry (in the vicinity of the landing site) the navigator will monitor altitude, velocity and range-to-target displays and, if necessary, he will manually initiate drogue chute deployment to commence the landing sequences. This will occur at an altitude between 100,000 ft and 45,000 ft with the vehicle less than 15 miles from the target.

C. DISPLAY AND CONTROL SUBPANEL DESCRIPTIONS

1. Seven-Inch Scope (24)

The pilot and navigator each have a 7-in. scope in the center of their displays. The scope functions primarily as a re-entry situation (footprint) indicator which will be used to perform re-entry guidance.

The 7-in. scope will also be used to display computer data as desired. During landing operations, the 7-in. scope will display the TV camera picture of the landing area. The navigator's prime use of the 7-in. scope is to examine mid-course trajectory errors during guidance operation. Alternate use includes redundant showing of the pilot's displays.

2. Ten-Inch Scope (6)

A 10-in. cathode ray tube is located directly in front of both the pilot-commander and navigator-pilot.

One purpose of the 10-in. scope is to display the output of the computer. By exercising the computer controls in conjunction with display controls, the operator can display on the 10-in. tube face, a large variety of guidance and trajectory data available either directly from computer store or by demand computation. This function would normally be the concern of the navigator.

Another function of the 10-in. scope is to display the view of terrain below the vehicle, during landing operation, as seen by a TV camera. This function will normally be the concern of the pilot.

3. Scope Display Control (33)

Both the navigator-pilot and pilot-commander positions have a scope display control panel located just to the right of the 7-in. scope. These controls permit switching of data from the printer, TV Camera and computer to either the 7-in. or 10-in. scope. Ordinarily, each crew member will be concerned with separate tasks, therefore, independent controls are provided. However, the duplicate controls provide flexibility in the event of failure of certain equipments. Figure VI-14 illustrates the functional relationship of the scopes, the scope display controls and the associated equipments.

4. Slide Projector and Controls (16)

Various information items are contained on slides and viewed on a projection screen of approximately 7-in. x 9-in. The complete assembly is mounted in the center of the console with the projector and selector mechanism mounted on the rear of the screen. A wide angle screen provides an adequate view to both the navigator and commander.

The slide projector is used for presenting check lists, star maps, information tables, operating procedures, maintenance procedures, etc. Selector controls below the screen allow rapid access to the stored information.

5. Computer Control (23)

A computer control panel is provided at the left of the navigator-pilot's 10-in. scope and a similar panel at the right of the pilot-commander's 10-in. scope. Controls permit readout of computer functions onto the cathode ray tube displays.

The navigator-pilot's position includes panel controls to establish which position is in control of the computers and to permit entry into the computer of data such as basic angles, occultation data and point tracking data from the manual tracker. A similar set of data entry controls is provided at the manual tracker location rather than at the pilot-commander's computer control panel to permit an operator to enter data directly from the tracker location.

6. Attitude Propulsion and Vernier Engine (3)

An attitude propulsion system display panel is centrally located to the left of the pilot-commander's 7-in. scope, provided on the main panel. This panel indicates the condition and functioning of the reaction jet propulsion system for controlling the attitude of the vehicle. The temperature, pressure, and remaining pounds of both the fuel and oxidizer supplies are continuously displayed. A total on-time counter provides a digital readout of the total seconds of use remaining. Valve lights show which jets are operating in roll, pitch and yaw control. A master switch transfers the monitor of all attitude information from the spacecraft system to the command module system at the beginning of re-entry.

Vernier propulsion jet operation is also shown and controlled from this panel.

7. Flight Control Display Group (14)

Two identical groups of displays for both the pilot and navigator provide spacecraft control information.

Flight reference indication. An "outside-in" flight reference indicator has a symbol of the spacecraft superimposed on a reference field to display the pitch, roll and yaw attitude of the spacecraft. Along the edges of the flight reference indicator are three small meters which display roll angle rate, pitch angle rate and yaw angle rate.

Re-entry vertical axis indicator. At the left of the flight reference indicator is a tape-type instrument which quantitatively presents the prime re-entry parameters, vertical acceleration (g) flight path angle (d), and lift-to-drag ratio (L/D). The g is sensed by an accelerometer, and the flight path angle and L/D are derived from computer calculations.

Thermal protection management display. At the right of the flight reference indicator is a display to aid the pilot in thermal management during re-entry. The indicator presents the temperature of the internal wall in per cent of permissible maximum (2200° F), the temperature of the supper alloy radiant shield in per cent of permissible maximum (2200@ F), and the amount of ablator material remaining on the re-entry vehicle. The indicator also displays a prediction of the amount of ablator material that will be consumed in the remainder of the re-entry flight. This indicator is driven by computer generated data; inputs to the computer being signals from contact probes embedded in the thermal protective material.

Inertial velocity. Below the flight reference indicator is a computer-derived numeric readout of inertial velocity. This indicator is also used for displaying the velocity error during spaceflight velocity corrections.

Inertial altitude. Directly above the flight reference indicator is presented a numeric readout of inertial altitude.

8. Automatic Stabilization and Control System (ASCS) (28)

This unit operates as a control panel for the spacecraft autopilot in automatic modes. With it the navigator or pilot-commander can provide damping of the spacecraft, and can select hold and control modes for stabilization and maneuvering. Along the bottom of the panel is a series of lighted pushbuttons to select an autopilot mode during the re-entry profile. These outer loops provide the capability of holding constant the most critical parameter during a particular portion of the re-entry phase (, g, lift/drag, temperature).

9. Printer (Alpha-Numeric) (31)

A printer is located at the left side of the navigator-pilot and the right side of the pilot-commander positions. All manual inputs and certain selected equipment parameters will be permanently recorded on the printer record paper. The printer will be controlled from the display control panel and also from the computer control panel. The printer output will normally be viewed at one of the 7-in. or 10-in. display tubes, but can also be viewed as hard copy.

10. Astro-Inertial Platform Control (27)

This centrally located panel controls operation of the astro-inertial platform. Slew controls are provided for the platform star tracker as well as the platform itself. Synchro repeaters are provided to permit visual check of platform operation.

11. Miniature Inertial Platform Panel (27)

A control panel for the miniature inertial platform is located centrally on

[REDACTED]

the right side of the main panel. Align, auto slew, and cage and uncage buttons permit erection and control of the platform. Two manual slew knobs are provided to permit manual slewing of the platform to the drive position. A 3-position mode select switch permits selection of the automatic or manual modes or to a slave mode which slaves the platform to inputs from the computer.

12. Timer and Sequence Indicator (15)

The timer and sequence indicator panel is just to the right of the centrally located slide projector. The instrument includes an elapsed time indicator which begins to function at zero minus 10 sec, and shows elapsed mission time in seconds, minutes and hours. Mission time appears as total hours rather than day and hour due to lack of day-night orientation in space flight.

Time to occurrence of next event can be set into one of the three time displays as hours, minutes and seconds to occurrence. As time of occurrence approaches, crew members can see directly the time remaining before the event shall occur. All major flight events are listed on tapes for display in the window. To set the proper event into the window, the serrated wheel is rotated to the proper position. A timer select switch permits changing the displayed time in any of the three displays. Time is adjusted by activating the toggle switch to "increase", which slews the time readout at high speed. Activating the start button for each display, starts the count toward zero.

Two stop clock timers are provided. The stop clock timer has two main usages:

- (1) During navigation operations, the time between sightings can be accurately recorded.
- (2) During thrust periods, a readout of the duration of the thrust can indicate the accuracy of the correction, since amount of thrust x duration = total correction made. Two toggle switches are provided to select manual or automatic mode of start and stop.

13. Communication Control (26)

A centrally located panel between the two 10-in. scopes permits selection of communication equipment by either the pilot-commander or navigator-pilot. Push button selection is provided with integral light indication of which equipment is operating and which is malfunctioning. Controls are provided for space antenna directional control.

14. Message Command (25)

This panel is centrally located on the lower portion of the main console near the pilot-commander. It is used to obtain various coded messages from

computer storage, which are then automatically transmitted to earth through the communication system. The panel contains a keyboard consisting of four letters and six numbers. A large number of computer messages can be selected by alpha-numeric coding.

15. Radar Altimeter Control (39)

Basic control of the radar altimeter is exercised from a centrally located panel in the center console. Switches are provided for on-standby-off control and mode selection. A direct numerical readout is provided to register the altimeter output readings prior to computer processing. Rotary antenna pointing controls are also provided.

16. Spacecraft Guidance Command (41)

A subpanel located immediately below the system status panel contains a grouping of combination light-switches identified with spacecraft guidance command. The light-switch on the left labeled "normal control", when lit, indicates that guidance functions are under the astronaut's direct control. At periodic intervals, e.g., 1 hr, another light identified as the "automatic programmer alert" light will flicker to show that switch-over to automatic programmer control will shortly take place.

When this occurs, a vehicle contained guidance programmer assumes control of such functions as star tracker operations and computer operational functions. This condition is indicated by the lighting of an "auto programmer control" light. When in automatic command, a switching circuit gives ground based radio guidance the option to assume vehicle guidance control, which is indicated by the fourth light. The astronaut will normally determine by switch engagement the mode of vehicle guidance command he desires. If he is physically disabled, the system will automatically switch first to automatic programmer and then possibly to ground control.

17. Control Stick (46)

A multiple-purpose, two-axis electrical control stick is provided for pitch and roll control of spacecraft attitude. The stick is of light weight, "pencil stick" design and has use during ascent, in space and during re-entry and landing operation. It incorporates a switch for manual start and stop control of midcourse propulsion.

18. Toe Pedals (47)

Toe pedals of the differential ankle design are provided for spacecraft yaw attitude control. The pedals enclose the front of the foot back to the instep and rotate about a pivot axis under the arch of the foot.

19. Abort Control (48)

A double action abort handle will be mounted on or near the right-hand arm of the pilot's seat. The design and position of the abort control will permit instantaneous operation, even when arm movement is constrained.

20. Major System Status (1)

A light panel, centrally located at the top of the forward console, indicates to both pilot-commander and navigator-pilot the operational status of major subsystems. Subsystems whose status is critical to pilot functions are shown by lights located on the right-hand side in arrangement related to system priority. Systems critical to navigator functions are located on the left. Subsystem status will be indicated by color coding. A malfunction indication on one of these gross status lights would immediately signal action by the spacecraft commander. The Saturn booster, guidance system, electrical power system, and communication system are typical of the subsystems whose status is shown on this panel.

21. "Q" Meter (11)

A "q" meter is provided at both the pilot-commander's and the navigator-pilot's position. This instrument shows dynamic pressure to an accuracy of about 5%. This information is used during re-entry and for abort decisions during launch. The "q" measurement is obtained from the computer.

22. Pressure Altimeter (12)

The barometric altimeter is located at each position to the left of the flight reference indicator. It is a single revolution indicator with a range from sea level to 100,000 ft. The dial face will have reference marks at the nominal drogue and main chute deployment altitudes. The expected instrument accuracy is ± 1000 ft. The static port for the instrument is located in a protected area on the aft face.

23. Standby Stability Indicator (13)

A standby stability indicator is located just to the left of each of the flight control display groups. The instrument provides backup for the flight reference indicator and provides pitch, yaw and roll information. It is used to monitor automatic attitude control performance and is also used by the pilot during manned attitude control. The instrument will be useful in recovery from tumbling during space flight, since the display is in simple form.

[REDACTED]

24. Sequence Lights and Controls (10)

Combined launch sequence and warning lights are arranged in chronological order from top to bottom along the left side of the main panel for observation and activation by the navigator-pilot. During normal launch operation, each sequence light illuminates green and remains on during the event. If an operational event, such as second stage ignition, does not occur at its normal time, the sequence light becomes a red warning light. Immediately, upon observation of a red light the navigator-pilot backs up the event manually by pulling the D-ring control. If this manual backup operation successfully causes the event to occur, the red light is extinguished and the green light illuminates. If the manual backup is not successful, the mission must be aborted. At the termination of an individual event, the green light is extinguished.

25. Flap System Display (8)

A flap system display is centrally located above the slide projector. This display provides information about the functioning of the hot gas servo power source and actuation of the aerodynamic control flaps. Fuel pressure, fuel quantity remaining, and system pressure parameters are displayed. Three flap position indicators are provided to indicate that the flaps have been deployed successfully and are functioning properly. A switch permits switching hot gas power from the flaps to the landing system winch.

26. Re-entry Sequence Lights and Controls (42)

Two combined landing sequence and warning lights are arranged on the right of associated re-entry event controls on this panel. The operation of this panel is similar to that of the "sequence lights and controls" panel in that the occurrence of the major events is registered by lights, and backup controls are provided for each primary operation mission module separation and drogue chute deployment events are covered.

27. Corrections Data Panel (40)

This is a backup display panel to provide direct readout of trajectory correction information. The functions of the panel are two-fold:

- (1) To provide direct access to the computer generated navigation solutions to be available, even if the forward console data display equipment fails.
- (2) To provide direct readin to the computer from the communication system and the communicated (from earth) navigation solutions from the ground facilities.

[REDACTED]

D. IMPLEMENTATION

A study was undertaken to identify appropriate techniques to be used in implementing Apollo's guidance system displays and operator controls. Both current state-of-the-art techniques, as well as advanced display mechanization techniques, have been selected.

1. Techniques

Electroluminescent materials, solid-state switching and microminiature packaging should be used in fabricating a large number of the Apollo display and control units.

Electroluminescent materials offer the advantages of reliability, low power consumption and multicolor capability in numerous display applications. Electroluminescent material brightness and usable life, currently adequate for Apollo applications, will measurably benefit from state-of-art improvements within the next two years.

Electroluminescent lamp materials should be used as an area illuminant in basic applications as well as in segmented forms for:

- (1) Thermometer-type displays (columnar form)
- (2) Meter-type displays (row form),
- (3) Digital-type displays (an ordered matrix form).

The multicolor capability of electroluminescent phosphors, plus the potential change in chromaticity with variation in excitation signal, provides the basis for excellent readability based on color contrast and brightness differentiation. Nearly all display subpanels should employ these materials.

Current solid-state switching techniques and practices are sufficiently well developed to find numerous applications in Apollo's display circuitry. Improvements in techniques and new concepts will undoubtedly occur during the next two years; full advantage should be taken of these anticipated improvements. Specific circuit applications include logical selection matrices and electronic counters. In certain areas, solid-state switching should be applied to power circuits, particularly in situations where high levels of reliability are required. For these applications, state-of-art components such as the silicon-controlled rectifier should be used.

Microminiature packaging should be employed in the display circuitry to obtain improved reliability and reduced package size and weight. The basic form of fabrication should be micro-modules in which thin-film circuit elements are vacuum-deposited on a mechanically stable base. Uncased transistors should be added as "lumps". Among the display circuitry packaged in this way are

~~CONFIDENTIAL~~

d. Meter display

Based on considerations of improved reliability and future growth inherent with solid-state devices, horizontal meter-type displays will be implemented by solid-state readouts rather than by moving coil meters. Readout is accomplished through utilization of a row of electroluminescent lamp segments activated by microminiature packaged power gates and enabling logic. Such meter displays will be used in the attitude propulsion and vernier engine panel (3).

e. Servoed vertical tape-type displays

Vertical tape-type servoed displays should be used in some of the Apollo display instruments where the required measurement and display range makes the equivalent solid-state display impractical. In these instances, the basic indicator operates as a closed loop self-balancing bridge and contains a reference bridge circuit, servo-amplifier, servo-motor and tape-device mechanism and position feedback transducers. The ablator material indicator of the flight control display group (14) typifies this instrument.

f. Attitude instruments

Two types of attitude instruments appear in the Apollo display design.

One of these, the standby stability indicator (13) is the mechanization of several meter movements into one display instrument for use as angular or angular rate indications.

The second attitude indicator is that which occupies the central position in the flight control display group (14). The display embodies the principle of a moving symbol with respect to a fixed reference. The spacecraft symbol is servo-positioned and has full 360° of roll freedom. Yaw and pitch freedom are displayed respectively over the width and height of the display. The horizontal and vertical director (command) needles are servo-positioned and provide a range over the total area display. The angular rate indicators may be either contemporary galvanometers or solid-state meter-type readouts. The choice of readout will be based on final system requirements input data form and reliability. Instruments quite similar to this have been engineered and produced by Minneapolis-Honeywell. Two such displays are the DJG 158A Attitude Indicator, developed for Hughes Aircraft Company, and the DJG 227A Flight Director - Attitude Indicator, developed for the AVRO-105.

g. Cathode ray tubes

One of the considerations (leading to the particular choice of printer, TV camera, kinescope arrangement for display of guidance parameters) was the prospect of mechanizing the display readout with standard design cathode ray tubes. The use of such standard CRT's will lead to considerable cost savings,

~~CONFIDENTIAL~~

gating and logic circuits, instrument servo amplifiers and scope deflection, switching, pattern generation and amplifier circuits.

2. Mechanization

In the Apollo displays, an important and frequent usage is found for status boards, numerical readouts, moving column displays, meter displays, vertical tape displays, attitude instrument and cathode ray tubes.

A brief description of the instrumentation design of these key display and control elements will explain further the equipment mechanization plan.

a. Status boards

Status board elements of numerous display subpanels, including the sequence lights and controls panel (10) and the major systems status panel (1), will be designed to use electroluminescent material. Included in this application class are the lighted pushbuttons which appear on numerous display subpanels. The utilization of electroluminescent materials for status boards could result in a reduction of power consumption up to 10 to 1 over incandescent lamps in the same application with subsequently lowered induced heat loads. Excitation will be by means of piezo-resonant, ferro-resonant or standard solid-state power gating techniques.

b. Numerical readouts

Because of advantages in reliability, speed of response, and low power consumption, electroluminescent lamp segments will be used to generate numerical data displays. By comparison, servoed drum-type counters suffer from slow speed, significant power consumption and the reliability limitations of mechanical devices. Piezoelectric gating techniques and microminiaturized logic networks should be used to drive the readouts. Typical displays appear on the timer and sequence indicator (15) and the radar altimeter control panel (39).

c. Vertical moving column display

Several of the vertical moving column meter-type displays can be implemented with solid-state moving light column techniques rather than conventional vertical tape systems, with considerable savings in power consumption, size and weight and with improved reliability. In these displays, electroluminescent lamp segments, arranged in columns, are energized sequentially and accumulatively in an upward direction. The temperature indicators of the flight control display group illustrate a typical display application.

and benefits in reliability and availability; these advantages would not, of course, be obtained with special purpose display guns. While the specific choice of the 7-inch and 10-inch scope tubes is not yet final, certain characteristics can be cited:

- (1) The tubes will be of ruggedized construction, and will of necessity possess a small overall length to screen width ratio.
- (2) Medium resolution, short persistence screens will be employed since there is no requirement for the tube display storage.
- (3) The 7-inch and 10-inch scope screens will differ in luminescent color and will be basically monochromatic, since study results do not show requirements for multicolor capability that cannot be met by simple fitters and perhaps spot deposits of additional color phosphor in selected screen areas.
- (4) Deflection circuitry to drive the tubes should be largely solid-state in design.

VII. ERROR ANALYSIS

A. INTRODUCTION

The error analysis confirms the applicability of the selected system to the Apollo mission. The mission is basically comprised of 2 phases: the inertially guided and the ballistic free-fall.

The former encompasses all mission phases where the space vehicle is under the influence of forces over and above that of celestial bodies such as the earth, moon, and sun. These forces include atmospheric drag and lift, and applied thrust from the booster and spacecraft propulsion system. The inertially guided phases include ascent and injection to the translunar trajectory, abort, lunar orbit injection, ejection into the transearth trajectory from the lunar orbit, earth atmospheric re-entry, and the application of velocity corrective thrust during midcourse and lunar orbit. Analysis of the inertially guided phases has been confined to ascent and earth atmospheric re-entry, inasmuch as these represent the most stringent requirements on navigation equipment. Equipment specifications determined by these phases of the flight include the astro-inertial platform, the miniature inertial platform, and the telesextant (when operating as a separate optical unit to make navigational and inertial reference measurements).

The ballistic free-fall phases include translunar, lunar orbit and transearth. Analysis has been confined to the final region of the transearth phase prior to re-entry, since this region entails the most stringent system requirements. The transearth navigation requirements are governed by the need to:

- (1) Deliver the space vehicle to a re-entry corridor whose equivalent vacuum perigee does not exceed 10 mi (3 sigma) to ensure that the atmospheric re-entry shall be accomplished without exceeding the constraints of heat rate, total heat and the load limits.
- (2) Establish the initial conditions of velocity and position at the start of re-entry to assure the desired landing point accuracy. Equipment specifications determined by this phase of flight are the telesextant and the astro-inertial platform (when employed to measure range and line of centers to the earth or moon with respect to an inertial reference). The digital computer is common to all phases of flight and for the purpose of error analysis, it is assumed that the error from this source is negligible in comparison to that induced by instrumentation.

Analysis of the astro-inertial navigation system covering the ascent and earth atmospheric re-entry has been performed by ARMA Division of American Bosch Arma Corporation in accordance with the Martin requirements and system concept (see Ref. II-1). ARMA inertial components were used as a basis

~~CONFIDENTIAL~~

for gyro and accelerometer performance. The errors introduced by these components can be considered as representative of typical inertial components.

B. SUMMARY OF RESULTS

1. Ascent and Injection Navigation

Navigation during this phase employs inertial techniques only. At injection to translunar trajectory, the errors in the position and velocity data will be as follows:

- (1) Down-range component of position error (1.6 naut mi).
- (2) Cross-range component of position error (0.2 naut mi).
- (3) Vertical component of position error (0.2 naut mi).
- (4) Down-range component of velocity error (1.5 ft/sec).
- (5) Cross-range component of velocity error (1.1 ft/sec).
- (6) Vertical component of velocity error (7.9 ft/sec).

2. Earth Re-entry Navigation

The re-entry trajectory starts at an altitude of 400,000 ft and is terminated at an altitude approximating 80,000 ft. The vehicle is guided through re-entry inertially. Final errors in the inertial system arise from the following 3 categories:

- (1) Errors in the inertial components.
- (2) Errors in the stellar alignment of the platform prior to re-entry.
- (3) Errors in the initial position and velocity furnished by the mid-course navigation system.

The following tabular data summarizes the errors in position and velocity due to these 3 categories at the end of re-entry (80,000 ft altitude) based upon an 8200-naut mi range trajectory. The errors are given in a rectangular coordinate system aligned as follows:

x = Down-range at re-entry point

y = Cross-range at re-entry point

z = Vertical at re-entry point

~~CONFIDENTIAL~~

where the re-entry point is taken at an altitude of 400,000 ft.

	<u>Inertial Components</u>	<u>Inertial Platform Alignment</u>	<u>Initial Position and Velocity at Re-entry (400,000 ft)</u>
Error in x(mi)	1.6	0.9	3.5
Error in y (mi)	0.3	0.04	1.4
Error in z(mi)	0.6	0.3	0.86
Error in \dot{x} (ft/sec)	8.6	6.3	17.3
Error in \dot{y} (ft/sec)	6.4	1.1	11.4
Error in \dot{z} (ft/sec)	8.9	5.2	15.2

It is evident that initial position and velocity data obtained from the transearth navigation phase represents the predominant source of error.

The one-sigma position errors in the local vertical coordinate system at the end of re-entry (80,000 ft) are:

- (1) Down-range component 3.6 naut mi.
- (2) Cross-range component 1.41 naut mi.
- (3) Vertical component 2.0 naut mi.

3. Transearth Navigation

It is assumed that navigation during this phase employs telesextant and time measurements to determine the re-entry corridor and the initial conditions of position and velocity at re-entry. Further, assuming that observations are made between 99,000- and 40,000-naut mi, and that the final midcourse correction is applied to the vehicle at the latter position, the re-entry corridor error is better than 10 naut mi (3 sigma). For observations between 40,000 and 13,000 naut mi, the one-sigma error in re-entry initial conditions is:

- (1) Velocity (1.3 ft/sec).
- (2) Range Distance (0.75 naut mi).
- (3) Vertical Velocity (2.0 ft/sec).
- (4) Altitude (0.15 naut mi).

These values reflect the use of a radio altimeter for improving the accuracy of the initial conditions.

C. ANALYSIS OF THE INERTIALLY GUIDED PHASES

1. General Remarks

This section will discuss the performance expected during the inertially guided phases of a lunar mission. These phases have been chosen because they represent the most severe test of system performance. Said phases include:

- (1) Ascent and injection into translunar trajectory including:
 - (a) First powered boost to start-of-parking orbit.
 - (b) Parking orbit.
 - (c) Final thrust into translunar orbit.
- (2) Injection into lunar orbit.
- (3) Exit from lunar orbit.
- (4) Re-entry into earth's atmosphere.

In the following pages we shall present a quantitative analysis of expected inertial guidance accuracy during the ascent and re-entry phases. Since these phases have the most stringent performance requirements, it is felt that analysis of the injection and exit from lunar orbit are unnecessary at this time.

2. Performance Analysis Assumptions

For practical reasons, the performance analysis for any complicated system requires the introduction of many simplifying assumptions. However, in order to indicate the usefulness of the performance estimate, these assumptions must be described and justified. Therefore, the more important assumptions underlying this analysis will be discussed below.

a. Independence of error parameters

A basic assumption of this analysis is that the errors of each component of the inertial navigation system can be defined by a finite number of independent error parameters. As an example of such error parameters, we might look at a typical component such as an accelerometer. Some of the error parameters for an accelerometer are: the zero offset, the scale error and the non-linearity. Each one of these parameters is a constant that established the errors that will be produced by the accelerometer under various conditions. The assumption concerning the finite number and independence of these parameters has been justified on the basis of laboratory tests.

b. Magnitude of error parameters

It is assumed that, for a large sample, the various component errors will have a mean value of zero. This is justified on the basis that the component trimming procedures eliminate all systematic errors. Therefore, the specified component error parameter magnitude is the root mean square (RMS) of the random residual errors for a large sample. The random residual errors may represent random instabilities in the components or random errors in the trimming procedures.

c. Passive guidance system

For reasons of simplicity, the performance analysis was conducted under the assumption that the vehicle carried a perfect guidance system in addition to the real guidance system. It was assumed that the perfect guidance system controlled the vehicle's trajectory, while the real system merely reported its estimate of the vehicle's present velocity and position. The error of the navigation system was then defined to be the difference between the positions and velocities as reported by these 2 systems.

This conceptual situation eliminates the two-way coupling that exists between the trajectory and the component errors. This coupling arises from the fact that many of the navigation errors are functions of the components of the impressed acceleration profile. However, the assumption can be justified since the component errors for any reasonable inertial guidance system will be very small and, therefore, the resulting coupling will be extremely small.

d. Gravity feedback

The accelerations due to gravity are computed within the navigation system as a function of position, and algebraically added to the accelerometer outputs in order to solve the vehicle's equations of motion. This addition of gravity has an interesting effect on the propagation of errors. An inertial navigation error of almost any kind will eventually cause the computation of an erroneous component of gravitational acceleration which, in turn, influences the propagation of navigation errors. This effect of gravitational acceleration necessitates a direct simulation of the inertial system, including the effect of error parameters, to arrive at a valid accuracy analysis for extended time and pure inertial operation. For short time missions, or aided inertial systems, much simpler methods are applicable.

e. Addition of errors

It is assumed that the total RMS navigation error can be obtained by taking the square root of the sum of the square (RSS) of the individual RMS navigation errors at injection or at any other time. This assumption is justified on the basis that the individual component error parameters have zero mean. The relation between the magnitude of the error parameters and the magnitude of the navigation errors is essentially linear over the range of the error parameters. The assumptions concerning the mean value and independence of the various

~~CONFIDENTIAL~~

component errors are in close agreement with reality and justified elsewhere in this section. The assumption concerning the linear relationship between the magnitude of the error parameters and the resulting navigation errors cannot be justified mathematically for the case of the unaided inertial navigation system. However, it has been determined empirically that the relationship between the component parameters and the resulting navigation errors is approximately linear for the trajectories analyzed.

f. Statistical interpretation of errors

It is assumed that the total RMS navigation errors represent the standard deviation or one sigma value of a normal distribution with a zero mean. Since the individual distributions all have zero mean values the resulting normal distribution will also have a zero mean value.

3. Astro-Inertial Navigation System's Acceleration Errors

An inertial navigation system utilizes accelerometers to measure vehicular thrust acceleration information and processes this information in a computer, so as to solve the vehicle's equations of motion. Thus, the performance analysis for such a system can logically be divided into 2 separate parts. The first part concerns the navigation errors caused by errors in acceleration measurement, and the second part concerns the navigation errors caused by processing of that data in the digital computer. The data processing errors during inertial navigation have been evaluated (see Section 3. 2. 2 of Ref. II-1) and were found to be negligibly small. Therefore, the present system performance analysis is primarily concerned with the data measuring portion of the inertial navigation system.

The data measuring operation is accomplished by 3 single-degree-of-freedom accelerometers. In order to be compatible with the vehicular equations of motion that are solved by the airborne navigation computer, these accelerometers must provide data concerning the separate components of the vehicle's acceleration in an inertially fixed rectangular coordinate system. This is accomplished by mounting the accelerometers mutually perpendicular to each other on a platform that is gyro-stabilized to a known orientation in inertial space. Therefore, it can be seen that errors in the system's thrust acceleration data gathering are caused by accelerometer transducing errors and accelerometer orientation errors. The instantaneous magnitude of the thrust acceleration errors depends on the magnitudes of the performance parameters that describe the behavior of the inertial components, the time, and the vehicular acceleration profile.

4. Method of Performance Analysis Through Simulation

The performance analysis is carried out by a direct simulation of the inertial system including physical phenomena which give rise to component errors. Briefly stated these simulations are carried out as follows:

~~CONFIDENTIAL~~

- (1) The rectangular components of the vehicle thrust profile on the mission under investigation are fed to the computer. This simulates the ideal acceleration data as it would be measured by a perfect inertial platform.
- (2) The ideal acceleration data is subjected to a series of mathematical operations which simulate the manner in which the ideal data is modified by equipment errors.
- (3) The acceleration data, including the effects of equipment errors, is fed to a simulation of the airborne digital computer, which determines vehicle position and velocity, including the gravity feedback computation. The resulting position and velocity simulate the data which would be generated by an inertial system on the given trajectory with the assumed equipment performance data which has been fed to the computer.

In this study it was considered of interest to be able to separately examine the effects of individual component errors. To accomplish this, the following sequence was employed:

- (1) A simulated run was made assuming perfect hardware. The resulting position and velocity was considered standard trajectory data.
- (2) A series of simulated runs were made. On each run a single error source was given its actual specified value. All other error sources were assumed zero. This was done for each error source in the system.
- (3) The difference between standard trajectory position and velocity and the position and velocity data (from each of the runs with individual error sources) was determined vs time. These results give the time history of the errors in position and velocity for each individual error source.
- (4) The position and velocity errors from individual error sources were combined to give overall position and velocity errors vs time for the entire system.

The inertial system simulation described above (ARMA Program EA-9) solves the following equations:

Position and velocity are computed by

~~CONFIDENTIAL~~

$$X_c = \int \dot{X}_c dt + X_o + K_1$$

$$Y_c = \int \dot{Y}_c dt + Y_o + K_2$$

$$Z_c = \int \dot{Z}_c dt + Z_o + K_3$$

$$\dot{X}_c = \int \ddot{X}_c dt + \dot{X}_o + K_4$$

$$\dot{Y}_c = \int \ddot{Y}_c dt + \dot{Y}_o + K_5$$

$$\dot{Z}_c = \int \ddot{Z}_c dt + \dot{Z}_o + K_6$$

where

$$\ddot{X}_c = A \ddot{X}^* - G_o \frac{X_c}{R_c^3}$$

$$\ddot{Y}_c = A \ddot{Y}^* - G_o \frac{Y_c}{R_c^3}$$

$$\ddot{Z}_c = A \ddot{Z}^* - G_o \frac{Z_c}{R_c^3}$$

The above symbols are defined as:

X_c, Y_c, Z_c = Computed components of vehicular position.

$\dot{X}_c, \dot{Y}_c, \dot{Z}_c$ = Computed components of vehicular velocity.

$\ddot{X}_c, \ddot{Y}_c, \ddot{Z}_c$ = Computed components of total vehicular acceleration.

$A \ddot{X}^*, A \ddot{Y}^*, A \ddot{Z}^*$ = Components of vehicular thrust acceleration as given by the platform.

X_o, Y_o, Z_o = Components of the initial position.

K_1, K_2, K_3 = Errors in the components of the initial position.

$\dot{X}_o, \dot{Y}_o, \dot{Z}_o$ = Components of the initial velocity.

K_4, K_5, K_6 = Errors in the components of the initial velocity.

~~CONFIDENTIAL~~

The components of vehicular thrust acceleration as given by the platform are computed in accordance with the following formula:

$$A \ddot{X} = A X' + K_{10} + K_{11} A X' + K_{12} A X'^2 + K_{13} A X'^3 + K_{14} A X' A Y' \\ + K_{15} A X' A Z' + K_{16} A Y' A Z' + K_{17} A Z' + K_{18} A Y'$$

$$A \ddot{Y} = A Y' + K_{20} + K_{21} A Y' + K_{22} A Y'^2 + K_{23} A Y'^3 + K_{24} A X' A Y' \\ + K_{25} A X' A Z' + K_{26} A Y' A Z' + K_{27} A X' + K_{28} A Z'$$

$$A \ddot{Z} = A Z' + K_{30} + K_{31} A Z' + K_{32} A Z'^2 + K_{33} A Z'^3 + K_{34} A X' A Y' \\ + K_{35} A X' A Z' + K_{36} A Y' A Z' + K_{37} A X' + K_{38} A Y'$$

where:

$$A X' = A X + \theta_z A Y - \theta_y A Z$$

$$A Y' = -\theta_z A X + A Y + \theta_x A Z$$

$$A Z' = \theta_y A X - \theta_x A Y + A Z$$

and:

$$\theta_x = K_{40} + K_{41} t + K_{42} A X + K_{43} A Y + K_{44} A Z + K_{45} A X A Y \\ + K_{46} A X A Z + K_{47} A Y A Z + K_{48} \int A X dt + K_{49} \int A Y dt \\ + K_{50} \int A Z dt + K_{51} \int A X A Y dt + K_{52} \int A X A Z dt + K_{53} \int A Y A Z dt$$

$$\theta_y = K_{60} + K_{61} t + K_{62} A X + K_{63} A Y + K_{64} A Z + K_{65} A X A Y \\ + K_{66} A X A Z + K_{67} A Y A Z + K_{68} \int A X dt + K_{69} \int A Y dt \\ + K_{70} \int A Z dt + K_{71} \int A X A Y dt + K_{72} \int A X A Z dt + K_{73} \int A Y A Z dt$$

$$\begin{aligned}
\theta_z = & K_{80} + K_{81}t + K_{82}A_x + K_{83}A_y + K_{84}A_z + K_{85}A_xA_y \\
& + K_{86}A_xA_z + K_{87}A_yA_z + K_{88}\int A_x dt + K_{89}\int A_y dt \\
& + K_{90}\int A_z dt + K_{91}\int A_xA_y dt + K_{92}\int A_xA_z dt \\
& + K_{93}\int A_yA_z dt
\end{aligned}$$

The above symbols are defined as follows:

A_x^*, A_y^*, A_z^* = Rectangular components of vehicle's thrust acceleration as sensed by platform (including accelerometer errors and misalignment errors).

A_x', A_y', A_z' = Rectangular components of vehicle's thrust acceleration as seen by the accelerometers in a rotated (misoriented) coordinate system.

A_x, A_y, A_z = True rectangular components of vehicle's thrust acceleration.

e_x, e_y, e_z = Angular misorientation of accelerometer about the X, Y, Z axes of the navigational coordinate system.

$K_{10} \rightarrow K_{18}$ = Error parameters of the X axis accelerometer.

$K_{20} \rightarrow K_{28}$ = Error parameters of the Y axis accelerometer.

$K_{30} \rightarrow K_{38}$ = Error parameters of the Z axis accelerometer.

$K_{40} \rightarrow K_{53}$ = Error parameters that cause misalignment of the accelerometers about the X axis.

$K_{60} \rightarrow K_{73}$ = Error parameters that cause misalignment of the accelerometers about the Y axis.

$K_{80} \rightarrow K_{93}$ = Error parameters that cause misalignment of the accelerometers about the Z axis.

5. Discussion of Ascent and Re-Entry Trajectories Assumed for Performance Analysis. The performance of the Apollo Astro-Inertial Navigation System was analyzed for a typical Apollo lunar mission. The ascent portion of this trajectory was generated by "run 990 rerun 0" of ARMA'S Digital Computer Ascent Trajectory Program AS-3. This run utilized the thrust acceleration characteristics of the C-2 Saturn Booster with 2 hydrogen peroxide upper stages. The trajectory was shaped to provide injection into a circular parking orbit at an altitude of approximately 650,000 ft. The vehicle was then allowed to coast for approximately 63 min. The engines were then re-ignited to boost the vehicle into a lunar trajectory. The important characteristics of the ascent trajectory are summarized below:

Summary of Trajectory Conditions at
Injection Into Circular Parking Orbit

Time from launch	9.7 min
Inertial velocity	25,680 fps
Path angle	0°
Altitude	650,000 ft
Down-range distance over earth	1250 naut mi

Summary of Trajectory Conditions at
End of Circular Parking Orbit

Time from launch	73 min
Inertial velocity	25,680 fps
Path angle	0°
Altitude	650,000 ft
Down-range distance over earth	16,000 naut mi

Summary of Trajectory Conditions at
Injection into Lunar Orbit

Time for launch	75.8 min
Inertial velocity	36,030 fps
Path angle	+3°
Altitude	765,000 ft
Down-range distance over earth	16,915 naut mi

The rectangular components of the vehicle's thrust acceleration as a function of time are shown in Fig VII-1.

The atmospheric re-entry portion of the performance analysis trajectory was generated by "run 50 rerun 3" of ARMA's Digital Computer Re-entry Simulation Program RE-1. This run assumed the following vehicular parameters:

$$L/D = 0.5$$

$$W/CDA = 60 \text{ lb/sq ft}$$

The initial conditions for the re-entry trajectory were:

Inertial velocity	36,080 fps
Path angle	-8°
Altitude	400,000 ft

The altitude, velocity, distance traveled, and aerodynamic acceleration of the resulting trajectory as functions of time are shown in Fig VII-2, 3, 4 and 5.

6. Error Analysis Results

The performance of the proposed inertial navigation system has been analyzed for the ascent and re-entry phases of the lunar trajectory discussed in the previous section. ARMA's three-dimensional digital computer error analysis program EA-9 was utilized to determine the performance that would result from the recommended inertial navigation system. This program simulated the exact behavior of an unaided inertial navigation system with the performance parameters that have been specified. Twenty-four separate simulated error analyses trajectories were run to determine the effect that each individual type of performance parameter had on the system's performance during the

Apollo ascent trajectory. Each run assumed that the inertial navigation system was perfect with the exception of one type of error or performance parameter. Each of these runs was then compared to a standard or perfect trajectory in order to determine the navigation errors that result from that parameter. It was then assumed that the relationship between these performance parameters and the resulting navigation errors was approximately linear and that the overall RMS system error was obtained by taking the root sum square (RSS) of the individual navigation errors resulting from the RMS value of the individual error parameters.

Thirty separate simulated error analyses trajectories were run to determine the effect that the individual types of error parameters (24 runs) and initial condition errors (6 runs) had on the system's performance during the atmospheric re-entry trajectory. Once again, each run assumed that the inertial navigation system was perfect except for 1 type of system error. Each run was compared to a standard re-entry trajectory to determine the navigation errors resulting from that error parameter.

The numerical values of the individual performance parameters that were used for this analysis were obtained from the component data given in Section 4.2 of Ref. II-1, as modified by the assumed operating conditions (and count-down procedures). The numerical values for the actual constants (K's) used in each run of the EA-9 error analysis program were then obtained by taking the root sum square (RSS) of the RMS values of the functionally similar performance parameters. The assumed operating conditions and the numerical values of the constants (K's) used for each analysis run are given below.

Numerical values of EA-9 constants used for analysis of Inertial Navigation System on Apollo Ascent Trajectory follow:

Accelerometer zero offset (K10, K20, K30)	$4.3 \times 10^{-6} \text{G(RMS)}$
Accelerometer zero offset due to cross acceleration (K17, K27, K28, K37)	$6 \times 10^{-6} \text{G/CrG(RMS)}$
Accelerometer scale offset (K11, K31)	$6.1 \times 10^{-6} \text{G/G(RMS)}$
Accelerometer scale offset due to cross acceleration (K15, K35)	$1 \times 10^{-6} \text{G/G/CrG(RMS)}$
Accelerometer second order non-linearity (K12, K32)	$3 \times 10^{-6} \text{G/G}^2 \text{(RMS)}$
Accelerometer third order non-linearity (K13, K33)	$0.3 \times 10^{-6} \text{G/G}^3 \text{(RMS)}$

~~CONFIDENTIAL~~

Misorientation of accelerometers about the X axis (K_{40})	1.36×10^{-3} deg. (RMS)
Misorientation of accelerometers about the Y axis (K_{60})	1.36×10^{-3} deg. (RMS)
Misorientation of accelerometers about the Z axis (K_{80})	2.1×10^{-3} deg. (RMS)
Gyro drift rate due to spring torques (K_{41} , K_{61} , K_{81})	0.001°/hr (RMS)
Gyro drift rate due to mass unbalance of ball along spin axis (K_{48} and K_{90})	0.021°/hr/G (RMS)
Gyro drift rate due to mass unbalance of gimbal along spin axis (K_{48})	0.018°/hr/G (RMS)
Gyro drift rate due to mass unbalance of ball along outer wire axis (K_{68} and K_{70})	0.0135°/hr/G (RMS)

It should be noted that none of the remaining component performance parameters or EA-9 error analysis constants could cause navigation errors on the 2 dimensional trajectory analyzed. It should also be noted that many of performance parameters that were investigated above cause navigation errors that were completely negligible.

a. Ascent

The operating conditions that were assumed for the ascent trajectory analysis include:

- (1) Ground alignment of inertial platform with pendulums and an optical link.
- (2) Calibration of gyro spring torques and mass unbalance less than 48 hr before injection.
- (3) Calibration of accelerometer zero and scale less than 48 hr before injection.
- (4) Control of internal platform temperature to within 0.15°C (RMS).

~~CONFIDENTIAL~~

(5) Control of power supply frequency to within 1% (RMS).

The RMS navigation errors contributed by the critical system performance parameters, at lunar injection, are shown below:

Performance Parameters	sm	sm	sm	fps	fps	fps
	X	Y	Z	X	Y	Z
X Accelerometer zero offset (K_{10})	0.108		0.42	1.47		-1.11
X Accelerometer scale offset (K_{11})	0.22		0.42	2.45		-1.06
X Accelerometer second order non-linearity (K_{12})	0.23		0.43	2.55		-1.11
X Accelerometer third order non-linearity (K_{13})	0.07		0.13	0.745		-0.322
X Accelerometer zero offset due to Z acceleration (K_{17})	0.08		0.15	0.818		-0.385
Y Accelerometer zero offset (K_{20})		0.007			0.10	
Y Accelerometer zero offset due to X acceleration (K_{27})	0.15	0.02	0.29	1.68	0.079	-0.745
Z Accelerometer zero offset (K_{30})	-0.352		-0.358	-2.71		0.213
Misorientation about X axis (K_{40})		0.03	-0.05		-0.432	-0.066
Fixed drift rate about X axis (K_{41})	-0.15		-0.29	-1.676	-0.197	0.807
Drift rate due to gyro gimbal unbalance along spin axis (K_{48})	-0.28	-0.008	-0.48	-3.04	-0.68	0.94
Drift rate due to gyro ball unbalance along spin axis (K_{48} and K_{90})	-0.21	-0.11	-0.40	-2.587	-0.395	0.632
Misorientation about Y axis (K_{60})	-0.41		-0.55	-3.175		0.683
Misorientation about Z axis (K_{80})	0.15	-0.14	0.29	1.677	0.528	-0.745

The rms navigation errors for the overall astro-inertial navigation system, at lunar injection, are:

X Component of position error	0.778 stat mi
Y Component of position error	0.182 stat mi
Z Component of position error	1.285 stat mi
X Component of velocity error	7.51 fps
Y Component of velocity error	1.07 fps
Z Component of velocity error	2.72 fps

Plots of the overall system RMS navigation errors are shown as functions of time in Fig VII-6 and 7.

It should be noted that the rectangular components of the above navigational errors are completely dependent on each other in a statistical sense and must therefore be treated as such in any extension of the performance analysis. It may therefore be of interest to present the RMS navigation errors at lunar injection in terms of a local vertical coordinate system. The RMS navigation errors of the overall system in such a coordinate system are:

Down range component of position error	1.6 stat mi
Cross range component of position error	0.18 stat mi
Vertical component of position error	0.232 stat mi
Down range component of velocity error	1.52 fps
Cross range component of velocity error	1.07 fps
Vertical component of velocity error	7.91 fps

b. Re-entry

Let us next consider the results of the performance analysis for the atmospheric re-entry portion of the mission. The numerical values of the constants used for analysis of the inertial navigation system on the Apollo re-entry trajectory were:

Accelerometer zero offset (K_{10}, K_{20}, K_{30})	4.3×10^{-6} G (RMS)
Accelerometer zero offset due to cross acceleration ($K_{17}, K_{27}, K_{28}, K_{37}$)	6×10^{-6} G/CrG (RMS)
Accelerometer scale offset (K_{11}, K_{31})	6.8×10^{-6} G/G (RMS)

Accelerometer scale offset due to cross acceleration (K_{15} , K_{35})	$1 \times 10^{-6} \text{G/G/CrG (RMS)}$
Accelerometer second order non-linearity	$3 \times 10^{-6} \text{G/G}^2 \text{ (RMS)}$
Accelerometer third order non-linearity	$0.3 \times 10^{-6} \text{G/G}^3 \text{ (RMS)}$
Misorientation of accelerometers about X, Y and Z axis (K_{10} , K_{20} , K_{30})	$2.1 \times 10^{-3} \text{ deg (RMS)}$
Gyro drift rate due to spring torques (K_{41} , K_{61} , K_{81})	0.001/hr (RMS)
Gyro drift rate due to mass unbalance of ball along spin axis (K_{48} and K_{90})	$0.15^\circ/\text{hr/G (RMS)}$
Gyro drift rate due to mass unbalance of gimbal along spin axis (K_{48})	$0.018^\circ/\text{hr/G (RMS)}$
Gyro drift rate due to mass unbalance of ball along outer wire axis (K_{68} & K_{70})	$0.051^\circ/\text{hr/G (RMS)}$
X-Component of initial position error (K_1)	0.8 stat mi (RMS)
Y-Component of initial position error (K_2)	1.15 stat mi (RMS)
Z-Component of initial position error (K_3)	0.17 stat mi (RMS)
X-Component of initial velocity error (K_4)	1.3 fps (RMS)
Y-Component of initial velocity error (K_5)	12.0 fps (RMS)
Z-Component of initial velocity error (K_6)	2.0 fps (RMS)

The operating conditions that were assumed for the above analysis include:

- (1) In-flight alignment of the inertial platform with the stellar alignment nulling device prior to re-entry.
- (2) Calibration of gyro spring torques and accelerometer zero within 48 hr of re-entry.

~~CONFIDENTIAL~~

- (3) Calibration of gyro mass unbalances and accelerometer scale within 30 days of re-entry.
- (4) Control of internal platform temperature to within 0.15°C (RMS).
- (5) Control of power supply frequency to within 1% (RMS).
- (6) Determination of initial conditions (except for Z component of position and velocity) by use of midcourse navigation technique aided by radio altimeter data.
- (7) Determination of Z component of initial position and velocity by use of a radar altimeter.

The RMS navigation errors contributed by the critical system performance parameters at the termination of the Apollo re-entry trajectory (80,000 ft altitude) are shown below:

Performance Parameters	mi X	mi Y	mi Z	Ft/Sec X	Ft/Sec Y	Ft/Sec Z
X Component of initial position error (K1)	-2.352	0	-0.736	-10.35	0	-9.69
Y Component of initial position error (K2)	0	0.989	0	-0.0046	2.9325	0.0046
Z Component of initial position error (K3)	-1.4382	0	-0.1343	-8.1131	0	7.21
X Component of initial velocity error (K4)	-1.573	0	0.08	-9.686	0	6.896
Y Component of initial velocity error (K5)	0	-0.96	0	0	11.064	0
Z Component of initial velocity error (K6)	-1.26	0	-0.42	-5.482	0	6.254
X Accelerometer zero offset (K10)	-0.14	0	0.02	-0.837	0	0.642
X Accelerometer scale offset (K11)	0.078	0	0	0.395	0	-0.362
X Accelerometer second order nonlinearity (K12)	-0.24	0	0.01	-1.429	0	1.056

~~CONFIDENTIAL~~

Performance Parameters	mi X	mi Y	mi Z	Ft/Sec X	Ft/Sec Y	Ft/Sec Z
X Accelerometer third order nonlinearity (K13)	0.17	0	-0.01	1.043	0	-0.738
X Accelerometer zero offset due to Z acceleration (K17)	-0.05	0	0	-0.196	0	0.265
Y Accelerometer zero offset (K20)	0	-0.04	0	0.002	-0.044	0.002
Y Accelerometer zero offset due to acceleration (K27)	0.54	0	-0.25	3.586	-0.180	-3.070
Z Accelerometer zero offset (K30)	-0.02	0	-0.05	0.070	0	-0.105
Misorientation about X axis (K40)	0.62	-0.04	-0.22	3.952	-0.123	-2.758
Fixed drift rate about X axis (K41)	0.54	-0.01	-0.26	3.059	-0.088	-3.085
Drift rate due to gyro gimbal unbalance along spin axis (K48)	0.70	0.01	-0.30	3.247	-0.050	-4.112
Drift rate due to gyro ball unbalance along spin axis (K48 and K90)	0.47	0.28	-0.23	2.969	6.390	-2.298
Misorientation about Y axis (K60)	0.52	0	0.02	3.247	0	-3.142
Misorientation about Z axis (K80)	0.54	0	-0.25	3.586	1.099	-3.070

The overall terminal error can be attributed to the following 3 categories:

- (1) Errors in inertial component.
- (2) Errors in stellar alignment of platform prior to re-entry.
- (3) Errors in initial position and velocity furnished by midcourse navigation method.

Each of these categories is summarized below.

The RMS terminal navigation errors due to the performance parameters of the inertial navigation system's inertial components were:

X Component of terminal position error	1.59 stat mi
Y Component of terminal position error	0.28 stat mi
Z Component of terminal position error	0.62 stat mi
X Component of terminal velocity error	8.55 f p s
Y Component of terminal velocity error	6.40 f p s
Z Component of terminal velocity error	8.92 f p s

The RMS terminal navigation errors due to the initial orientation errors of the inflight stellar alignment system were:

X Component of terminal position error	0.97 stat mi
Y Component of terminal position error	0.04 stat mi
Z Component of terminal position error	0.33 stat mi
X Component of terminal velocity error	6.25 f p s
Y Component of terminal velocity error	1.11 f p s
Z Component of terminal velocity error	5.19 f p s

The RMS terminal navigation errors due to errors in the initial position and velocity data furnished by the midcourse navigation method were:

X Component of terminal position error	3.45 stat mi
Y Component of terminal position error	1.37 stat mi
Z Component of terminal position error	0.86 stat mi
X Component of terminal position error	17.3 f p s
Y Component of terminal position error	11.43 f p s
Z Component of terminal position error	15.2 f p s

Finally, the RMS terminal navigation errors for the overall navigation system were:

X Component of terminal position error	3.95 stat mi
Y Component of terminal position error	1.41 stat mi
Z Component of terminal position error	1.11 stat mi
X Component of terminal position error	20.3 f p s
Y Component of terminal position error	13.16 f p s
Z Component of terminal velocity error	18.3 f p s

It should be noted that the various navigation errors resulting from any one performance parameter are completely dependent on one another in a statistical sense, and must be treated as such in any extension of the performance analysis. It may therefore be of interest to present the components of the navigation errors, at re-entry termination, in terms of a local vertical coordinate system. The terminal RMS errors of the overall navigation system, in such a coordinate system are:

Downrange component of terminal position error	3.58 stat mi
Cross range component of terminal position error	1.41 stat mi
Vertical component of terminal position errors	2.00 stat mi
Downrange component of terminal velocity error	27.3 f p s
Cross range component of terminal velocity error	13.16 f p s
Vertical component of terminal velocity error	1.5 f p s

It is interesting to note that the terminal navigation errors contributed by the system's erroneous initial position and velocity conditions represent the predominant errors. Therefore, it can be concluded that terminal accuracy of the proposed inertial navigation system is primarily limited by the assumed accuracy of the midcourse navigation system.

D. ERROR ANALYSIS OF MIDCOURSE NAVIGATION SYSTEM

1. Introduction

The most critical phase of midcourse navigation from the standpoint of accuracy is that of transearth. This is due to the stringent requirements of:

- (1) Delivering the space vehicle to a re-entry corridor which will permit atmospheric re-entry without exceeding the constraints of heat rate, total heat, load limits and the apogee of the subsequent skip.

~~CONFIDENTIAL~~

- (2) Establishing the initial conditions of velocity and position of the inertial system at the start of atmospheric re-entry so as to assure the desired landing point accuracy. In view of this, the error analysis has been performed for the final region of the transearth trajectory prior to atmospheric re-entry.

The technique of computation for midcourse navigation has been described in Section II-B2-f. This technique will accept various types of measured data and compute the space vehicle trajectory, utilizing redundant data in a least squares routine to minimize the trajectory errors resulting from errors in measurement. Due to the complexity of the computation of the described technique, a full scale digital computer program is required to obtain the final error analysis. Since only a limited time is available for this study, such a simulation was not available but will be performed in the next phase of the program. However, by making simplifying assumptions, a preliminary error analysis has been performed which should closely approximate the final simulation.

In the described technique, a minimum of six independent pieces of information and the corresponding time are required to determine the trajectory. For the purpose of this analysis, the source of information will be confined to:

- (1) Sextant observations, the measurement of the angle between a landmark (on the earth or moon) and a known star.
- (2) Stadia observations, the measurement of the included angle of the earth disc with the telesextant from which the absolute value of range between the vehicle and earth (or moon) can be computed.

Each sextant and stadia observation represents an independent piece of information so that various combinations of 6 of these readings will constitute sufficient, though minimum, data to permit computation of the trajectory. For the moment, only the case of the minimum 6 independent pieces of information (observations) will be considered. An important consideration is the method of grouping the 6 observations and their location along the trajectory. Some characteristic combinations of groups are as follows:

- (1) A pair of sextant observations taken simultaneously between a common landmark and two known stars describes a line in space. Thus the 6 sextant observations can be separated into 3 groups of 2 sextant observations.
- (2) Two sextant observations between a common landmark and two known stars plus a third sextant reading on a second landmark describes a vector in space. For this condition, the 6 observations can be separated into two groups of 3 observations.

~~CONFIDENTIAL~~

When the space vehicle is close to the earth (or moon), all observations will be taken on the common body. In the middle region between the earth and moon, the 3 observations are distributed between the two bodies.

- (3) Similarly, two sextant observations between a common landmark and two known stars plus a stadia observation describes a vector in space. The 6 observations can be separated into two groups consisting of 2 sextant and 1 stadia observation.

The number and grouping of observations cited above represents the minimum number of observations which will provide a solution to the trajectory equations. There are families of solutions, however, so that additional observations will be required to resolve the ambiguity and uniquely determine the particular solution. In as much as there will generally be wide spacing between these solutions, the accuracy and redundancy of these additional observations are not critical. In general, the optimum grouping and redundancy of all observations which yield the greatest accuracy will be determined from an overall digital simulation study.

As the spacing between each group of observations is increased, there is a reduction in the trajectory errors resulting from equipment and landmark errors. In as much as only a finite time and distance along the trajectory is available, it becomes desirable to reduce the number of groupings in order to permit wider spacing between the groups. The relative advantages of these methods of groupings becomes a matter of comparing total errors for each case, taking into account the relative effect of error partial variations and equipment and landmark accuracies.

In order to reduce the magnitude of random errors, redundant observations will be taken for each of the 6 independent pieces of information, the method of obtaining the best least squares solutions with this data being described in Section II-B2-f. For purposes of this error analysis, the observations within a group are considered to be taken at one instant of time so that the position distribution reduces to a point. In actual practice, the observations will be distributed in time and position due to the time required to take observations in a moving vehicle. The methodology of the described computational technique takes this distribution into account.

It has been indicated that 3 groups of 2 telesextant observations will yield sufficient information to determine the trajectory for the three dimensional case. For the coplanar assumption to be used in the analysis (i. e. the landmark lies in the trajectory plane), 4 groups of single sextant observations are required to determine the trajectory. The remaining two observations, as needed to satisfy the required number of 6 independent pieces of information, determines the trajectory plane orientation in space. Although the error analysis is performed for 4 points along the trajectory, due to the coplanar

~~CONFIDENTIAL~~

assumption, this will reduce to 3 points in actual practice in as much as landmarks which lie outside of the trajectory plane can be selected.

2. Analysis

The assumptions made as to the characteristics of the trajectory are:

- (1) The representation is that of a limited two body problem with the earth as the central force.
- (2) The trajectory is considered to be parabolic for ranges less than 45,000 naut mi, and all error coefficients are determined on this basis. In as much as the actual trajectory has an eccentricity of the order of 0.97, this assumption is reasonable.
- (3) The trajectory parameters are: p (semi-latus rectum), e (eccentricity), T (perigee time) and ζ (angle between an inertial reference and the major axis of the trajectory). The system parameters, however (which are of greater significance in the error analysis), are altitude, velocity, flight path angle, and range distance at the nominal re-entry altitude of 400,000 ft, (these system parameters being computed from the trajectory parameters). In computing the error partials, these system parameters will be computed, for convenience, at perigee. The discrepancy between the error partials, determined at perigee and at an altitude of 400,000 ft, is not excessive.
- (4) All landmarks are assumed to lie in the trajectory plane. This will reduce the analysis to that of a coplanar problem.

When taking sextant readings on landmarks in order to compute the local vertical and absolute range, there exist many combinations of locations of landmarks and stars which will affect the overall accuracy. For the purpose of this analysis, the following assumptions are made:

- (1) The sextant observations will measure the angle between the reference star and an earth landmark. It is assumed that both the star and the earth landmark lie in the trajectory plane with the landmark being located along the local vertical between the vehicle and the earth mass center. Thus the sextant observation will be a measure of the angle Θ indicated in Fig. VII-8, the indicates inertial reference being determined by the direction of the known star.
- (2) Range will be obtained both from stadia and sextant observations. The former is the poorer of the two due to uncertainties in the edge of the earth disc. Range is derived from sextant observations of a pair of earth landmarks with respect to a

~~CONFIDENTIAL~~

known star. The error in range determination is a minimum when the landmarks lie in the vicinity of the diametrically opposite edges of the viewed earth disc, and approaches infinity as the landmarks approach the local vertical between the vehicle and the earth mass center. It will be assumed that the landmarks are symmetrically located at 45° from the local vertical.

The above assumptions will apply to ranges from the earth, which are approximately less than 45,000 naut mi. For ranges greater than this value, sextant observations will be taken on both earth and lunar landmarks with the assumption that the landmarks lie along the geocentric and selenocentric local verticals. Knowing the ephemeris of the moon, there is sufficient information to specify the vehicle position by triangulation.

Two cases for the determination of the trajectory will be considered:

Case I: Sextant observations and time measurements will be made at 4 points along the trajectory. This is equivalent to measuring the local vertical with respect to an inertial reference at 4 trajectory points.

Case II: Sextant and stadia observations and time measurements will be made at 2 points along the trajectory. The alternate method of determining range by sextant observations on 2 landmarks will be evaluated. This is equivalent to measuring the range vector at 2 trajectory points.

The 4 points and 2 points respectively cited above represent the minimum number of readings required to describe the trajectory. Aside from the obvious approach of reducing the equipment errors, the system error can be reduced by:

- (1) Taking additional observations in the vicinity of each point. Assuming that the errors are random and uncorrelated but with the same standard deviation, there will be a decrease in the standard deviation by $1/\sqrt{k}$ if k observational readings are taken at each point along the trajectory.
- (2) Increasing the spacing between the points. Increasing the spacing will reduce the error partials and thus the effect of errors, both random and systematic, on the system parameters.

The error partials for Cases I and II are developed in Appendix D. The errors considered are:

- (1) dr_p : Radius error at perigee.

- (2) dV_p : Velocity error at perigee.
- (3) $dV_{zp} = V_p d\gamma_p$: Vertical component of velocity error at perigee where V_p is velocity at perigee and $d\gamma_p$ is the flight path angle error at perigee.
- (4) $dx_p = r_p d\theta_p$: Range error at perigee where r_p is the perigee radius and $d\theta_p$ is the range angle error at perigee.

It is assumed that all errors are random and uncorrelated. For Case I, the error can be characteristically expressed as follows:

$$dr_p = \sqrt{\frac{1}{k} \left(\frac{\partial r_p}{\partial \theta} d\theta \right)^2 + \frac{1}{k} \left(\frac{\partial r_p}{\partial l} dl \right)^2}$$

where:

$d\theta$ is the mean deviation of the sextant error.

dl is the mean deviation of the earth landmark error.

$\frac{\partial r_p}{\partial \theta}$ is the RMS value of the error partials and equal to

$$\sqrt{\sum_{n=1}^k \left(\frac{\partial r_p}{\partial \theta_n} \right)^2}$$

$\frac{\partial r_p}{\partial l}$ is the RMS value of the error partials and equal to

$$\sqrt{\sum_{n=1}^k \left(\frac{\partial r_p}{\partial l_n} \right)^2}$$

k is the number of redundant readings at each point.

The errors dV_p , dV_{zp} and dX_p are similarly defined. For Case II, the error partials can be characteristically expressed as follows:

$$dr_p = \sqrt{\frac{1}{K} \left\{ \left(\frac{\partial r_p}{\partial \theta_1} d\theta_1 \right)^2 + \left(\frac{\partial r_p}{\partial \theta_2} d\theta_2 \right)^2 + \left(\frac{\partial r_p}{\partial r_1} dr_1 \right)^2 + \left(\frac{\partial r_p}{\partial r_2} dr_2 \right)^2 \right\}}$$

where $d\theta_1$, $d\theta_2$ is the mean deviation of the total error at the subscript point including the effect of sextant and landmark errors.

dr_1 , dr_2 is the mean deviation of the total error in range at the subscript point including the effect of sextant and landmark errors.

The error partials apply to the subscript point.

The errors dV_p , dV_{zp} and dX_p are similarly defined.

3. Measurement and Landmark Errors

The assumptions made relative to the sources of errors are:

- (1) The time measurements are considered to be ideal.
- (2) The telesextant errors are considered to be random with a standard deviation of 5 arc seconds (2.4×10^{-5} radians). The bias and scale factor errors of the sextants can be accounted for by inflight calibration of the instrument using pairs of known stars as a reference.
- (3) The landmark error is 0.2 naut mi and the earth disc error is 2 naut mi. The latter number is used for stadia observations.

The range and local vertical errors to be used for Case II are plotted in Figs. VII-9, -10, -11, -12. The error equations for range obtained by stadia and sextant observations are shown in Figs. VII-10 and VII-11. When range is obtained by sextant observations solely on earth landmarks, it is assumed that the landmarks are located symmetrically at 45° to the instantaneous local vertical. For ranges greater than 45,000 naut mi, the method of triangulation as indicated in Fig. VII-12 is employed. The errors arising from triangulation are a strong function of the trajectory. As the vehicle approaches the earth-moon line,

there is a marked increase in range error due to the fact that the included angle between the line of sight between the vehicle and the earth and lunar landmarks approaches 180°. The error curve indicated in Fig VII-9 was computed, based on a typical 3-1/2 day trajectory.

4. Results

There are two requirements that must be met. First, the re-entry corridor tolerance must be realized, and the initial conditions at re-entry must be commensurate with the required landing point accuracy. Furthermore, it is desirable to make the final trajectory corrections as far from the re-entry corridor as feasible in order to conserve propulsion fuel. Once a correction impulse is applied to the space vehicle, all past observations are lost and the trajectory determination procedure will have to be initiated again. In view of these considerations, the sequence of operation will be as follows:

- (1) Observations will be made over the interval starting at 100,000 naut mi and terminating at about 40,000 naut mi in order to determine the trajectory and compute velocity corrections. The final trajectory correction to assure the re-entry corridor tolerance will be made at the latter range.
- (2) In order to establish the re-entry initial conditions, observations will be initiated after the final trajectory correction has been made and will continue as long as feasible.

a. Re-entry corridor

For Case II, the re-entry corridor errors were determined with the initial observation point at 99,000 naut mi (20 hr from perigee) and the final observation point at 40,260 naut mi (5 hr from perigee). Due to the long ranges considered here, the assumption of a parabolic trajectory was not valid and the exact form of the error equations (i. e., eccentricity less than unity) cited in Appendix D was used. The one sigma vacuum perigee error can be expressed as follows:

$$d\mathcal{R}_p = \sqrt{\begin{matrix} (d\theta_1 0.33 \times 10^5)^2 + (d\theta_2 0.33 \times 10^5)^2 \\ (d\mathcal{R}_1 0.040)^2 + (d\mathcal{R}_2 0.22)^2 \end{matrix}}$$

Employing the errors for $d\theta_n$ and dr_n using sextant observations and triangulation for the corresponding range from Fig. VII-9, the vacuum perigee is 3 naut mi. The 3 sigma re-entry corridor is 18 naut mi. Assuming that 9 observations are taken at each point and that the errors are random, the 3 sigma re-entry corridor is 6 naut mi. The largest contributor to this error is the range term $\frac{\partial r_p}{\partial r_2} dr_2$ at 40,260 naut mi. This is due to the magnitude of the error

partial and the large error in range derived from sextant observations as can be seen in Fig. VII-9. When employing stadia observations at the 40,260 naut mi point, the 3 sigma re-entry corridor is 8 naut mi.

b. Re-entry initial conditions

For Case I, two conditions were investigated corresponding to different spacing between the four adjacent points. All observations were initiated at a range of 45,000 naut mi. The error partials are tabulated in Table VIII-1, -2. As was anticipated, an increase in the spacing between adjacent points reduced the magnitude of the error partials. The condition of maximum spacing will be further considered.

For Case II, a number of conditions were investigated corresponding to various spacing between the 2 observation points. The first point (r_1) was taken at 40,000 naut mi and the last point (r_2) over a range from 33,400 naut mi to 13,000 naut mi. The trend is indicated in Fig. VII-13 for the $\partial p/\partial e$ and $\partial p/\partial \lambda$. As the ratio between the initial and last point increases, corresponding to an increase in spacing, $\partial p/\partial e$ decreases, $\partial p/\partial r_1$ decreases and the $\partial p/\partial r_2$ increases. The net effect on perigee altitude and velocity is to decrease these values as the ratio r_1/r_2 increases. The condition of maximum spacing will be further considered, the error partials being tabulated in Table VII-2.

Using the assumed telesextant and landmark errors and error data from Fig. VII-9, the one sigma errors can be summarized as follows:

$$\begin{aligned} \text{Case I: } dr_p &= 3.1 \text{ naut mi} \\ dV_p &= 14.5 \text{ ft/sec} \\ dV_{zp} &= 89 \text{ ft/sec} \\ dX_p &= 17.6 \text{ naut mi} \end{aligned}$$

TABLE VII-1

Error Partial for Case I

Range (nm)	Time (hr)	$\frac{\partial \Delta P}{\partial \epsilon}$ nm/rad	$\frac{\partial V_p}{\partial \theta}$ ft/sec rad	$\frac{\partial V_p}{\partial l}$ ft/sec nm	$\frac{\partial V_{ip}}{\partial \theta}$ ft/sec rad	$\frac{\partial V_{ip}}{\partial l}$ ft/sec nm	$\frac{\partial X_p}{\partial \theta}$ nm/rad.	$\frac{\partial X_p}{\partial l}$ nm/nm	
45,000	6.0								
25,980	2.7	1.14×10^5	5.3×10^5	29	34×10^5	135	6.7×10^5	27	
15,000	1.2								
8,600	0.6								
<hr/>									
45,000	6.0								
37,500	4.5	6.1×10^5	30.5×10^5	90					
25,980	2.7								
15,000	1.2								

All error partials are RMS values - ex. $\left(\frac{\partial \Delta P}{\partial \theta} = \sqrt{\sum_{n=1}^4 \left(\frac{\partial \Delta P}{\partial \theta_n} \right)^2} \right)$

TABLE VII-2

Range (nm)	Time (hrs)	Error Partial for Case II							
		$\frac{\partial R_p}{\partial \theta_n}$ nm/rad	$\frac{\partial R_p}{\partial h_n}$ nm/nm	$\frac{\partial V_p}{\partial \theta_n}$ ft/sec rad.	$\frac{\partial V_p}{\partial h_n}$ ft/sec nm	$\frac{\partial V_{2p}}{\partial \theta_n}$ ft/sec rad	$\frac{\partial V_{2p}}{\partial h_n}$ ft/sec nm	$\frac{\partial X_p}{\partial \theta_n}$ nm/rad	$\frac{\partial X_p}{\partial h_n}$ nm/nm
40,262	5.0	0.13×10^5	0.150	0.65×10^5	0.75	0.48×10^5	4.0	17,000	0.80
13,539	1.07	0.13×10^5	0.420	0.65×10^5	2.10	0.24×10^5	15.0	9500	2.70

Case II: (Stadia observations for range)

$$d r_p = 3.4 \text{ naut mi}$$

$$d V_p = 16.5 \text{ ft/sec}$$

$$d V_{zp} = 100 \text{ ft/sec}$$

$$d X_p = 18 \text{ naut mi}$$

Case II: (Sextant observations for range)

$$d r_p = 1.6 \text{ naut mi}$$

$$d V_p = 8.0 \text{ ft/sec}$$

$$d V_{zp} = 54 \text{ ft/sec}$$

$$d X_p = 10 \text{ naut mi}$$

The propagation coefficients relating the initial conditions at re-entry and the landing point accuracy for a typical 8200 naut mi re-entry trajectory are as follows:

$$\frac{\partial X_L}{\partial r_p} = 8.5 \text{ naut mi/naut mi}$$

$$\frac{\partial X_L}{\partial V_p} = 1.2 \text{ naut mi/ft/sec}$$

$$\frac{\partial X_L}{\partial V_{zp}} = 0.7 \text{ naut mi/ft/sec}$$

$$\frac{\partial X_L}{\partial X_p} = 2.95 \text{ naut mi/naut mi}$$

Assuming that nine redundant observations are made at each point (i. e. $k = 9$), the errors for Case II become:

$$d r_p = 0.6 \text{ naut mi}$$

$$\begin{aligned} dV_p &= 2.6 \text{ ft/sec} \\ dV_{zp} &= 18 \text{ ft/sec} \\ dX_p &= 3.3 \text{ naut mi} \end{aligned}$$

The landing point errors will be:

$$\begin{aligned} dX_L \text{ (due to } dr_p) &= 5.1 \text{ naut mi} \\ dX_L \text{ (due to } dV_p) &= 3.2 \text{ naut mi} \\ dX_L \text{ (due to } dV_{zp}) &= 12.6 \text{ naut mi} \\ dX_L \text{ (due to } dX_p) &= 9.7 \text{ naut mi} \end{aligned}$$

The errors in initial conditions are excessive so that alternate methods will be required. The errors in altitude (dr_p) and altitude rate (dV_{zp}) will be reduced by the use of an on-board radio altimeter, the accuracy of the latter being 0.15 naut mi and 2 ft/second respectively.

In the vicinity of re-entry, the error in altitude rate (dV_{zp}) is primarily a function of dT and the error in range (dX_p) is primarily a function of dT and $d\delta$. The error term dT is the stronger function of the two accounting for over 80% of the total error. When the radio altimeter is used, the error in altitude rate is reduced by a factor of 9 from 18 ft/sec to 2 ft/sec. Inasmuch as dV_{zp} and dX_p are strong functions of the same error, dT , it is possible to account for much of the range error. Based upon this approach, the range error will be reduced from 3.3 to 0.75 naut mi as altimeter data becomes available to update altitude rate. Similarly, the velocity error dV_p can be reduced from 2.6 to 1.3 ft/sec by use of radio altimeter data. These initial conditions are employed in Section VII-C to determine the detail terminal accuracy.

5. Conclusions

The achieving of a 3 sigma re-entry corridor of 10 naut mi or better, raises no real problems. The initial conditions, however, obtained from this phase of flight represents the largest contributor to the error in landing point. For the long range of re-entry flight of 8200 naut mi, and initial condition of $dr_p = 0.15$ naut mi, $dV_{zp} = 2$ ft/sec., $dV_p = 1.3$ ft/sec and $dX_p = 0.75$ naut mi, the landing point accuracy is 3.6 naut mi in range and 1.4 naut mi in cross range. For short re-entry ranges, the landing point accuracy will be reduced to about 2 naut mi one sigma.

~~CONFIDENTIAL~~

By optimizing the location and spacing of the observation points and the smoothing of data by the use of redundant observations, the accuracy of the initial conditions can be improved.

~~CONFIDENTIAL~~

~~CONFIDENTIAL~~

VIII VENDOR STUDIES

A. METHOD OF APPROACH

It was recognized in the beginning of the study that The Martin Company is not in the inertial or astro-inertial guidance business and would, therefore, require assistance from established firms in these fields. This is not to say that Martin is uninformed on this subject. Studies dating back to early 1952 have included inertial systems for Matador, a fighter-bomber, a tactical bomber, Hounddog, Skybolt, medium range ballistic missiles, Titan, Minuteman and various space guidance studies. In addition, Martin is producing inertially guided Mace, Titan and Pershing missiles.

This study concentrated on companies that have produced satisfactory hardware in the fields of inertial guidance, astro-trackers and digital computers, on the assumption that companies who had exhibited a good background in the field could repeat their performance on Apollo. A number of companies with promising development programs was eliminated because we believe that their developments will not be ready in time for Apollo.

We decided that we would ask vendor assistance in two areas--systems and components. Inertial system companies were asked to study hardware requirements, GSE requirements, subsystem tie-in, performance, and the like. Component companies were asked to define the characteristics and limitations of the various subsystems in a space guidance system.

B. SYSTEM VENDORS CONTACTED

Accordingly, the following companies were contacted, regarding the guidance system:

- (1) Autonetics
- (2) AC Spark Plug
- (3) Arma
- (4) Bendix (Eclipse-Pioneer Division)
- (5) GPI (Kearfott Division)
- (6) Litton
- (7) Minneapolis-Honeywell
- (8) Nortronics
- (9) Sperry

Preliminary proposals were sought from these companies early in the Apollo study. AC Spark Plug and Nortronics indicated previous commitments

~~CONFIDENTIAL~~

and Litton did not respond. The other companies verbally presented their capabilities as well as their studies to date on guidance systems for the Apollo vehicle in mid-December 1960.

C. COMPARISON OF SYSTEM VENDORS

The comparison of the qualifications of these companies is shown in Table VIII-1. They were rated at the time as follows in order of preference:

Autonetics. This company has long been in the field of astro-inertial systems as well as pure inertial systems. No company has developed as many different systems or has the production capacity of Autonetics. In addition, it was apparent that Autonetics had studied the specific requirements and had a solution to the Apollo guidance problem. Autonetics also displayed some background in the re-entry field from Dyna-Soar work with another prime contractor.

Arma. This firm's detailed knowledge of the guidance problems of ascent and the lunar mission re-entry is based on JPL and Dyna-Soar studies. Although an overall mission study had not been considered, the analysis capability was apparent from the Arma presentation. The background in the inertial guidance system for Atlas also was taken into consideration.

Sperry. This company exhibited its latest work in components: fluid sphere gyro, 3-axes integrating accelerometer and "exotic" star tracker. Sperry showed a thorough knowledge of man's capability in the guidance loop, based on extensive studies.

Minneapolis-Honeywell. This company discussed gyros which were sufficiently accurate to eliminate star trackers. These were of the exotic type-- electrostatic suspension. Some of the techniques and equipment required for the Apollo mission had been studied.

GPI (Kearfott). Indicated a knowledge of the Apollo mission, but except for advanced developments, such as solid-state photo-detectors, their solutions were routine.

Bendix (Eclipse-Pioneer). The system capability presented involved present Pershing work; that is, air-bearing gyros. Their approach in gyro suspension involves forced air suspension of the output axis of the gyro. This calls for a considerable air supply for long-term operation or a closed cycle operation. An advanced sun tracker was also presented. This unit contained no moving parts and has a tracking accuracy of about 7 minutes of arc. Their appreciation of the overall Apollo guidance problem was lacking and the impression was that little space guidance work had been done. However, in the field of human factors and displays for space vehicles, a considerable amount of study had been made.

In evaluating these companies we felt that Autonetics and Arma were equally capable. Autonetics was strong in number of systems developed, hardware

~~CONFIDENTIAL~~

TABLE VIII-1

Apollo Guidance System Vendor Comparison

Company	Inertial Guidance Background	Digital Computer Background	Optical Background	Manned Systems	Space Guidance Studies	Unique Concepts & Components
Minneapolis-Honeywell	ISIP (exp), MIG platform, ASROC, miniature platform design	Limited	Star tracker & horizon scanner designs	Numerous aircraft auto-pilots	SR-183 lunar observatory (G & C) Dyna-Soar (Martin)	Electrostatic gyro eliminates star tracker requirement
Arma	Titan and later Atlas inertial guidance system	Atlas guidance system digital computer (prod)	Stellar-inertial for mobile Atlas (des)	Simulation studies for space guidance	Space guidance--simulation programs	Gravity gradient, vibrating string accelerometer
Sperry	X-15, B-58, Sergeant, SINS, miniature celestial inertial system (des)	Limited	Star trackers (dev)	Numerous aircraft autopilots and simulation studies for space guidance	Several space guidance studies	3-axes integrating accelerometer (dev), fluid sphere gyro (dev)
GPI	Several exp systems, SUBROC	ASROC, SUBROC, Centaur	Solid-state star tracker (dev), sun tracker (dev)	Numerous simulators from Link Aviation	SLOMAR (Martin-Denver)	Solid-state tracker (dev)
Bendix (Eclipse-Pioneer)	Pershing (prod), miniature platform (des)	Company sponsored efforts only	Sun tracker (des)	Numerous autopilots and space studies	Dyna-Soar proposal	Moving tape displays, optical storage devices
Autonetics	NAVAHO, SINS, A3J, Minuteman, B-70, Hound-dog and various experimental systems. Miniature celestial inertial system	VERDAN, Minuteman and various development systems	N2, N3 (limited productions)	Various autopilots and fire control systems. Space guidance studies, Dyna-Soar	Dyna-Soar, Apollo, orbital bomber	Free rotor gyro, quartz accelerometer, earth landmark tracking

LEGEND:
 dev = development
 prod = production
 exp = experimental

~~CONFIDENTIAL~~

problems, and astro-tracker work. Arma had only one system, Atlas, in its background but appeared very strong in knowledge of lunar guidance analysis particularly in ascent and re-entry.

Sperry and Minneapolis-Honeywell (also about equal) both exhibited knowledge of the space guidance problem. Sperry seemed conversant with the problems associated with using the navigator in the loop. Minneapolis-Honeywell discussed advanced components that could not phase in to early Apollo missions.

GPI and Bendix presented conventional approaches to the Apollo guidance problem. GPI demonstrated knowledge of components and Bendix showed that they understood how the astronaut would fit into the operation.

We recognize that all of the above companies are experienced and knowledgeable in their fields. It is imperative that the selected company have prior experience on lunar mission programs: such is the case with both Autonetics and Arma.

We also recognized that no company in the country had all of the capabilities required for taking over all the aspects of the Apollo guidance system. These may be listed as:

- (1) Background in automatic star tracking;
- (2) Development and production of basic components in an astro-inertial guidance system
- (3) Development of subminiature platforms of the 15-lb class with the performance of considerably larger units
- (4) A strong background in design, development, test and operational use of digital computers in a ballistic environment
- (5) A background in design, development and test of astro-inertial systems.
- (6) An extensive knowledge of space guidance problems
- (7) Experience in both manual and automatic precise optical instruments
- (8) Experience in advanced, long range radio altimeters.
- (9) A thorough knowledge of the problems of integrating a human operator in a guidance system and particularly in the space guidance field

We decided then that we would work with the top four companies on the guidance system to be sure to cover all of the problem areas, but Sperry and Minneapolis-Honeywell declined because of the press of other projects.

~~CONFIDENTIAL~~

D. DEFINITION OF SYSTEM VENDOR EFFORTS

Early in February 1961, Autonetics and Arma were given the Martin guidance concepts and statements of work; the guidance concepts to be the basis for their studies. These concepts included:

- (1) On-board capability for performing all guidance functions.
- (2) Two-system, two adjacent window approach.
- (3) Automatic and manual capability.
- (4) Astro-inertial platform and manually operated optical instrument for basic system inputs, with both instruments having navigational capabilities
- (5) Structural tie between angular measuring subsystems
- (6) Two-body computation
- (7) straightforward techniques and development equipment

Taking into consideration the peculiar qualifications of these companies, separate statements of work were prepared. Briefly, Autonetics was asked to study:

- (1) Equipment definition including reliability, size, weight, power, abort, self-checking, navigation and steering equations.
- (2) Identification and coupling problems between guidance subsystem and other vehicle systems.
- (3) Environmental control requirements and solutions.
- (4) Definition of GSE requirements including azimuth alignment, calibration, program read-in and check-out.
- (5) Definition of countdown procedures as well as the sequence of operation during the mission.
- (6) Mechanization problem in the restricted 3 (or more) body navigation and guidance approach for comparison with the two-body method.
- (7) Installation problem.
- (8) Overall error analysis with emphasis on the midcourse and lunar orbit phases.

~~CONFIDENTIAL~~

The Arma assignments were:

- (1) Conceptual, mechanization and performance analysis of the ascent phase.
- (2) Conceptual, mechanization and performance analysis of the re-entry phase.
- (3) Conceptual, mechanization and performance analysis of the lunar orbit guidance problem.
- (4) Definition of the digital computer requirements.
- (5) Study of number of observations, smoothing and the mechanization required.
- (6) Study of occultation technique, analysis and the problem of whether manual or automatic techniques should be used.
- (7) Definition of rendezvous guidance technique.
- (8) Conceptual and analysis study of abort guidance.
- (9) Study of the overall guidance system error analysis.

E. COMPONENT VENDOR EFFORTS

Even the combination of Arma and Autonetics did not cover all of the subsystem areas, such as miniature platform and manually operated optical units. Therefore, information was requested from a number of "component" companies on the above items as well as on astro-inertial platforms and digital computers. Investigation of the radio altimeter was rather limited because of the conventional nature of this unit.

The subsystem and component companies which were asked to submit design proposals are listed below:

Telesextant

Kollsman
Mergenthaler
Perkin-Elmer

Digital Computer

IBM
Litton
Librascope
Texas Instruments

Analog Computer

Electronic Associates
Reeves Instruments

Raytheon

Miniature Platform

Litton

Kearfott

Minneapolis-Honeywell

Astro-Inertial Platform

Nortronics

Litton

Inputs on the telesextant were also forthcoming from Autonetics and Arma, the latter company having chosen to work with Keuffel and Esser for their manual instrument. Therefore, actually five companies were asked to contribute in this area. Mergenthaler did not respond, and time did not permit a follow-up with Perkin-Elmer. Other than Arma and Autonetics, the detailed work in this area was done with Kollsman, who was given our specific requirements as detailed in IV-D-4. That company's background in the field of automatic star trackers and manual optical units is well known and will not be further explored in this report.

Also in the field of digital computers, Arma and Autonetics were asked to supply information. Therefore, 6 companies were asked to participate. Librascope decided not to participate. A number of companies is developing small platforms. The three selected were considered representative of the miniature platform field.

The number of companies developing astro-inertial platforms is limited, Autonetics and Nortronics being the only ones who have produced this type of unit. Litton, however, is in final development of an astro-inertial system under a Navy contract. Therefore, information was sought on this unit. A combined Arma-Kollsman astro-inertial platform was also considered.

F. VENDOR CONTRIBUTIONS

The material received from the above system and component companies was extensive. Arma supplied a detailed study of the guidance system concept, mechanization and operation (see Ref II-1). The Autonetics report was more cursory and philosophical (see Ref II-2). Arma's approach was one of a purely manual input system with no automatic navigation capability. Autonetics went to the other extreme, providing automatic navigation not only in the astro-inertial platform but in the telesextant. As has been observed in earlier chapters of this report the selected Martin approach is somewhere in between.

~~CONFIDENTIAL~~

As mentioned earlier, only Kollsman, other than Arma and Autonetics, supplied information on the telesextant (Ref. IV-2). Their report described an instrument which specifically met the Martin requirement. It was apparent from this report that Kollsman had considered carefully both the instrument design and the environment in which the instrument would operate.

No specific proposal requests were issued for the miniature platform since material on representative units already existed. Therefore, information on platforms in development at Litton (Ref. IV-1), Kearfott (Ref. VIII-1 and Appendix H) and Minneapolis-Honeywell (Ref. VIII-2 and Appendix I) was studied for applicability to the Apollo guidance system.

Digital computer proposals were received from IBM (Ref. VIII-3 and Appendix N), Litton (Ref. VIII-4 and Appendix M) and Texas Instruments (Ref. VIII-5 and Appendix L). These companies were given the Martin guidance concepts and equations around which a preliminary design of a digital computer was made. The proposals received generally followed out concepts but did not detail how sextant readings would be handled and did not include Chapman's re-entry technique; however, these items were included in Arma's design. Raytheon's and analog contributions are discussed in Chapter III of this report.

A proposal for an astro-inertial platform for Apollo application, from Nortronics was not available because of previous commitments, but Nortronics' work in this field is well known by The Martin Company. The modifications required to the A-11 system have been considered. This unit is described in Appendix F. Information was also available on Litton's astro-inertial work--their LN-5 system (Ref. VIII-6 and Appendix E).

G. UTILIZATION OF VENDOR CONTRIBUTIONS.

In general, equipment that most nearly fits the Apollo requirements is described in the main body of this report. Other equipment is described in the Appendices. In no case was final equipment selection made.

The Autonetics N-20 astro-inertial platform, representative of size, weight, complexity and accuracy required for this subsystem, is described in Chapter IV. Not enough information was available from Nortronics, and the Litton unit did not appear to fit directly into the guidance system because of weight and accuracy considerations.

Information on the digital computer was received from five companies. The Arma computer was described in the main body of this report for the following reasons:

- (1) Close liaison was maintained with this company on specific requirements.
- (2) Their computer was small in size and weight.
- (3) No moving parts were used.

~~CONFIDENTIAL~~

- (4) Advanced packaging techniques were used.
- (5) Their computer was in an advanced state of development.

The Litton P-300G miniature platform was chosen for inclusion in the main body of this report because of its advanced state of development, light weight, and its use of long life gas-bearing gyros.

The Kollsman design of the telesextant is included in the main body of the report because of the close liaison with this company; hence their design specifically fit the Martin requirements and the background of Kollsman in the field of star trackers and manually operated optical instruments.

In addition, information from the Arma and Autonetics studies was used in the guidance system report, for example, Arma's ascent and reentry error analysis. Information received on equipment and not used in the main body of the report is included in the Appendices.

H. SUMMARY

Two of the best inertial guidance companies were engaged in the Apollo study. These companies have already contributed to the Atlas and Minuteman ICBM's. Martin is also aware of the AC Spark Plug efforts in the Titan ICBM and Mace programs. The Apollo study, Mace and Titan background coupled with Pershing experience, has given The Martin Company a unique awareness of the latest technology in pure inertial navigation.

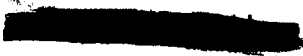
Unfortunately, time did not permit the evaluation and incorporation of the excellent work done in the Apollo guidance area by NASA-STG, NASA-Langley, NASA-Ames, NASA-Marshall and NASA-Lewis. In addition companies such as Nortronics were not available for study inputs. Companies and agencies such as Bell Avionics, MIT, and STL, although cognizant of space guidance problems, did not receive full evaluations.

In the guidance area, some 20 companies were approached and about 12 responded. In the study itself, about 40 engineers from the various companies contributed to the study on a full time basis.

It will be seen, then, that an overall survey has been made of the guidance capabilities of companies in this country. Therefore, The Martin Company is in an advantageous position for working with NASA in making decisions for subcontracting the Apollo guidance system and its various subsystems when a development contract is awarded.

~~CONFIDENTIAL~~

~~CONFIDENTIAL~~



IX. RELIABILITY

Apollo's guidance system must possess ultra-high reliability to protect the human crews and to ensure its planned vital contribution to overall mission success.

The system has therefore been allocated a reliability goal of 98.50%.

A consistently-maintained conservative and prudent approach dictates the use of only proven circuitry and mechanical design rather than laboratory models and concepts. Other components and techniques already far along the developmental path have also been incorporated into Apollo's guidance system.

A. DESIGN ANALYSIS

The reliability analysis for the planned electronic portion of the Apollo guidance system has been completed. The analysis is based on various assumptions pertaining to system use time, and modes of operation during the lunar orbit mission. Variance from these assumptions (listed below) may result in a different reliability for the guidance system.

The analysis is based on the catastrophic failure of parts; it does not include the effects of parametric variations.

1. Assumptions

- a. It is assumed that the electronic portion of the Apollo guidance system is composed of an astro-inertial platform, a telesextant, a miniature platform, and two identical digital computers.
- b. The digital computers operate in active redundancy for seventeen hours during each translunar and transearth flight.
- c. The telesextant also operates for seventeen hours during the translunar and transearth phases.
- d. The miniature platform operates during the boost and re-entry phases.
- e. The miniature platform, together with the telesextant, may substitute for the astro-inertial platform.
- f. Each component, or black box, of the electronic guidance system is assumed to be operable immediately prior to launch.

~~CONFIDENTIAL~~

B. FAILURE RATE DATA

The assumed MTBF's (mean time between failures) for Apollo's guidance system components are tabulated below.

TABLE IX-1

Component MTBF (hours)

<u>Component</u>	<u>Mission Phase</u>	
	<u>Boost Re-entry</u>	<u>Orbit Translunar Transearch</u>
Astro-Inertial Platform	50	5,000
Computer	10	1,000
Miniature Platform	75	7,500
Telesextant	150	15,000

The equivalent guidance system phase failure rates are tabulated in Table IX-2.

The operational modes of the electronic guidance system for the various lunar mission phases, plus the system equivalent phase failure rates, are illustrated in Fig. IX-1.

Listed in Table IX-3 are the equivalent system failure rates during the time starting from the middle of the previous phase to the time ending at the middle of the one under which it is listed. These failure rates are presented to aid safety calculations. For estimating purposes, it is assumed that each component is operable at the beginning of each midphase interval.

C. SELECTED SYSTEM

The reliability analysis of the selected guidance system indicates that the probability of success of the electronic portion of the guidance system is 0.9939.

~~CONFIDENTIAL~~

ER 12007-2

TABLE IX-3

Failure Rates Of Equipment (Guidance safety)

Component/ Equipment	No. of Units	Hourly Failure Rate		Mission Phase Failure Rate									
		Count- down Trans- lunar Trans- earth Lunar Orbit Recov- ery	Boost Re- entry Landing	Count- down	Boost	Coast	Trans- lunar flight	Lunar orbit	Trans- earth flight	Re- entry	Landing	Re- cov- ery	
Astro-inertial Platform, Miniature Plat- form, Telexant Computer					2	0	101	270	327	238			

A subsequent report received from Arma analyzed their proposed system. Arma evolved a somewhat different guidance system philosophy. The failure rates utilized were more optimistic than those set forth above; said rates indicated a probability of mission guidance success of .99994.

D. ADDITIONAL INVESTIGATION

An investigation was conducted to determine the effect that additional computer redundancy would have on the overall reliability of the electronic guidance system:

Gains in system reliability may be accomplished by expanding the degree of "building block," thereby increasing subsystem redundancy. However, a trade-off must be made in exchange for the reliability gained by this redundancy in terms of increased system cost, weight, and power consumption.

An investigation was made to determine the guidance system's sensitivity to additional computer redundancy.

Two basic guidance system reliability estimates are available. These estimates entail the very conservative preliminary estimate, and that made by Arma in their document CX-13, 184. Both estimates considered "double" active redundant computers.

E. CALCULATIONS

1. Preliminary Analysis System

<u>System or subsystem type</u>	<u>Mission Failure Rate</u>
Platforms	.004902
Computers (Q each .0334285)	
Two redundant	.001117
Three redundant	.000037
Platforms and 2 computers (p=.993981)	.006019
Platforms and 3 computers (p=.995061)	.004939
System mission failure rate improvement	

$$\frac{6019-4939}{4939} = 18\%$$

~~CONFIDENTIAL~~

System reliability improvement

$$\frac{.995061 - .993981}{.993981} = .108\%$$

2. Arma Estimate

Platforms	.000030
Computers (Q each .00577)	
Two redundant	.000030
Three redundant	.000000
Platforms and 2 Computers (p= .99994)	.000060
Platforms and 3 Computers (p= .99997)	.000030
System mission failure rate improvement	

$$\frac{.000060 - .000030}{.000060} = 50\%$$

System reliability improvement

$$\frac{.99997 - .99994}{.99994} = .003\%$$

F. CONCLUSIONS

1. Increase Based on Preliminary Estimate Data

The preliminary estimate data set forth above indicates that an additional redundant computer improves the system mission failure rate 18%. However, the reliability factor increases from .993981 to .995061 - - an increase of .108%.

2. Increase Based on Arma Estimate

Based on Arma data, an additional redundant computer improves the system mission failure rate approximately 50%. However, the reliability factor increases from .99994 to .99997 - - an increase of .003%. Since both of these reliability estimates for the guidance system exceed those specified, it is anticipated that the operational system will meet or exceed the goal.

~~CONFIDENTIAL~~

3. Computer Redundancy

The sensitivity of the guidance system reliability factor to additional computer redundancy is largely dependent upon the actual reliabilities of the platform system and the individual computers. The reliability factor improvement to be expected by additional computer redundancy is between .003% and .108%.

~~CONFIDENTIAL~~

~~CONFIDENTIAL~~

X GUIDANCE CONCLUSIONS

A. CONCLUSIONS DEVELOPED

From the previous chapters a number of important points and conclusions have developed. These may be enumerated as follows:

1. Conceptual Studies

Both two-body and four-body approaches have been proven feasible. It has also been shown that the computer required for the four-body concept is not much heavier or more complex than that required for the two-body. Therefore, either concept may be used, with more study required for optimization. The goal in the two-body study is to arrive at a completely manual system.

2. Re-entry Studies

A number of re-entry guidance techniques have been studied and the Chapman approach has definitely proven feasible. This technique, therefore, tentatively is selected. Other techniques, such as optimum equilibrium glide, equations of motion, etc., show promise but require additional study.

3. Mechanization

The two system approach has been shown to possess greater reliability than is actually specified for the Apollo mission. This approach also brings the astronaut directly into the navigational function, utilizing his capabilities to the fullest and placing him in full command of the vehicle. Further, the selected approach provides automaticity for emergency operation.

4. Operation

It was shown in the operational sequence that the required functions were compatible with the timing of the various phases of the mission. The occultation technique was also shown to be feasible.

5. Displays

A very flexible display system has been presented. The use of cathode ray tubes allows various parameters and formats to be displayed on a common unit. The integration of this subsystem with the crew was also demonstrated.

6. Accuracy

From the error analysis, it was shown that by making a final correction at 40,000 naut mi from the earth, the arrival within the re-entry corridor was better than 10 mi. By making navigational measurements from that point in to

near the re-entry point, initial condition accuracy at re-entry resulted in 2.0 and 3.5 naut mi (one sigma), for short and long range respectively, at the landing point.

7. Vendor Studies

A close look was given to the industries' capabilities in the fields of space guidance systems and components. The component areas included astro-inertial platforms, miniature platforms, digital computers, manually operated optical navigation instruments and radio-altimeters. Tentative selection of components was based on availability and compatibility with Martin Apollo guidance requirements. Studies have also shown the components development times are compatible with the Apollo development schedule. From 2 to 2-1/2 years or less is required for delivery of qualified production units in all areas except the astro-inertial platform. From 2-1/2 to 3 years is required for this subsystem.

8. Reliability

Through the use of redundant systems and the selection of highly reliable individual components, the system reliability surpasses the goals previously set. Higher reliability is attained by integration of the astronaut into the system and his ability to switch subsystems from one system to another.

B. RECOMMENDED RESEARCH AND STUDY

The study has shown that the Apollo mission is feasible from a guidance standpoint. It is recommended, however, that several items receive further research and study in parallel with a development effort. These items, over and above the aforementioned two-body, four-body and re-entry guidance studies, include:

- (1) Development of small size accurate digital pick-offs. Accuracy goal should be one arc/second.
- (2) A study of the optical window problem in space to arrive at an optimum solution. Items such as glare, condensation, differential pressure, differential temperature, refraction and sealing should be considered.
- (3) An investigation of operating optical and electro-mechanical equipment in a space environment. Consideration should be given to the effect on seals, lubricants, bearings, slip rings and brushes and to the temperature problem.
- (4) A study of the astronaut's performance capabilities in the guidance field. This should include a simulation of the space environment as

seen by the astronaut (planetarium). The simulator should include naked eye stars visible in space. Questions that need to be answered are:

- (a) With the additional stars seen in space, is identification of a given star a problem?
 - (b) How accurately can optical measurements be made?
 - (c) How rapidly can readings be taken?
 - (d) When does fatigue become a problem?
- (5) An overall simulation (digital) should be set up to determine optimum times for corrections, how many corrections, accuracy based on instrument errors and other sources, number of readings and smoothing requirements.

~~CONFIDENTIAL~~

~~CONFIDENTIAL~~

~~CONFIDENTIAL~~

XI. ATTITUDE CONTROL SYSTEM

A. INTRODUCTION

The Apollo attitude control system acquires and maintains required vehicle attitudes or attitude rates throughout all mission phases. An overall functional block diagram of this system is shown in Fig. XI-1. The variations in vehicle configuration, control environments and control requirements require such disparate controls that the system may actually be considered as a group of subsystems, sharing a common guidance system and power supply but differing functionally in the flight phases in which they are operational. These subsystems, listed below, are also divided by function, configuration or environment as shown:

- (1) Boost phase
 - (a) Ascent
 - (b) Coast
 - (c) Injection
- (2) Abort
 - (a) Launch escape tower (aerodynamic)
 - (b) 15.6 K engine (nonaerodynamic)
- (3) Midcourse
 - (a) Coast
 - (b) Midcourse translation corrections
 - (c) Lunar orbit injection and ejection
- (4) Re-entry
 - (a) Reactive controls
 - (b) Aerodynamic controls

The configurations during these flight phases are shown in Fig. XI-2. The subsystems are listed in Table XI-1.

The boost phase control system, consisting of gimbaleed engine control of three Saturn stages and reaction attitude jet control during the S-IV stage coast

TABLE XI-1

Apollo Attitude Control Subsystems

Autopilot	Type of Control	Configuration	Period of Operation	Comments
1. Boost phase	(a) Proportional control via gimbaled engine (3 stages) (b) On-off control (?) via attitude jets during S-IV coast phase	Three stage Saturn booster with Apollo vehicle	From launch until Apollo separation from S-IV stage	Design of this system is not included in present effort
2. Launch Escape Propulsion System	Proportional control using injection thrust vectoring technique	Command module plus launch escape tower	Prelaunch until tower jettisoned at 300,000 ft	Aborts or turnarounds past 300,000 ft use 5.6K engine and its associated control system
3. Midcourse	(a) Proportional control with adjustable limit cycle via pulse modulated attitude jets during coasting flight and vernier velocity adjustment (b) Proportional control via pulse modulated vernier translation jets in P&Y during 15.6K engine operation	Command and propulsion/equipment modules	Between separation from S-IV stage and separation of command and propulsion modules	This system has been breadboarded and is being tested with analog simulation of vehicle
4. Re-entry	(a) P, Y&R reaction control via pulse modulated jets at dynamic pressure 10 psf (b) P&Y aerodynamic control and reaction control at dynamic pressures >math>70 \text{ psf}</math>	Command module Model 410	From separation of propulsion modules until deployment of drogue chute	This system has been breadboarded and is now being tested with three dimensional analog of a parabolic re-entry

period, depends on the booster design and as such is not part of the present Apollo vehicle design effort. Consideration must be given, however, to integrating it with the rest of the Apollo flight control system. The remaining subsystems are discussed separately in sections B, C and D of this chapter.

The various flight regimes require different methods of obtaining control torque. These methods were selected after a study of the requirements and tradeoff studies with alternative methods. Those chosen, with their periods of operation, are listed below:

- (1) Thrust vector control (gimbaled engine)--ascent with three Saturn stages.
- (2) Thrust vector control (injection technique)--controlled flight abort.
- (3) Fixed reaction jets (pulse modulated)--midcourse coasting, midcourse and lunar velocity corrections, and re-entry roll control.
- (4) Aerodynamic flaps-pitch and yaw control via three flaps on the Model 410 command module used in re-entry flight environments where the aerodynamic pressure exceeds 10 psf.

Manual and automatic control modes are provided during all flight phases. Manual control is provided through a two-axis finger operated electric side stick controller (pitch and roll) and toe pedals (yaw). Although this configuration is heavier and structurally more complex than a three-axis side arm controller, it is the preferred system for tracking functions, especially during high accelerations (See Ref. III-10). Since the most critical periods of possible manual control (abort and re-entry) will involve high accelerations, the manual system must be selected accordingly.

Rate damping is provided about all axes to allow the pilot to concentrate on tracking and reorientation functions. Triple redundancy is provided in the rate damping loops to enhance reliability. Current planning entails the use of three body-mounted rate gyros per axis as the primary source of rate information with RC networks as possible backup. Although more reliable, RC networks are restricted somewhat in that the derivatives of the Euler angles (which these networks yield) are not equal to the body angular rates, especially for large gimbal angles. (See Appendix V for a brief treatment of the relationship between the body rates and Euler angle derivatives.)

Ref III-10 NASA TN D-337 "Centrifuge Study of Pilot Tolerance to Acceleration and the Effects of Acceleration on Pilot Performance" by Brent Y. Creer, Captain Harold A. Smedal and Rodney C. Wingrove.

~~CONFIDENTIAL~~

The automatic control mode will also permit a somewhat similar form of manual control by varying the orientation settings or dialing the autopilot. Manual control will therefore always be through electrical systems; no purely mechanical backup will be provided. This is partially because of the difficulty in providing a pulse modulated hypergolic bipropellant system with this feature, and partly because the weight of a mechanical system may be better used in aiding reliability elsewhere.

Although the subsystems or autopilots are discussed in the subsequent sections as somewhat separate entities, the design will be integrated to use as many common sections or modules as possible. For example, the midcourse and re-entry autopilots differ in the nozzle combinations used for obtaining pitch, yaw and roll forces, but are both pulse modulated systems sharing many common sections. The launch escape tower autopilot, although it is the sole system using an injection thrust vector technique, also will have amplifiers and demodulators similar to those used in the midcourse and re-entry autopilots. With interchangeable modular construction and adjustable gains, it will be possible to utilize parts of control systems not in use (or whose function is completed) to effect repairs. Although the extended length of Apollo missions make redundancy a necessity, the modular switching feature is a desirable additional assurance. Easy in-flight checkout and modular interchangeability is therefore considered a design criterion.

The use of the guidance computer as a midcourse and re-entry autopilot is a possibility which will be studied further. Preliminary consideration indicates that a digital computer is well suited for operating a pulse modulation system. Further investigation must be made, however, concerning reliability, computer loading and other aspects of the problem.

Autopilots for the midcourse and re-entry phases have been designed and built for test purposes. A breadboard midcourse system has been demonstrated. Preliminary test data indicate that the special combination of pulse width and pulse rate modulation designed for this system is meeting expectations. The re-entry autopilot has been tied into an analog simulation of the equations of motion to demonstrate its capability during a simulated parabolic re-entry.

Inputs to the system, in addition to the rates mentioned previously, will consist of attitude information from the platform (which has been resolved into the body axes) and commands generated by the computer. During the coasting periods, when the main orientation requirement involves keeping the heat radiators facing deep space, pitch and yaw information may be obtained from the sun-seeker coupled with platform roll signals.

Growth potential is included in the system design for rendezvous and lunar landing missions. The rendezvous system will use the present attitude controls operated automatically, coupled with additional vernier translation jets under pilot control. This system is described in Chapter XII. Under the lunar landing

concept, the 15.6 K engine will be used for takeoff only. The attitude control system employing the vernier translation jets will be capable of providing the necessary control during this function.

The following subsections are devoted to individual discussions of the abort, midcourse and re-entry systems concerning the requirements, system selection and preliminary design. Appendices give additional information on limit cycles (Appendices T&U) and the relation between body rates and Euler angle derivatives (Appendix V).

B. ABORT CONTROL SYSTEM

1. System Requirements

The abort control system described in this section is concerned only with abort operations utilizing the launch escape tower and does not consider mission aborts occurring after the tower is jettisoned. This late abort, or turnaround, will utilize the 15.6K engine and its associated attitude control system described in Section C of this Chapter: "Midcourse Attitude Control."

The abort tower is used for all abort operations from launch throughout the atmospheric flight region or up to 300,000 feet. The abort configuration during this period is merely the Model 410 command module with the abort tower attached (see Fig. XI-3). The command module will include the re-entry reaction and aerodynamic attitude controls which will be available for abort control purposes. The range of aerodynamic forces and the control torques required, however, will preclude the use of these systems for primary control forces.

To minimize the chance of collision between the booster and the aborting command module, it is necessary to follow some optimum abort trajectory based on the booster behavior immediately prior to separation. This behavior--in terms of vehicle attitudes, velocity vector and angle of attack--will be used by the computer to continuously calculate the optimum abort trajectory, abort plane and the steering commands necessary to achieve them.

The optimum angle for abort thrusting is between 10° and 15° from the initial velocity vector (see ER 12003). When the vehicle's pitch plane and the abort plane coincide, the command angle will be the difference between 15° and the angle of attack (α) at initiation of abort. The command angle will not, therefore, exceed 15° .

The abort plane is defined as that which includes the vehicle's longitudinal axis (\bar{p}) and the velocity vector (\bar{V}). This plane generally will be the same as the vehicle's pitch plane, since the ascent trajectory will be achieved through pitch commands. If the angle between the vectors (generally α), is less than some certain value (whose determination considers permissible angles of attack), the vehicle's pitch plane will be used automatically. The computer will resolve the

~~CONFIDENTIAL~~

abort plane and trajectory requirements into requisite pitch, yaw and roll steering commands. The abort plane concept automatically limits the maximum angle of attack of the aborting vehicle to 15° ; this angle further decreases during thrusting..

The abort rocket thrust is approximately 130,000 pounds and lasts about 3 seconds. The distance--16 feet and the thrust alignment tolerances permit up to 4340 foot-pounds of disturbing torque.

The tower remains attached to the module after burnout to provide aerodynamic stability at speeds below Mach 2. It is then jettisoned, after opening of drogue chute. At speeds above Mach 2 the tower is jettisoned immediately after burnout and the re-entry control system provides attitude control.

2. System Selection

The turning rates, damping requirements, and possible thrust asymmetries discussed in the previous section indicate the necessity for large control forces and the desirability of proportional control. More complete discussions of the system selection are set forth in ER 12007 and ER 12017, entitled "Onboard Propulsion" and "Aerodynamics", respectively. Only a relatively brief discussion is presented here.

An aerodynamic control system was found to be impractical because of the size of the control surfaces involved, their effect on stability in the face of possible controls malfunction, and the necessity for an auxiliary reaction system during the final phases of aerodynamic flight.

The high torques required (50,000 foot-pounds minimum), and the proportional control feature make thrust vector control superior to attitude jets mounted on the tower. Thrust vector control also enjoys considerable weight and complexity advantages. The high torques and the response of this type system also are preferred from a controls standpoint.

Consideration of nozzle gimbaling, jet vanes and an injection technique led to the selection of the latter as the most promising. In the injection system, a substance such as freon is injected at the proper place and pressured into the exhaust nozzle; this induces a thrust deflection by the shock wave which occurs. This system is described in the propulsion report, but from a controls standpoint may be considered as similar to a gimbale engine system in which the thrust vector may be moved but which does not yield positive position information as from a followup potentiometer.

3. System Design

A basic block diagram of the injection vector control system is shown in Fig. XI-4. Preliminary information indicates the injection servo loop transfer

~~CONFIDENTIAL~~

function is approximately equivalent to a second order system with a natural frequency of 400 rad/sec and a damping ratio of unity. The dynamic response of this system with a loop gain of 150 sec^{-1} is also shown in Fig. XI-4.

The system will be stabilized with attitude information from the platform, and rate information from the body mounted rate gyros; it will receive the trajectory steering commands from the computer. The control system block diagram is shown in Fig. XI-5. To meet abort requirements the system must be fairly fast, but with limited overshoot. A natural frequency of 3.0 rad/sec and a damping ratio of 0.6 have been selected; these give an essentially damped response in two seconds. The response of such a system to a step input of 15° is shown in Fig. XI-6. The configuration allows aerodynamic damping to be neglected for the preliminary design (according to information on the Mercury abort configuration).

The maximum thrust deflection is assumed to be $\pm 1.09^\circ$. With a thrust of 130,000 pounds and a moment arm of 16 feet, the maximum control torque is 39,750 foot-pounds. The gain of this system will approximate 135,000 ft-lb/rad. The system will therefore yield proportional control to attitude commands up to 16.9° . The root locus shown in Fig. XI-7 indicates a damping variation of 0.5 to 0.7 for a gain change exceeding $\pm 25\%$. The ratio of rate to displacement gain required is 0.41. Although the system is basically simple, structural considerations may require the addition of filters.

C. MIDCOURSE ATTITUDE CONTROL

1. System Requirements

The midcourse attitude control system operates in the period between separation of the propulsion and equipment module from the Saturn S-IV booster, and the separation of the command module for re-entry. This period is assumed to be two weeks, and since it will be spent entirely out of the atmosphere, reactive control is required. The control situations during this period are varied and include both coasting and translation boosting phases. Since a period is prolonged, it is quite important to handle these differing requirements as efficiently as possible.

The operational modes and requirements for the midcourse control system are listed and discussed as follows:

a. Cancellation of separation tipoff rates and displacements

The tipoff rates and displacements will be minor since the S-IV booster will be shut down at separation. The only disturbances will be those caused by the disconnecting operations and these will not be sufficient to define the required system control torque or appreciably affect fuel expenditure.

~~CONFIDENTIAL~~

(2) Injection thrust vector control.

(3) Separate attitude jets.

The choice of attitude jets was made primarily from a weight and reliability standpoint. An additional controls interest was that the system should be proportional. This is obtained by using pulse modulation techniques. An additional refinement was added by using the 15.6K engine pitch/yaw attitude control jets as the vernier translation jets, by making their thrust parallel to the longitudinal axis. In this manner the propellant expended for attitude control also adds to the desired velocity increment.

The rest of the midcourse flight (which involves limit cycling, reorientations and at least a backup control capability during the vernier translation jet operation) will be handled by the "coasting" autopilot. This control system will also furnish roll control during operation of the 15.6K engine. The use of a high specific impulse propellant and an economical limit cycle fuel expenditure rate are the primary goals of this system.

Since the system should be able to provide control during the vernier translation jet operation, the torque available should be 200 foot pounds or more. With the moment arms available, a thrust level of 25 to 30 pounds is therefore desirable. This criterion eliminates reaction wheels as the sole system because of the weight penalty, in addition to the necessity for velocity desaturation.

Table XI-8 shows the relative advantages and disadvantages of the various systems considered. A detailed discussion of the more promising types of systems is as follows:

a. Pulse modulated linear system

This system used high specific impulse hypergolic propellants such as UDMH and nitrogen tetroxide. It operates economically under limit cycle conditions because of its low minimum impulse (or low minimum control rate)*, and its

*The limit cycle propellant expenditure rate is given by the following relation (see Appendix U derivation):

$$Q = \frac{r I_t^2}{6(\Delta \theta) I I_{sp}} \text{ lbs/sec}$$

where

r = moment arm

I_{sp} = specific impulse

I_t = minimum impulse

$\Delta \theta = 1/2$ deadspot band in radius

I = moment of inertia

~~CONFIDENTIAL~~

b. Solar orientation for heat radiation

This is the normal mode of operation during the lunar mission. The greatest percentage of time will be devoted to this function. The heat radiators, located on the sides of the vehicle, must be kept facing deep space. The vehicle centerline will therefore be maintained aligned to the sun within $\pm 3^\circ$ in the yaw plane. Although roll and pitch requirements are less stringent, they will also be taken as $\pm 3^\circ$. The transmitting and receiving antennas will be gimballed and situated to preclude conflicting demands for vehicle orientation. Earth-moon guidance will not require continuous star tracking; therefore, during most of the coasting flight, the dominant attitude control requirements will be a rather loose solar orientation.

c. Reorientation or slewing

The vehicle must be slewed every time an operation is to be performed which cannot be done in the nominal, sun oriented position. Some examples of these operations, and the estimated number of reorientations required during a two week lunar expedition, are as follows:

(1) Star observations for navigation (27)	54
(2) Midcourse velocity corrections (9)	18
(3) Scientific observations (6)	12
(4) Initial and final orientation (1 each)	<u>2</u>
Total	86

The navigational star observations may require a change in pitch attitude only, while the midcourse translation corrections will probably require a three-axis change. It is, therefore, difficult to predict the number of reorientations to be required, but an estimate is necessary to obtain propellant requirements. For simplicity and conservatism, it may be assumed that each reorientation involves all three axes, and that the roll moment of inertia equals that of pitch and yaw. The total reorientation may then be considered as 258 turns. The propellant required is a function of the number of turns, and the turning rates. The mass and configuration of the vehicles under consideration will required an expenditure of approximately 0.06 pound of fuel ($I_{sp} = 280$ seconds) for a change in attitude rate of 1° per second.*

* Using the relation: Q lb of propellant = $\frac{\Delta W I}{57.3 I_{sp}}$

where ΔW = change in angular rate in deg 1 sec
 I = moment of inertia in slug ft²

~~CONFIDENTIAL~~

I_{sp} = specific impulse

r = moment arm of thrust

Thus, if the 258 turns were made at rates of 10° per second, approximately 310 pounds of propellant would be expended. Since this would be the major part of the midcourse attitude control propellant requirement, the obvious indication is the importance of not using high turning rates. The necessity of keeping the heat radiators facing deep space as much as possible is the primary reason for setting some minimum turning rate.

d. Orientation maintenance for navigation and scientific observations

A limit cycle with a deadspot of $\pm 0.5^\circ$ and maximum rate of 10° per hour is assumed acceptable for both automatic and manual stellar angular measurements and any scientific observations required.

e. Vernier translation and lunar orbit boosting

Lunar orbit velocity adjustments will be made with a 15.6K engine firing up to 286 seconds. The disturbing torque from the thrust asymmetries of this engine may reach 650 foot-pounds which is by far the largest disturbance of any duration to be expected. This disturbing torque is based on reasonable maximum tolerances in thrust alignment and center-of-gravity location.

Midcourse vernier velocity corrections will be made approximately nine times during a lunar flight for a total velocity change of up to 525 fps. A thrust of about 1200 pounds will be used for vernier velocity corrections and the maximum disturbing torque will be on the order of 50 foot-pounds, assuming the same tolerances on thrust alignment and center-of-gravity position as before.

f. Fuel requirements

The operational modes and requirements discussed above indicate (1) the size of the control torques necessary as discussed under the next section, entitled "System Selection," and (2) the total torque impulse required. Fuel expenditure estimates may be made by considering the requirements as follows:

Disturbing torque impulse. The disturbing torque impulse from the 15.6K engine will be 71,500 foot-pounds seconds or less 14,000 foot-pounds seconds additional may be attributed to the vernier translation engines and disturbances due to accelerating and decelerating the main pump turbine and the turbine generators. Thus, the torque impulse will be 85,500 foot-pounds seconds. Gyroscopic moments are minor since only the relatively small turbine generators will be rotating during attitude changes. Disturbing moments due to solar radiation, solar wind plus electro- and magneto-dynamic effects are also negligible compared to the better known effects, but will have some effect on fuel

~~CONFIDENTIAL~~

Limit cycle. Unless certain special rate- and displacement-nulling systems are used, the inherent nonlinearities of the system will yield an attitude limit cycle. During most of the flight the deadspot of the limit cycle could be quite large ($+30^\circ$) without disturbing the operation of any other system. Although a deadspot of this size is undesirable, the fact that a reasonable deadspot is permissible, coupled with the large moments of vehicle inertia indicate that a system can be designed which would allow the vehicle to limit cycle for two weeks with less than 10 pounds of fuel. (See Appendix T and Appendix U for discussions of limit cycle fuel expenditure rates for two general types of systems "on-off" and "impulse response".) As mentioned previously, stellar observations are expected to require much smaller deadspots and also lower rates than are usually required, and the system must be capable of adjusting the deadspot and/or operating for short periods of time with a minimal deadspot.

It is seen from the above discussion that propellant requirements will be in the neighborhood of 160 pounds for attitude control alone, not including margin for unpredictables and assuming a somewhat theoretical limit cycle fuel expenditure rate. Most of this requirement is a function of moment arm and specific impulse, and not a function of the type of reactive system involved.

2. System Selection

The salient criteria for selecting a midcourse control system from the discussion in the previous section are:

- (1) Maintenance of good attitude control with a disturbing moment of up to 650 foot-pounds.
- (2) Maintenance of an economical limit cycle.

These criteria indicate the control system should have the following characteristics:

- (1) Proportional control, especially during midcourse vernier and lunar orbit velocity corrections.
- (2) A low minimum impulse capability during limit cycle operation.
- (3) High specific impulse propellant with short ignition delay times.

An initial decision was made to separate the pitch/yaw attitude control for use during the 15.6K engine operation from that for use during the coasting flight. This prevents the system in use for almost two weeks from being sized for less than five minutes of the flight. The following systems were considered for attitude control during the operation of the 15.6K engine:

- (1) Gimbaled engine.

~~CONFIDENTIAL~~

TABLE XI-2

Attitude Control Systems Comparison

<u>System</u>	<u>Advantages</u>	<u>Disadvantages</u>
Pulse modulated bipropellant jets	Proportional control, high specific impulse	More complicated electronics
Bipropellant or monopropellant two level bang-bang	Good specific impulse	Requires complicated system to switch either feed systems or combustion chambers, not proportional
Inertia wheel plus reaction system	Proportional control for small disturbances	System heavy and relatively complex
Compressed cold gas proportional system	Simple, proportional control	Weight penalty from low specific impulse propellant
One level bang-bang	Simple	Not proportional, thrusts high enough for disturbances are wasteful during limit cycling

~~CONFIDENTIAL~~

expenditure. The total torque impulse which should be allotted for use at the crew's discretion is difficult to calculate, but various investigations* indicate that the individual torques and times of application will be small. Torques imparted by the crew will either be accompanied or closely followed by an equal and opposite counter torque. In the latter case the rate imparted will be cancelled, but a net displacement will remain. Thus the crew disturbances will tend to be self-cancelling and will not effect fuel expenditure in the same manner as thrust asymmetries and turbine accelerations but rather through their effect on the limit cycle (providing there is an appreciable deadspot). The total disturbing torque impulse for estimating fuel expenditure is allotted as follows:

Thrust asymmetries 15.6K engine	71,500 ft lb/sec
Vernier engines	10,000
Accelerating rotating equipment	4,000
Crew disturbances	8,000
Solar radiation, solar wind, electro- and magneto-dynamic effects plus margin	<u>6,500</u>
Total	100,000 ft lb/sec

Less than 50 pounds of propellant (with a specific impulse of 280 seconds) will be required to provide 100,000 ft-lb/sec of counter torque impulse with the moment arms available in the vehicle.

Reorientation or slewing. This was discussed previously under operational modes and requirements where it was noted that, if the estimated number of reorientations for a lunar mission were transformed into an equivalent number of turns about a single axis at 10° per second (or with a change in angular rate per turn of 20°/sec), the fuel requirements would be approximately 310 pounds (for $I_{sp} = 280$ sec). Since the only reason for setting any minimum turning rate is because of the heat radiator requirements (which are not stringent), it is evident that somewhat less than 310 pounds may be allotted for reorientation. Thus, if a turning rate of 3° / sec is arbitrarily chosen, the fuel requirement may be considered as 100 pounds.

* WADC Technical Report 59-94, "Man's Ability to Apply Certain Torques While Weightless"-Ernest Dzendolet and John F. Rievley.
WADC Technical Report 60-129, "Manual Application of Impulses While Tractionless"-Ernest Dzendolet.

Some advantages of this system are:

- (1) It requires less complicated hardware.
- (2) Systems of this type have had extensive flight testing.
- (3) It could be manually operated easier than the PM system.

The disadvantages include:

- (1) It is only capable of nonlinear control.
- (2) The complications involved in using propellants with specific impulses as high as the PM system will at least partially negate its possible advantage in simpler hardware, for example, the monopropellants hydrozine, $I_{SP} = 235$ seconds, requires heaters, and bipropellant. require injectors.

c. Flywheel and jet reaction system

In this system flywheels are used to give linear control during small disturbances, and the jet system controls the larger disturbances and also "unloads" the flywheels when they become velocity saturated.

Advantages of this system are:

- (1) No reaction mass is expended during the limit cycle or for small disturbances (unless biased in one direction and desaturation required).
- (2) Linear control of small disturbances.

Its disadvantages include:

- (1) It is the heaviest system, and the only function of the flywheels is accomplished with less weight by the other system.
- (2) It requires the most complex autopilot.
- (3) It does not give linear control during the larger disturbances when most desirable.
- (4) It requires the most accurate prediction of the magnitude, direction and duration of disturbances during the mission since any advantages are lost if velocity desaturation is required too often.

A relative pound-weight comparison of the systems in significant areas is as follows.

ability to limit cycle below the sensitivity threshold of rate gyros. Proportional control is obtained by varying the thrust pulse width or repetition rate as a function of the input signal; this yields an apparent thrust which is proportional to the error, although the system is basically on-off. The system may use pulse rate modulation (PRM), pulse width modulation (PWM) or a combination of the two dependent on signal level (PM). These systems are under investigation by Marquardt, Tapco, Bendix and others; tests are being planned by both NASA and Martin.

Advantages of pulse modulation include:

- (1) It gives linear control without the use of proportional valves.
- (2) It yields superior limit cycle operation with thrust levels required by the disturbing torques.
- (3) It uses propellants with a specific impulse as high or higher than any competing system.
- (4) It is as light or lighter than any competing system because of (2) and (3).
- (5) It uses the same propellants as the vernier translation control system which simplifies the tankage problem.
- (6) It is inherently more adaptable to a digital autopilot, which will possibly aid in redundancy.

Some disadvantages are:

- (1) Its inherently great number of actuations during linear control is a possible reliability problem.
- (2) It has not yet been flight tested.
- (3) The power required for injector operation may exceed comparable requirements of other systems.

b. Two-level on-off system

This system could use a stored gas, a monopropellant and catalyst, or hypergolic bipropellant. The low thrust level of this system is designed for an economical limit cycle; the high thrust level is designed for the largest disturbing torques. The system could be designed so that the high and low thrust jets could be used individually and in combination so that a three-level system is attained.

~~CONFIDENTIAL~~

where:

- K = system gain in ft-lbs per radian
- m = ratio of rate to displacement gain
- I = moment of inertia
- τ = system time delay.

A damping ratio of 0.6 and a natural frequency of 1.0 radians per second were chosen for design values. This yields a system gain (K) of 12,500 foot-pound per radians and, with an available control torque of 1800 foot-pounds, the saturation displacement is 8.25° . The root locus of this system is shown in Fig. XI-9. The rate to displacement gain ratio (m), which is a function of the damping ratio and natural frequency, is 1.21. The saturation rate is therefore 6.82° per second.

The root locus indicates the small effect rather large gain (K) variations have on the system stability. There is also enough margin in the system time delay (τ) to indicate that possible changes due to such factors as experimental results should not require basic changes.

b. Coasting attitude control

This control system used the vernier attitude jets to maintain attitude control during the entire midcourse portion of a lunar flight, except for pitch and yaw control during operation of the 15.6 K engine. The attitude nozzle placement is shown in Fig. XI-1. The system has two modes of operation, proportional control (by pulse modulation), with essentially no deadspot during translation velocity corrections, and limit cycle control, in which the allowable deadspots vary from $+0.5^\circ$ to $+30^\circ$. These modes are discussed in the following sections.

Proportional control. This design is similar to that discussed previously for the 15.6 K engine pitch and yaw control system. In this system, however, a damping ratio of 0.5, and a natural frequency of 0.75 radians per second were selected for pitch and yaw control. The attitude jet thrust was selected to be 30 pounds to provide both adequate control torque and a suitably economical limit cycle. (The yaw channel uses two 15-pound jets simultaneously. Note configuration.) The control torque varies from approximately 270 foot-pounds to 390 foot-pounds as the center-of-gravity shifts with fuel consumption. Since the largest disturbing torque of any duration will be less than 60 foot-pounds this provides an adequate margin.

Figure XI-11 shows a block diagram of this system, which is similar except for constants to the 15.6 K engine attitude control. The system gain (K) is 7025 foot-pounds per radian and, with the minimum control torque of 270 foot-pounds, the saturation displacement is 2.3° . With the maximum control torque the saturation displacement is 3.3° .

~~CONFIDENTIAL~~

	<u>Pulse modulation</u>	<u>Two-level jet</u>	<u>Flywheel</u>
Propellant	160	160	190
Thrust units	24 (12 units)	48 (24 units)	24 (12 units)
Electronics	<u>20</u>	<u>15</u>	<u>30</u>
Total poundage	204	223	244

Weight of flywheel system for small disturbances and limit cycle included with propellant weight for large disturbances and reorientation.

The weights are near enough to each other not to be a deciding factor. However, weight plus the performance advantages of the pulse modulation system predicated its selection.

Figure XI-2 shows the midcourse configuration with the attitude jet positions on the propulsion module.

3. System Design

Midcourse attitude control, as developed in the preceding sections, is composed of the 15.6K pitch/yaw attitude control system and the coasting attitude control system. Their preliminary designs are discussed separately as follows.

a. 15.6K engine pitch/yaw control

This system acquires and maintains desired vehicle attitudes and rates during the operation of the 15.6K engine, using the four pulse modulated 300-pound thrust vernier translation engines for control torque (see Fig. XI-2 for the configuration). Attitude displacement signals are furnished by the inertial platform resolved into the appropriate body angles. Rate signals are obtained from the body mounted rate gyros because of the lack of correspondence between actual body rates and Euler angle derivatives under certain conditions, (see Appendix V. RC networks may be used for lead, either as the primary system or as a rate gyro backup, if further investigation indicates that the flight conditions permit.

In the preliminary design, crosscoupling may be ignored and pitch and yaw considered as separate identical channels. A simplified block diagram of a pitch/yaw channel is shown in Fig. XI-8. The open loop transfer function is:

$$\frac{K/I (1 + m s)}{s^2 (1 + \tau s)}$$

~~CONFIDENTIAL~~

The root locus of this system (pitch/yaw) is shown in Fig. XII-12. The rate to displacement gain ratio (ω) required by the damping ratio and natural frequency is 1.33, and the saturation rate is 1.73° per second. As before, the gain (K) and time constant (τ) margins are sufficient to prevent reasonable variations from requiring basic changes.

The roll control system is similar to the pitch/yaw channels. Its block diagram and transfer function are shown in Fig. XI-13. The control moment resulting from the 15-pound thrust yaw/roll jet couple and the 6-foot moment arm is 180 foot-pounds. This is high for the roll limit cycle, but is necessitated by both the roll and yaw control torque requirements. The maximum roll disturbing torque is approximately 30 foot-pounds from the thrust asymmetries of the vernier translation jets. (The vernier translation jets may provide their own pitch and yaw control during vernier velocity corrections, but roll control from the coasting system will always be required.)

The nominal damping ratio is 0.5 and the natural frequency is .75 radian per second. The root locus is shown in Fig. XI-14. The ratio of rate to displacement gain (ω) required is 1.33. The system gain (K) is 3460 foot-pounds per radian, and the saturation displacement and rate are 2.98° and 2.24° per second, respectively. The root locus shows that the gain and time constant tolerances are sufficient to indicate that the basic system will not require change.

Limit cycle. A pulse modulated control system will limit cycle with (1) deadspot rates which depend on the minimum control impulse of the system, and (2) a deadspot magnitude which is either deliberately selected or is inherent in the system. The equation for the fuel expenditure rate, developed in Appendix U is:

$$\text{lb/sec} = \frac{r I_t^2}{G \Delta e I I_{sp}}$$

where:

I_t = minimum impulse in lb-sec

r = moment arm in feet

Δe = one-half the deadspot in radians

I = moment of inertia in slug ft²

I_{sp} = specific impulse in seconds (280 sec).

It is evident that the expenditure rate varies as the square of the impulse. The minimum pulse width, which a 30-pound thrust system is capable of, is approximately .005 second. Using this, a deadspot of +0.5°, and the other system

~~CONFIDENTIAL~~

parameters, the fuel expenditure for a two-week limit cycle will be 1.64 pounds for pitch, 1.64 pounds for yaw and 1.83 pounds for roll.

In a pulse modulation system, the following relation holds:

$$T_h \cdot r \cdot R \cdot d = K \epsilon_e = \text{Torque}$$

where

T_h = thrust in pounds

r = moment arm in feet

R = pulse repetition rate in pulse/sec

d = pulse width

K = system gain in ft-lb/rad

ϵ_e = error signal in radians-- a function of ϵ and $\dot{\epsilon}$

and

$$0 \leq R d \leq 1$$

Since the limit cycle fuel expenditure rate varies as the square of the impulse, it is desirable to design the system so that the deadspot ϵ_e value calls for the minimum pulse width. In a pulse width modulation system (PWM), it is therefore necessary to change the repetition rate (R) when the deadspot is changed, or the system gain (K) selected for proper proportional operation must change. For small deadspots the repetition rates are so low that an unacceptable delay problem arises.

A pulse rate modulation (PRM) system does not have this problem (or the comparable problem of changing the pulse width with changes in deadspot) because the limit cycle will inherently use the systems minimum pulse width and, within limits, is not concerned with the repetition rate. This system has several disadvantages, however, the chief of which is the high repetition rates required during disturbances of any magnitude.

A combination pulse-width and pulse-rate modulation system is being developed. This system acts as a PRM system with small signals and with changes in the deadspot, and with larger signals it acts as a combination pulse rate and pulse width system. This prevents the required pulse rate from becoming too high. Since the minimum pulse width must be repeatable, a conservative value of .010 second was investigated, although 0.003 to 0.005 second appears attainable. The limit cycle fuel expenditure for two weeks $\pm 0.5^\circ$ deadspot and this pulse width is 6.6 pounds for pitch, 6.6 pounds for yaw and 7.3 pounds for roll, totaling 20.5 pounds.

This fuel expenditure is acceptable and is obtained with a system whose lead (or m value) was selected for proportional control. However, a deadspot of

~~CONFIDENTIAL~~

$\pm 3^\circ$ is permissible and, although this deadspot is not compatible with linear operation (with the control torque available), the system could be operated in a simple on-off manner except during velocity corrections and stellar observations. This would merely require changing the value of m to the optimum value or near it as developed in Appendix T and introducing the capability of changing between two modes of operation: (1) proportional operation with a small but adjustable deadspot, and (2) on-off operation with a large deadspot. The total two-week limit cycle fuel expenditure for the second system would be approximately 15 pounds. It therefore appears that decreasing the minimum pulse width will be more rewarding.

4. Mechanization

A breadboard of the yaw/roll channels has been constructed to test the operation of the system with the analog computer and also to test the circuit design. Results of the analog program are discussed in the following section.

Silicon semiconductors are used for all active elements, and the circuits are designed for operation in an ambient temperature of up to 125°C . This is much greater than the expected maximum temperature. Radiation, a second consideration in semiconductor design, will have little effect on performance because of (1) the allowed radiation level (due to the crew, and (2) the relative independence of the circuit operation on the semiconductor parameters because of the design.

A complete discussion of the autopilot mechanization, including circuit diagrams and operating characteristics, will be found in Appendix W.

5. Analog Program (A/P)

To validate much of the previous material, a tie-in of the breadboard coasting A/P was made with the analog computer. The computer simulated the system attitudes and disturbing conditions and furnished resultant error signals to the A/P. Figure XI-15 shows the block diagram of the A/P analog computer hook-up. Figure XI-17 is a photograph of the breadboard A/P unit.

Results of the studies with the analog computer indicate that the A/P performs its assigned tasks and is stable under all disturbing influence to which the system was subjected.

The plot shown in Fig. XI-17 typifies the A/P limit cycle, the system response to 1° and 3° steps and the newly established limit cycles. Figure XI-18 shows system response to a step input.

One of the limits of the simulation was that, over long periods of time, the natural machine drift for "open loop type" integrations in the computer approaches limit cycle rates and displacements. The drift rates were kept down by

~~CONFIDENTIAL~~

blasing off as much of the apparent machine drifts as possible by small opposing rates. Machine drift was thus maintained at a maximum level of 0.25 volt for a 6-minute running time.

D. RE-ENTRY ATTITUDE CONTROL SYSTEM

1. Introduction

The re-entry attitude control system on the Model 410 command module operates from the time of separation of the command and propulsion modules, throughout the re-entry operation. The flight regime includes both aerodynamic and nonaerodynamic phases which may alternate because of skip maneuvers. Sensor information is provided by the inertial platform, computer and body mounted rate gyros.

Configurations of the reactive and aerodynamic controls are shown in Fig. XI-2. Provision is made for both automatic and manual control of this system. Manual control is with an electric side stick control and toe pedal. This combination was selected for optimum pilot performance (see Ref. III-10).

The following sections are devoted to a more detailed discussion of the reaction and aerodynamic controls design.

2. Reaction System Requirements

The Model 410 configuration will employ four pairs of jets which will furnish pitch and yaw control when the dynamic pressure is less than 10 psf, and roll control during the entire re-entry flight. The nozzle configuration is shown in Fig. XI-2.

Requirements for the reactive pitch and yaw system are: (1) to cancel any tip-off rates incurred in separation from the propulsion module, (2) to maintain the proper orientation outside of the aerodynamic region, and (3) to cancel all crew, equipment and aerodynamic disturbances in the region of dynamic pressures less the 10 psf. These requirements are relatively easy to meet.

The roll control system provides control in both the space and aerodynamic regions of the re-entry flight. Since the disturbances will be small, the requirements are comparatively minor in the nonaerodynamic region. In the aerodynamic region, however, an estimated 1000 foot-pounds of control torque will be required at maximum q to handle disturbing moments due to yaw/roll coupling

Ref. III-10 NASA TN D-337 "Centrifuge Study of Pilot Tolerance to Acceleration and the Effects of Acceleration on Pilot Performance" - by B. Y. Creer, H. A. Smedal and R. C. Wingrove.

and axial misalignment of the vehicle. Since the system must be compatible with pilot control, consideration must also be given the magnitude of the control accelerations and the relative accelerations of the roll and pitch/yaw axes in regard to pilot preferences.

3. Reaction System Selection

The roll reaction system is most critical because of its operation in the aerodynamic region. This factor, and the use of a similar system on the propulsion and equipment module, makes a pulse modulated proportional system using high specific impulse hypergolic bipropellants the best choice.

Advantages of this system are:

- (1) Proportional control gives the best response to the roll commands required by the guidance system.
- (2) During manual control the system may be used as a proportional system or as an on-off system with several thrust levels.
- (3) The specific impulse is as high or higher than competitive systems.
- (4) The re-entry reaction autopilot may be integrated with the midcourse autopilot, decreasing complexity and increasing reliability.

Comparison of this system with competitive re-entry systems is similar to the comparison for midcourse controls; this comparison is shown in Table XI-2.

4. Reaction System Design

The roll control torque requirements (1000 foot-pounds) and the nozzle arrangement required by the Model 410 configuration (see Fig. XII-2) dictate a pitch and yaw torque of 500 foot-pounds. Since the moment of inertia about the pitch and yaw axes is about 3250 slug ft² the pitch/yaw control acceleration is about 8.8°/sec².

The system will be mechanized similarly to the midcourse system so that the same autopilot may be used with appropriate gain changes. The block diagram of pitch/yaw channel is shown in Fig. XII-20. Choosing a damping ratio of 0.5 and a natural frequency of 1.5 radians per second, the system gain (K) is more than 310 foot-pounds per radian. The saturation displacement is thus 3.9°.

The pitch/yaw channel root locus is shown in Fig. XI-20. The required value of rate to displacement gain ratio is 0.66; this yields a saturation rate of 6° per second.

The roll control torque of 1000 foot-pounds gives a roll control acceleration of $50.5^\circ / \text{sec}^2$ with a roll moment of inertia of 1130 slug ft^2 . For design purposes, tentative values for the damping factor and the natural frequency of 0.45 and 2.5 radians per second were chosen. These values must be made compatible (according to pilot preference) with the aerodynamic pitch/yaw system parameters, but the above values are suitable for a preliminary examination.

The block diagram and the transfer function of the roll control loop are shown in Fig. XI-21. The system gain (K) is 8440 foot-pounds per radian, and the saturation displacement is 6.8° . The root locus is shown in Fig. XI-22. The required value of rate to displacement gain (m) is .357, and the saturation rate is 19 degrees per second. These values are, of course, dependent on the tentative values of damping factor and natural frequency which may be changed because of human factors or other considerations.

5. Aerodynamic System Requirements

a. Aerodynamic stability coefficients

The aerodynamic stability analysis to date has been restricted to the pitch and roll axis with the assumption being made that the stability in yaw would be analogous to a previous analysis conducted on a lifting body similar to the Model 410 vehicle.

L-2-C configuration. Aerodynamic test data obtained from NASA, Langley Field were used to determine the pitch stability coefficients. This information consisted of C_n , C_a , and C_m versus angle of attack (α) data which were obtained at Mach 6.7. For the purpose of this analysis these coefficients were assumed to be invariant with Mach number.

From observation of the pitching moment coefficient versus angle of attack curves for various offset cg locations, it was decided that it would be desirable to limit control surface deflections to $\delta = 90^\circ$ maximum. To trim at max C_{L_L} with this limitation requires a 2% forward location of the cg using flap configuration F-1 (chord = 1.748 ft, span = 2.32 ft). It was necessary to develop pitching moment curves for the 2% cg location from the 1% and 3% cg locations for which data were available. These data are presented in Fig. XI-23. Since the stability analysis was to be conducted for the angle of attack producing maximum C_{L_L} ($\alpha = 55^\circ$), $C_{m\alpha}$ was determined for this angle of attack. The pitching moment coefficient per deflection of the control surface, $C_{m\delta}$ was determined by constructing Figs. XI-23 and XI-24.

From equations (7) and (8) of Appendix X it can be seen that K_a and ω_n are functions of q for any particular vehicle configuration and angle of attack. A plot of K_a and ω_n versus q for the L-2-C configuration is shown in Fig. XI-25.

~~CONFIDENTIAL~~

A corresponding plot of K_a and ω_n vs. q for the integrated W-1 configuration is shown in Fig. XI-26. Table XI-3 shows a tabulation of q , ω_n and K_a for the L-2-C configuration.

Table XI-3

q	ω_n	K_a
18.61	0.47	0.10
170	1.41	0.88
369	2.08	1.91
450	2.30	2.34
634	2.73	3.29
800	3.06	4.15

b. Stability characteristics of the Model 410 vehicle

The Model 410 vehicle has in general certain static characteristics similar to those of the W-1 configuration. The geometry can be altered to be provided with sensitive adjustments for trim and stability. In conjunction with appropriate pitch flaps, stability and control are maintained over the large range of angles of attack desirable for versatility in permissible re-entry trajectories. It is desired to trim at maximum C_L which occurs at $\alpha = 30^\circ$ with the pitch flap fully retracted. To provide a high lift attitude without a pitch flap, we must trim at (L/D) which occurs when $\alpha = 13^\circ$.

Pitching moment coefficient data appears in Fig. XI-27 for the basic geometry and for the aft end flattened. The basic geometry refers to a spherical nose and 18° semicone without flaps. The pitching moment coefficient data is presented assuming that $l = 12.5$ feet with a nominal reference.

area of 100 ft^2 . The basic shape was found to be statically stable for cg. locations forward of $x/l = 0.65$ measured from the nose and trimmed at $= 0.11$ measured downward from the cone axis.

The pitching moment coefficients for the aft flattened Model 410 is also shown in Fig. XI-27. "Aft flattened" refers to a geometric modification where 20% of the reference length (\mathcal{L}) of the 18° cone, measured from the flat side of the cone, is removed. This modification decreases stability but allows an increase in the trim angle by a large amount for a given cg location. This can be observed by noting the positive slope of the C_m vs α curve for various values of

~~CONFIDENTIAL~~

An alternate modification to the basic shape is the nose tip-up for which the pitching moment coefficients are also shown in Fig. XI-27. A 5° tip-up refers to a geometric modification where the entire nose portion forward of Station 50 is tilted upward 5° with respect to the cone axis. This increases stability as indicated by the larger negative slope of the pitching moment coefficient versus α .

c. Directional stability

The basic Model 410 command module is to some extent directionally unstable without side flaps for the cg at 0.6351. In Fig. XI-28 plot of yawing moment coefficient, C_n versus sideslip angle, β_0 for various angles of attack is shown. Side flaps are required to provide directional stability to the configuration, to trim for misalignments and to provide yaw damping. The basic Model 410 configuration without flaps is more directionally stable than the W-1 configuration without flaps.

6. Aerodynamic System Selection

a. Adaptive autopilot analysis

Because of the wide variations in dynamic pressures encountered during a typical re-entry the rate damping gain would normally be programmed to change with a change in K_a . To avoid this gain programming, it was decided to investigate a pseudo-adaptive autopilot design similar to that described in Ref. III-12.

The form assumed for the proposed adaptive autopilot of the pitch axis is shown in Fig. XI-29. Ideally this system would operate such that the inner loop $\frac{\dot{\theta}_o}{\dot{\theta}_c} \approx 1$, where $\dot{\theta}_o$ is the vehicle pitch rate and $\dot{\theta}_c$ is the pitch rate com-

manded by the model. Under this condition of operation, the closed loop transfer function is

$$\frac{\theta_o}{\theta_i} = \frac{1}{1 + \frac{s}{K_\theta} + \frac{s^2}{K_\theta/T_\theta}} \quad (1)$$

~~CONFIDENTIAL~~

where Θ = vehicle pitch angle

Θ_i = input or commanded pitch angle

K_Θ = model gain

T_Θ = model time constant.

Thus it can be seen that the response characteristics are determined by the gain and time constant of the model. Assuming an ideal inner loop, the natural frequency and the damping ratio are given by the following expressions:

$$\omega_{n1} = \sqrt{\frac{K_\Theta}{T_\Theta}} \quad (2)$$

$$\zeta_1 = \frac{1}{\sqrt{K_\Theta T_\Theta}}$$

For an ideal inner loop the choice of $K_\Theta = 2$ and $T_\Theta = 0.3$ was based on achieving a reasonably rapid response with a small amount of overshoot. Substitution of these values in equation (2) and (3) yields the following:

$$\omega_{n1} = \sqrt{\frac{K_\Theta}{T_\Theta}} = \sqrt{\frac{2}{0.3}} = 2.58 \text{ rad./sec.} \quad (4)$$

$$\zeta_1 = \frac{1}{2\sqrt{K_\Theta T_\Theta}} = \frac{1}{2\sqrt{2 \times 0.3}} = 0.645 \quad (5)$$

In reality, the inner loop is not ideal. The assumed values for the transfer functions of the various components of the block diagrams shown in Fig. XI-29 are given below:

$$(6) \quad \frac{\dot{\Theta}}{\delta E} = \frac{K_a}{s^2 + \omega^2}$$

$$\omega \leq 3 \text{ rad./sec.}$$

$$K_a \leq 4.15$$

for the L-2-C Configuration

$$\frac{\dot{\delta}_A}{\delta} = \frac{1}{1 + T_S} \quad (7) \quad T_S = 0.01 \text{ sec.} \\ \text{(Rate Servo)}$$

$$\text{Rate Gyro} = H = \frac{\omega_G^2}{s^2 + 2\zeta\omega_G s + \omega_G^2} \quad (8)$$

The derivation of Eq. (6) will be shown in Appendix X. The rate gyro has a natural frequency of 26 cps and a damping ratio of 0.5. Substituting these values into H yields:

$$H = \frac{(141)^2}{(s + 81.5 + j141)(s + 81.5 - j141)}$$

The open loop transfer function at the inner loop is given by GH, where:

$$GH = \frac{K_a \omega_G^2}{(s^2 + \omega^2)(1 + 0.01s)(s + 81.5 + j141)(s + 81.5 - j141)}$$

The poles and zeros of GH representing the airframe, servo and rate gyro were plotted and the root locus of GH was determined and is shown in Fig. XI-30. The root locus was found to be unstable for values of gain greater than zero. It was desired to have the root locus pass through the point $S = -15 + j30$ giving a damping ratio of 0.45 at this point. To determine the lead network transfer function to give the desired characteristics, the following technique illustrated in Fig. XI-31 was employed. The amount of lead required at the design point of $S = -15 + j30$ was determined and divided by two. It was found that the lead circuit must furnish 85° lead at this point. A line from the origin to the design point and a line parallel to the real axis through the design point was then constructed. The obtuse angle formed by the intersection of the two lines was bisected and using the design point as the vertex, the desired lead angle was constructed such that the lead angle was bisected by the obtuse angle bisector. The intersection of the included sides of the lead angle with the real axis then gives the desired poles and zeros for the lead network (The pole being the

~~CONFIDENTIAL~~

intersection which the the greatest distance from the origin and the zero being the closed intersection with the origin.)

A root locus plot of the inner loop of the pseudo-adaptive control system with lead circuit constants of $\alpha = 13$ and $T = 0.017$ is shown in Fig. XI-32. With the introduction of the lead circuit the open loop transfer function is:

$$G'H' = \frac{K_a K_r \omega_g^2 (1 + 0.107s)}{(s^2 + \omega^2)(1 + 0.00823s)(1 + 0.015s)(s^2 + 163s + 26524)} \quad (11)$$

$$G'H' = \frac{K(1 + 0.107s)}{(s^2 + \omega^2)(1 + 0.00823s)(1 + 0.015s)(s^2 + 163s + 26524)} \quad (12)$$

Where $K = K_a K_r \omega_g^2$

$$G'H' = \frac{K(1 + 0.107s)}{(s^2 + \omega^2)(1 + 0.00823s)(1 + 0.015s)(s + 81.5 + j141)(s + 81.5 - j141)} \quad (13)$$

~~CONFIDENTIAL~~

b. Rate saturation

In conjunction with the preliminary design of the autopilot, an investigation of the control system rate saturation has been conducted in an attempt to reduce control power requirements during re-entry. Since rate saturation acts like a nonlinear element, describing function techniques (described in Ref. III-13) were used. The purpose of this investigation was to specify the minimum surface deflection rates necessary to assure a stable operation in the frequency range of interest.

The effect of rate-limiting in the pseudo-adaptive autopilot is to produce a high frequency chatter at small amplitudes. The magnitude of this chatter is directly related to $\dot{\delta}_{\max}$, however, this $\dot{\delta}_{\max}$ limitation will not affect vehicle stability since a limit-cycle oscillation at high frequency and low amplitudes will have a negligible effect on the vehicle dynamics. Reduction of $\dot{\delta}_{\max}$ will affect the vehicle response, but this effect using the pseudo-adaptive technique is very difficult, if not impossible, to analyze unless the system is evaluated on the analog computer.

To have some basis for establishing $\dot{\delta}_{\max}$ by hand calculation, the simple control system shown in Fig. XI-33 was considered.

By use of describing function techniques, the system shown in Fig. XI-33 can be analyzed to establish the minimum value of $\dot{\delta}$ required for stable operation.

If the signal level (X) at the input to the nonlinear element is increased beyond the saturation level, the value at N decreases, causing the pole to move toward the origin. This distorts the root locus so that it crosses the imaginary axis at a much lower frequency. The resultant effect is to cause an instability to occur as a function of amplitude θ_i . The value of θ_i which would cause an instability to occur is extremely small, on the order of 2 degrees. Because of the effects of rate saturation in the pseudo-adaptive autopilot, along with the fact that in the lead circuit type of autopilot a programming of gains would be required to give us well-damped operation, a third autopilot configuration was considered.

7. Aerodynamic System Design

a. Position-rate-integral control system, L-2-C configuration

Previous studies conducted on the autopilot requirements of a lifting body returning from an earth orbital mission indicated, from a linear analysis, that a position-rate-integral type of autopilot would provide a stable re-entry operation. This analysis was later substantiated by a six degree of freedom analog simulation which included nonlinearities, crosscoupling and vehicle dynamics.

Because of the similarity of the aerodynamic transfer functions of the L-2-C, Model 410 and the integrated W-1 with the configuration previously studied, this type of autopilot was investigated as a possible configuration for the Apollo re-entry vehicle and is shown in the block diagram in Fig. XI-34.

The relations between the gains K_1 , K_2 and K_3 are given by

$$\frac{K_3}{K_1} = \frac{K_1}{K_2} = 0.5\omega_n \quad (14) \quad K_1 = 0.4 \quad (15)$$

Both K_3 and K_2 can be written as functions of ω_n .

$$K_3 = 0.2\omega_n \quad (16) \quad K_2 = \frac{0.8}{\omega_n} \quad (17)$$

The transfer function for this type of control system is given by

$$\frac{\theta_o}{\theta_i} = \frac{K_2 K_a N K_H (S^2 + K_V/K_2 S + K_3/K_2)}{1 + \frac{K_2 K_a N K_H (S^2 + K_V/K_2 S + K_3/K_2)}{S(S+NK_H)(S^2 + \omega_n^2)}}$$

The derivation of this equation is shown in Appendix Y.

The three flight conditions of max q, mid q, and min q were evaluated. As a preliminary determination of the effects of rate saturation, the hydraulic pole at -20 was moved towards the origin. When $N = 1/2$ the hydraulic pole has a value of -10 and $N = 1/4$ the hydraulic pole has a value of -5. Figs. XI-35 through XI-37 show the max q condition and the effects of rate saturation. As the pole moves toward the origin, the root locus is distorted such that it approaches its asymptote at much lower values of gain. Figs. XI-38 through XI-43 show the min q condition and the effects of rate saturation. Figs. XI-44 through XI-48 show the mid q condition and the effects of rate saturation. The effects of rate saturation on the mid q and the min q conditions are the same as that observed in the max q case, namely, as the pole moves toward the origin the root locus is distorted such that it approaches the asymptote at much lower values of gain. This causes the system to be very underdamped. For all the cases investigated the root locus plots show stable system operation. Although stable operation is achieved, the values of gain at the max q condition show operating damping ratios of about 0.2.

~~CONFIDENTIAL~~

In an attempt to obtain a well-damped operation over the flight profile, a constant gain of $K = 4$, was added in series with the position-rate-integral system. For the max q and min q case the damping ratio varies from $\zeta = 0.4$ to $\zeta = 0.6$. However, the damping ratio for the mid q case gives the overdamped value of $\zeta = 0.95$. This shows that for a fixed value of gain (K), the damping ratio varies from a well-damped to an overdamped and then back to a well-damped system as the dynamic pressure is increased to its maximum value. In order to have well-damped operation for all flight conditions it will therefore be necessary to program several steps of gain as a function of q .

b. Position-rate-integral control system for integrated W-1 vehicle

Because of the similarity in the aerodynamic transfer function for the integrated W-1 and L-2-C configuration, only the gain constants for the position-rate-integral system were modified for the stability analysis of the integrated W-1. From previous experience on the L-2-C configuration, it was noted from the root locus plots that an underdamped control system resulted for various possible aerodynamic flight conditions. By varying K_2 in the characteristic equation, $1 + F(S) = 0$, the root locus can be varied to give us better damping. The equations for the modified control system are:

$$K_2 = \text{constant} \tag{19}$$

$$\frac{K_1}{K_2} = \frac{K_3}{K_1} = 0.5 \omega_n \tag{20}$$

If the values of $K_2 = 0.4, 0.6,$ and 0.8 are used, the characteristic equation can be expressed as a function of ω_n . This is given by Eq. (21).

$$1 + \frac{K_2 K_a N K_H (S^2 + 0.5 \omega_n S + 0.25 \omega_n^2)}{S(S + N K_H)(S^2 + \omega_n^2)} \tag{21}$$

The advantage of using the given values of K_2 in conjunction with Eq. (20) is that all cases reduce to Eq. (21) as a result. This means that all of the poles and zeros will be coincident, however, the gain constant K_2 will be changed.

The following table is a tabulation of flight conditions and the corresponding damping ratios. These damping ratios are shown for values of $K_2 = 0.4$ and $K_2 = 0.6$.

TABLE XI-4

Flight Condition (psf)	Gain	Gain	ζ	ζ
	$K_2 = 0.4$	$K_2 = 0.6$	$K_2 = 0.4$	$K_2 = 0.6$
Max q, q = 476	120	180	0.4	0.62
Mid q, q = 238	60	90	0.3	0.5
Min q, q = 20	5	7.5	0.1	0.15
Min q, q = 5	1.3	1.9	0.05	0.1

For $K_2 = 0.4$, the control system is seen to be underdamped for mid q and min q flight conditions. In order to study the effect of varying K_2 , it was changed to 0.6. By using $K_2 = 0.6$, the characteristic equation remained the same as previously derived. With $K_2 = 0.6$, the damping ratios were increased such that at mid q an ideal damping ratio of $\zeta = 0.5$, at max q with a slightly overdamped value $\zeta = 0.62$ and at min q the underdamped value of $\zeta = 0.15$ were realized. With a more detailed study it may be possible to adjust the value of K_2 to obtain satisfactory damping throughout the entire flight regime.

As in the L-2-C configuration, the effects of rate saturation were observed by moving the hydraulic pole at -20 towards the origin. The effects on the root locus were the same as those observed in the L-2-C configuration, namely, that rate saturation causes the damping to decrease as the gain is increased. Figures XI-49 through XI-63 show the effects of rate saturation for the max. q, mid q and the min q cases.

c. Position-rate-integral control system Model 410 configuration

Because of the similarity of the aerodynamic characteristics of the Model 410 configuration with the L-2-C and the integrated W-1, the position-rate-integral system is recommended from the Model 410 configuration. Like the L-2-C and the integrated W-1, the Model 410 will have negligible aerodynamic damping. With negligible damping, the aerodynamic transfer function can be assumed to be of the form:

$$\frac{\theta}{-s} = \frac{K_a s}{s^2 + \omega_n^2} \quad (2.2)$$

$$K_a = \frac{f S C_{ms}}{I_{yy}} \quad (23)$$

$$\omega_n^2 = \frac{f S C_{m\dot{\alpha}}}{I_{yy}} \quad (24)$$

The root locus for the Model 410 will generally have the same shape as that of the L-2-C and the integrated W-1 but the position of the poles will vary slightly and the value of the aerodynamic gain will change slightly. It is felt with a more thorough study the gain constants in the position-rate-integral system law can be so adjusted to give a well-damped system.

d. System design summary

The linear aerodynamic stability analysis has been restricted to the pitch and roll axes because of the symmetry of the L-2-C and the integrated W-1 configurations. The three basic types of autopilots which were considered were of the lead circuit, the adaptive and the position-rate-integral type. Of the autopilots examined the position-rate-integral is recommended for the Model 410 because it is felt that the gain constants can be so adjusted to give good damping for all flight conditions. The effects of rate saturation in the hydraulic servo have been approximated and examined. It was approximated by moving the hydraulic pole at -20 towards the origin. It was found that rate saturation tended to decrease the damping and lower the gain of the overall control system. The effect of rate-limiting in the pseudo-adaptive autopilot produced a high frequency chatter at small amplitudes. The lead circuit type of autopilot was rejected because a programming of gains would be required.

~~CONFIDENTIAL~~

~~CONFIDENTIAL~~

XII. RENDEZVOUS CONTROL SYSTEM

A. INTRODUCTION AND DESIGN CRITERIA

1. Study Definition and Rendezvous Problem Description

The purpose of this study is to determine an orbital rendezvous technique and to evaluate the effects of implementing this technique on the Apollo spacecraft. Orbital rendezvous is defined as the precise simultaneous nulling of the position and velocity of a vehicle relative to a "target" satellite. This study will be limited to consideration of the problem from the time the spacecraft is injected into a prescribed orbit (which closely approximates the target vehicle orbit) until rendezvous is achieved. Within this study definition, it is then assumed that the ephemeris of the orbital target is known, the ascent inertial guidance techniques determined and the associated problems (such as inertial guidance programming, launch time tolerance) have been solved.

Space track is capable of locating a cooperative satellite (in this case the target satellite) in its orbit within a 3σ volume of uncertainty which is 10 nautical miles long (in the direction of satellite travel) and elliptical in cross-section with axes of 4 nautical miles (high) and 2 nautical miles (wide) respectively.

The onboard inertial guidance system will accomplish the ascent and injection guidance required to place the Apollo spacecraft in the vicinity of the satellite with which rendezvous is to be made. The anticipated bounds on the errors associated with injecting into the predetermined orbit on the prescribed schedule are presented below:

3σ Injection Errors

Altitude	4570 feet
Down range	3030 feet
Cross range	2560 feet
Velocity	3 fps
Flight path angle - in plane	.33 mils
Flight path angle - out of plane	.08 mils

These injection errors, based on previous studies conducted by The Martin Company, have been modified by estimated performance improvements realizable with the Apollo inertial guidance system.

~~CONFIDENTIAL~~

To accomplish rendezvous of two earth orbital satellites in essentially identical orbits requires that one of the vehicles involved have a system capable of acquiring the other (either optically or electronically), making a direct determination of relative position and rate, and cancelling these differences. Therefore, the Apollo spacecraft will require a system capable of acquiring the (cooperative) target and of determining position and rate differences, an attitude control system, and a maneuvering system to accomplish the terminally-guided rendezvous.

Previous studies conducted at The Martin Company and elsewhere have demonstrated the capability of a pilot to control manually a rendezvous operation. Visual observation of the target is made through a television display. This display may comprise the operator's sole source of information or it may be supplemented by radar-acquired range and range rate information. The rendezvous vehicle (Apollo) is slaved to some fixed reference and the operator achieves rendezvous by commanding actuation of maneuvering thrust units located along the vehicle's principal axes.

A system such as that briefly discussed above can be implemented on Apollo by the simple addition of the translation thrust units and controls. An automatic system can be implemented at the expense of additional complexity, i. e., search and acquisition radar, added computer utilization, a short range radar to supply range, range rate, angle and angle rate information plus the translation thrust units.

The complexity of an automatic system does not appear warranted for a manned-vehicle application. This statement is justified in the following section.

2. Manually Controlled Rendezvous System

This system is composed of a 1) television camera and monitor, 2) a control station from which the translation thrust units are operated, 3) translation thrust units and possibly 4) a simple radar to provide range and range rate data to the control station. All maneuvering commands are initiated by an operator (pilot). The pilot derives angle and angle rate data from the television monitor and either infers range and range rate data from the same source or obtains such data from the range and range rate radar.

One of the basic problems associated with this system is that of target recognition. For the large initial separation distances possible at the termination of the orbit injection phase (termination of inertial guidance also), the target satellite would first appear as a bright star on a television screen. This poses a problem of recognizing the target satellite, against a fixed star background. The recognition problem can be alleviated by proper choice of injection conditions. Tail chases (direct or inverse) are ruled out immediately for a passive satellite, because any relative motion is essentially along the line of sight and the very low drift rate of the target may be indiscernible from the star field itself. Any displacement of the rendezvous vehicle normal to the target

~~CONFIDENTIAL~~

vehicle path would be advantageous because the relative motion would then be normal to the line of sight. The most favorable arrangement would be to couple this normal displacement with a lead on the target and a velocity disadvantage. Then the apparent motion of the target satellite would be contrary to the fixed star field and recognition should be simple. The injection method would be to inject the rendezvous vehicle with a displacement normal to the target orbit, ahead of the target with a velocity deficiency. The displacement could be to either side of or below the target. A commanded attitude change would be made to properly orient the television camera.

In addition to the detection problem, a problem arises in the detector itself. A vidicon camera which had sufficient sensitivity and an adequate field of view such that a satisfactory search could be conducted at reasonable ranges, might not provide useful intelligence information after maneuvering close to the target. In other words, the acquisition phase would necessitate high sensitivity; and, optically, this would be accompanied by narrow fields of view. This problem may be met by having a large field of view for acquisition and a smaller fields of view for inspection. In the simulation program discussed later, a 90° field, a 10° field, and a 4° field were used for these purposes. Successful tracking would also require good target illumination; and, at long range, the foot-candle illumination of the target may border on the sensitivity threshold of the vidicon tubes.

In an attempt to gain more information on this rendezvous technique, The Martin Company has conducted an analog simulation program. Applicable portions of this study are described in the following section.

3. Analog Study

a. Description of problem

The analog simulation begins with injection of the rendezvous vehicle into orbit below and ahead of the target and with a velocity deficiency. It is also assumed to be automatically attitude-stabilized to the local earth vertical. The fore-aft (circumferential), right-left (lateral) and up-down (radical) jets are, therefore, always correctly oriented. Two translation thrust levels for coarse and fine control are available at the discretion of the operator.

The operator controls the vehicle from a control station, using information transmitted from the 90° field of view camera and displayed on a TV screen. The field of view may be switched to 10° or to 4° when desired; this will increase the size of the image 9 or 22.5 times, respectively. To do this without losing the image requires that the target satellite be very close and directly above the rendezvous vehicle; however, the stringency of this requirement is inversely proportional to the radial distance between the rendezvous vehicle and the target satellite.

~~CONFIDENTIAL~~

The nominal rendezvous situation simulated is as follows: Following injection, the rendezvous vehicle 48,000 feet below and 30,000 feet in front of the target satellite, with the target satellite gaining at 150 to 300 fps. The target satellite image appears as a point about 3/15 of the way down from the top of the TV screen and moves slowly down -- requiring from 100 to 200 seconds to reach the center if no thrust is applied. The lateral error is within +30,000 feet range, and 50 fps rate. The problem is to null the range and rate differentials with the translation jets so that rendezvous may be accomplished.

The information desired from the analog program is as follows:

- (1) Can a pilot achieve a rendezvous with a satellite using on-off thrust control?
- (2) What control accelerations are optimum for coarse and fine positioning?
- (3) What are the time and fuel requirements?
- (4) What would be the effect of any limit cycle in the attitude control system on the above subjects?

b. Description of simulation

Since the vehicle is stabilized to the local vertical axis system, the relative motion between vehicle and satellite is observed in the axis system. Equations of relative motion derived for this case (see Appendix AA) are as follows:

$$\ddot{y} = -\omega^2 y + \frac{T_y}{m}$$

$$\ddot{c} = 2\omega \dot{r} + \frac{T_c}{m}$$

$$\ddot{r} = 3\omega^2 r - 2\omega \dot{c} + \frac{T_r}{m}$$

where

\ddot{y} = relative lateral displacement, positive when the vehicle is to the left of the satellite (looking in direction of satellite travel).

\ddot{c} = relative fore-aft (circumferential) displacement, positive when the vehicle is behind the satellite.

\ddot{r} = relative vertical (radial) displacement, positive when the vehicle is above the satellite.

~~CONFIDENTIAL~~

ω = angular rate of satellite orbital motion (assumed circular).

T = thrust applied to vehicle, subscript denotes direction of thrust component.

m = mass of vehicle

An interesting problem in the analog of this system was the display or TV screen simulation. The circumferential and lateral positions of the target satellite relative to the rendezvous vehicle are indicated by corresponding positions on the screen. The relative radial distance, however, is indicated only by the relative size of the image. This simulation was accomplished with a Lissajou pattern by putting a 400 cps voltage on the X axis of the screen and a similar voltage shifted 90° out of phase with a passive phase shift network on the Y axis. Both voltages were inversely proportional to the radial distance between the satellite and vehicle (an approximation which assumes the circumferential distance C is relatively small). They were also inversely proportional to the field of view half-angle Θ (either 45°, 5°, or 2°). The distance on the screen representing the circumferential and lateral position is also directly a function of the corresponding distance and inversely a function of the radial distance and the tangent of the field of view half-angle. The voltages which simulate the satellite in size and position are:

$$V_x = \frac{-ky}{r \tan \Theta} + \frac{Rk \cos \omega_1 t}{r \Theta}$$

$$V_y = \frac{-kc}{r \tan \Theta} + \frac{Rk \sin \omega_1 t}{r \Theta}$$

where R is the satellite's radius, k is a constant, and ω_1 is 2×400 .

A "slant range" dot displaced relative to a reference mark was also displayed on the scope (Fig. XII-1) to give the pilot an integrated display. This displacement was a voltage proportional to the line of sight range obtained from the radar altimeter. The relative motion of the dot referred to the reference mark gave the pilot an indication of closing rate. The radar antenna was assumed locked on the target. The tracking function may be assumed to be the task of a second crew man.

~~CONFIDENTIAL~~

The operator's control panel has circumferential (fore-aft); lateral (right-left) and radial (up-down) thrust switches, each accompanied by a thrust level switch for coarse or fine control. Colored lights gave an indication of switch position. The photograph (XII-1) shows the latest control panel for this problem.

For experience with various possible situations, sets of initial conditions were calculated using various combinations permitted by the position envelopes, generally using maximum rate differences. To keep the operator from recognizing a problem too easily from the initial screen position, several problems were set up, each of which had the same initial screen position but greatly different actual positions and rates.

A typical problem begins with the pilot seated at the control panel facing the screen, with thrust levels set on high, and the field of view switch set on 90°. When the computer operator pushes the "operate" button, the satellite image moves toward the bottom of the screen, and also left or right at rates depending on the initial conditions. The pilot then throws the proper thrust switches to start the image moving toward screen center. He may also apply a short upward radial thrust if, in his judgment, he can center the image and switch to the small view screen before the radial distance becomes too small.

Since there is no damping, the pilot must be careful to apply counter-thrust well before the image reaches the center of the screen. The ideal is to apply counter-thrust such that rate and position are nulled simultaneously and the thrust immediately cut off. The pilot switches to the 4° lens as soon as the spot is approximately centered. At this time it is often advisable to switch to low level thrusts. He is then able to judge his radial distance from the image diameter and decide whether to continue coasting or apply upward or downward thrust. His intent at this time is to slow or stop his upward velocity close to the satellite and observe at close range. Having demonstrated the ability to make prolonged observations, the pilot then will proceed to move the vehicle upward to make contact.

The first tests were made to determine the optimum control accelerations. It was very difficult to judge on the basis of relative performance but, subjectively, most operators considered 15 ft/sec² for coarse control and 1.5 ft/sec² for fine control best. These accelerations were then used in all subsequent tests.

c. Presentations

The first presentation considered is the "out the window" display in which the pilot has only the information available by looking at an object of unknown size, distance and velocity. However, by assuming the velocity discrepancy to be between 150 and 350 fps, inferences concerning radial and circumferential distances may be made even when the image is only a point.

~~CONFIDENTIAL~~

~~CONFIDENTIAL~~

Since the satellite will appear as a point until it is very close when viewed on the 90° field, the pilot is unable to make distance and radial rate judgements based on size until he can use the 10° or the 4° field. This means that the lateral and circumferential range discrepancies must be nulled before reliable radial information may be obtained. This initial uncertainty makes it prudent to avoid boosting upward at the beginning unless the circumferential velocity discrepancy movement and the response to circumferential and lateral boosting definitely indicate a large radial distance.

The usual rendezvous path with this type of information is, therefore, a dog-leg with little radial adjustment until the circumferential and radial distances and rates are nulled sufficiently for small screen viewing, and then radial control until an observational position or contact is made. If there is difficulty in nulling the circumferential and lateral ranges, and if there is an upward rate due to the initial conditions and/or upward thrusting, then there is a likelihood of overshoot. This is because by the time a change in image size is noted on the large field, it is usually too late for downward thrusting to be effective.

It was learned that when circumferential and radial differential rate information was provided to the pilot on meters, he was able to fly a much more direct rendezvous path. This is due partly to the confidence generated by knowledge of the radial rate, since he now has some idea of how long it would take to null it. It was found to be easier to null range and rate simultaneously when the rate is known and not merely inferred from the rate of position change on the screen.

When range information was displayed on meters, or a line of sight range dot was displayed on the scope, improvements up to 50% in the figure of merit (which is the product of the time required and fuel expended) were noted, although some operators showed little improvement over their runs with rate information.

The presentations studied were:

- (1) Television display only.
- (2) Television display plus range and range rate (all axes).
- (3) Television display plus range and range rate (radial only).
- (4) Television display plus range only.
- (5) Television display plus range rate only.
- (6) Television display plus "Line of Sight" range dot on scope.

Evaluation of runs made with the attitude limit cycle indicate that its effect does not appear important.

d. Evaluation methods

The goals of each analog run were to close in on the satellite as quickly as possible, to hit it with as low a closing velocity as possible and to expend as little reaction mass as possible.

Since short close-in time, low final closing velocity and low fuel expenditure are incompatible, the product of closing time and the weight of reaction mass expended was used as a figure of merit to compare successful flights- i. e., which hit the satellite and had a satisfactorily low contact velocity.

e. Learning process

That there is a definite learning process involved in flying the vehicle to a rendezvous is evidenced by fewer misses and better figures of merit as the operator becomes more experienced (Fig. XII-2). Since there were only a limited number of initial conditions used, it was realized that once a pilot recognized a problem, he would be able to respond from memory rather than his estimate of the situation from the data. To avoid this as much as possible, the problems developed looked similar initially but were actually as different as possible in range and rate. This made it unwise to assume a knowledge of distance and rate from the initial screen position of the image.

Beginners appeared prone to make the following errors:

- (1) Starting reverse thrust when too near the desired position thus overshooting and consuming extra time and fuel. (Fig. XII-3)
- (2) Overthrusting, or controlling at too high rates, requiring extra fuel to kill off the high rates, and making control difficult near the target.
- (3) Not utilizing information on radial distance gained from image size and apparent reaction to circumferential and lateral thrusting; this often resulted in failure to thrust radially toward the target early in the maneuver when such procedure was warranted; the time to rendezvous thus became excessive.
- (4) Concentrating on one problem and forgetting others; e. g., by attempting only to center the image in only one direction at a time so much time would elapse by the time the narrow field of view could be used that a generally poor run would be made.
- (5) Changing thrust levels at the wrong time; if velocities were built up using high thrusts, and the thrust levels were then cut, the operator often had no real sense of how long to thrust at the low level to kill off the velocities.

People with various training and experience backgrounds successfully flew the problems after only a short briefing. Judging from quality of performance, however, it seemed that pilot training and/or some theoretical knowledge of undamped on-off control was helpful.

The ability of most people to make successful runs after only short periods of instruction and the continued improvement of experienced operators indicate that manual control of satellite rendezvous is feasible. (Figures XII-2 through XII-4) Although the objective initially was only to make contact at a low velocity, later runs showed that actual docking-type rendezvous could be accomplished, and the pilot could position himself at will.

f. Conclusions

The following conclusions were drawn from analysis of more than 400 analog runs:

- (1) A pilot is capable of making an orbital rendezvous with an on-off control system.
- (2) Initially, an acceleration of 15 ft/sec^2 for coarse position control and 1.5 ft/sec^2 for vernier control appeared to be about optimum for a pilot-controlled rendezvous. No clear-cut performance advantage is evident by use of these high accelerations, however. (It should be noted that an acceleration of 15 ft/sec^2 may acquire a thrust level too high to be practical for large vehicles.) The latest studies with heavier vehicles and the lower accelerations achievable ($3.2 - 4.9 \text{ ft/sec}^2$) demonstrated that one level of thrust is adequate for rendezvous and docking maneuvers.
- (3) Although time and propellant requirements are inversely related, it appears that a propellant weight of $1/8$ the vehicle loaded weight (propellant specific impulse of 280 sec) is sufficient to complete the rendezvous maneuver in a time somewhat less than 500 seconds for the initial conditions selected. (It should be noted that the Apollo Guidance System is capable of better injection accuracies than those used in this study. This should result in a reduction in both propellant required and time required to accomplish the rendezvous maneuver.)
- (4) An attitude limit cycle has very little effect on the pilot's ability to achieve contact, but does add to propellant requirements and requires greater pilot concentration.

B. TRANSLATION AND ATTITUDE CONTROL CONFIGURATIONS

Several systems for maneuvering during an orbital rendezvous are discussed in this section and compared in their operational and configuration requirements. The systems fall into two general categories in which 1) translation control is available along a single axis which is positioned by the attitude control system, or 2) translation control is available along all three axes which are automatically held to some inertial reference.

The present operational concept assumes a man in the loop possibly using radio direction-finding for initial acquisition, a television system for final acquisition, and a radar altimeter for line of sight range and range rate. The system could use tracking radar; however, in this case an automatic rendezvous seems indicated. In either case, the comparisons set forth in this section will remain substantially the same.

Three representative configurations and techniques are discussed below:

1. Single Axis Translation Control

The control nozzle positions of this system are shown in Fig. XII-5. Nozzles are located to thrust in opposite directions along the longitudinal axis. (A system with only one thrust direction in which the vehicle is rotated 180° for thrust reversal is conceivable, but would be inadequate for close positioning.) The system illustrated requires two forward facing nozzles on the mission module because it is not feasible to place a nozzle in front of the Model 410 command module.

A rendezvous would be effected with this system as follows: After injection, the pilot scans the volume of space in which the target is expected to be by gimbaling the TV camera. The vehicle is automatically held to some inertial reference giving the best field of view in the desired direction. If necessary, this position may be adjusted to change the scanning directions. When the target is acquired, the pilot centers it on the TV screen and maintains that position by gimbaling the camera. The TV camera gimbal angles and rates, and the range and range rate from the radar altimeter are fed into the computer. Using these data, the computer commands the attitude control system to adjust the body attitude until the thrust direction is proper for nulling the line of sight angular rate and establishing a closing rate commensurate with the displacement error. The computer may then fire the appropriate translation rocket, subject to override control by the pilot. It is desirable to null the line of sight angular rate prior to getting close to the target since the angular rate increases as the displacement decreases, and it is preferable to avoid situations requiring the body axes to be slewed at high rates or through large angles.

Some advantages of this system are:

- (a) It requires the least number of translation jets.
- (b) The translation jet is used most efficiently by being directed along the desired velocity vector (i. e., the velocity vector is not along the resultant of two thrust vectors as in the other systems).

Disadvantages include:

- (a) The computer operation is more complex and vital.
- (b) The attitude control requirements in some situations could be quite severe, as in nulling the line of sight angular rate at close range.
- (c) The final position and relative rate tolerances must, therefore, be greater.

2. Three-Axis Translation Control, Plus Attitude Control

Figure XII-6 shows the translation and attitude control nozzle positions for this system. Translation control is possible simultaneously along all three axes via six thrust units (the forward longitudinal axis unit consists of a pair of nozzles in the present configuration with the Model 410 command module). Attitude control is maintained with six additional thrust units.

One method of orbital rendezvous with this system is as follows: After injection, the pilot scans the volume of space expected to contain the target by gimbaling the TV camera. The body axes will be stabilized automatically to an inertial reference to give the desired field of view. When the target is acquired, the pilot centers it on the TV screen by aiming the TV camera and then locks the camera to the inertial platform. He next used the attitude jets to align two of the body axes with the x and y axes of the screen, and the third body axis with the line of sight. This axis will be "in and out" of the screen (z axis) and the other two axes will be "right and left" and "fore and aft" on the screen. The radar altimeter will furnish the range and rate data necessary to null the "in-out" displacement error, while the apparent motion of the target on the screen enables the pilot to null the errors along the other two axes.

An alternative method is similar, but the vehicle is kept oriented to local vertical during the acquisition phase and the TV camera is locked to the vertical body axis. The injection guidance technique is such that the target will be in view at injection or will enter into view within some time limit. The target may be distinguished from the stars since its motion will be opposite to the apparent motion of the star field. The displacement and rate nulling procedure is as before. (The analog simulation was made of this method.)

~~CONFIDENTIAL~~

Some advantages of this configuration are:

- (1) Comparatively simple in mechanization and operation.
- (2) Pilot is not dependent on the computer after injection except to stabilize vehicle attitude.
- (3) Fine position and rate control is possible.

Some disadvantages are:

- (1) More control rockets are required than in the single axis system.
- (2) It is inefficient in that the thrust vectors are not necessarily along the resultant velocity vector.

3. Three-Axis Translation Control, Combined with Attitude Control

Fig. XII-7 shows the nozzle configuration of this system, in which joint use of the reaction jets is made by attitude and translation control. Since the configuration does not permit the nozzles to be located at equal distances from the center of gravity, different thrust levels must be employed by the two jets when used for translation. In attitude control, when a couple is desired, the thrust levels must be the same. This requires either a proportional thrust system or high and low level nozzles and, in the latter case, the translation control is not actually combined with attitude control.

This system is a counterpart to the three-axis translation control, plus the attitude control system discussed previously, and would be operated the same in an orbital rendezvous.

The advantages of this system over that with separate attitude and translation is doubtful in the present Apollo configuration. The disadvantage is that, due to the vehicle configuration, the nozzles used for translation are not equally spaced from the center of gravity. This requires different thrust levels or high attitude control torque. Another disadvantage is that, in choosing the thrust level for any jet, consideration must be given both attitude and translation control requirements.

From the above discussion, and from Martin's previous experience, it is considered that the three-axes translation, plus an attitude control system, is the first system to consider for Apollo in that it seems to offer the best performance and the least problems.

~~CONFIDENTIAL~~

C. RENDEZVOUS SYSTEM FOR APOLLO

1. Utilization of Onboard Equipment

To achieve maximum efficiency in using the Apollo spacecraft as a rendezvous vehicle, it is desirable to utilize as much of the onboard equipment as possible. This utilization is as follows:

a. The steerable antennas and radio receivers

Following injection into co-orbit with the target satellite, these antennas (located on the mission module) will be erected. They will then be used to null on a signal transmitted by the target satellite. This determines the direction of the target with respect to the Apollo reference system and limits the search area.

b. The television camera and monitor

After the directional determination made above has been accomplished, the television camera is aimed in this direction and the monitor is scanned by the pilot for target identification. Once the target is located, the pilot can use this system to determine angle and angle rate data.

c. The radar altimeter

For the rendezvous operation, the radar altimeter is slaved to the television camera. This altimeter has a fairly large look angle and can be used as an aid in target detection. Once the target is located, the altimeter will provide range and range rate data.

d. The inertial guidance platform

The inertial guidance platform will be used to provide attitude stabilization data.

By proper use of the data derived from the above system (range, range rate, angle and angle rate), a pilot has adequate information to conduct a rendezvous operation.

The Apollo spacecraft, in an earth orbital mission, does not require the mission control and abort propulsion system. The propulsion requirements consist of attitude control functions and a de-orbit capability. The presently planned attitude control and vernier velocity propulsion system can provide both the control and de-orbit functions for the orbital mission. Additional thrust units and propellant are required for orbital transfer or rendezvous maneuvers. These requirements will be discussed in the following section.

~~CONFIDENTIAL~~

A new problem arises, however, in the environmental control and electrical power areas. Neither the lunar mission environmental control system nor the electrical power system are adequate for the earth orbital mission without being supplemented. It is tentatively planned to partially load the mission abort propulsion tanks with approximately 1000 pounds of liquid hydrogen and 800 pounds of liquid oxygen. This propellant will be utilized by those systems to meet a 14-day, earth orbit mission requirement.

With the exception of the equipments previously discussed and the added maneuver (translation) system (see the next section), all onboard systems remain unchanged for the orbital rendezvous mission.

2. Maneuvering System

The maneuvering system, consisting of thrust units, propellant system, propellant feed system, and command control system constitutes the only additional equipment required to provide Apollo with a rendezvous capability. The criterion for determining thrust level is allowable rendezvous time. This time is limited by two factors: man functioning as the control center, and the time dependence of the relative positions of the target and rendezvous vehicle, since the two orbits are not identical. The most serious limiting factor, however, is believed to be the man. He should be able to operate efficiently, watching the data display and maneuvering the vehicle for a period of one hour. Under any circumstances, he should be able to complete the rendezvous in a maximum time of three hours. To investigate the effect of a one-hour rendezvous time on thrust level, consider the case where the Apollo is injected at the center of the volume of uncertainty of the target with no relative velocity difference. In this case, the maximum vertical separation is 2-3/4 nautical miles, and the maximum longitudinal displacement is 5-1/2 nautical miles. To cancel this longitudinal displacement, accelerating 1/2 hour and decelerating 1/2 hour requires an acceleration of 0.0102 ft/sec^2 or approximately 5.0 pounds of thrust with a vehicle weight of 15,000 pounds. To cancel the vertical displacement in the same time requires 1/2 this thrust level.

It is not desirable, of course, to operate with such low thrust levels in a manned system, since the pilot should not be required to maintain thrust-on for extended periods of time and should be able to note easily the reactions to control applications. It is interesting, however, to see that it seems possible to obtain an acceptable rendezvous time with control accelerations low enough for fine positioning since this obviates the requirement for two thrust levels or proportional control. Thrust levels of 150 to 1500 pounds will satisfy both rendezvous time and fine positioning requirements, although the "on time" for a 150-pounds thrust is somewhat longer than desirable. The latest analog runs indicate that 1500 pounds was the optimum thrust level for the vehicle investigated.

~~CONFIDENTIAL~~

3. Rendezvous Operation

In a typical Apollo rendezvous operation, space track will provide the ephemeris of the orbital target. These data will be used to establish a nominal launch time. Launch must occur within the prescribed time limits or be held until the next precomputed opportunity. (In the case of Apollo, the target satellite will have been placed in orbit from the Apollo launch position and a direct ascent trajectory in the plane of the target orbit can be selected while maintaining reasonable reaction times.) Following launch, the vehicle will be inertially guided along some preselected nominal ascent trajectory and injected into co-orbit with the target satellite. The Apollo vehicle, at this time, will have some preferred orientation and desired velocity characteristics with respect to the target.

Following injection, the Apollo vehicle is automatically slaved to earth vertical and the search phase is initiated. The steerable antennas will be inflated and a radio-direction search begun. Concurrently, optical search can be in progress by use of the television system and periscope. Once the target satellite is identified, the pilot centers it on the television monitor screen by aiming the camera. The camera is then locked to the inertial platform. The pilot then commands an attitude change to align two of the body axes with x and y axes of the screen. The third body axis will then be the line of sight (range) axis and "in and out" of the screen. The other two axes will be "right and left" and "up and down" in the screen. The pilot then uses the radar altimeter data and the apparent motion of the target on the screen to determine displacement and radial errors along the "line of sight". He commands the required on-off operation of the maneuver thrust units to null these errors and hence accomplish rendezvous.

The vehicle weight in the configuration described above is 12,870 pounds. Using this weight and the relationship derived from the analog studies that the propellant required for rendezvous is approximately 1/8 the vehicle total weight (propellant $I_{SP} = 280$ sec) the propellant weight required can be calculated.

$$\frac{W_P}{W_V + W_S + W_P} = 1/8 \quad (1)$$

where

W_p = propellant weight required

W_v = vehicle weight = 12,870 pounds

W_s = rendezvous propulsion system inert weight

(includes tankage, thrust units, pressurization system, plumbing, etc.)

also assume

$$\frac{W_p}{W_s + W_p} = .85 \quad (2)$$

$$W_s = .1765 W_p$$

Substituting value of W_s in equation (1)

$$\frac{W_p}{W_v + 1.1765 W_p} = \frac{1}{8} = .125 \quad (3)$$

$$W_p = .1465 W_v = .1465 \times 12870 \approx 1900 \text{ lbs}$$

and

$$W_s = .1765 W_p = .1765 \times 1900 = 335 \text{ lbs}$$

The fuel requirements developed above are a conservative estimate, since the initial conditions investigated (below, ahead and slower) are a worst case. If the time required for rendezvous is not critical, the fuel requirements may be reduced by reducing the initial velocity differential. Nulling this velocity is then the primary fuel requirement.

Ideal initial conditions, from a fuel expenditure standpoint, would be injection at the same height and to the side of the target with as low a velocity discrepancy as possible. Considering acquisition of a friendly satellite with a radio and optical beacon, the initial difference may be minimized, since recognizing the satellite against the star field is not an unaided visual task.

~~CONFIDENTIAL~~

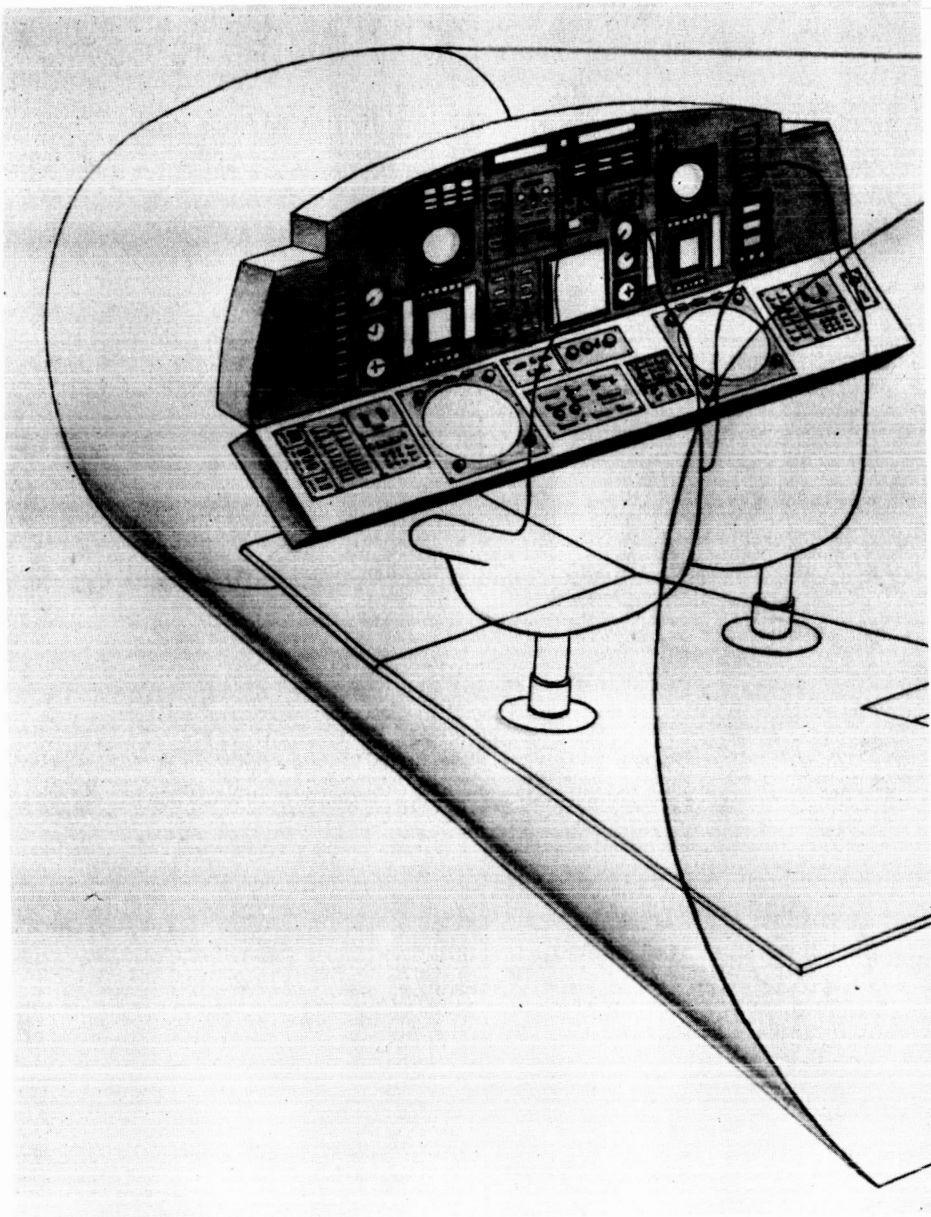


Fig. VI-1. Unitized Forward Console

~~CONFIDENTIAL~~

ER 12007-2

~~CONFIDENTIAL~~

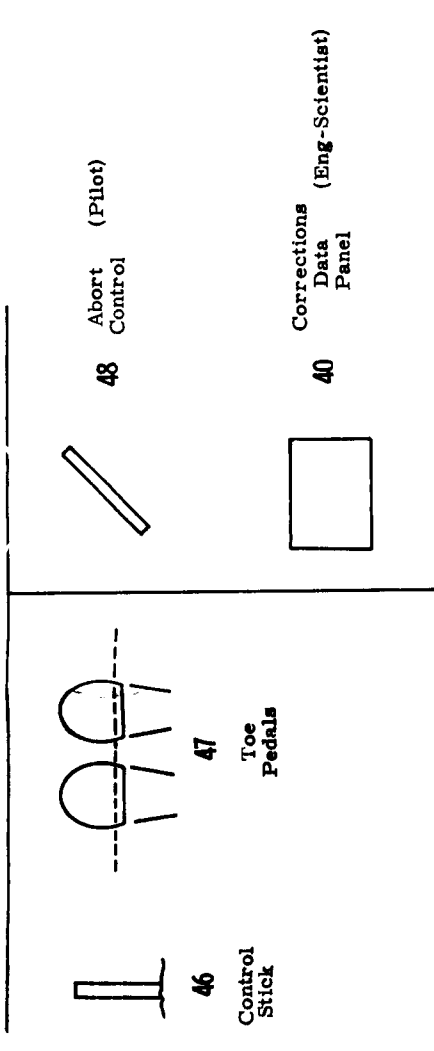
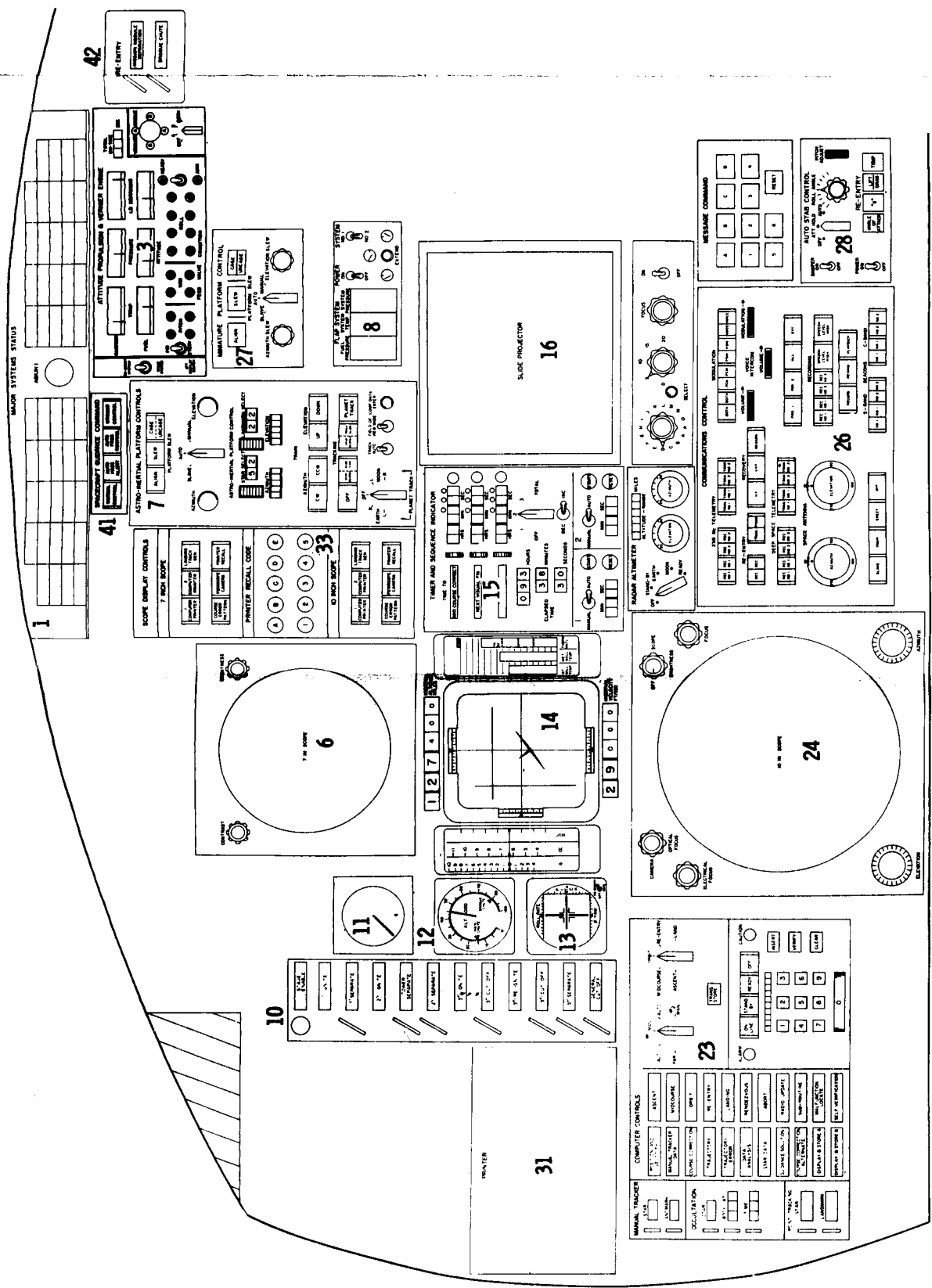


Fig. VI-2. Navigator - Pilot Displays and Operating Controls

~~CONFIDENTIAL~~

~~CONFIDENTIAL~~

TRAJECTORY DEVIATIONS

DATA TIME	3 hr 0 min 0 sec
PRESENT TIME	2 hr 12 min 0 sec

SYSTEM	A	B	C	D
ΔX mi	+15	+30	+18	+21
ΔY mi	+10	-14	+ 4	-40
ΔZ mi	+ 9	+30	- 1	+60
Δt sec	+ 5	+10	+ 8	+ 8
$\dot{\Delta X}$ fps	+ 2	+ 6	+ 3	+ 4
$\dot{\Delta Y}$ fps	+ 3	- 4	+ 1	-12
$\dot{\Delta Z}$ fps	+ 6	+10	0	+15

Fig. VI-3. Trajectory Deviations--10-inch scope (24) display

~~CONFIDENTIAL~~

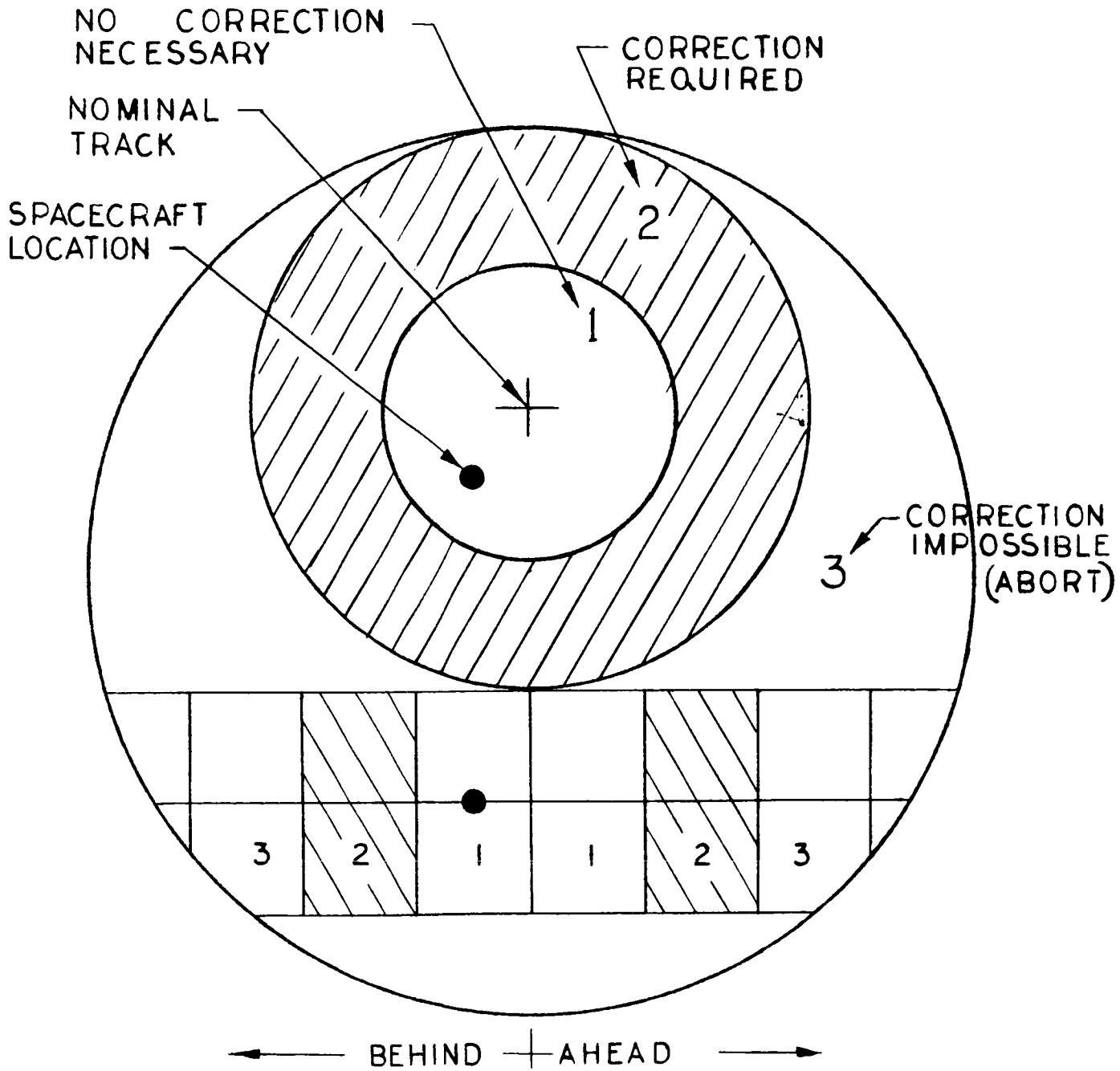


Fig. VI-4. Trajectory Deviations--7-inch scope (6) analog display

~~CONFIDENTIAL~~

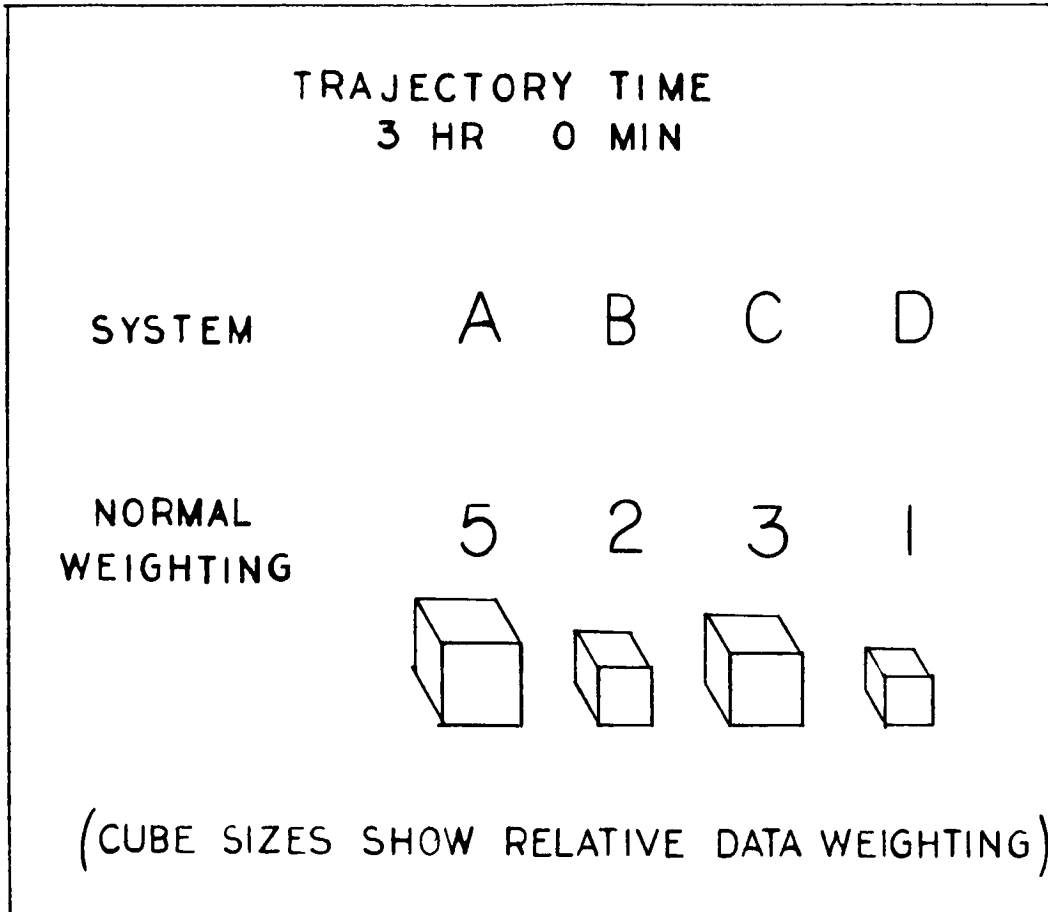


Fig. VI-5. Data Weighting--slide projector (16) display

~~CONFIDENTIAL~~
ER 12007-2

SYSTEM	A	B	C	D
INDIVIDUAL ACCURACY RATIO	1.3	1.0	0.7	0.8
TRIAL COMBINATION	1	2	3	4
RATIO	1.2	1.5	1.1	0.3
SYSTEM	A B C D	A B	A B D	C D
WEIGHT	5 2 3 1	1 1	5 3 1	1 1

Fig. VI-6. Data Selection by Trial Weighting Arrangement--10-inch scope (24) display

TRAJECTORY SOLUTIONS FOR
ABLE TIME AT 3 HR 0 MIN

TOTAL DELTA VELOCITY (ΔV)

BAKER TIME	NOMINALS	N-1	N-2	N-3	N-4
2		10	11	15	9
4		9	10	12	12
10		8	8	10	10
20		7	7	8	10
40		6	6	6	8

Fig. VI-7. Trajectory Solutions for Total Delta Velocity--10-inch scope (24) display

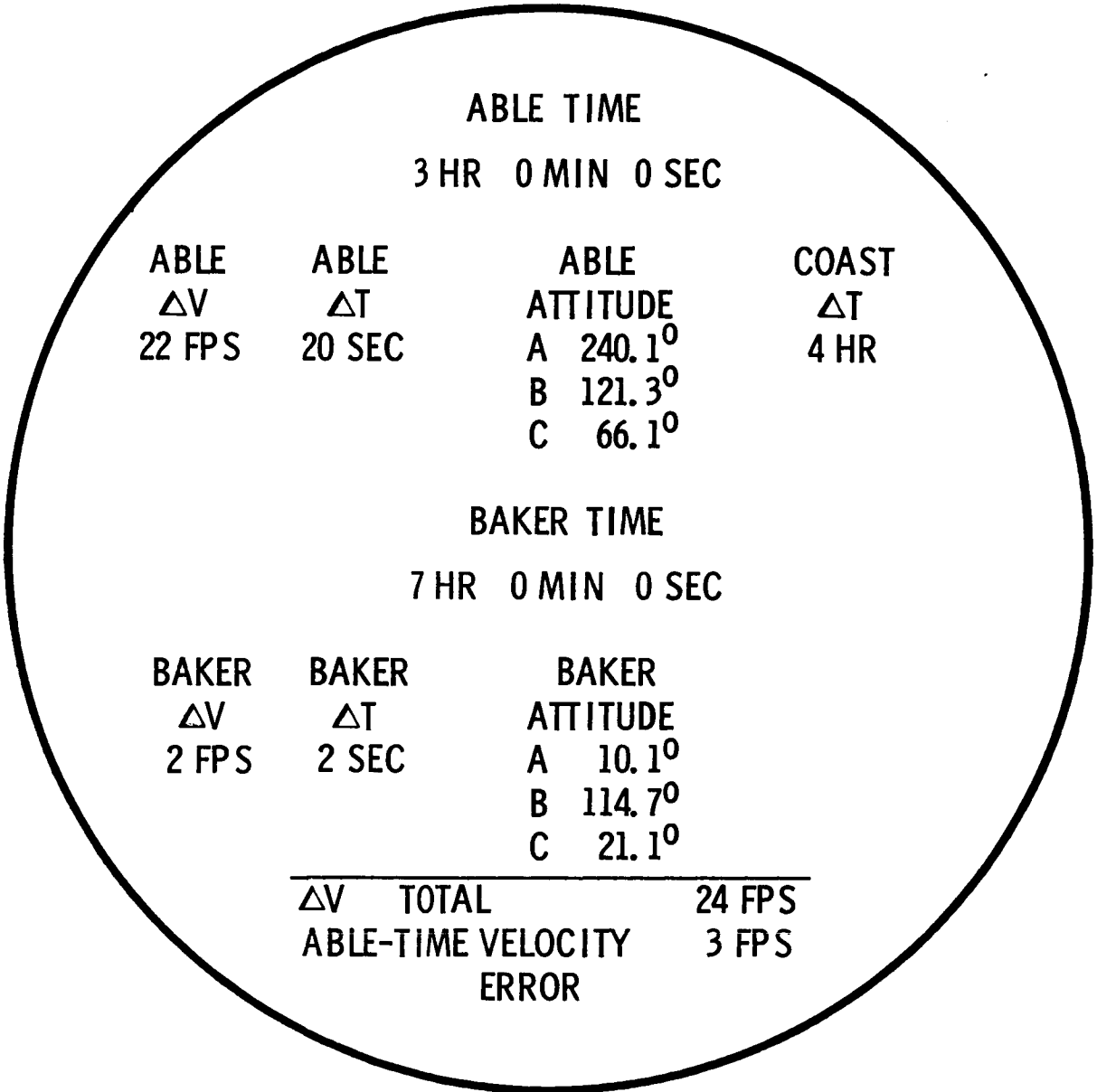


Fig. VI-8. Selected Course Correction Alternate--7-inch scope (6) display

~~CONFIDENTIAL~~

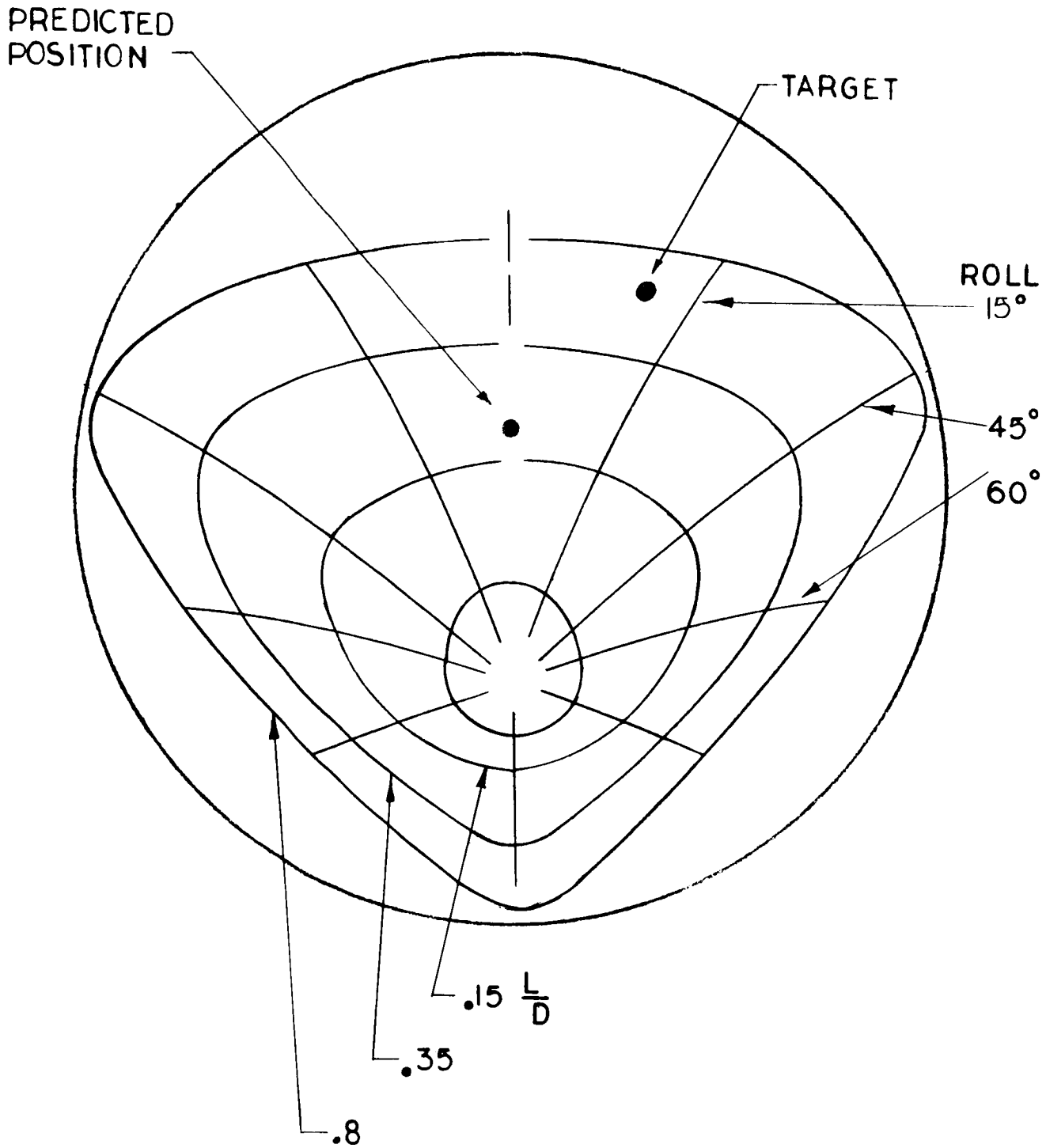


Fig. VI-9. Performance Capability Display--7 Inch (6) Scope

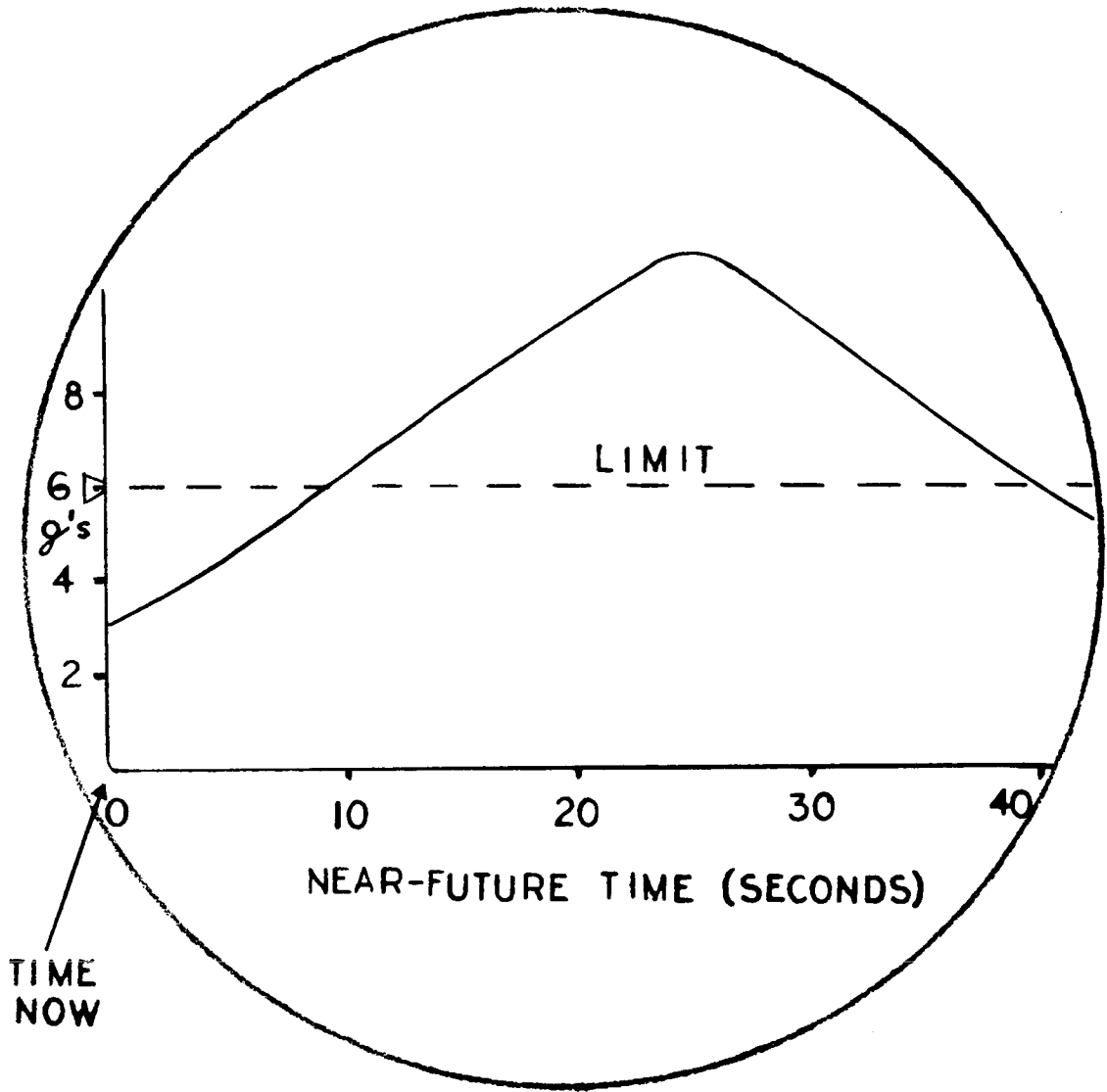


Fig. VI-10. Near Future g's--10-inch scope (24) display

~~CONFIDENTIAL~~

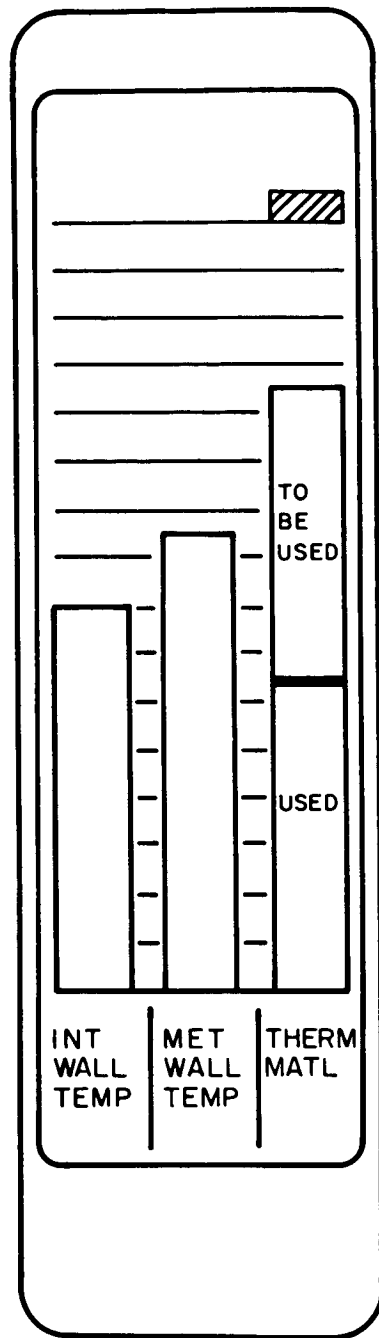


Fig. VI-11. Thermal Protection Management Display

~~CONFIDENTIAL~~

~~CONFIDENTIAL~~

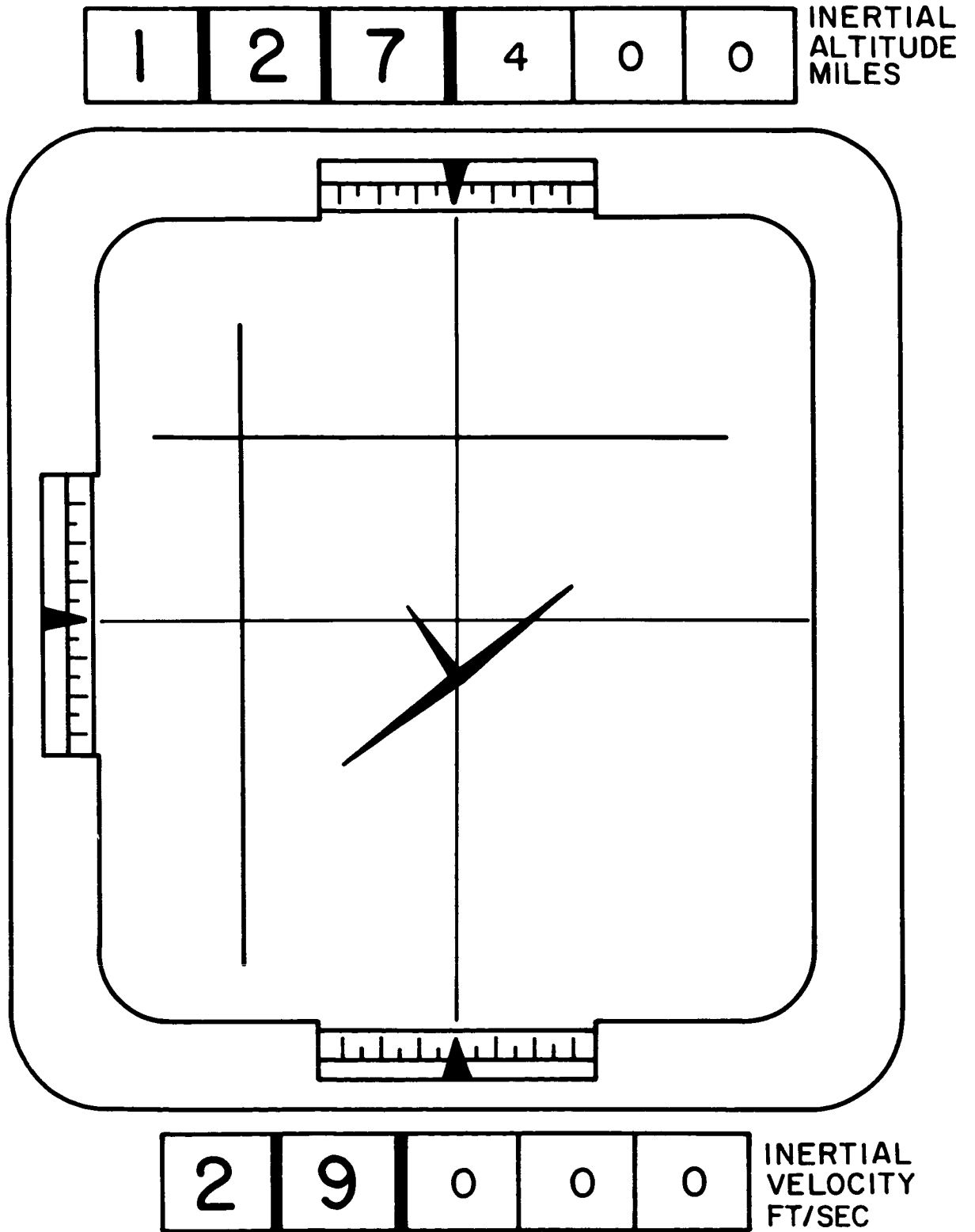


Fig. VI-12. Spacecraft Attitude Display

~~CONFIDENTIAL~~

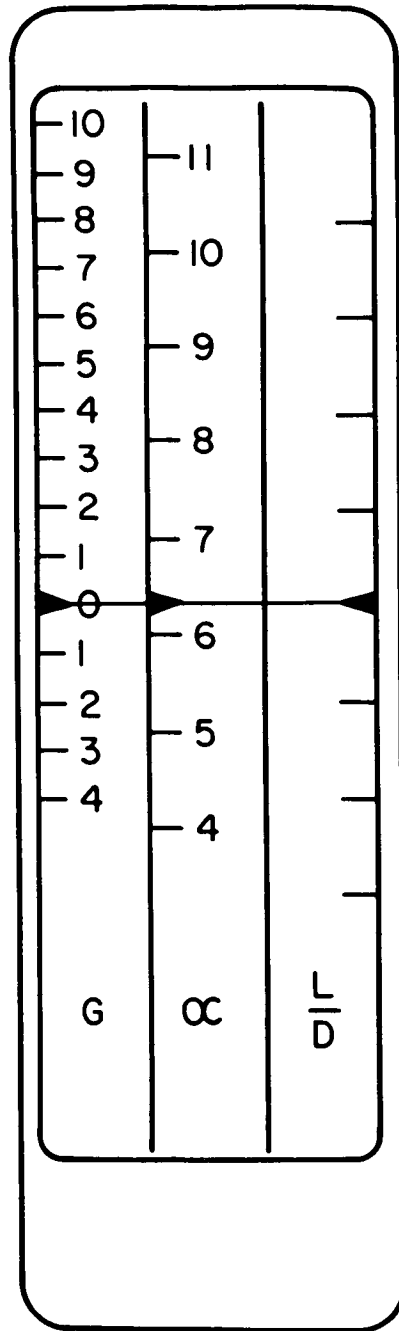


Fig. VI-13. Display for Gravity, Angle of Attack and Lift/Drag Ratio

~~CONFIDENTIAL~~

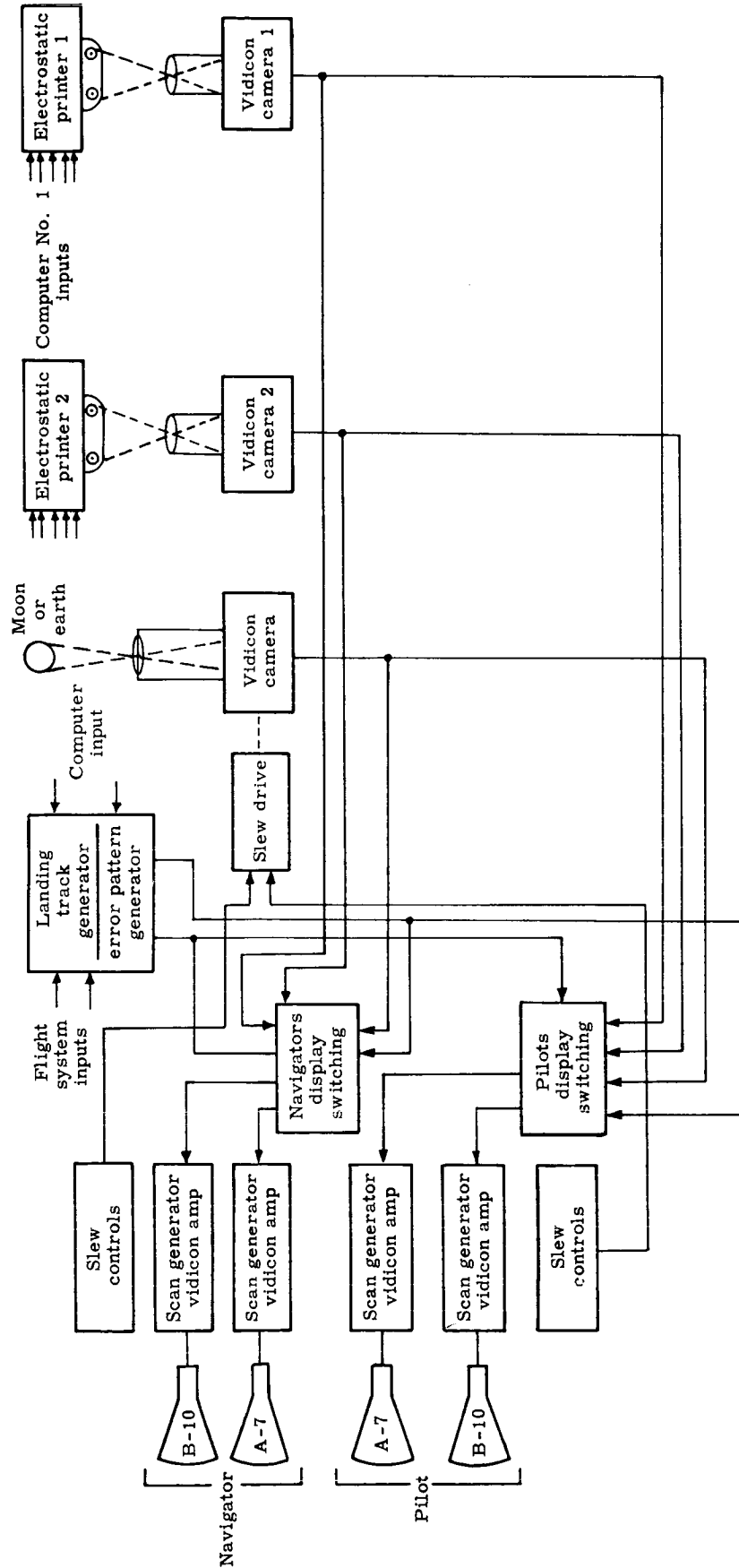


Fig. VI-14. Cathode-Ray Tube Display System--block diagram

~~CONFIDENTIAL~~

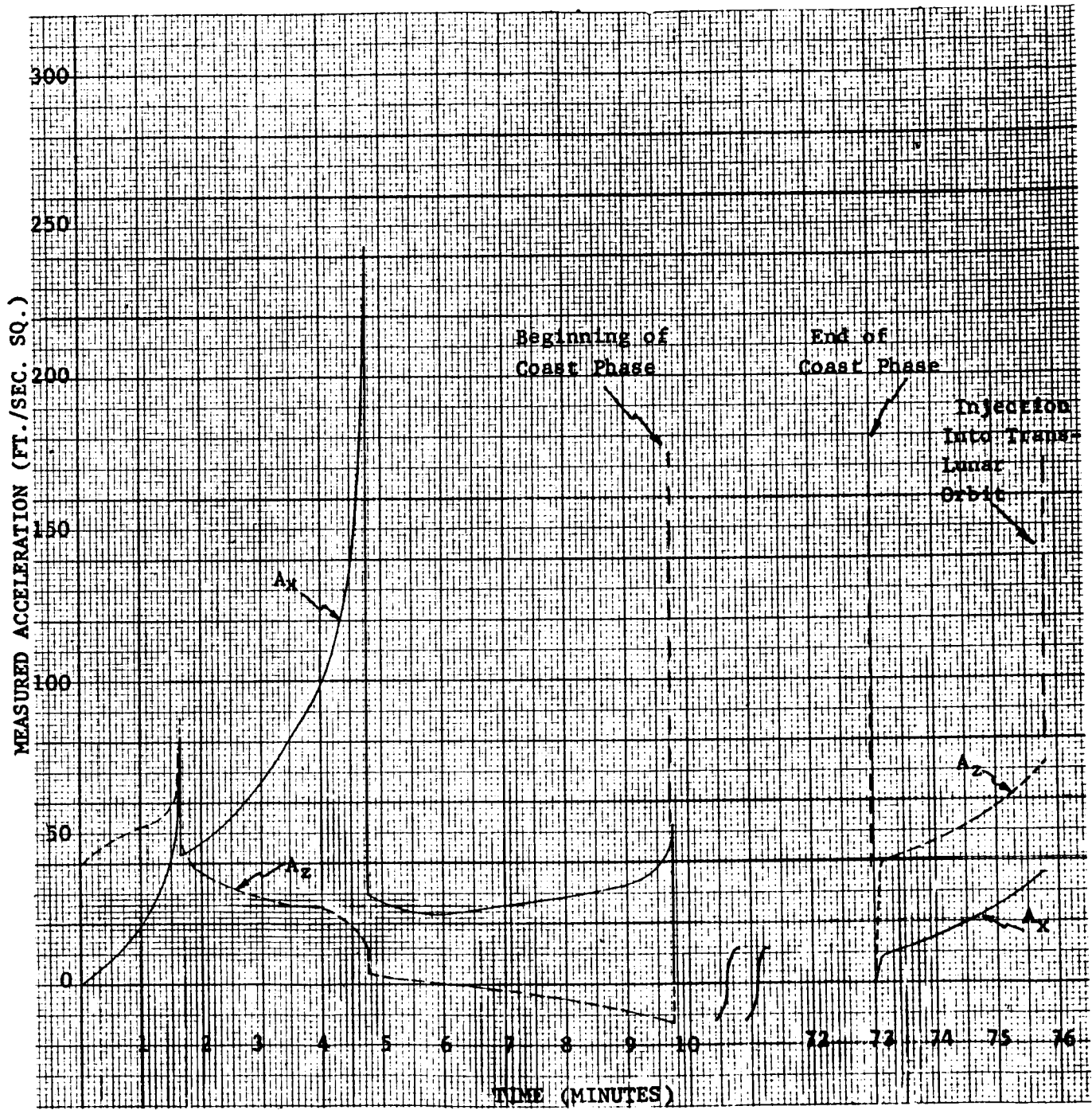


Fig. VII-1. Components of Acceleration for Ascent Phase of Apollo Mission

~~CONFIDENTIAL~~

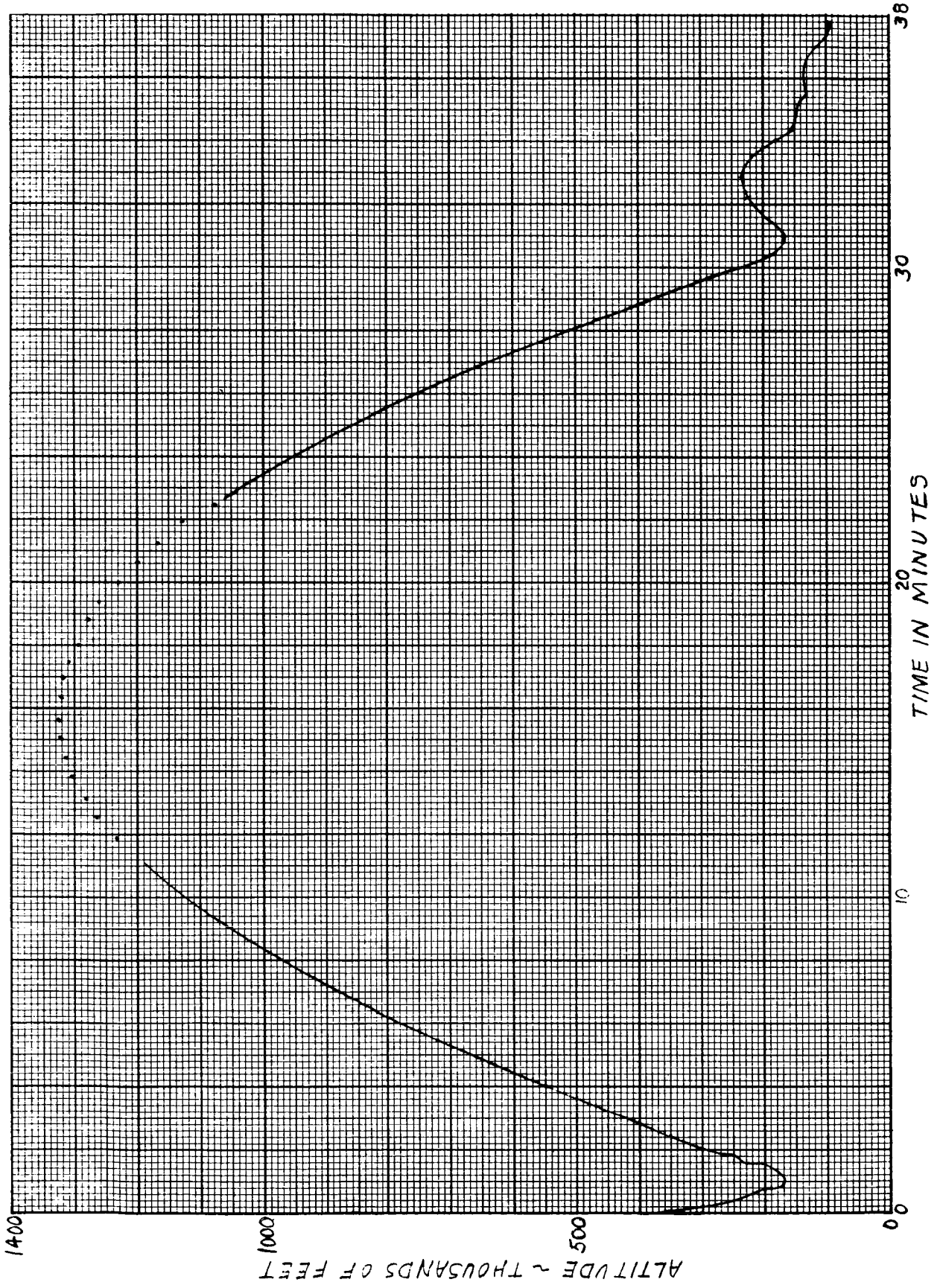


Fig. VII-2. Digital Plot of Altitude Versus Time

~~CONFIDENTIAL~~

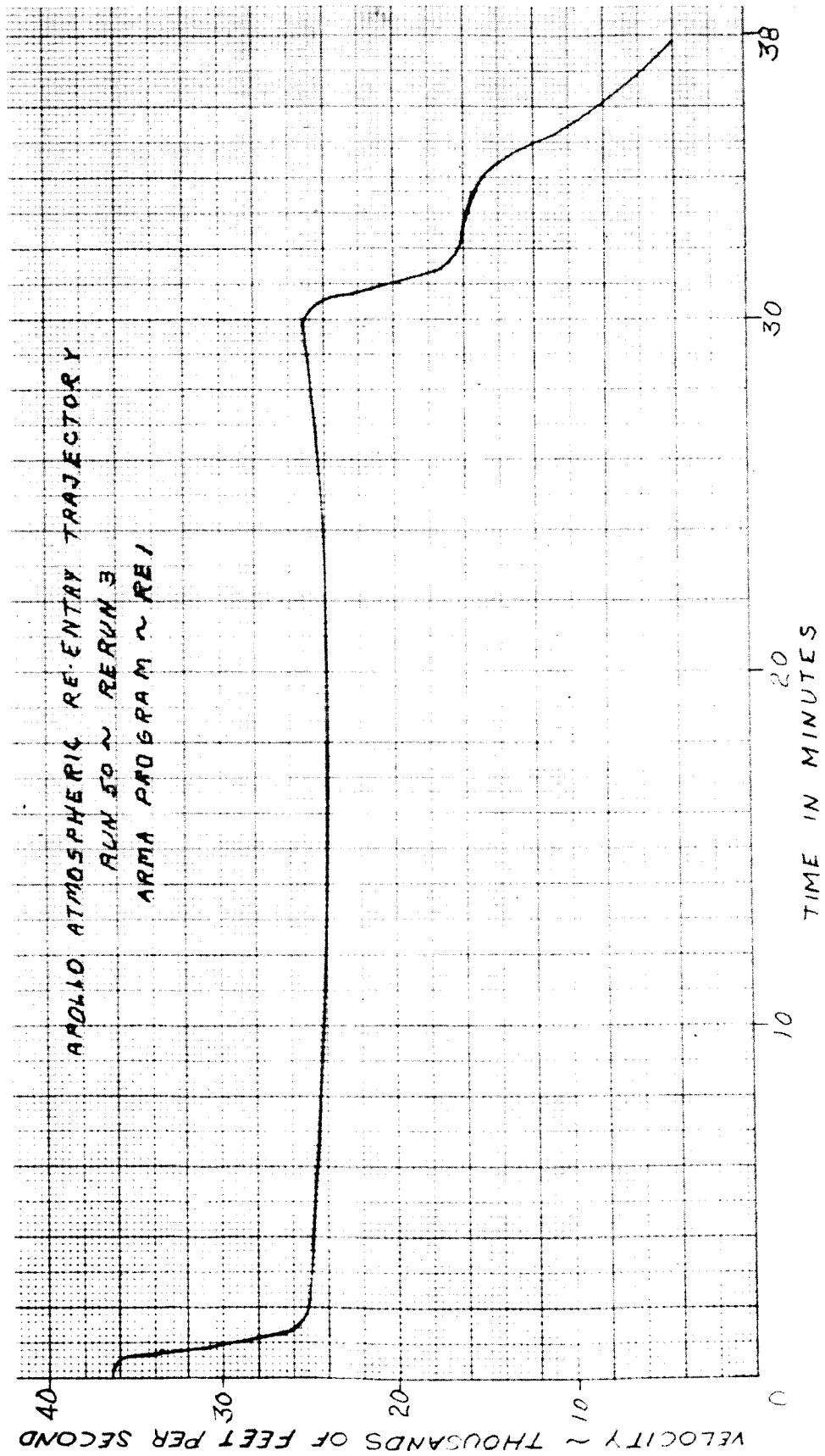


Fig. VII-3. Digital Plot of Velocity Versus Time

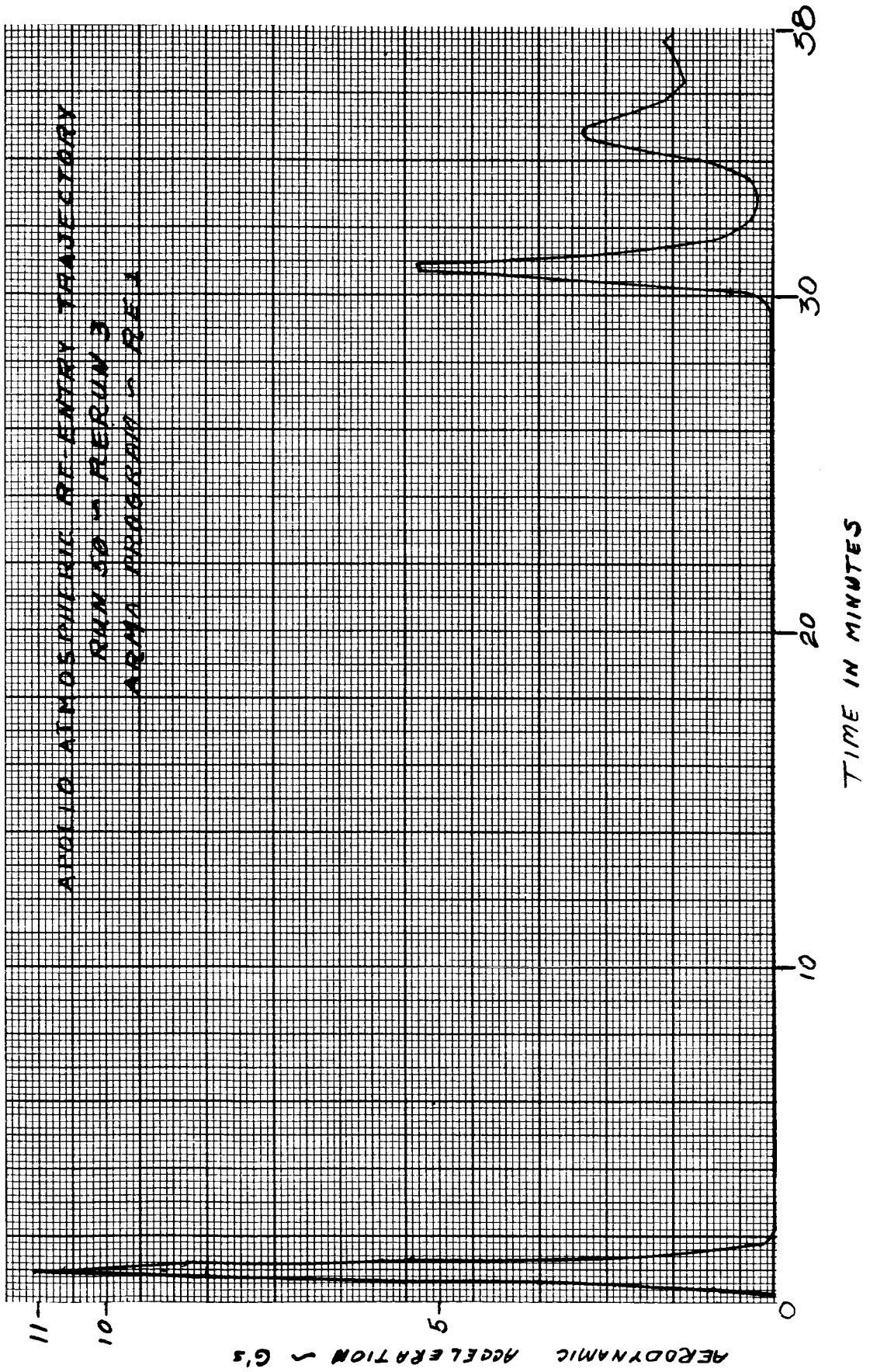


Fig. VII-4. Digital Plot of Total Aerodynamic Acceleration Versus Time

~~CONFIDENTIAL~~

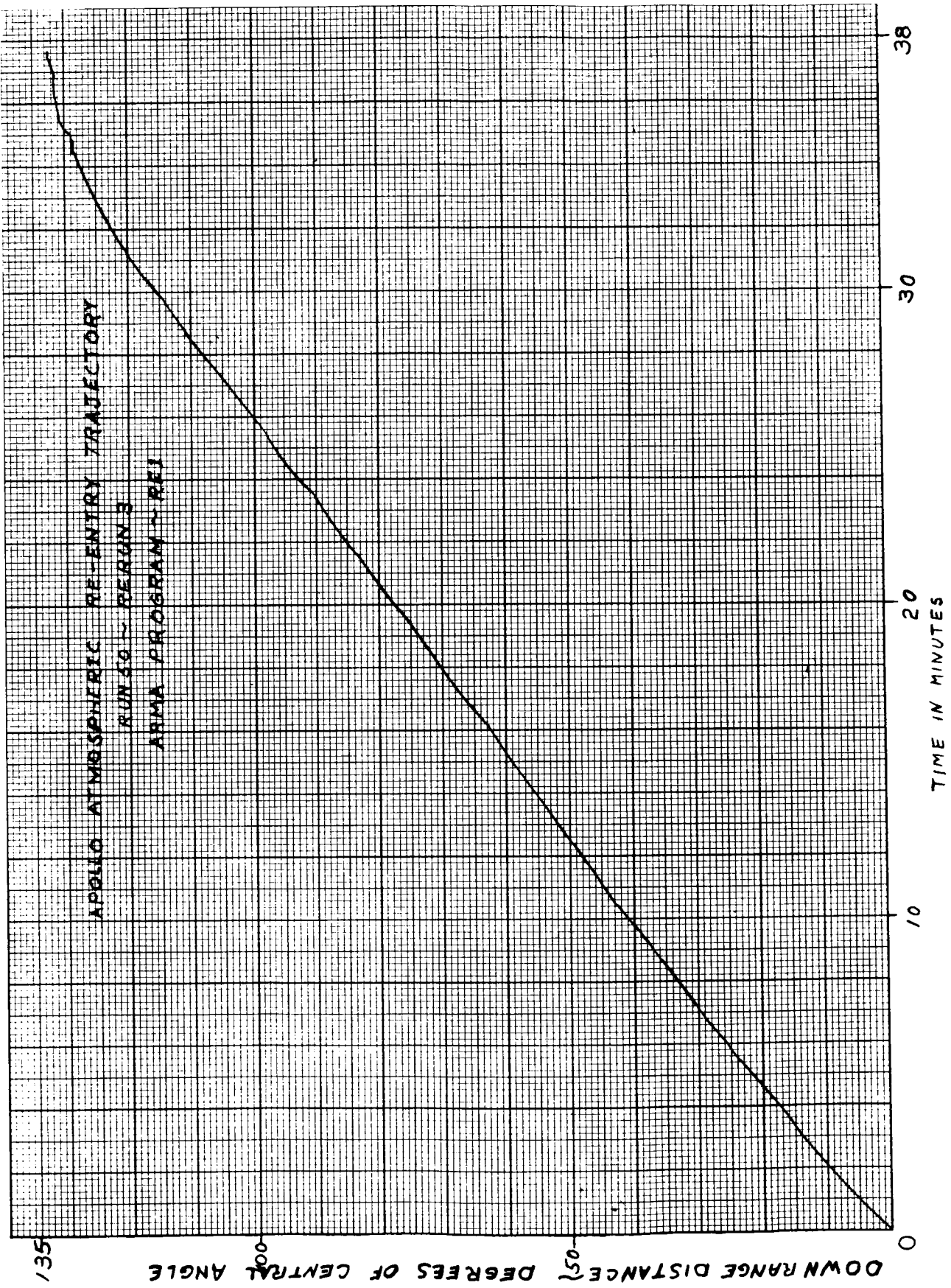


Fig. VII-5. Digital Plot of Distance Traveled Versus Time

~~CONFIDENTIAL~~

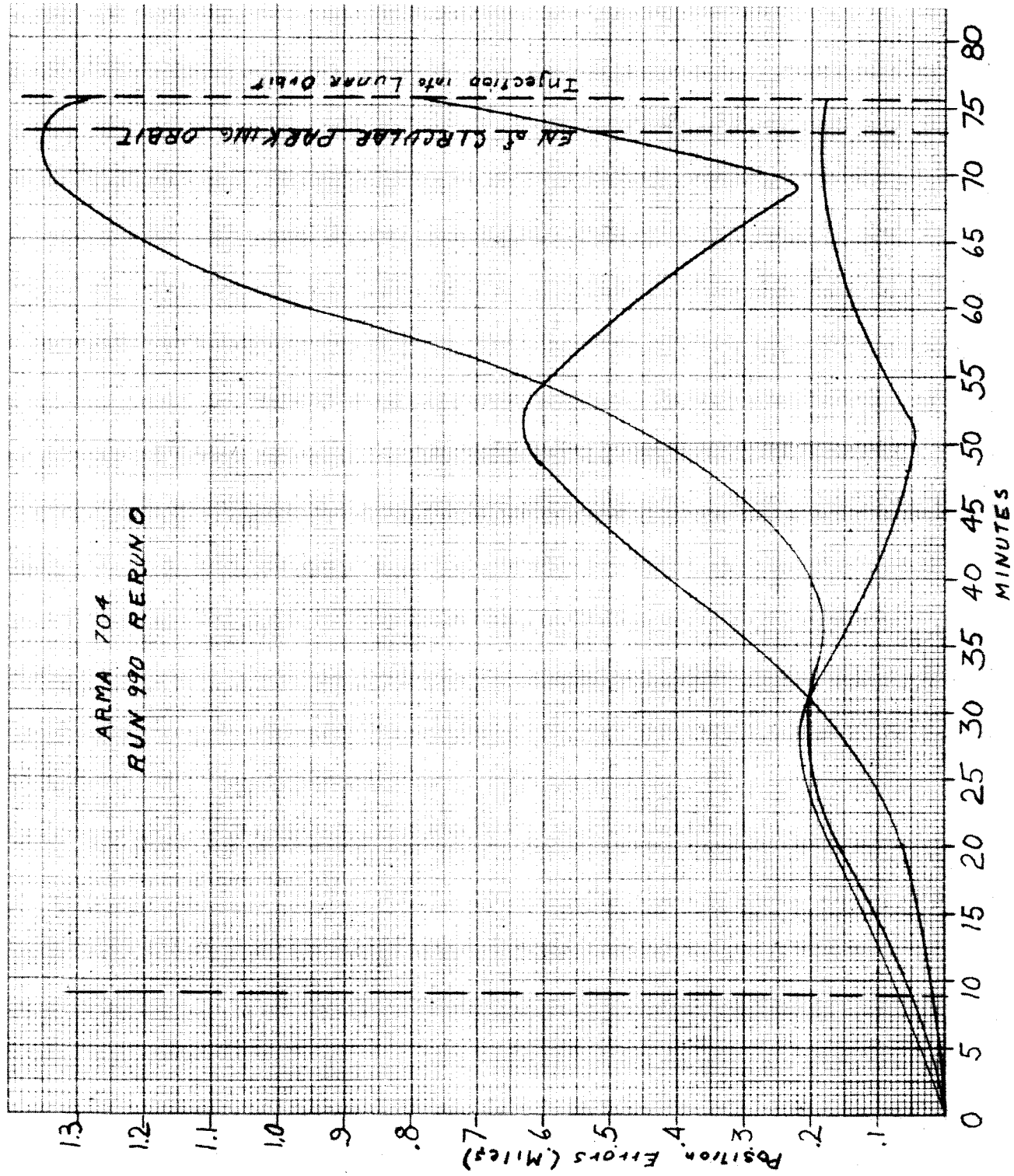


Fig. VII-6. Rectangular Components of Position Error Versus Time for Apollo Ascent Trajectory

~~CONFIDENTIAL~~

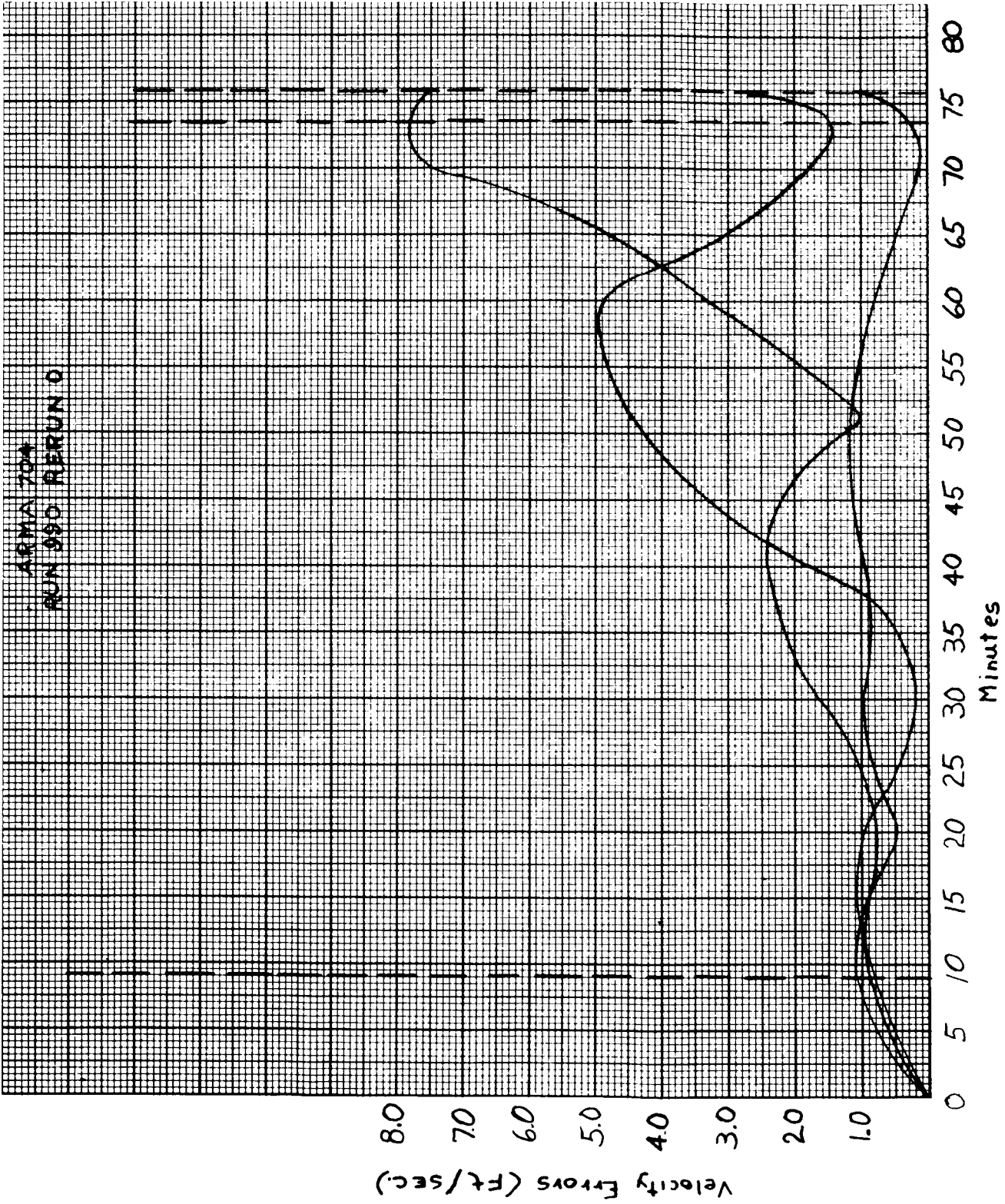


Fig. VII-7. Rectangular Components of Velocity Error Versus Time for Apollo Ascent Trajectory

~~CONFIDENTIAL~~

~~CONFIDENTIAL~~

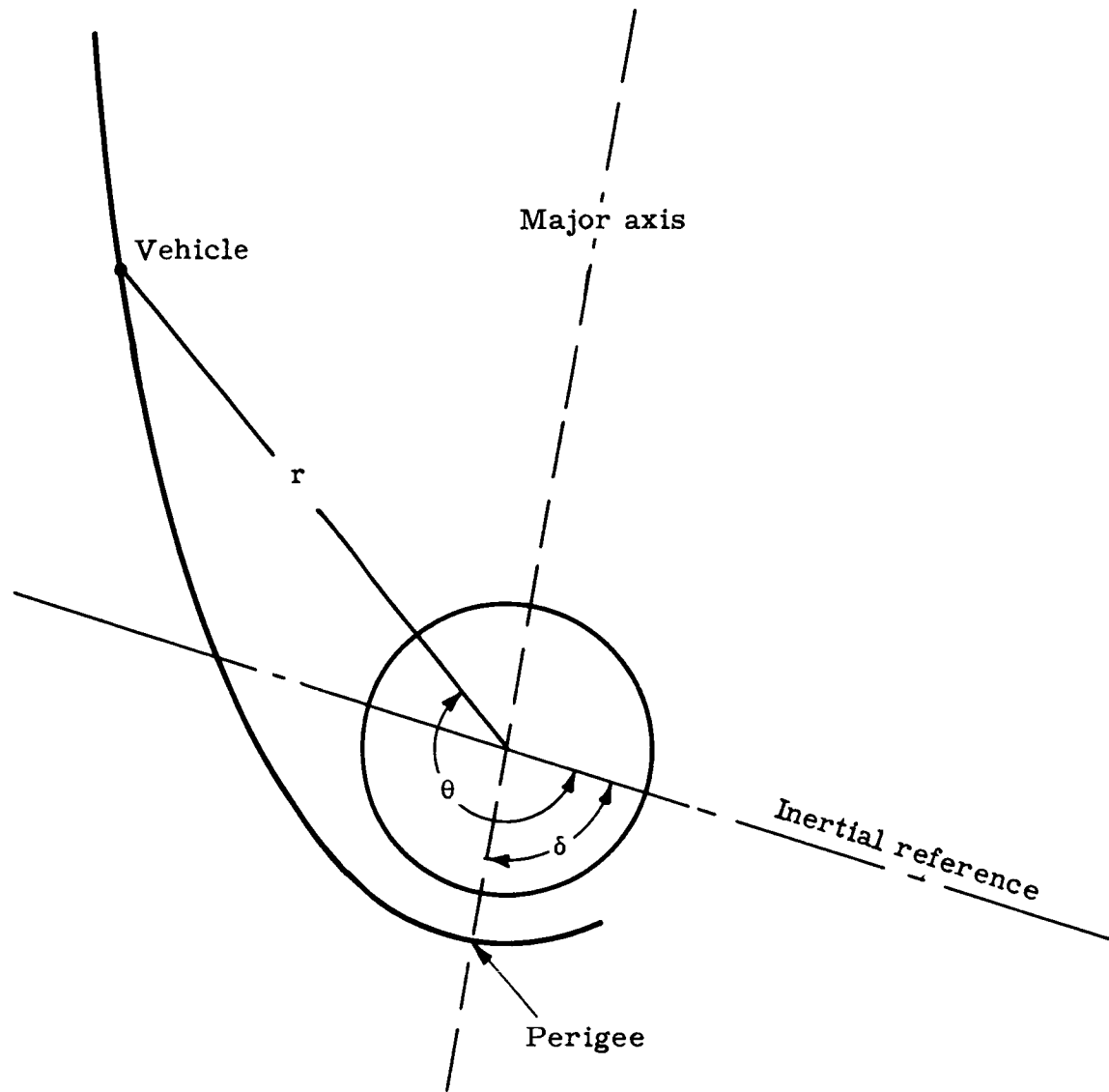


Fig. VII-8. Transearth Trajectory

~~CONFIDENTIAL~~

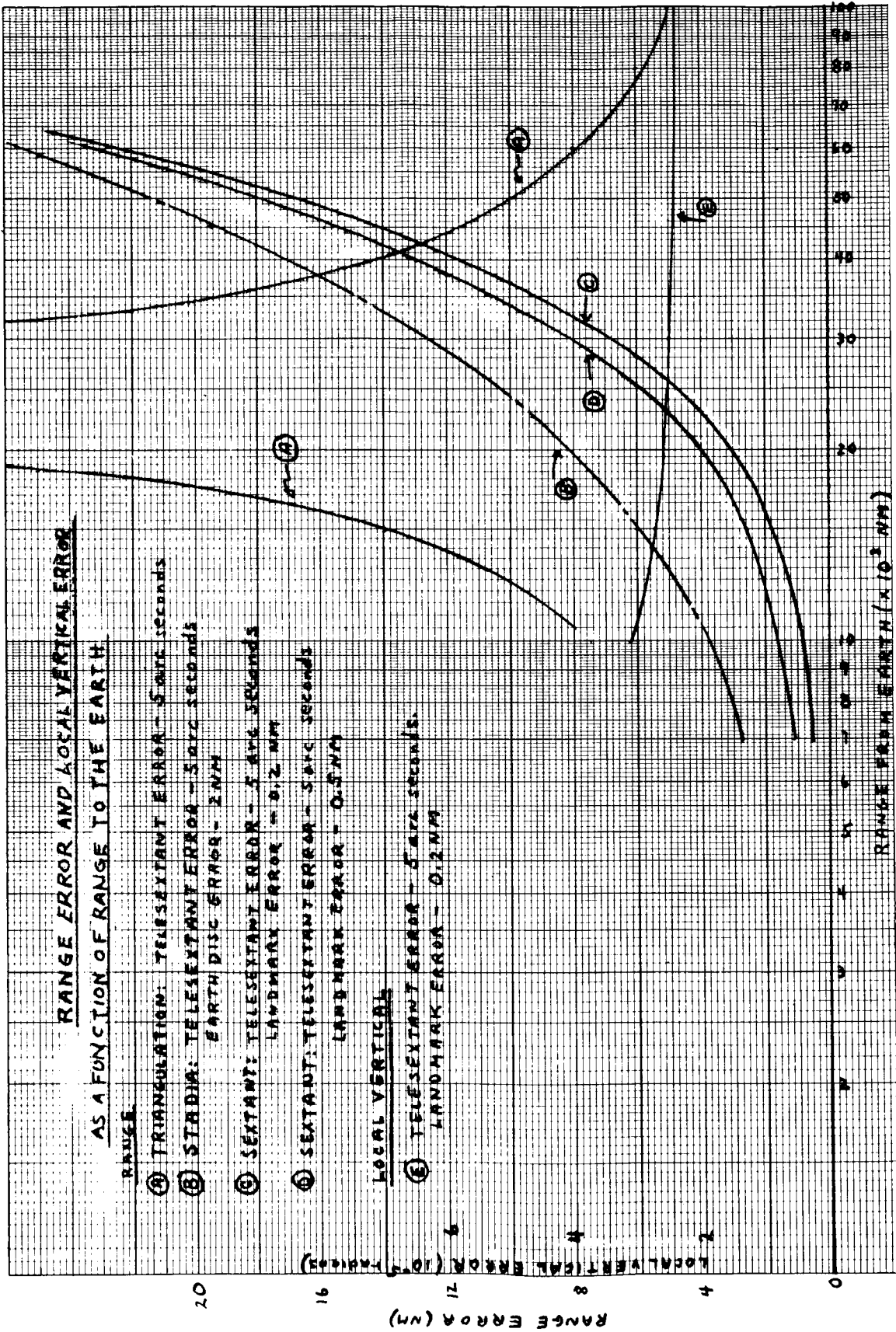
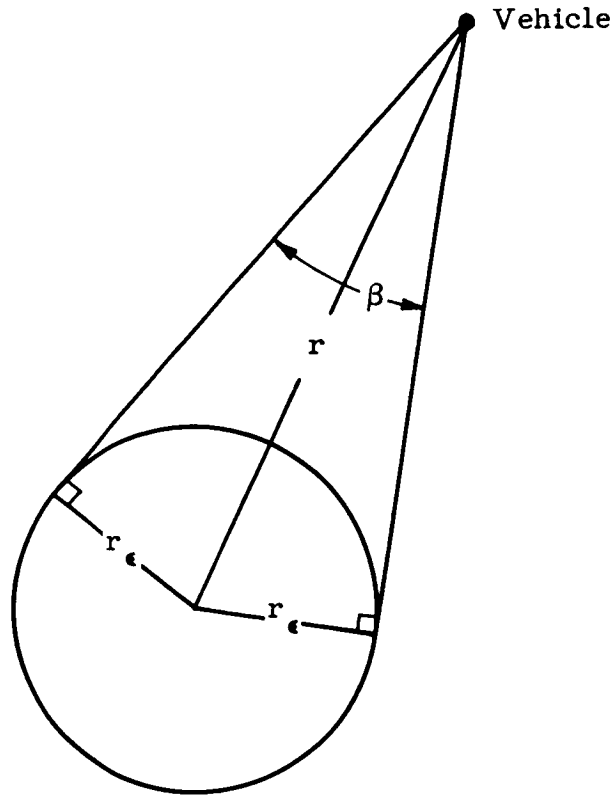


Fig. VII-9. Range Error and Local Vertical Error as a Function of Range to the Earth

~~CONFIDENTIAL~~



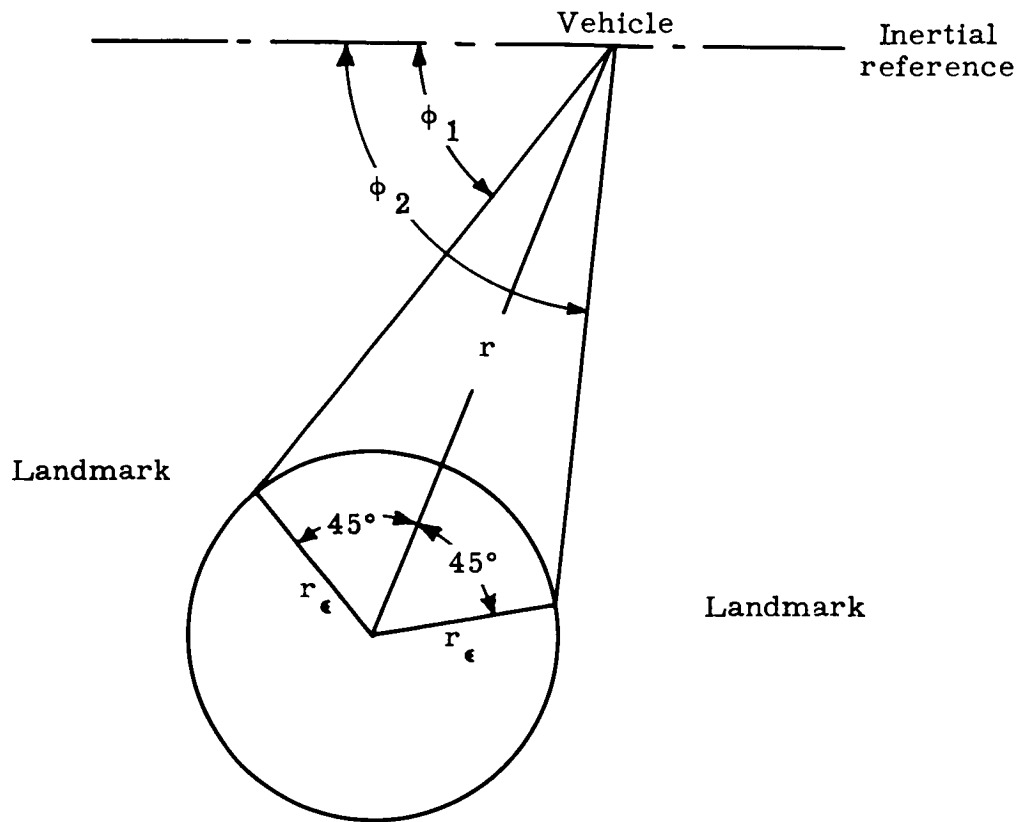
$$\Delta r = \sqrt{\left(\Delta \beta \frac{r^2}{2r_\epsilon} \sqrt{1 - \left(\frac{r_\epsilon}{r}\right)^2} \right)^2 + \left(\Delta r_\epsilon \frac{\sqrt{2}}{2} \frac{r}{r_\epsilon} \right)^2}$$

- Where Δr = error in range
- $\Delta \beta$ = telesextant angular error
- Δr_ϵ = uncertainty in the contour of the earth disc
- r = range from the vehicle to the earth center
- r_ϵ = radius of the earth
- β = stadia observation using the telesextant

Fig. VII-10. Stadia Errors

~~CONFIDENTIAL~~

~~CONFIDENTIAL~~

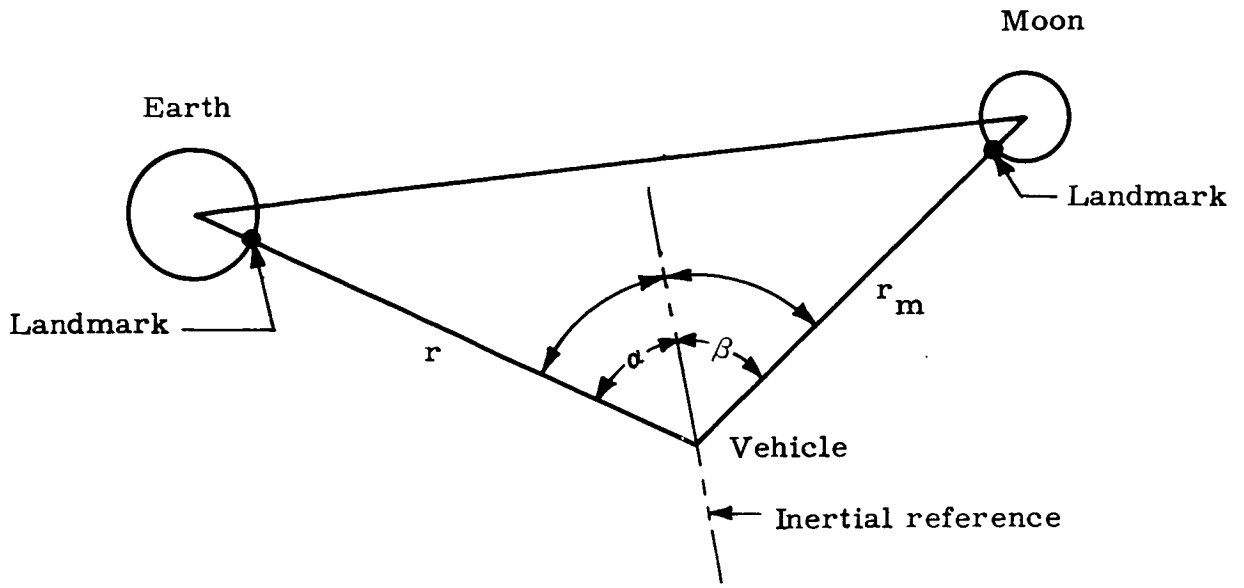


$$\Delta r = \sqrt{\left(\Delta r_{\epsilon} \frac{\sqrt{2}}{2} \frac{r}{r_{\epsilon}}\right)^2 + \left(\Delta l \frac{\sqrt{2}}{2} \left[\frac{\sqrt{2}}{2} \frac{r}{r_{\epsilon}} - 1\right]\right)^2 + \left(\Delta \phi r_{\epsilon} \left[\left|\frac{r}{r_{\epsilon}}\right|^2 - \sqrt{2} \frac{r}{r_{\epsilon}} + 1\right]\right)^2}$$

- Where
- Δr = range error
 - $\Delta \phi$ = telesextant angular error
 - Δr_{ϵ} = altitude error of the landmark
 - Δl = landmark error
 - r_{ϵ} = earth radius
 - ϕ_1, ϕ_2 = sextant readings

Fig. VII-11. Range Error Using Sextant Observations

~~CONFIDENTIAL~~



$$\Delta r = \Delta \alpha \left(r \frac{\cos \alpha + \beta}{\sin \alpha + \beta} \right) + \Delta \beta \left(\frac{r_m}{\sin \alpha + \beta} \right)$$

- Where Δr = range error
 $\Delta \alpha, \Delta \beta$ = telesextant angular errors
 r = range to the earth
 r_m = range to the moon
 α, β = sextant readings

Values for r , r_m , α and β are obtained from typical trajectories

Ideal lunar ephemeris data have been assumed. Land mark errors were found to be negligible for the cases considered.

Fig. VII-12. Range Errors Using Triangulations

~~CONFIDENTIAL~~

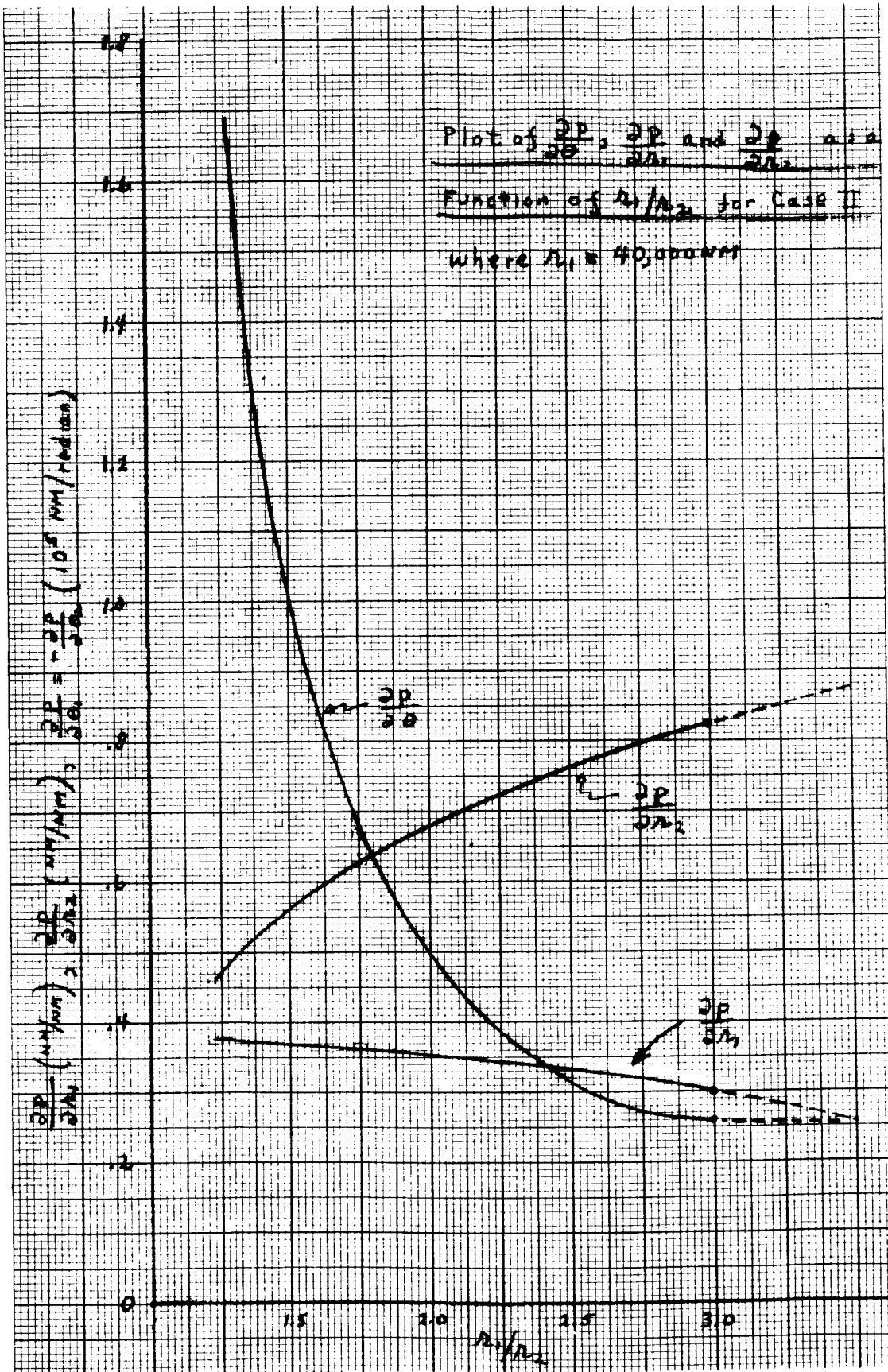


Fig. VII-13. Plot of Error Partial as a Function of $r1/72$ for Case II

~~CONFIDENTIAL~~

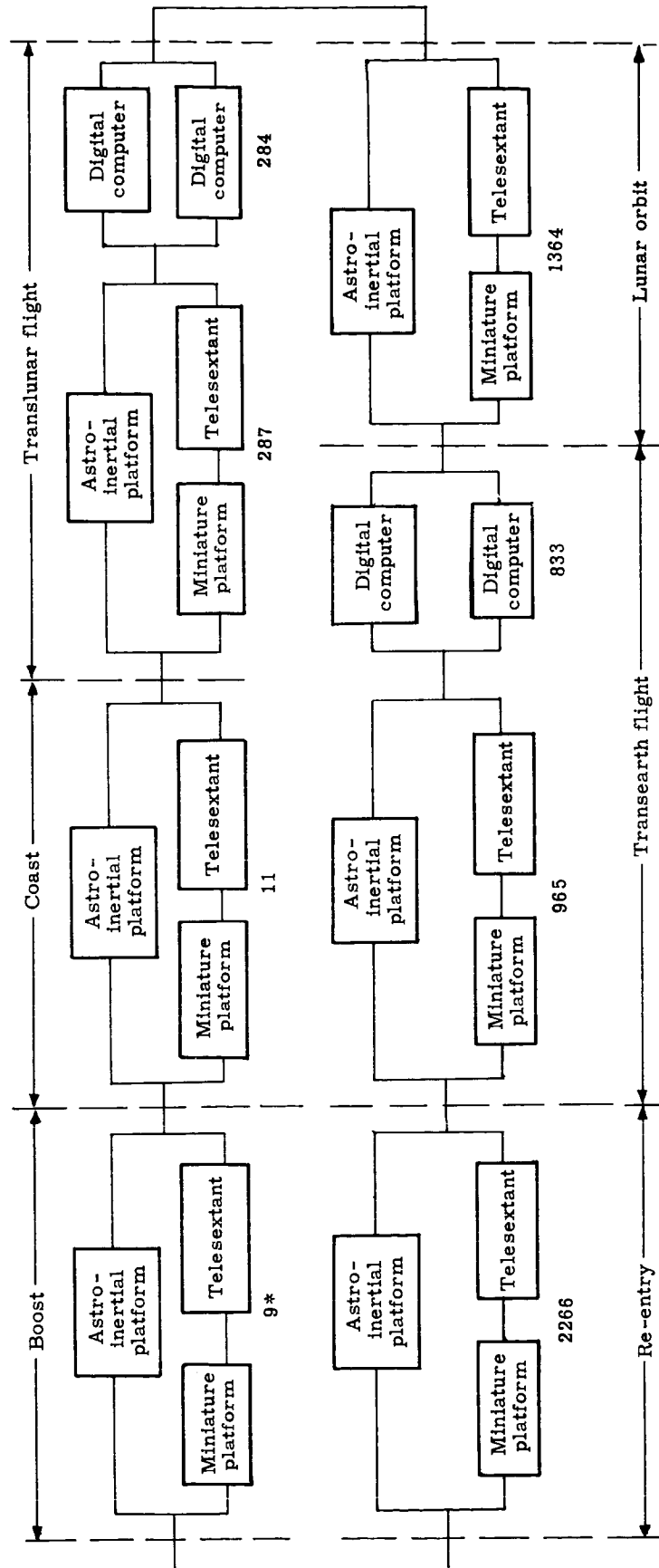


Fig. IX-1. Guidance Reliability Diagram

~~CONFIDENTIAL~~

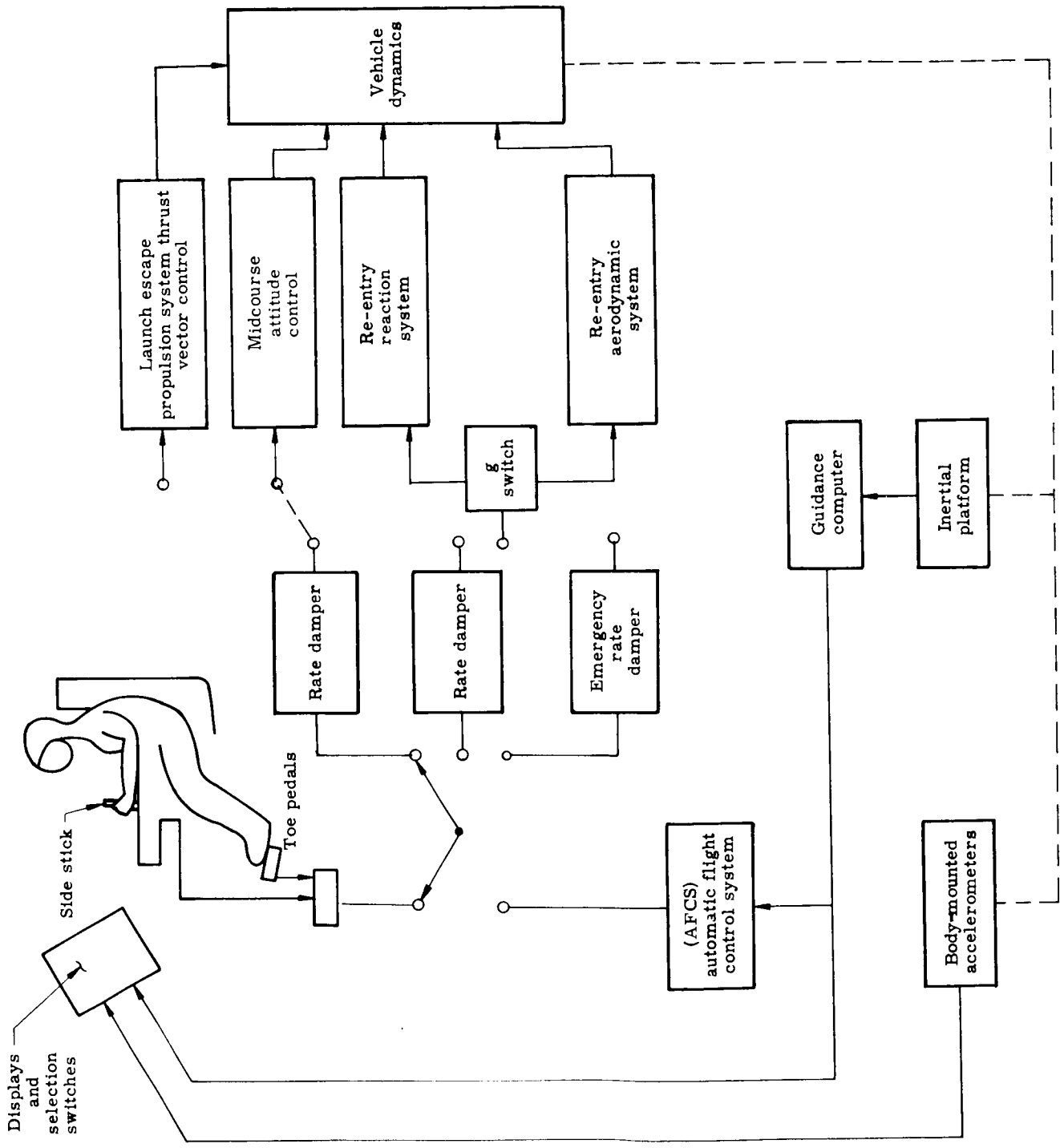


Fig. XI-1. Apollo Attitude Control System

~~CONFIDENTIAL~~

~~CONFIDENTIAL~~

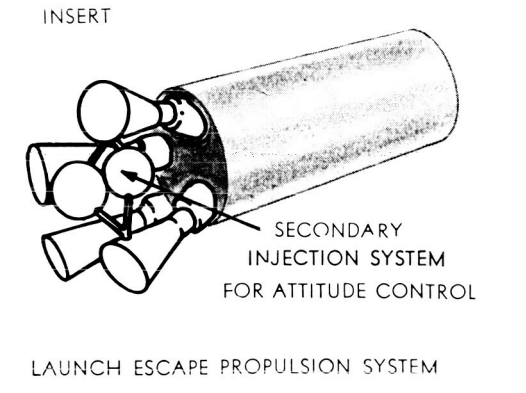
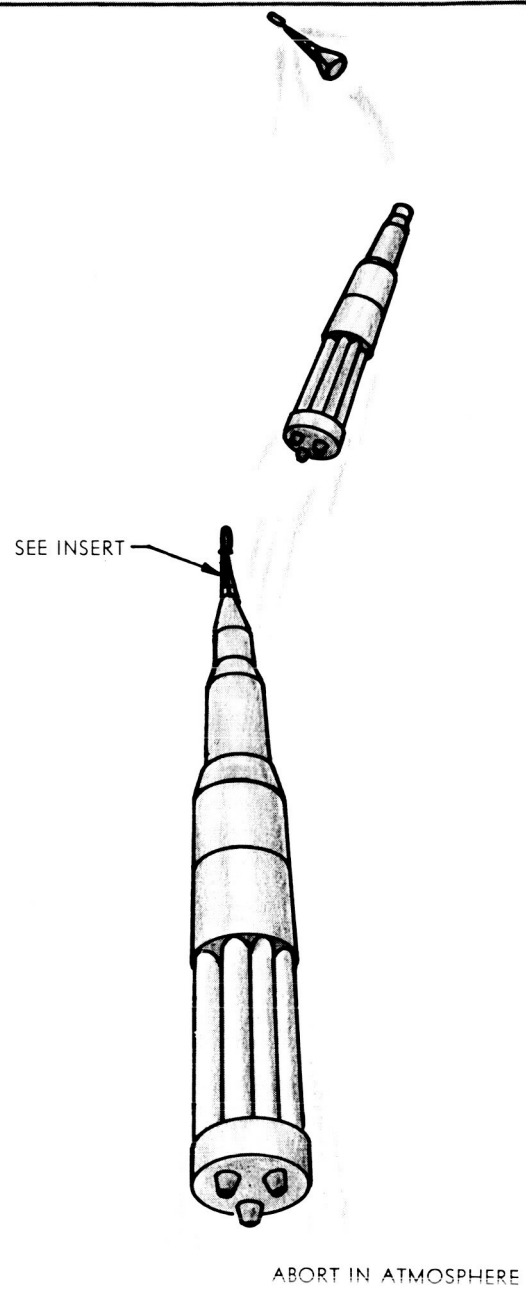
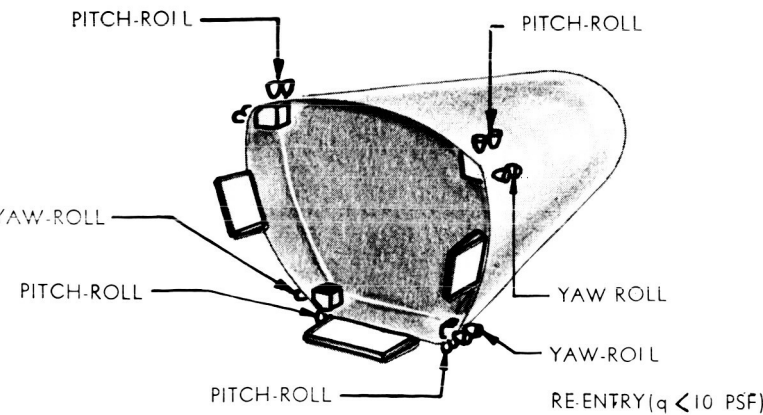
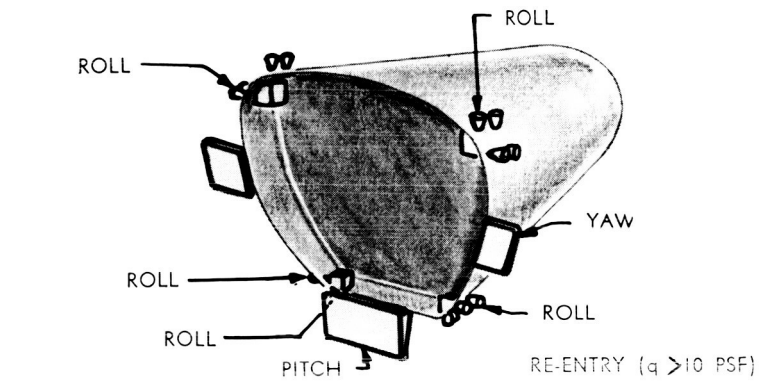
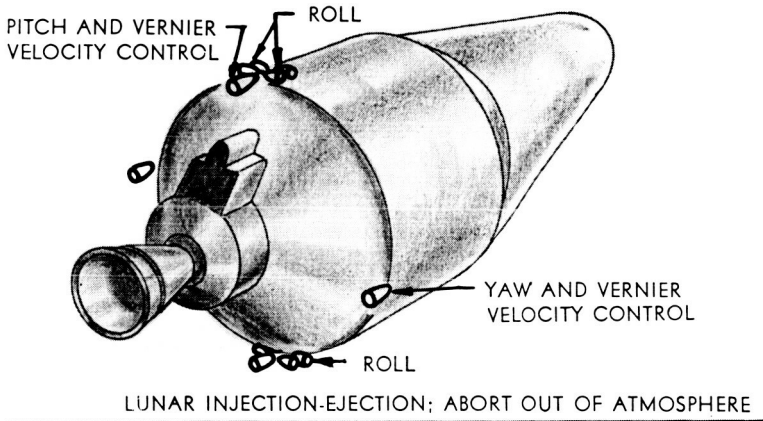
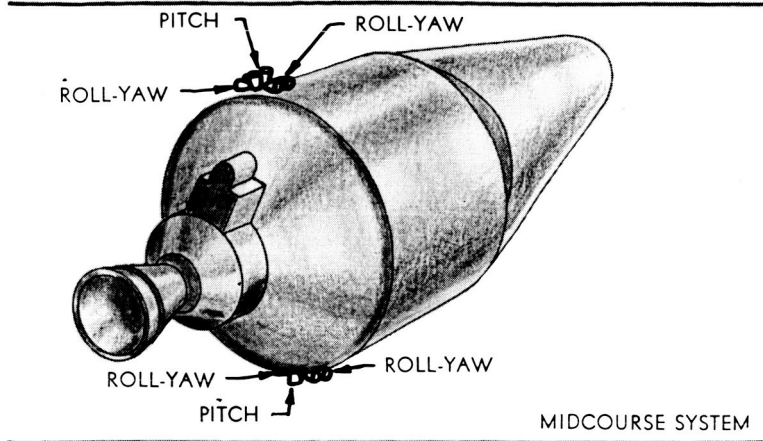


Fig. XI-2. Midcourse Configuration

~~CONFIDENTIAL~~

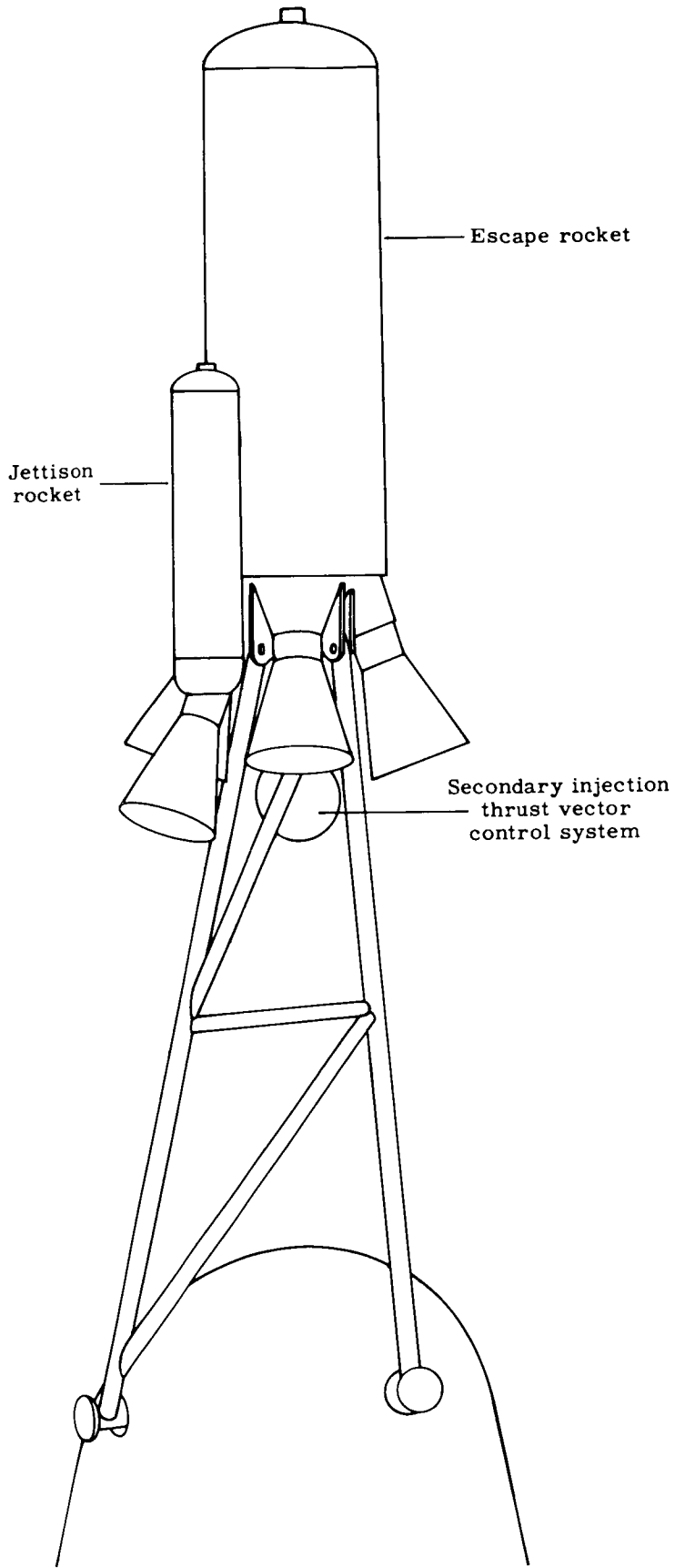
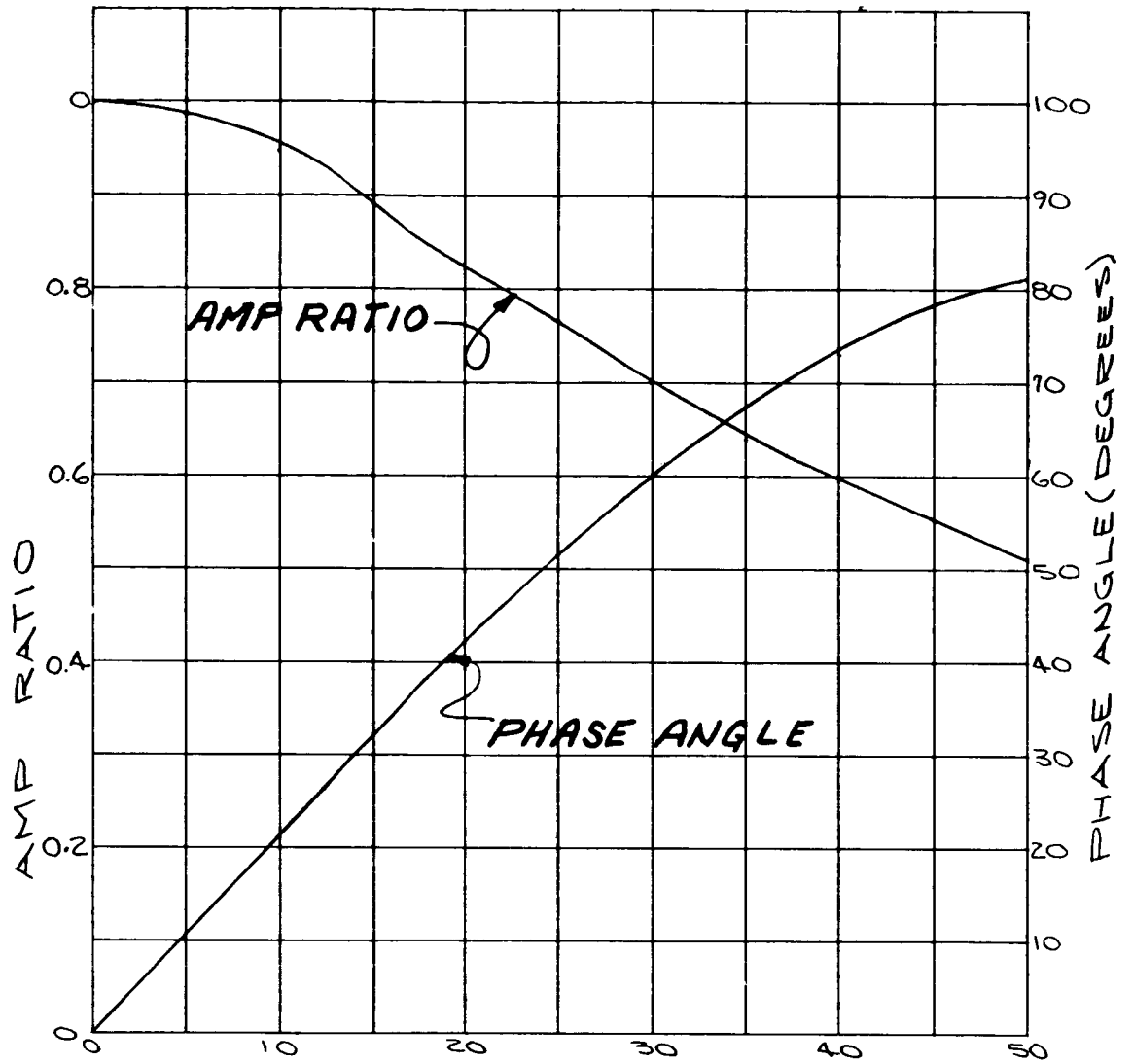


Fig. XI-3. Launch Escape Configuration



LIQUID INJECTION CONTROL

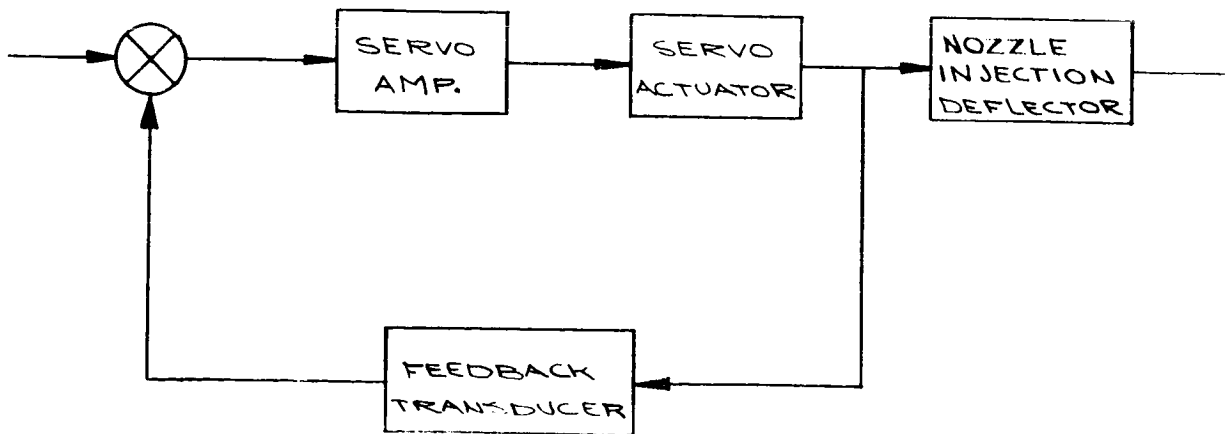
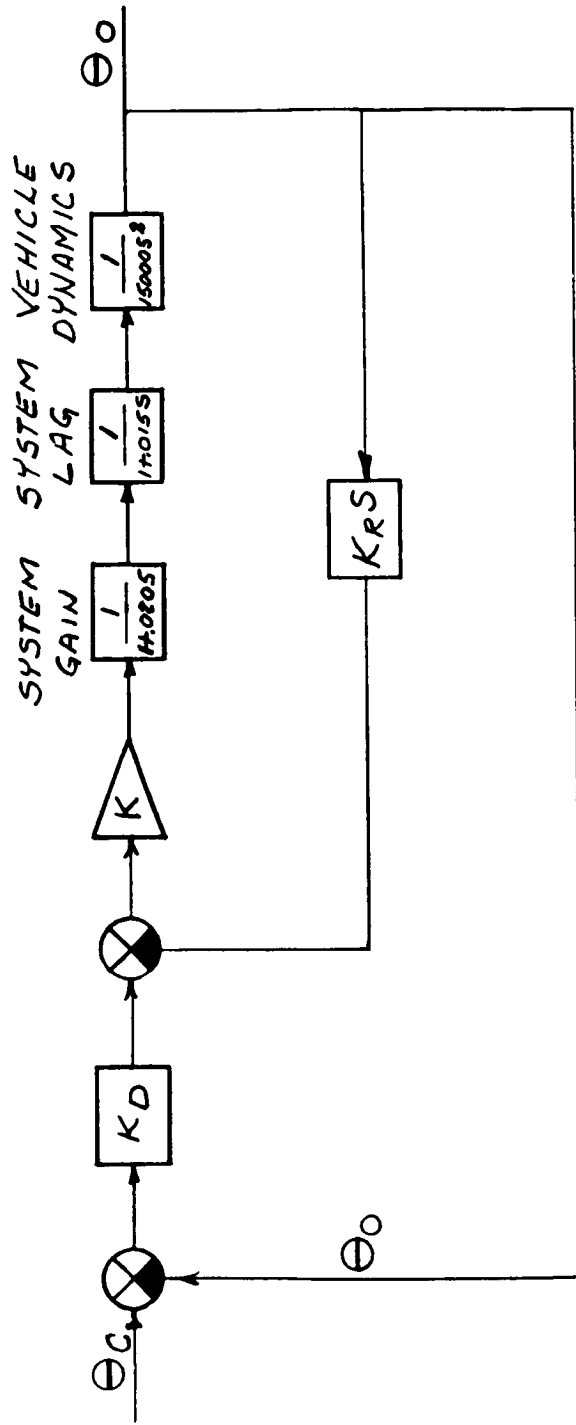


Fig. XI-4 Block Diagram and Dynamic Response of Liquid Injection Control System

~~CONFIDENTIAL~~



K : SYSTEM GAIN
 $KR/KD = m$: RATE TO DISPLACEMENT
 GAIN RATIO.

OPEN LOOP TRANSFER
 FUNCTION:
 $\frac{K/15000(17ms)}{s^2(17.0205)(17.0055)}$

Fig. XI-5. Functional Block Diagram, Launch Escape Pitch/Yaw Control Channel

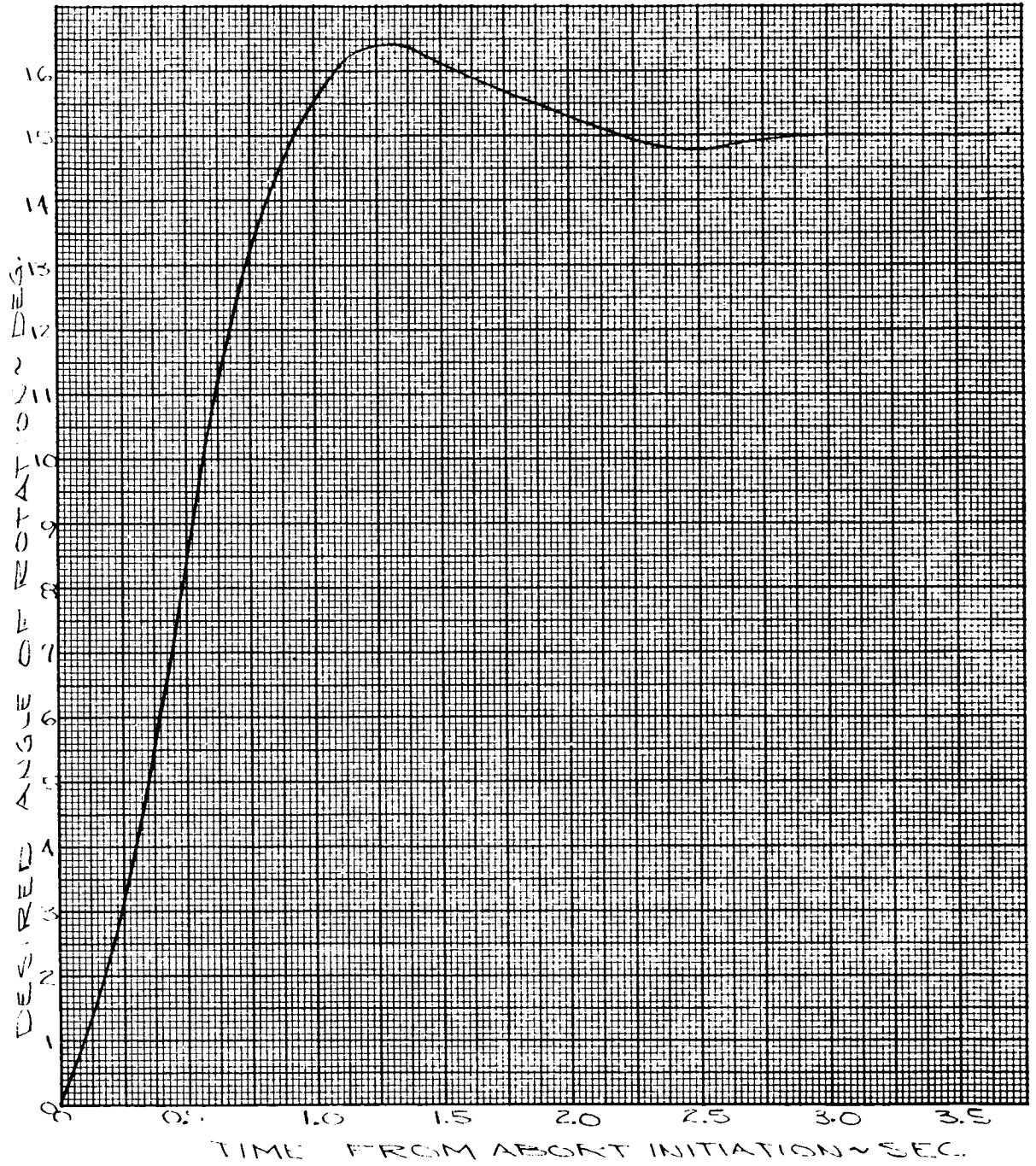


Fig. XI-6. Typical Response of Launch Escape Configuration to a 15° Step Input

~~CONFIDENTIAL~~

OPEN LOOP TRANSFER FUNCTION

$$= \frac{K/12500 (1+ms)}{s^2 (1+0.205s)(1+0.0055s)}$$

$\zeta=0.6$

$\zeta=0.7$

$\zeta=0.5$

3% +

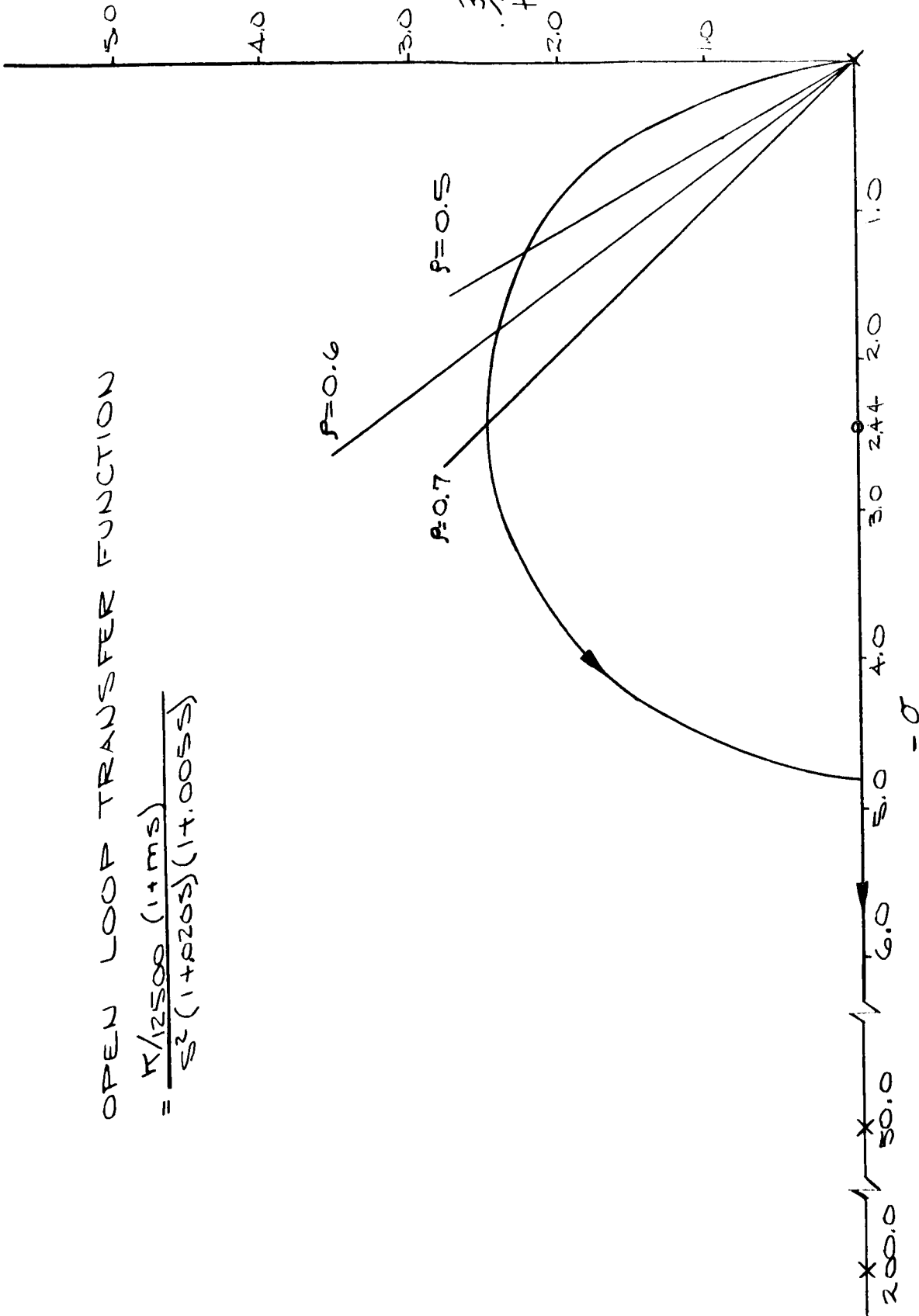
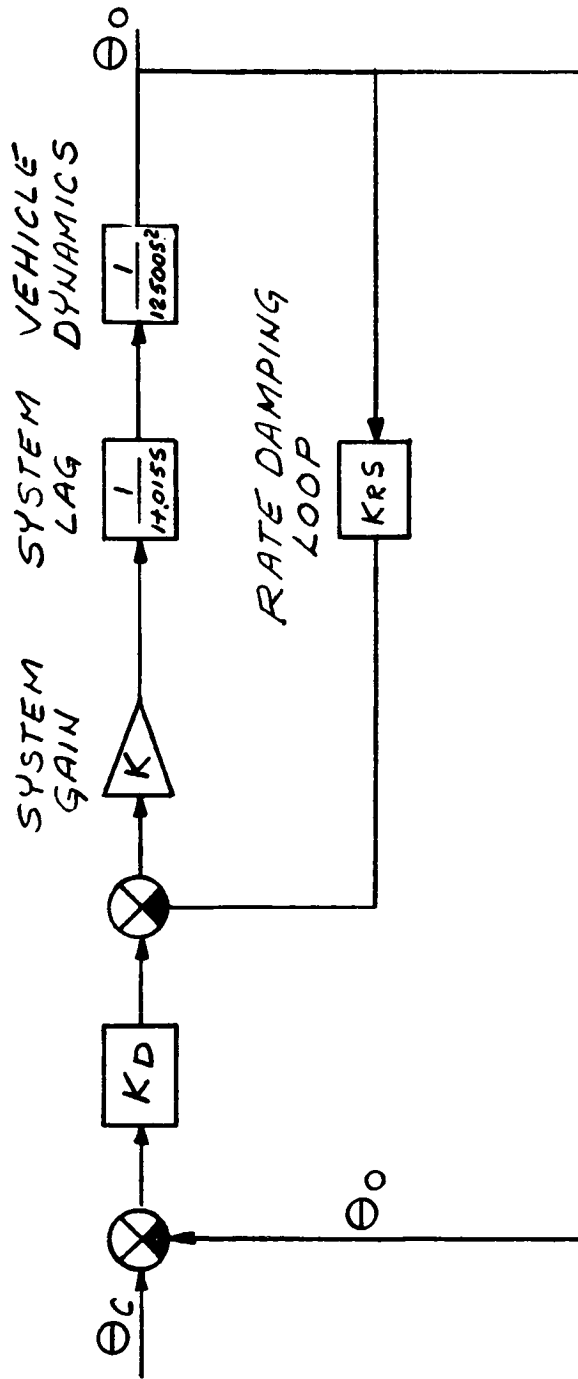


Fig. XI-7. Root Locus -- Launch Escape System Pitch/Yaw Channel

~~CONFIDENTIAL~~

~~CONFIDENTIAL~~



$K =$ SYSTEM GAIN
 $KR/K_D = \eta =$ RATE TO DISPLACEMENT GAIN RATIO.
 OPEN LOOP TRANSFER FUNCTION.
 $\frac{K/12500(1+ms)}{S^2(1+0.15S)}$

Fig. XI-8. Block Diagram Pitch/Yaw Control Channel During 15.6 k Engine Operation

~~CONFIDENTIAL~~

OPEN LOOP TRANSFER FUNCTION:

$$\frac{K(12500(1+ms))}{s^2(1+0.015s)}$$

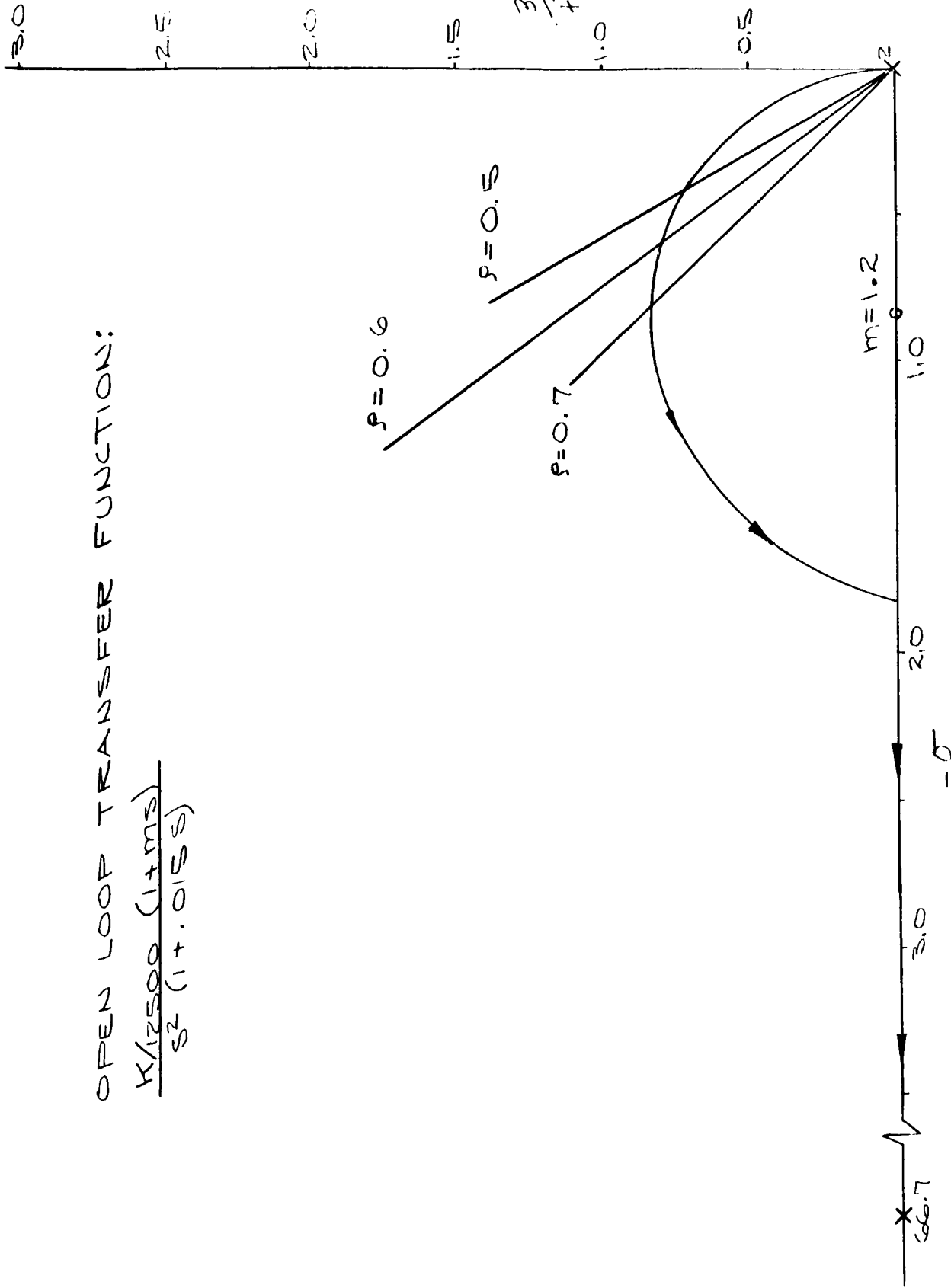


Fig. XI-9. Root Locus -- 15.6 k Engine Pitch/Yaw Channel

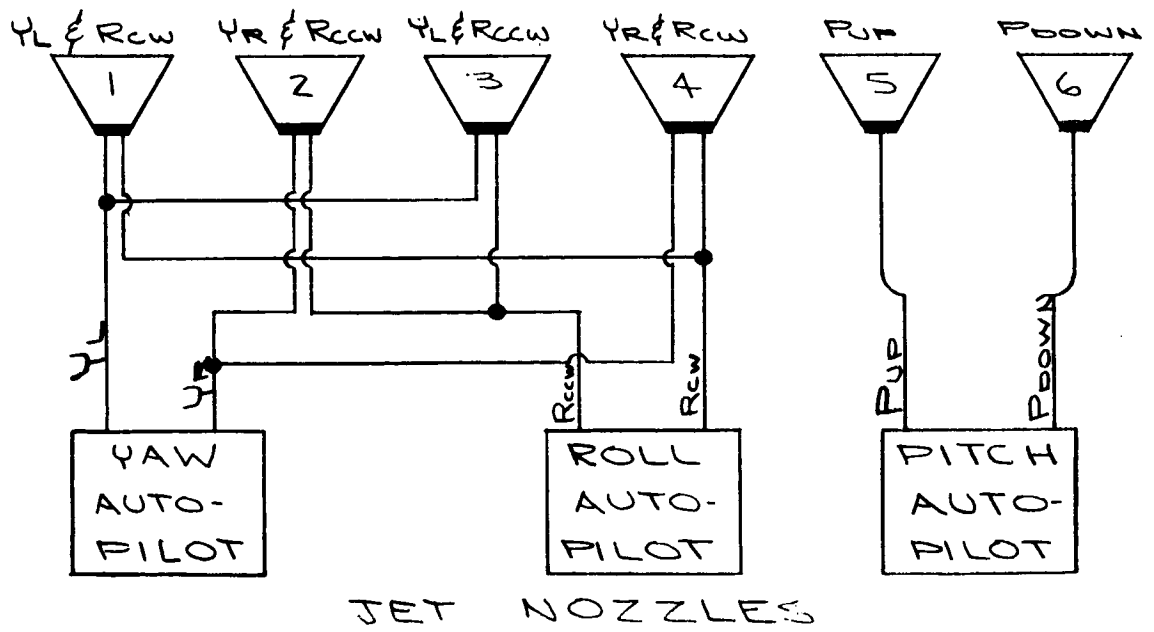
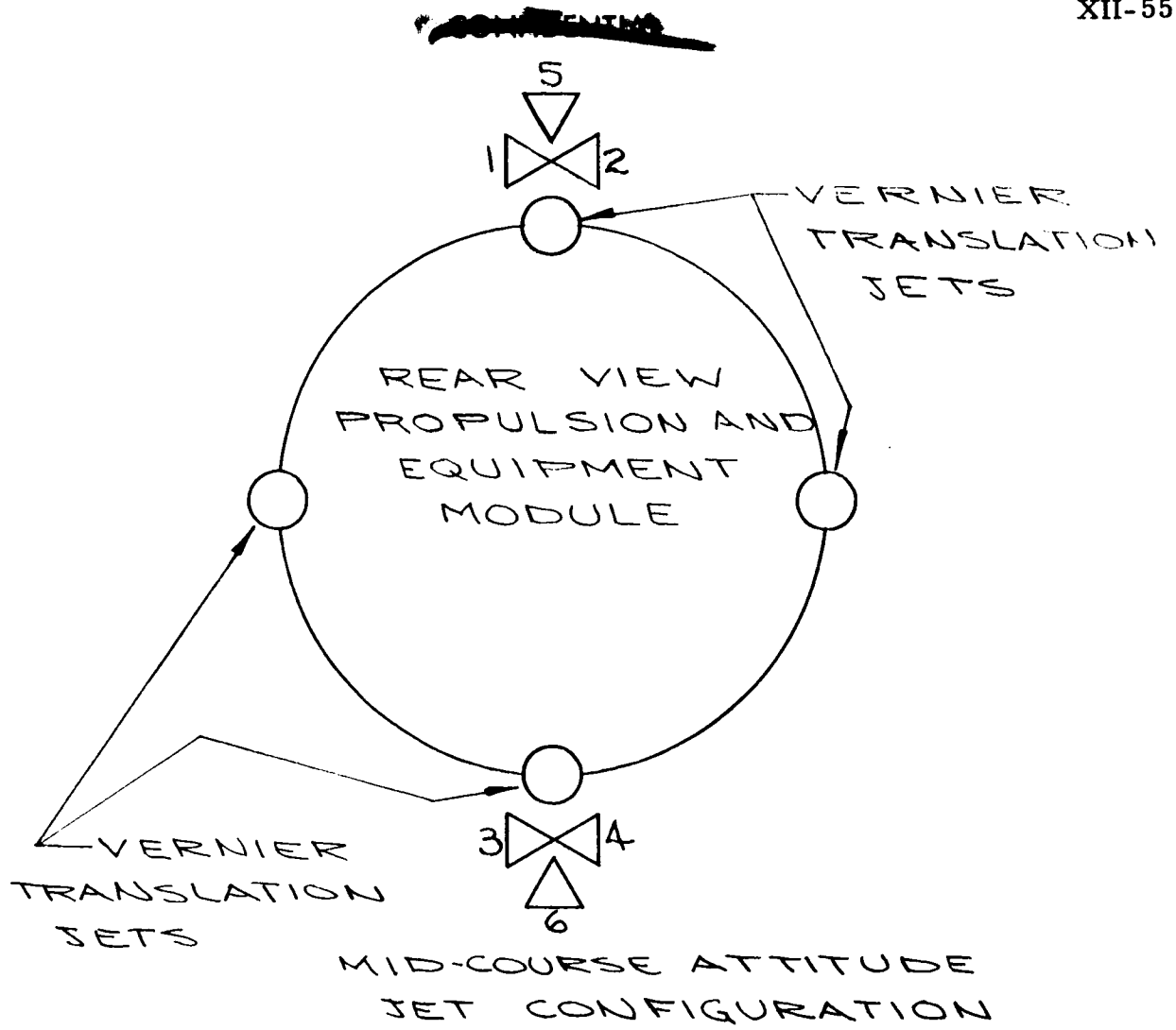
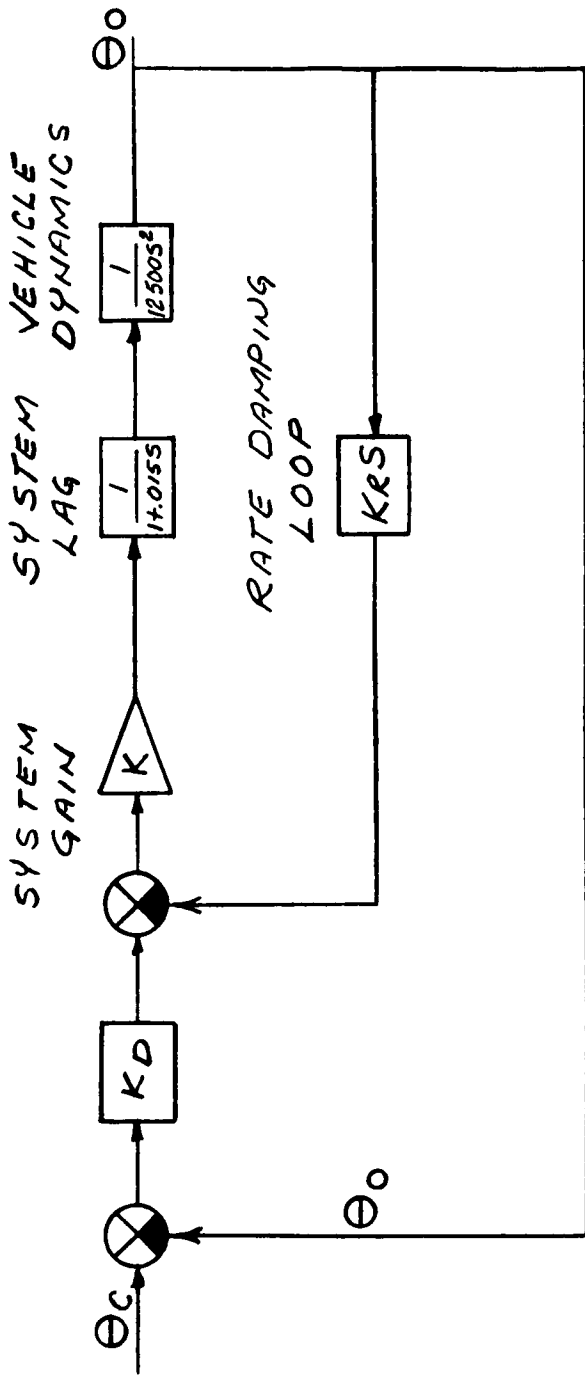


Fig. XI-10. Midcourse Attitude Control Nozzle Configuration

~~CONFIDENTIAL~~

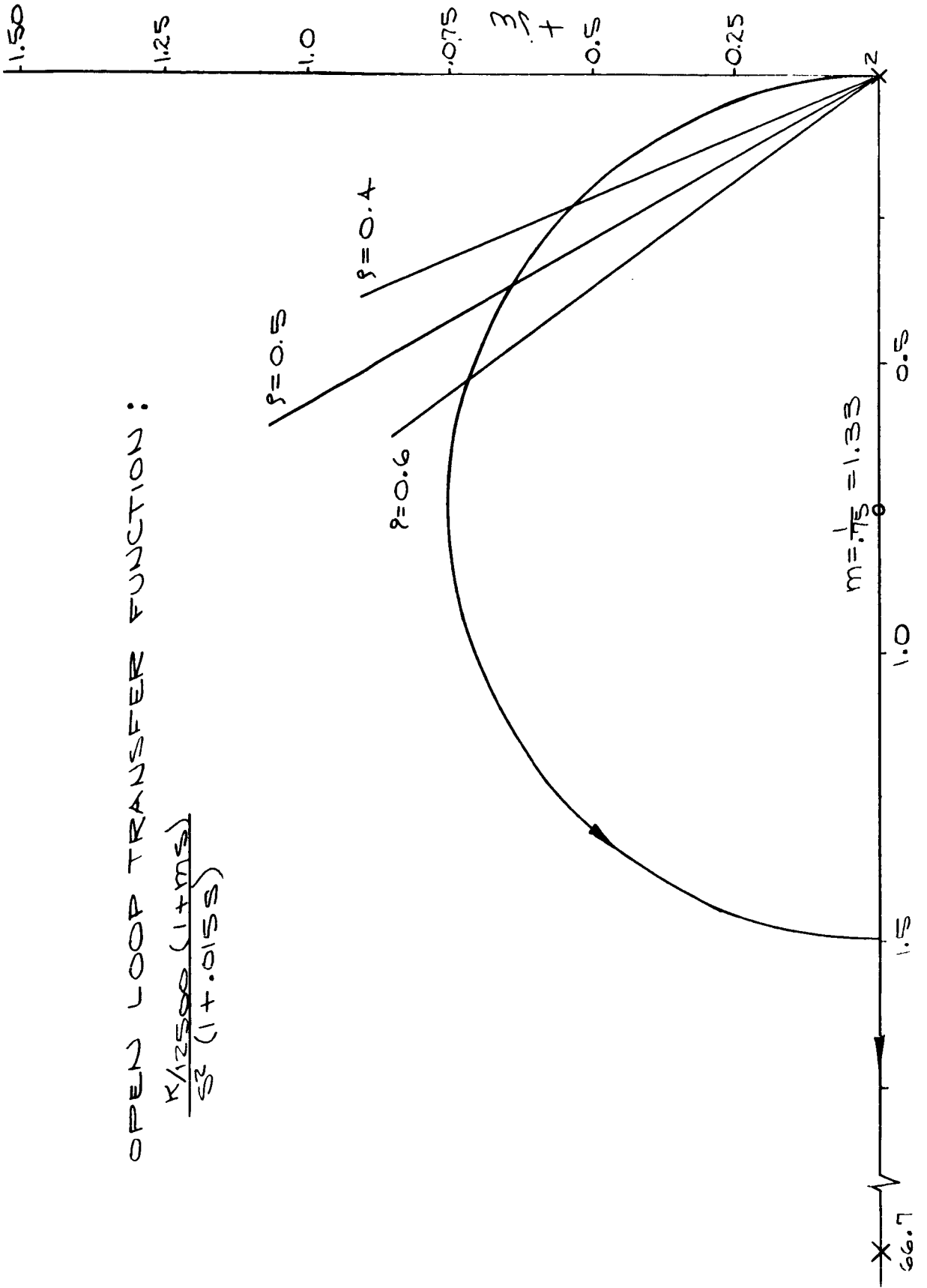


*K: SYSTEM GAIN
 KR/KD = m: RATE TO
 DISPLACEMENT
 GAIN RATIO.*

*OPEN LOOP TRANSFER
 FUNCTION:
 K/(12500(1+.015S)
 S²(1+.015S)*

Fig. XI-11. Functional Block Diagram Coasting, Autopilot, Pitch/
 Yaw Channel

~~CONFIDENTIAL~~

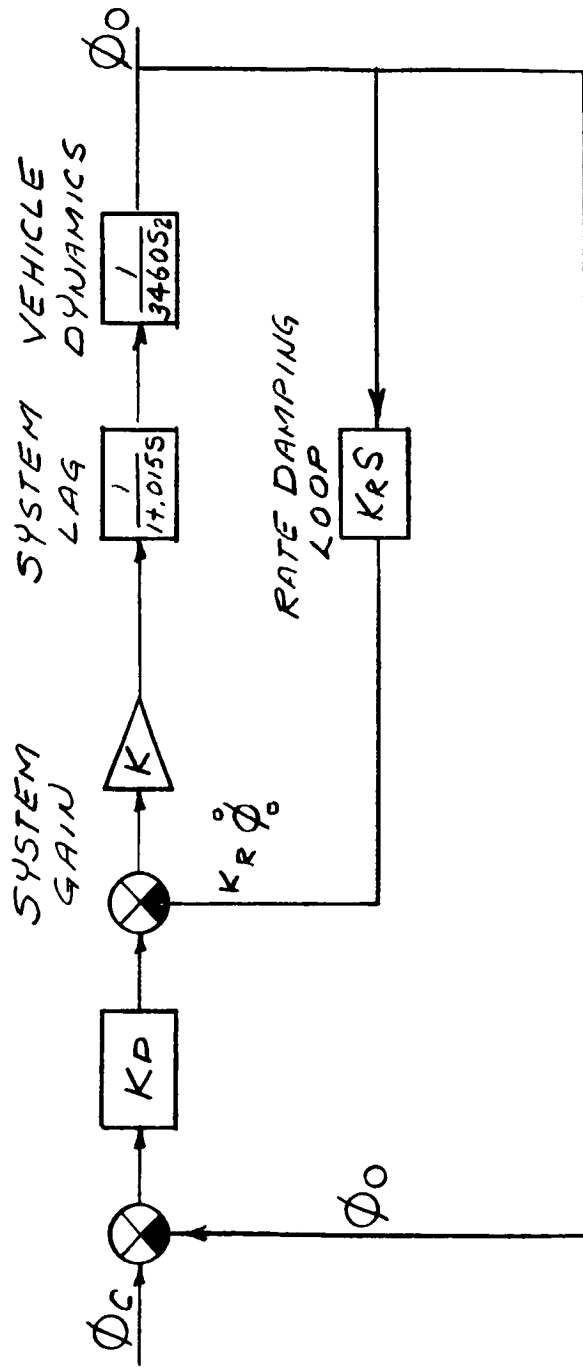


OPEN LOOP TRANSFER FUNCTION :

$$\frac{K/12500(1+ms)}{s^2(1+0.15s)}$$

~~CONFIDENTIAL~~

Fig. XI-12. Root Locus -- Coasting Flight Pitch/Yaw Channel



$K = \text{SYSTEM GAIN}$
 $K_R/K_D = m : \text{RATE TO DISPLACEMENT GAIN RATIO.}$
 $\text{OPEN LOOP TRANSFER FUNCTION:}$
 $\frac{K/3460(1+ms)}{s^2(1+0.155s)}$

Fig. XI-13. Functional Block Diagram. Midcourse Autopilot Roll Channel

~~CONFIDENTIAL~~

OPEN LOOP TRANSFER FUNCTION:

$$\frac{K/6150 (1+ms)}{s^2 (1+0.015s)}$$

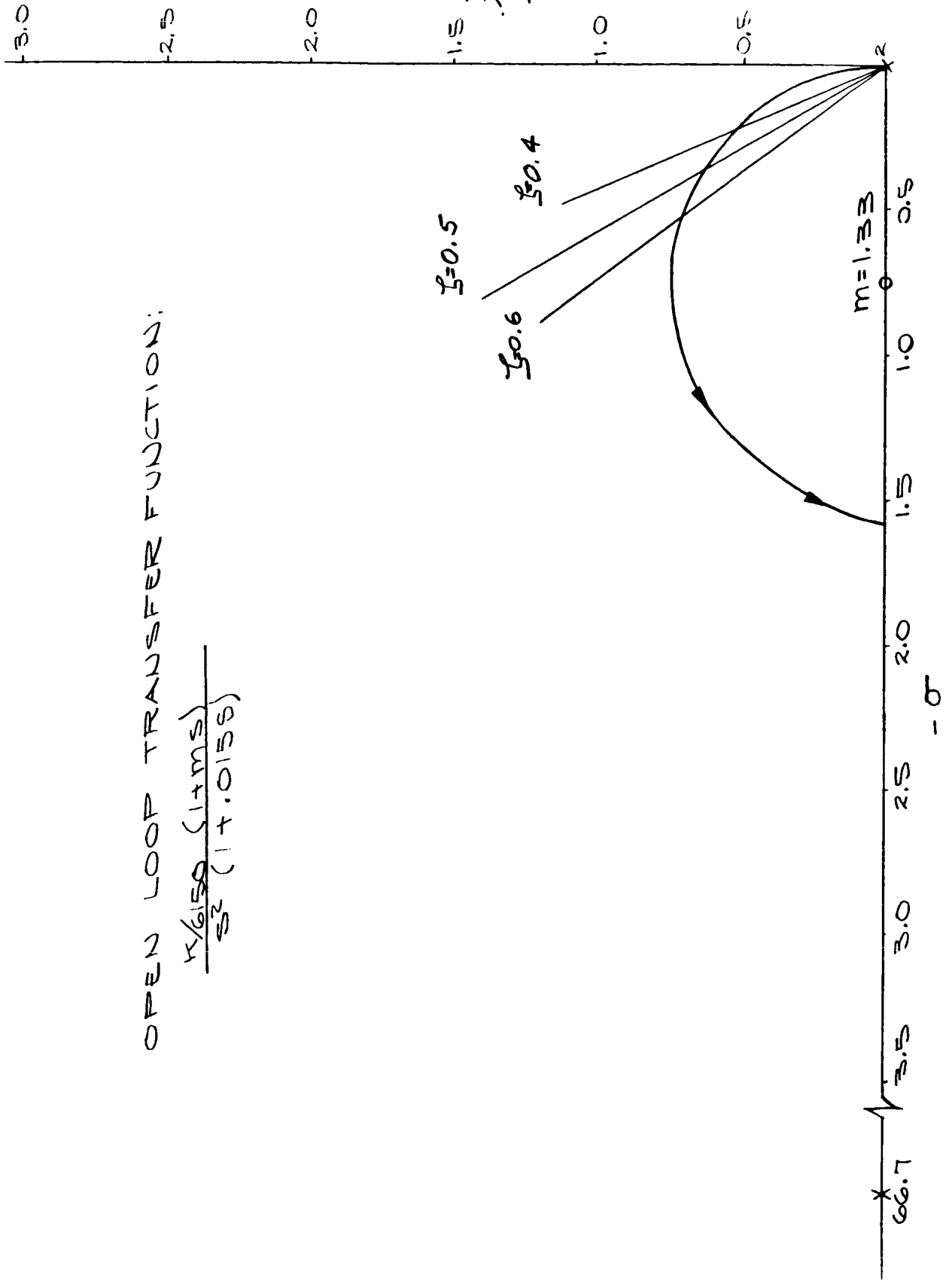
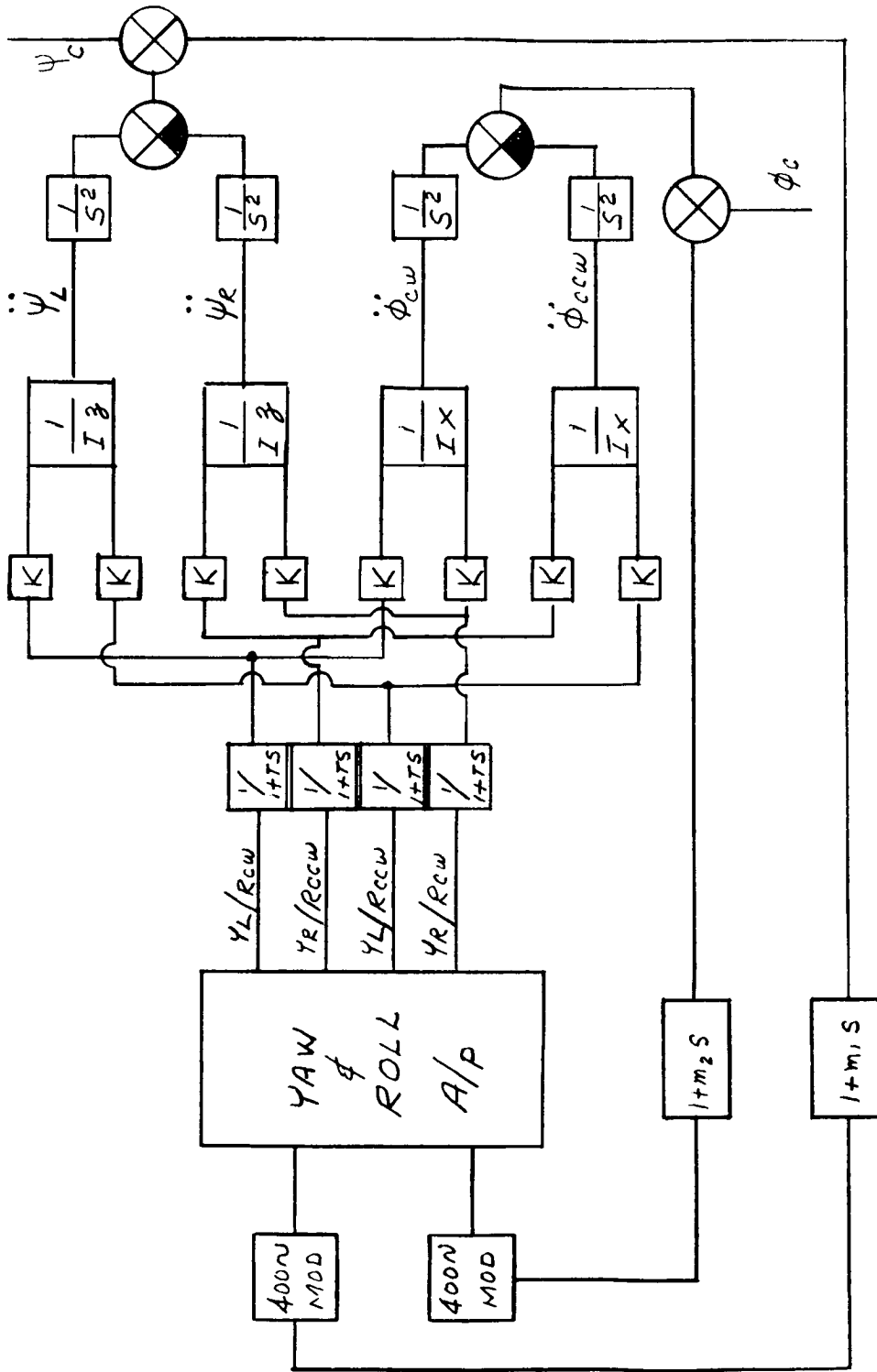


Fig. XI-14. Root Locus--Midcourse Roll Channel

~~CONFIDENTIAL~~



$I_z = 12,500 \text{ slug } f^2$
 $I_x = 3,460 \text{ slug } f^2$
 $\tau = .005 \text{ sec}$
 $m_2 = m_1 = 1.2$

$\ddot{\psi}_L \text{ MAX} = \ddot{\psi}_R \text{ MAX} = \frac{2 \times 180}{12500}$
 $\dot{\phi}_{CW} \text{ MAX} = \dot{\phi}_{CCW} \text{ MAX} = \frac{2 \times 45}{3460}$

Fig. XI-15. Block Diagram -- Autopilot/Analog Connection

~~CONFIDENTIAL~~

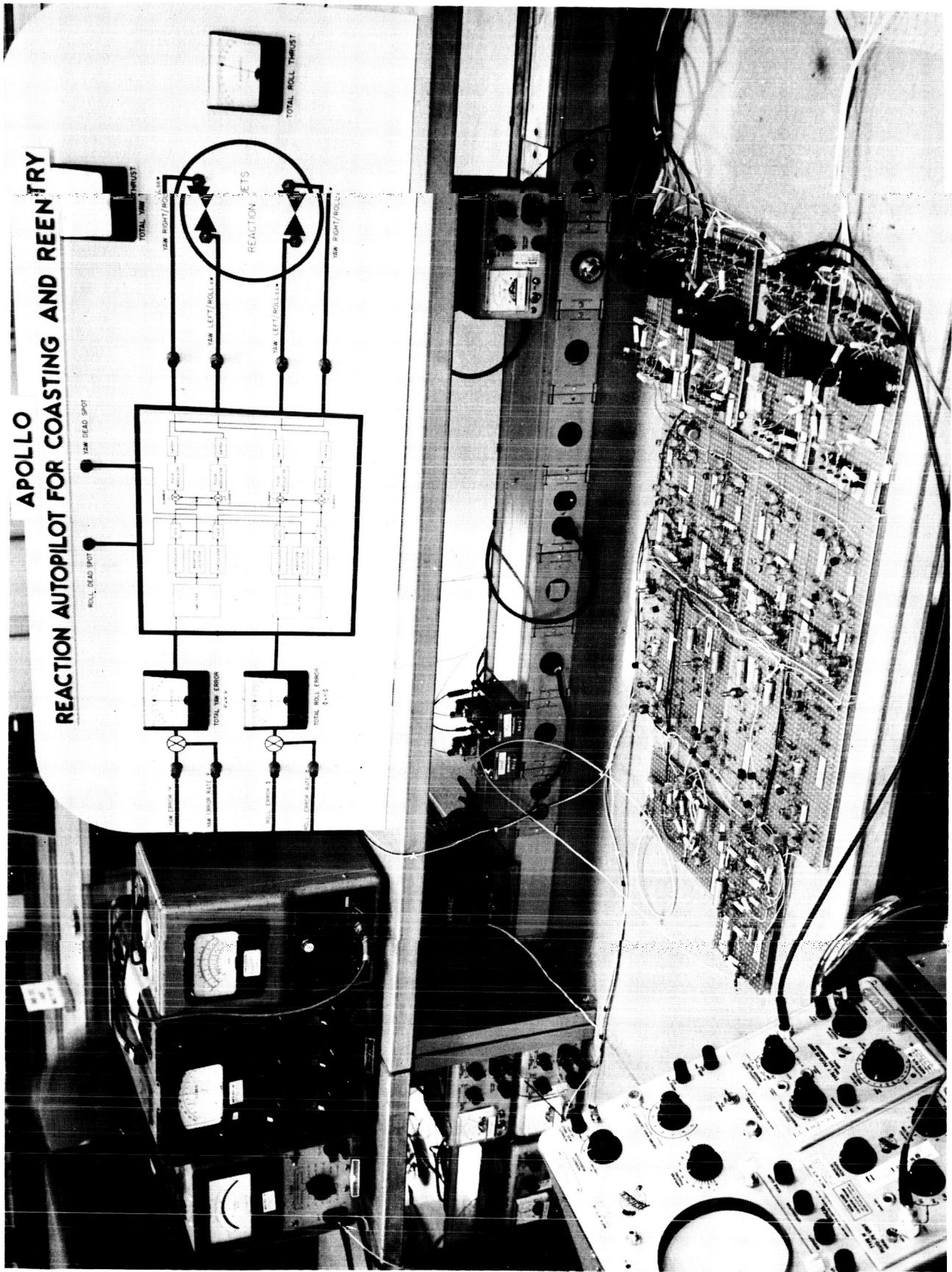


Fig. XI-16. Breadboard Apollo Reaction Autopilot for Coasting and Re-entry

~~CONFIDENTIAL~~

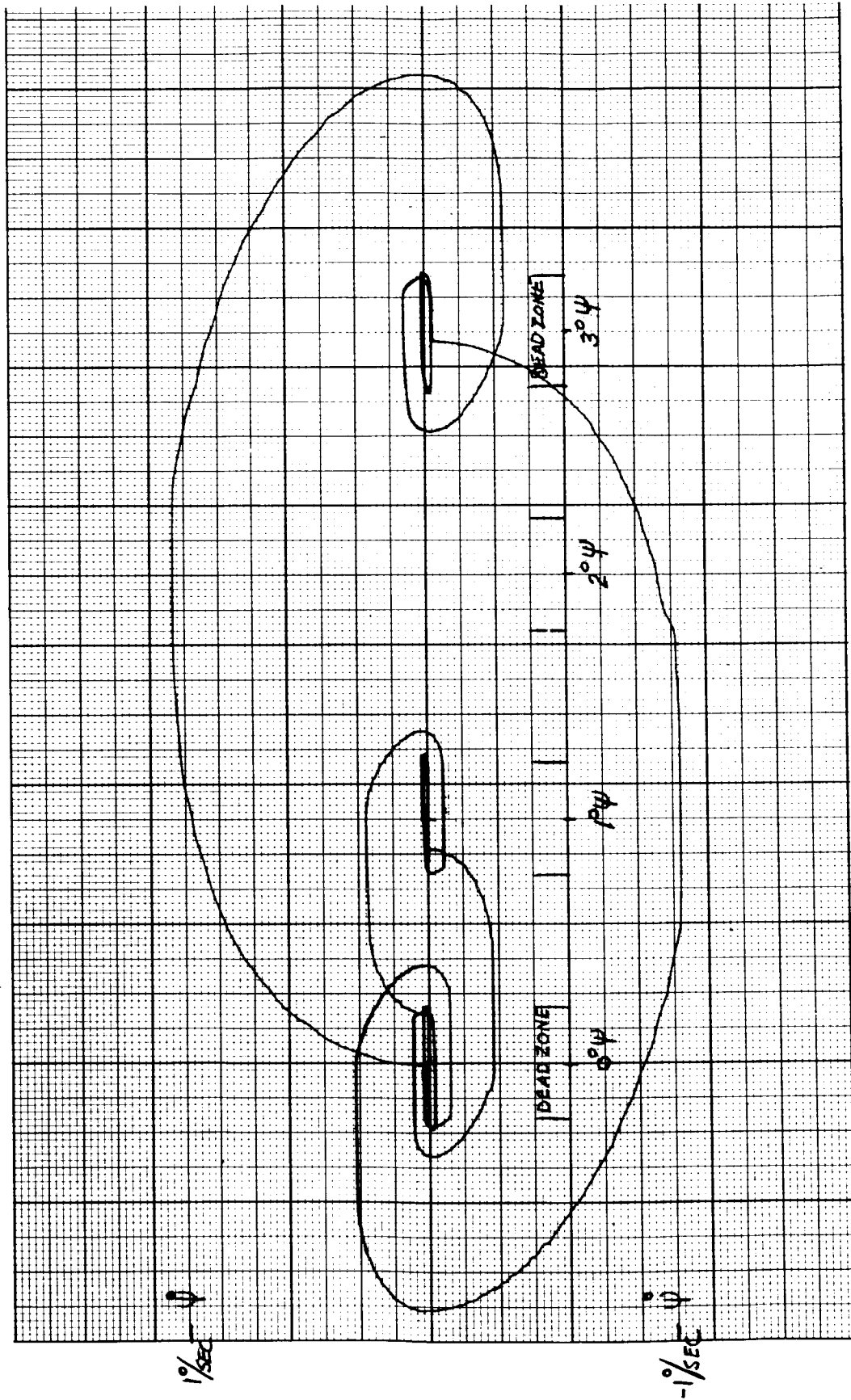


Fig. XI-17. X-Y Recorder Limit Cycle Tracing

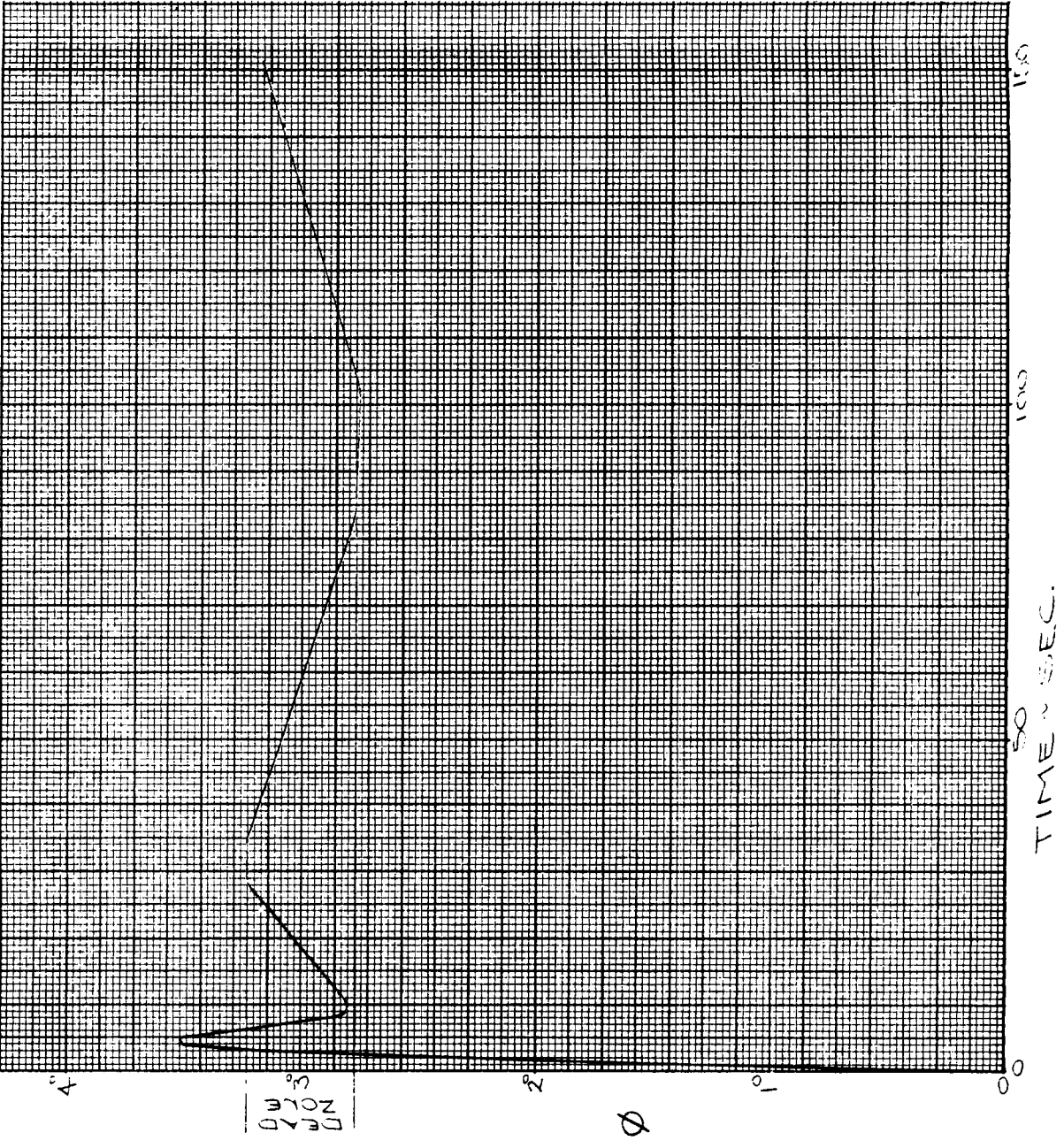
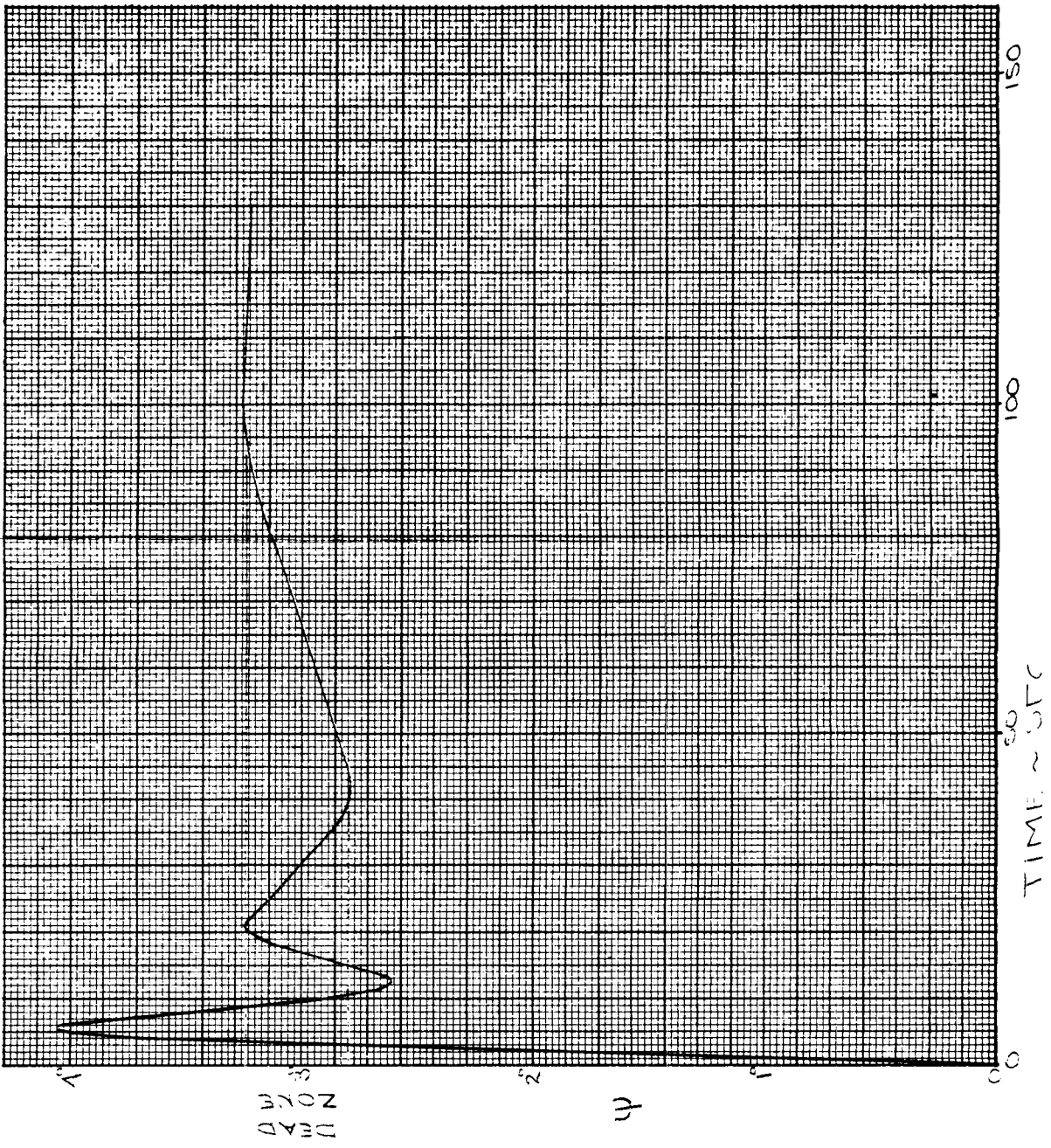
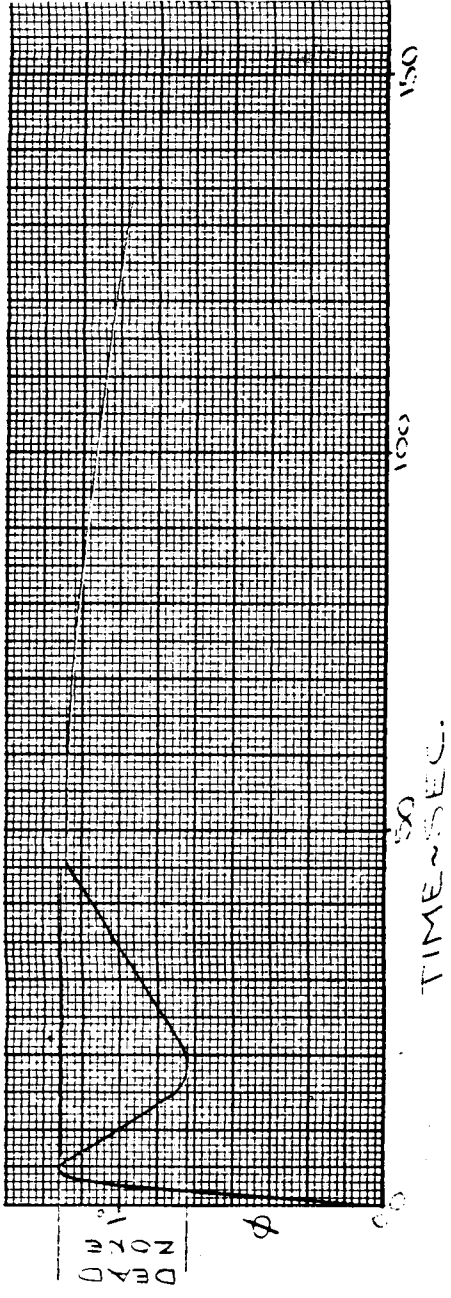
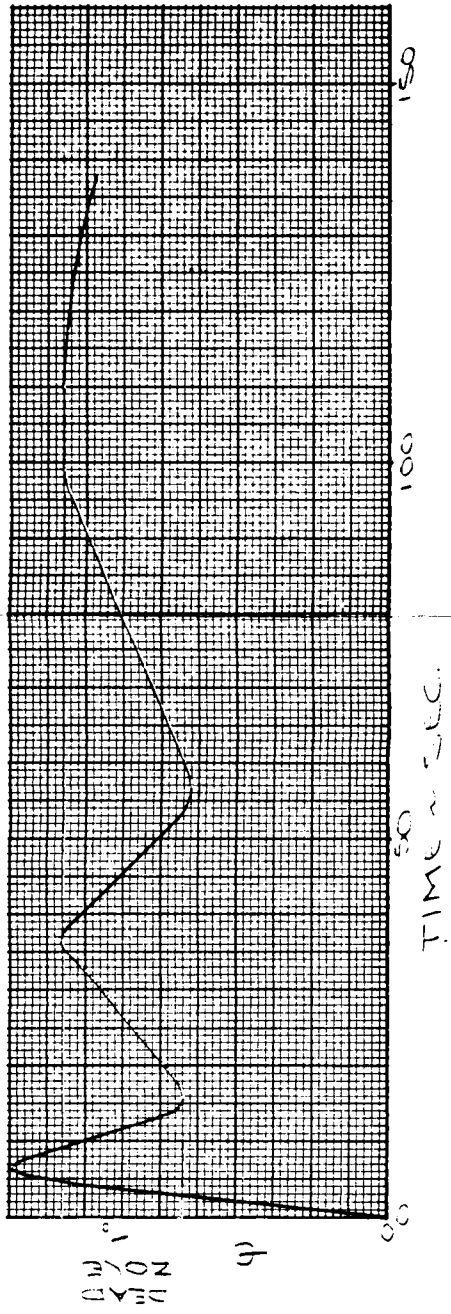


Fig. XI-18. Recorder Tracing A/P System Response to Step Input (Coupled)

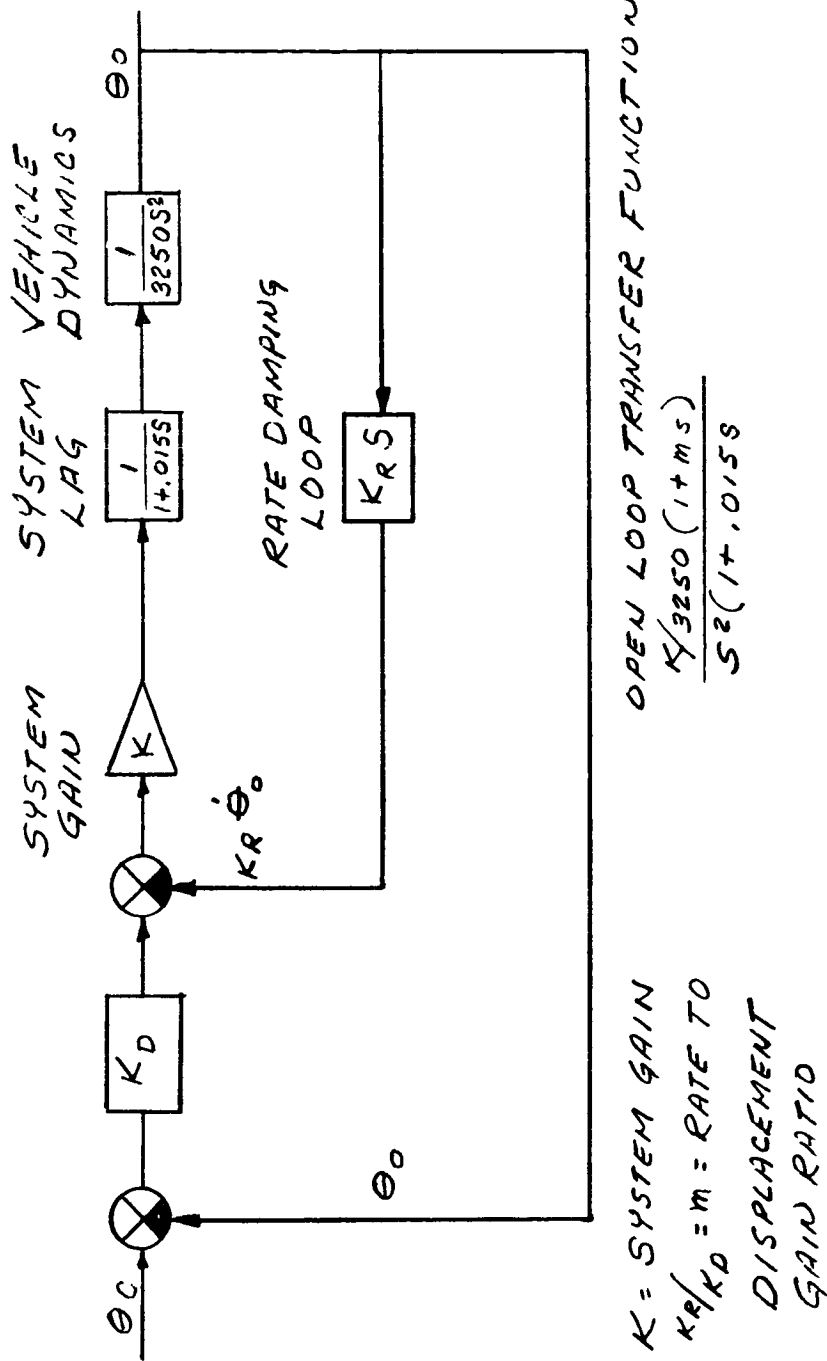
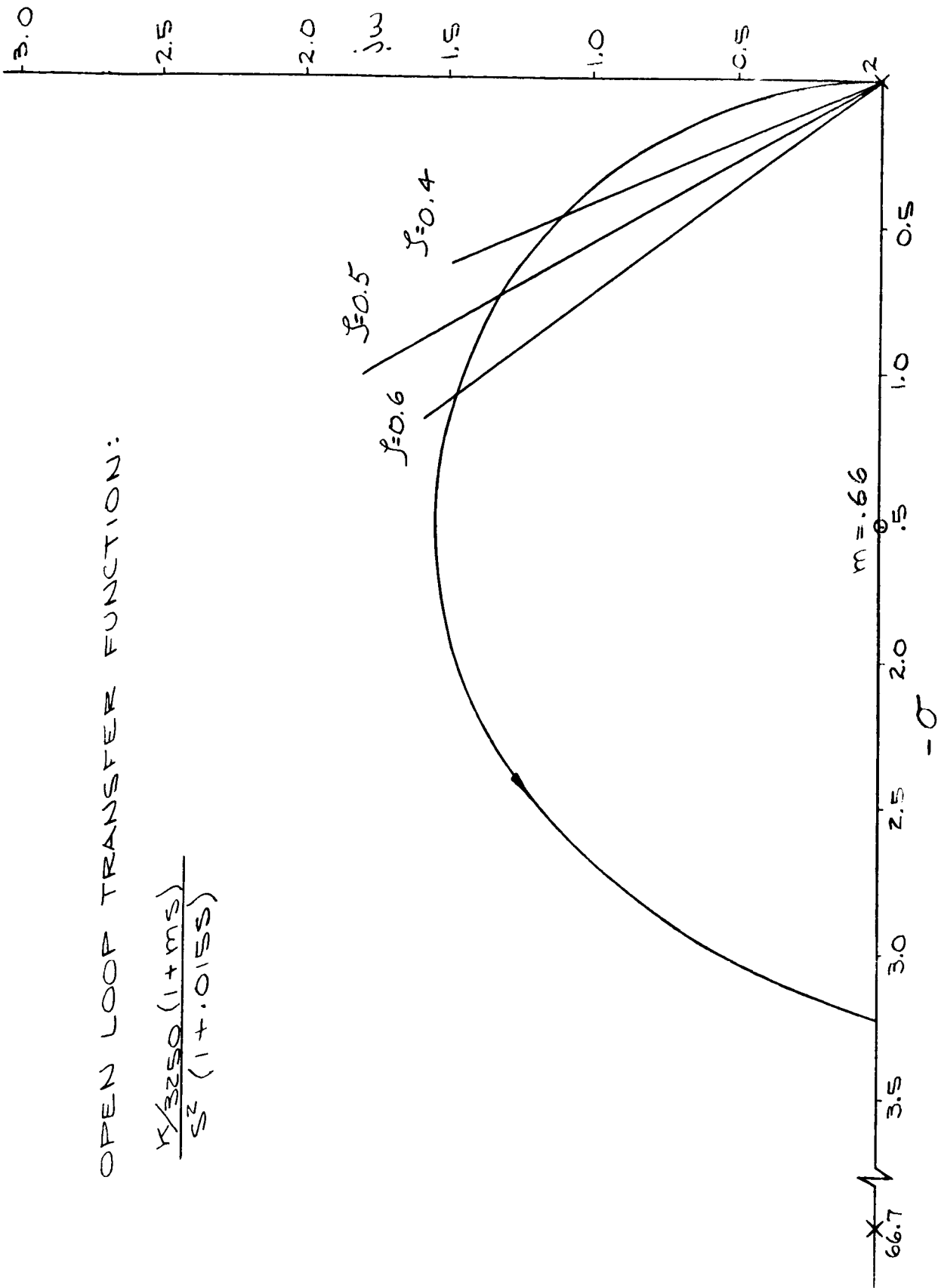


Fig. XI-19. Block Diagram--Re-entry Reaction Pitch/Yaw Channel

~~CONFIDENTIAL~~

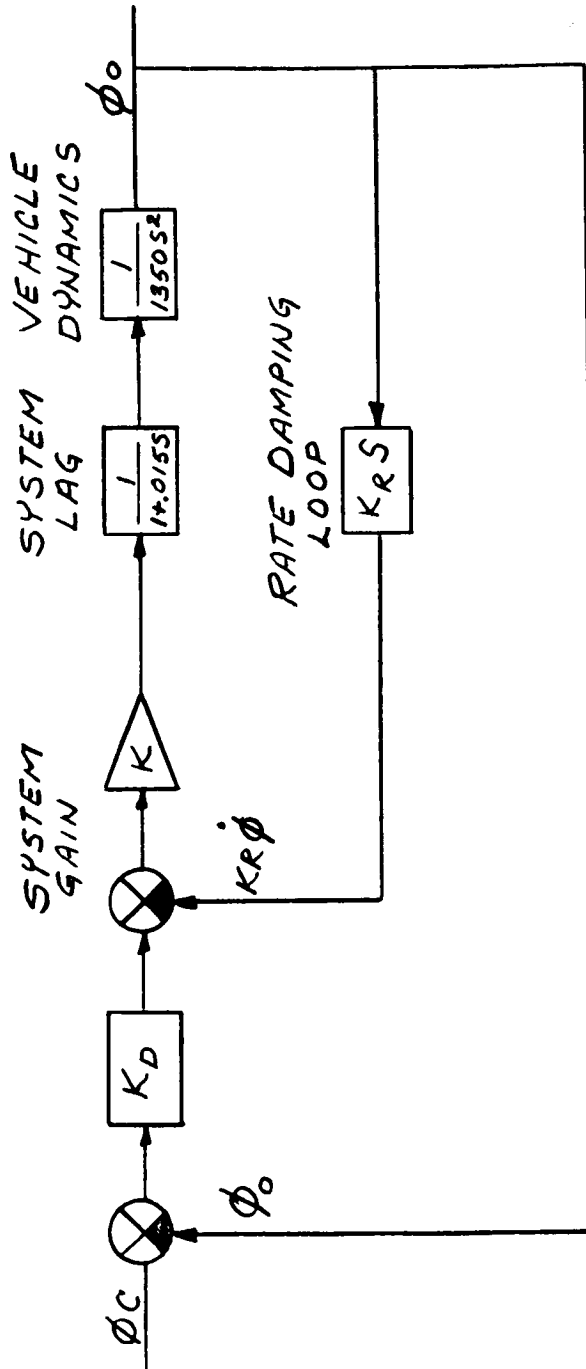


OPEN LOOP TRANSFER FUNCTION:

$$\frac{K/3250(1+ms)}{s^2(1+0.015s)}$$

~~CONFIDENTIAL~~

Fig. XI-20. Root Locus -- Re-entry Reaction Pitch/Yaw Channel



$K = \text{SYSTEM GAIN}$

$K_R/K_D = m = \text{RATE TO DISPLACEMENT GAIN RATIO.}$

$\text{OPEN LOOP TRANSFER FUNCTION}$

$$\frac{K/1350(1+ms)}{s^2(17.015s)}$$

Fig. XI-21. Functional Block Diagram Re-entry Roll Control Channel

OPEN LOOP TRANSFER FUNCTION:

$$\frac{K(1+s)}{s^2(1+0.15s)}$$

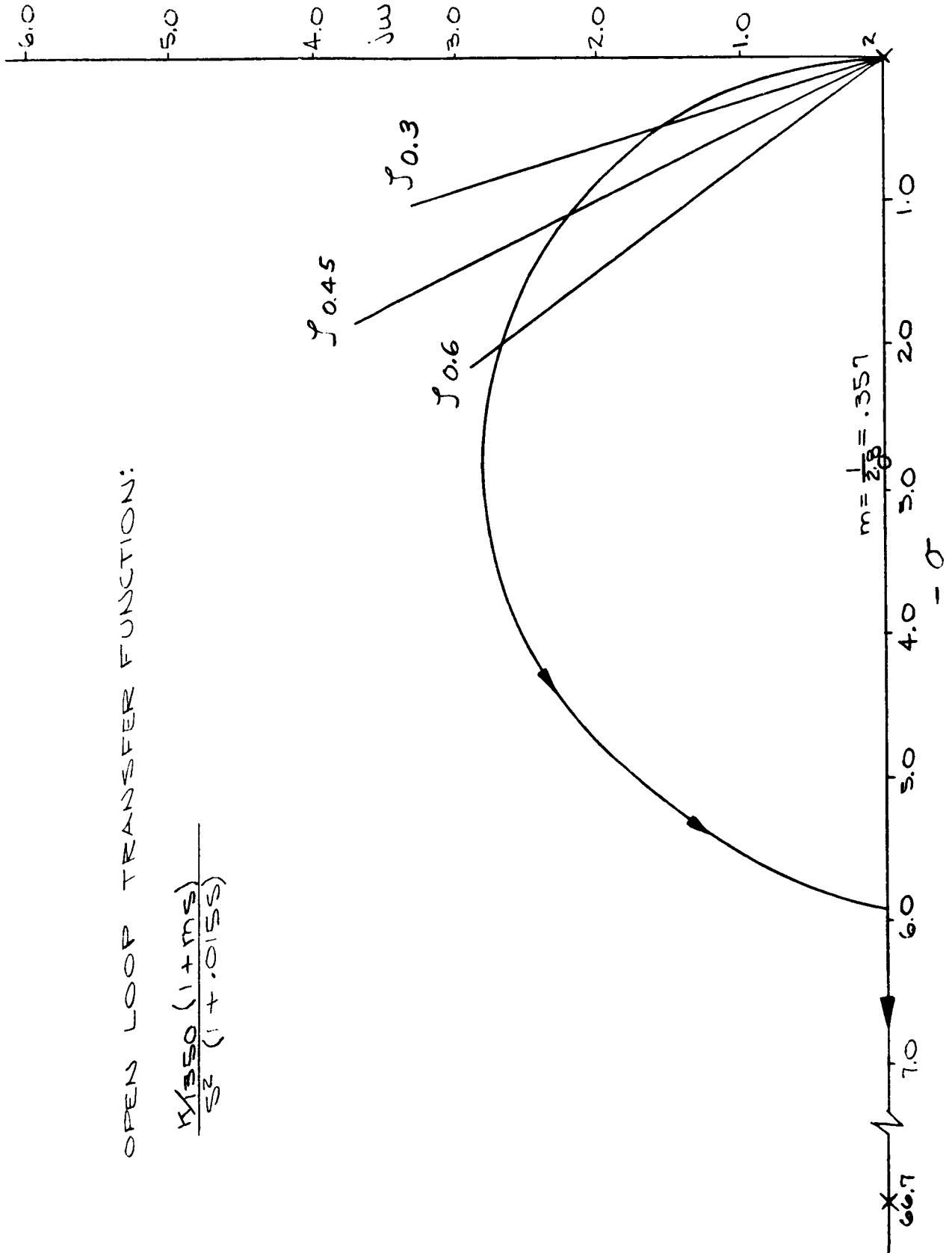


Fig. XI-22. Root Locus -- Re-entry Roll Channel

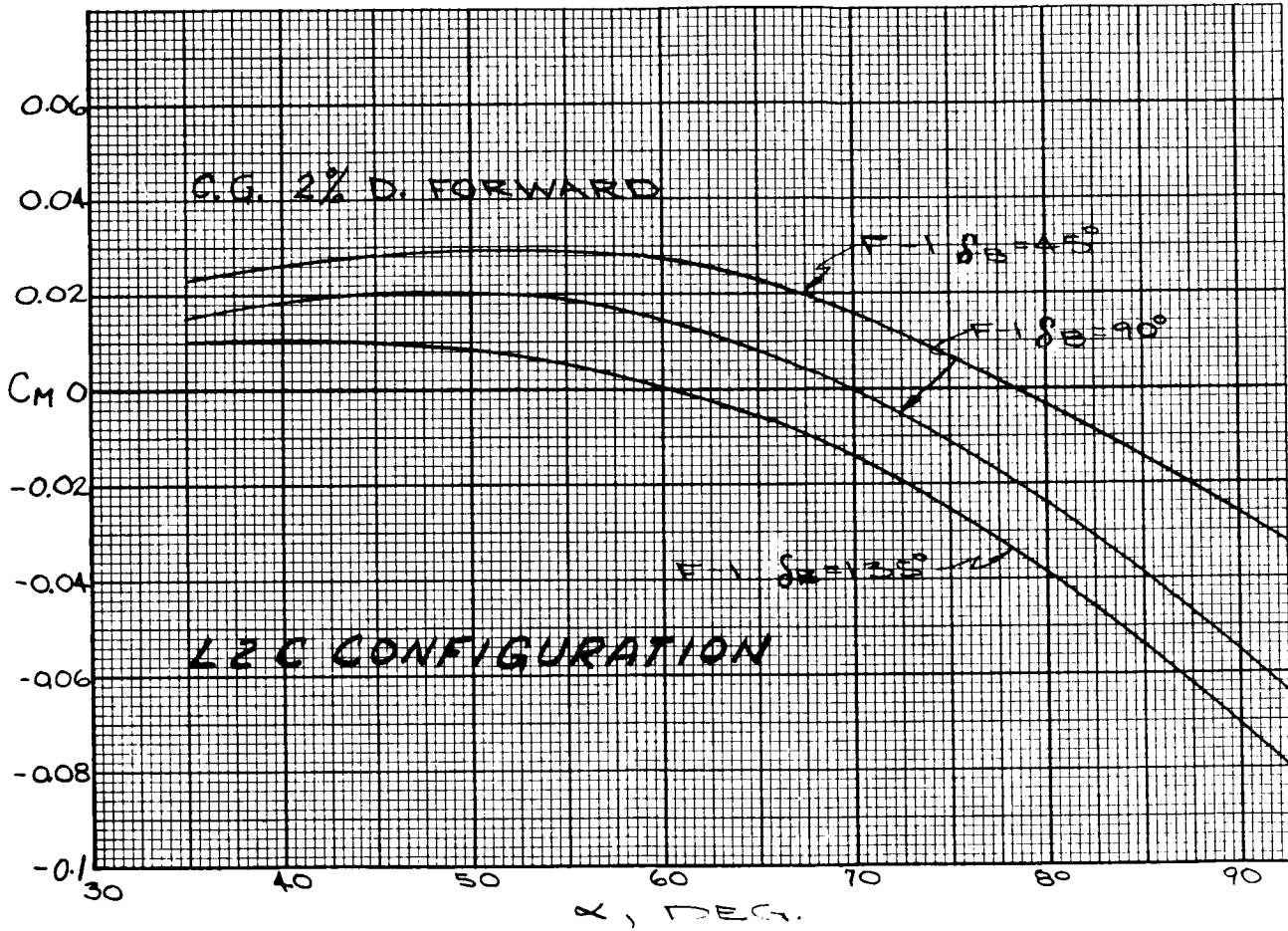


Fig. XI-23 Pitching Moment Coefficient Versus Angle of Attack

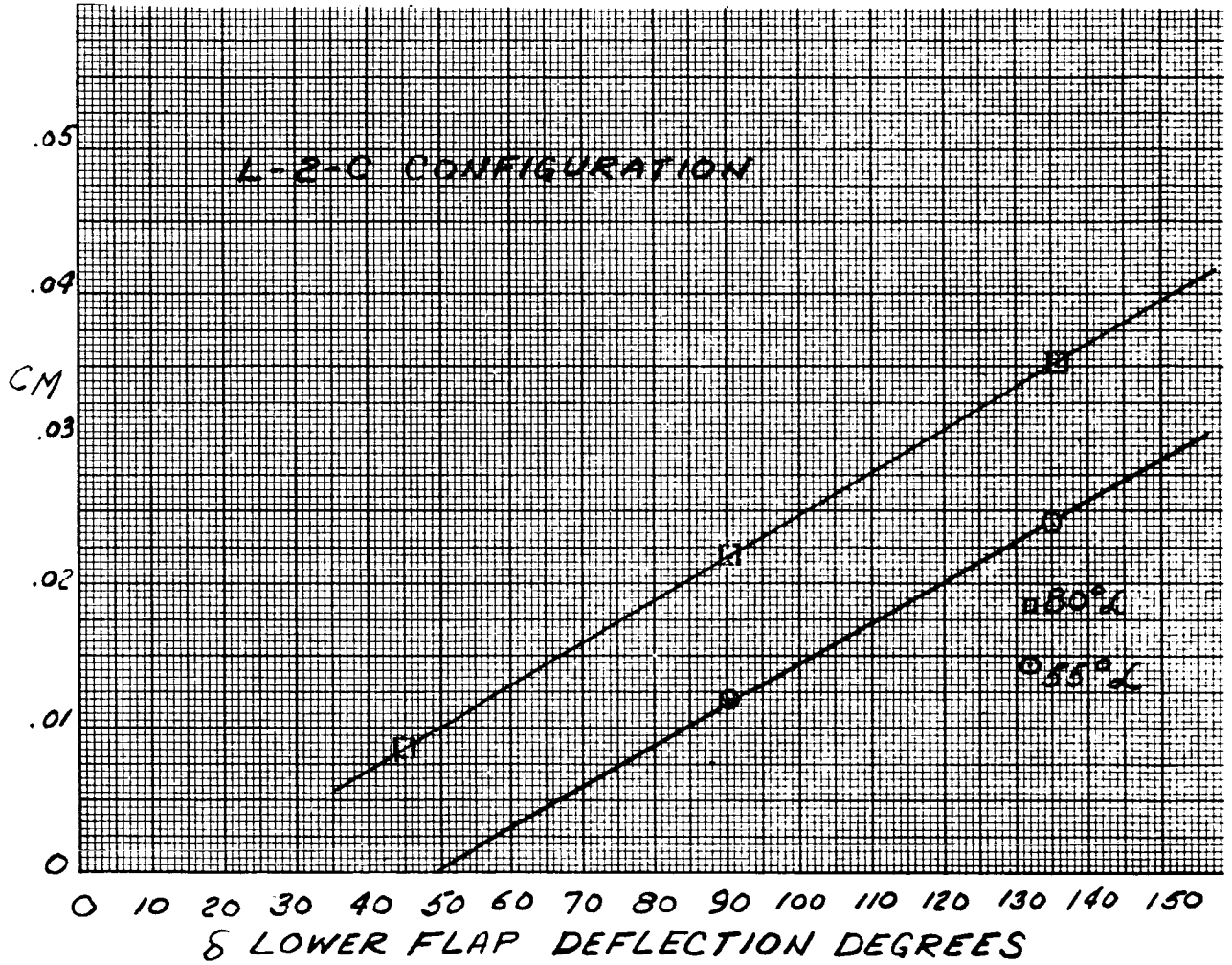


Fig. XI-24. Pitching Moment Coefficient Versus Lower Flap Deflection

~~CONFIDENTIAL~~

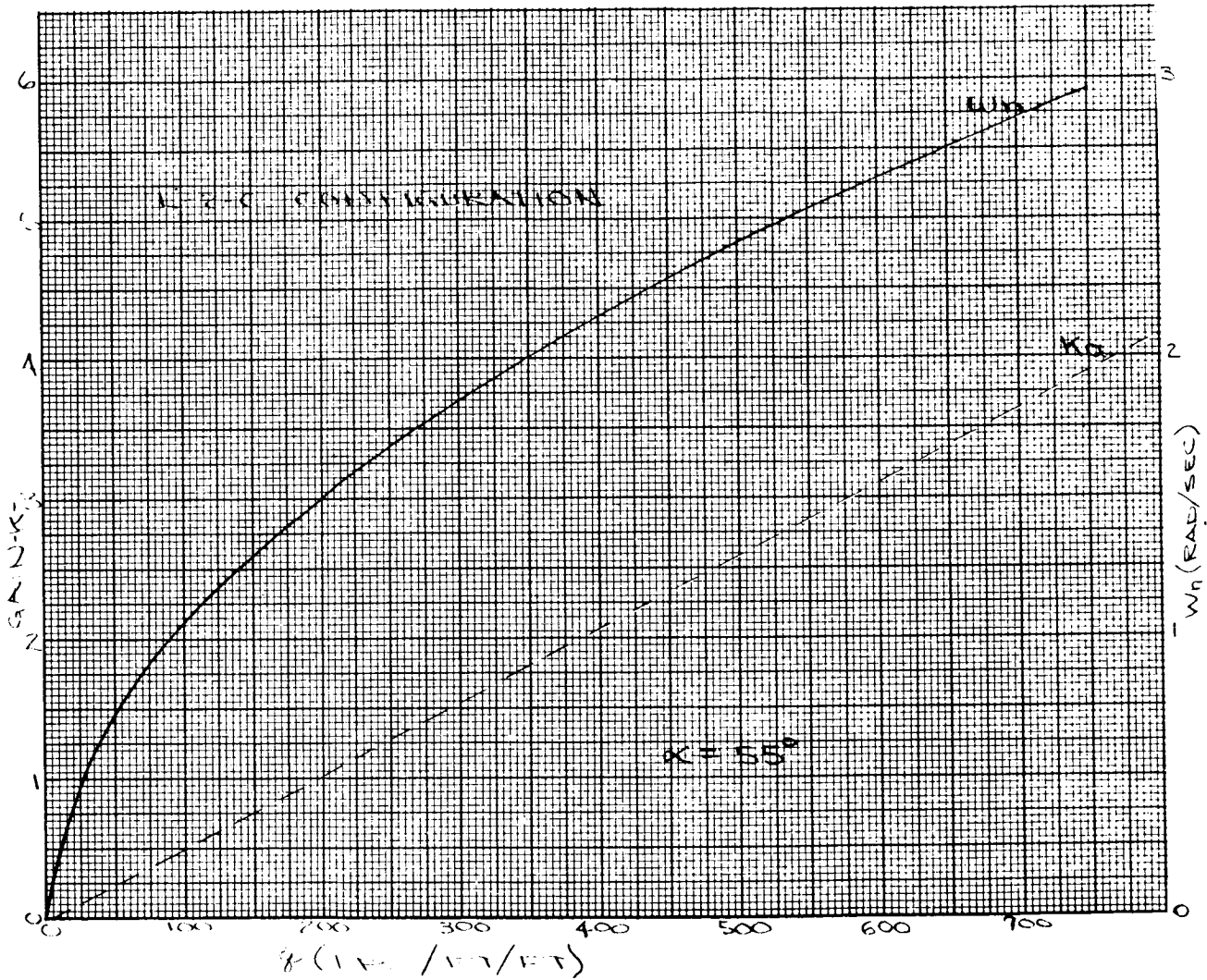


Fig. XI-25. Undamped Natural Frequency and Aerodynamic Gain Versus Dynamic Pressure

~~CONFIDENTIAL~~

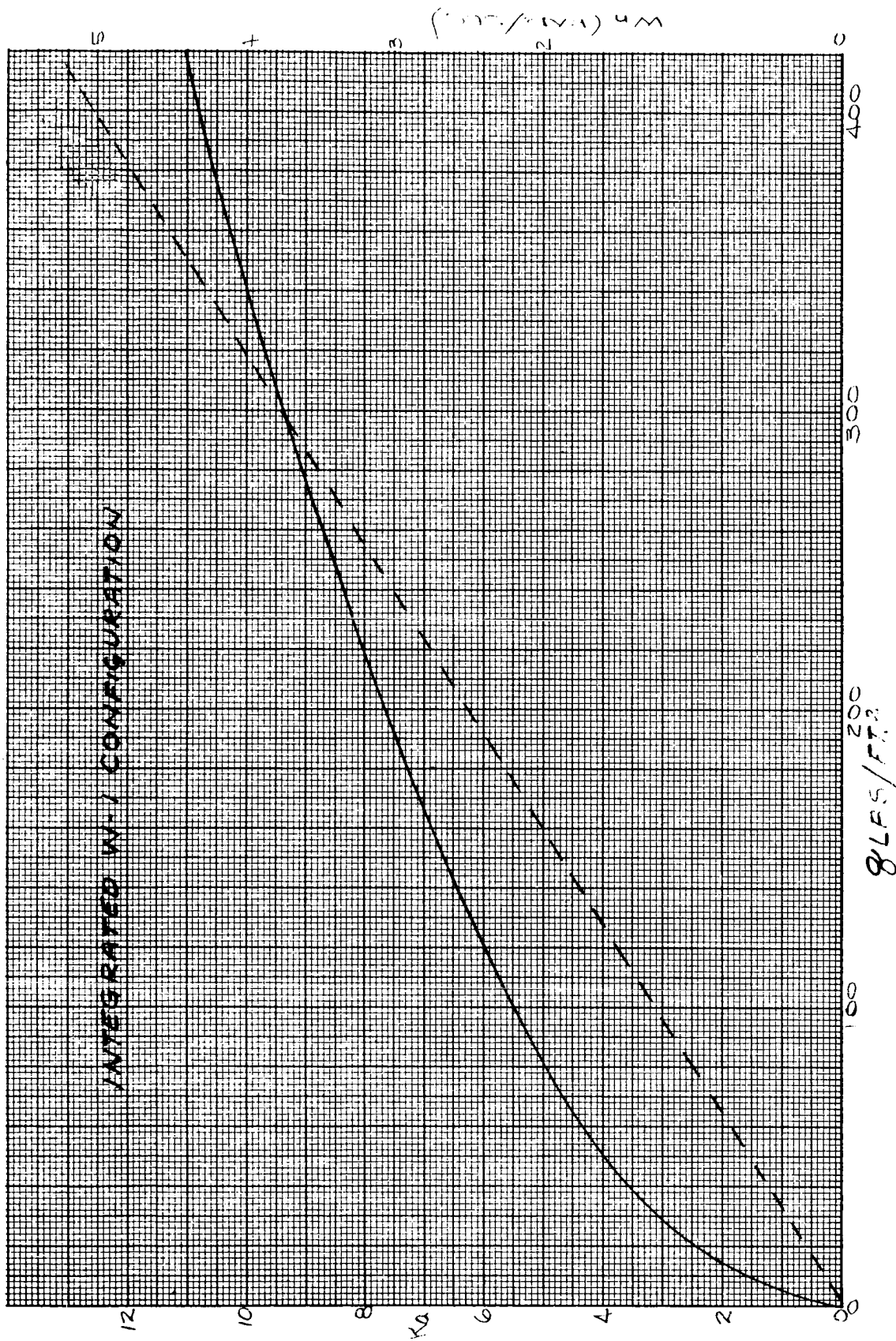


Fig. XI-26. Undamped Natural Frequency and Aerodynamic Gain Versus Dynamic Pressure for the Integrated W-1

~~CONFIDENTIAL~~

~~CONFIDENTIAL~~

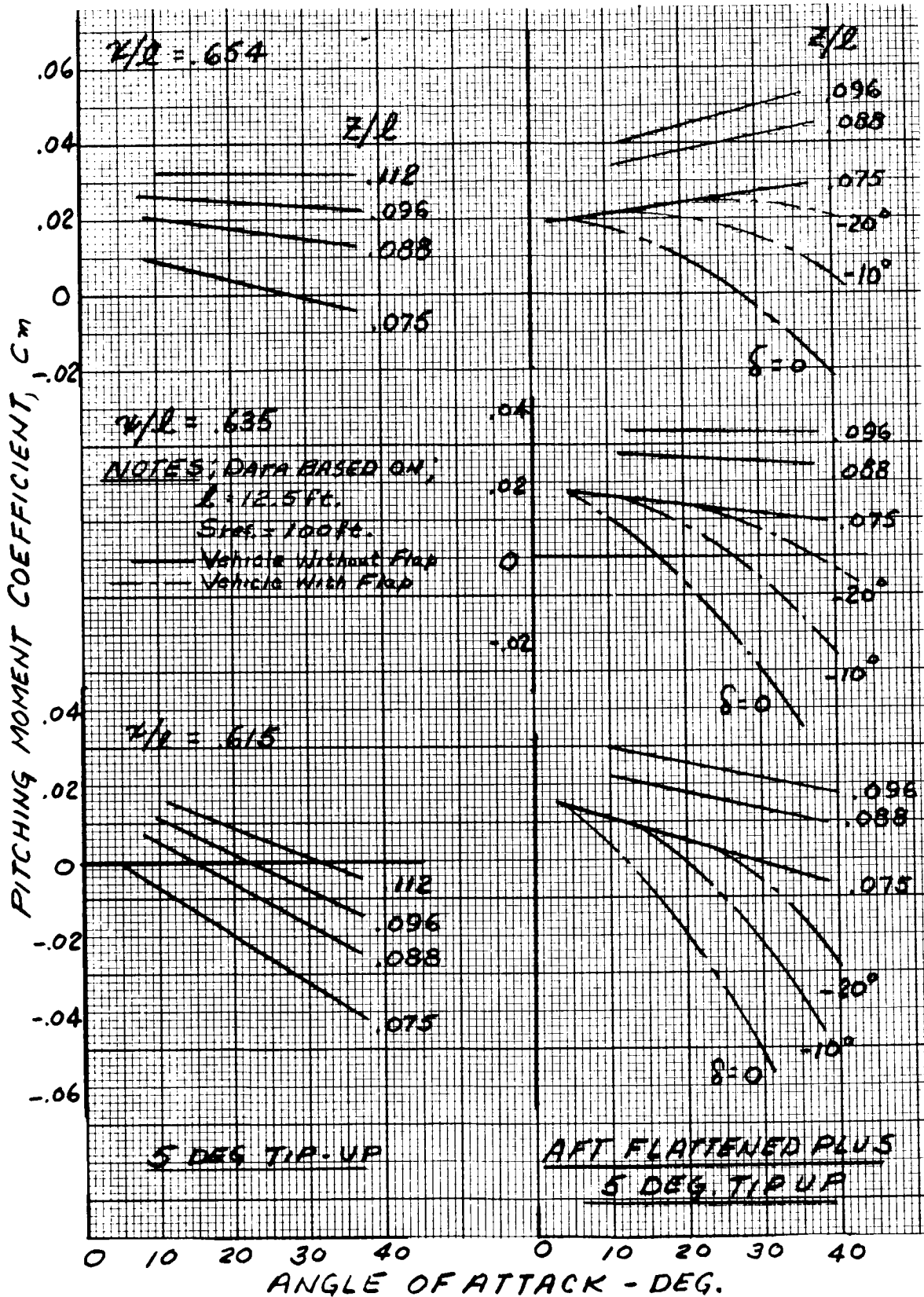


Fig. XI-27. Pitching Moments for the Model 410, 5 Degree Tip-up and Aft Flattened Plus 5 Degree Tip-up

~~CONFIDENTIAL~~

~~CONFIDENTIAL~~

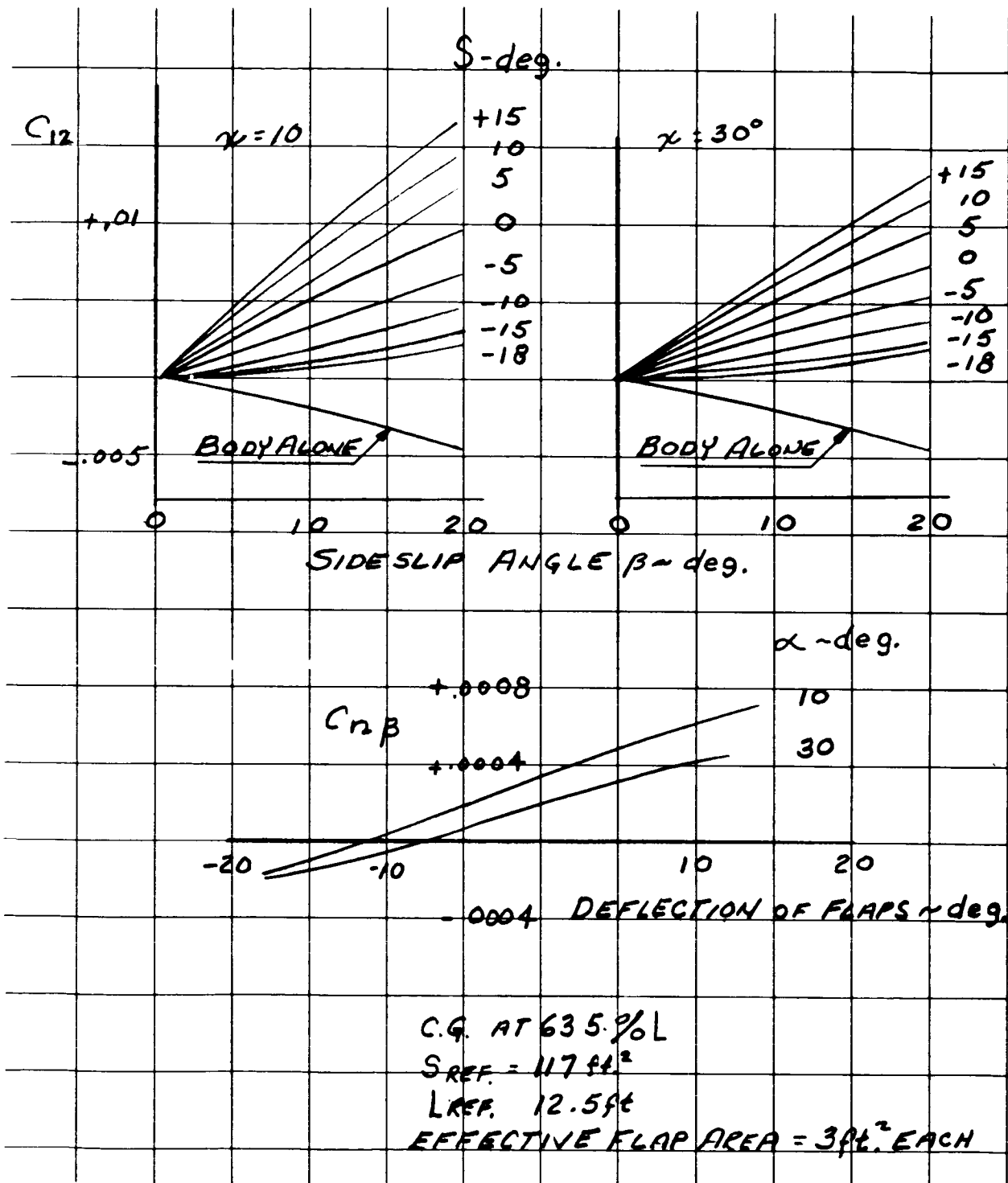


Fig. XI-28. Directional Stability of Model 410, Body Alone and with Flaps Equally Deflected

~~CONFIDENTIAL~~
ER 12007-2

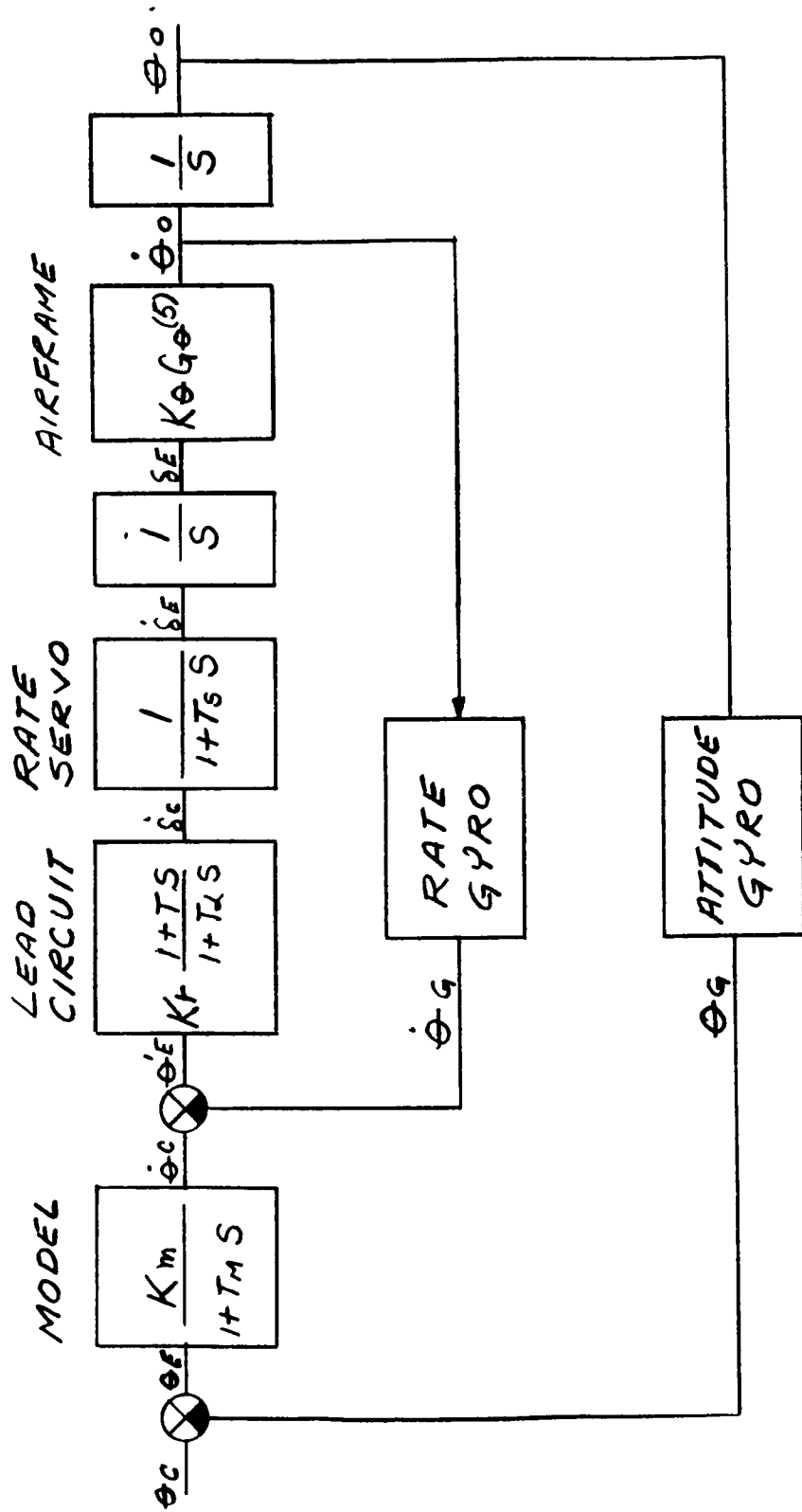


Fig. XI-29. Block Diagram of Adaptive Control System for Pitch Loop

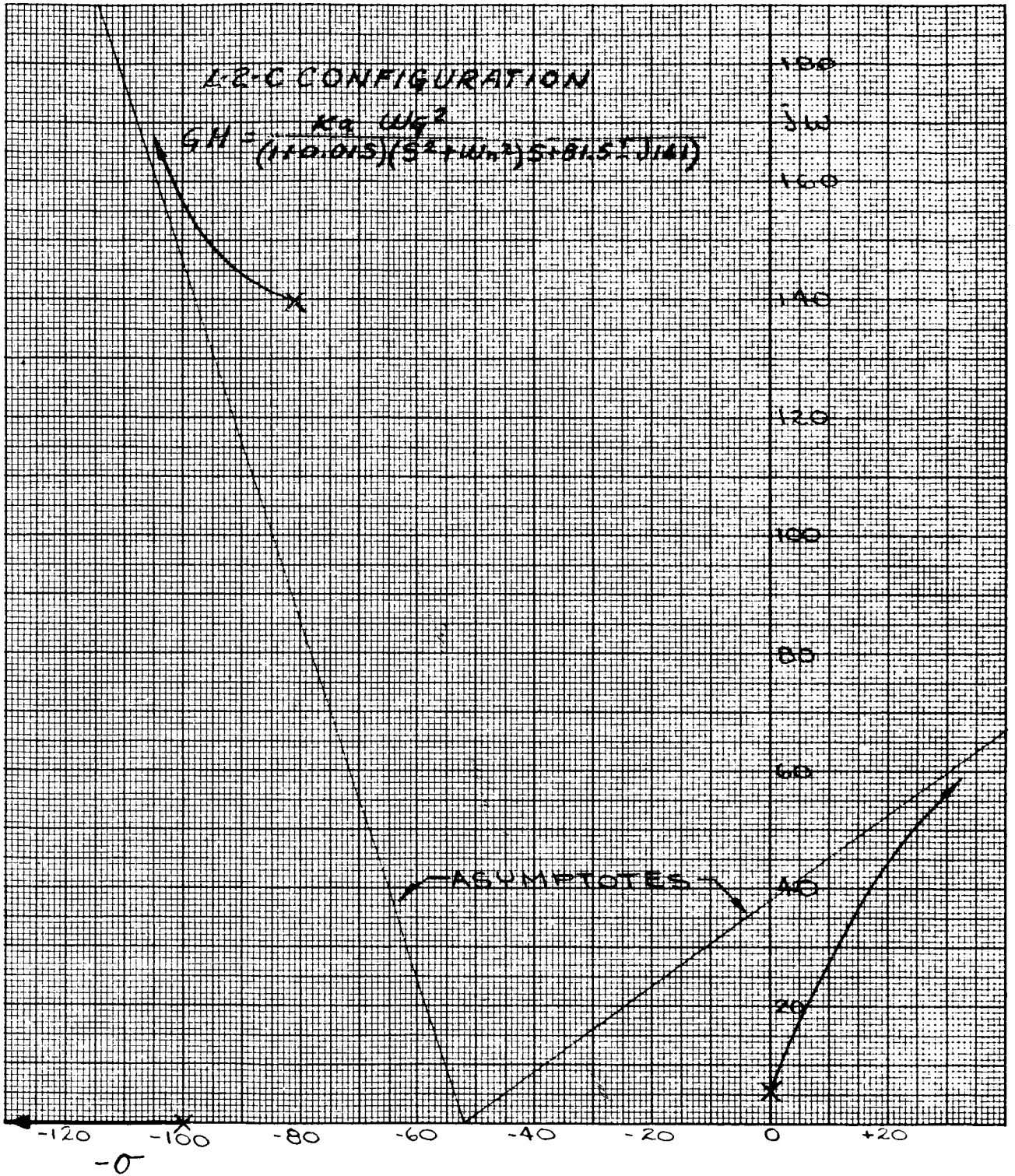


Fig. XI-30. Upper Half of Root Locus Before the Addition of a Lead Network

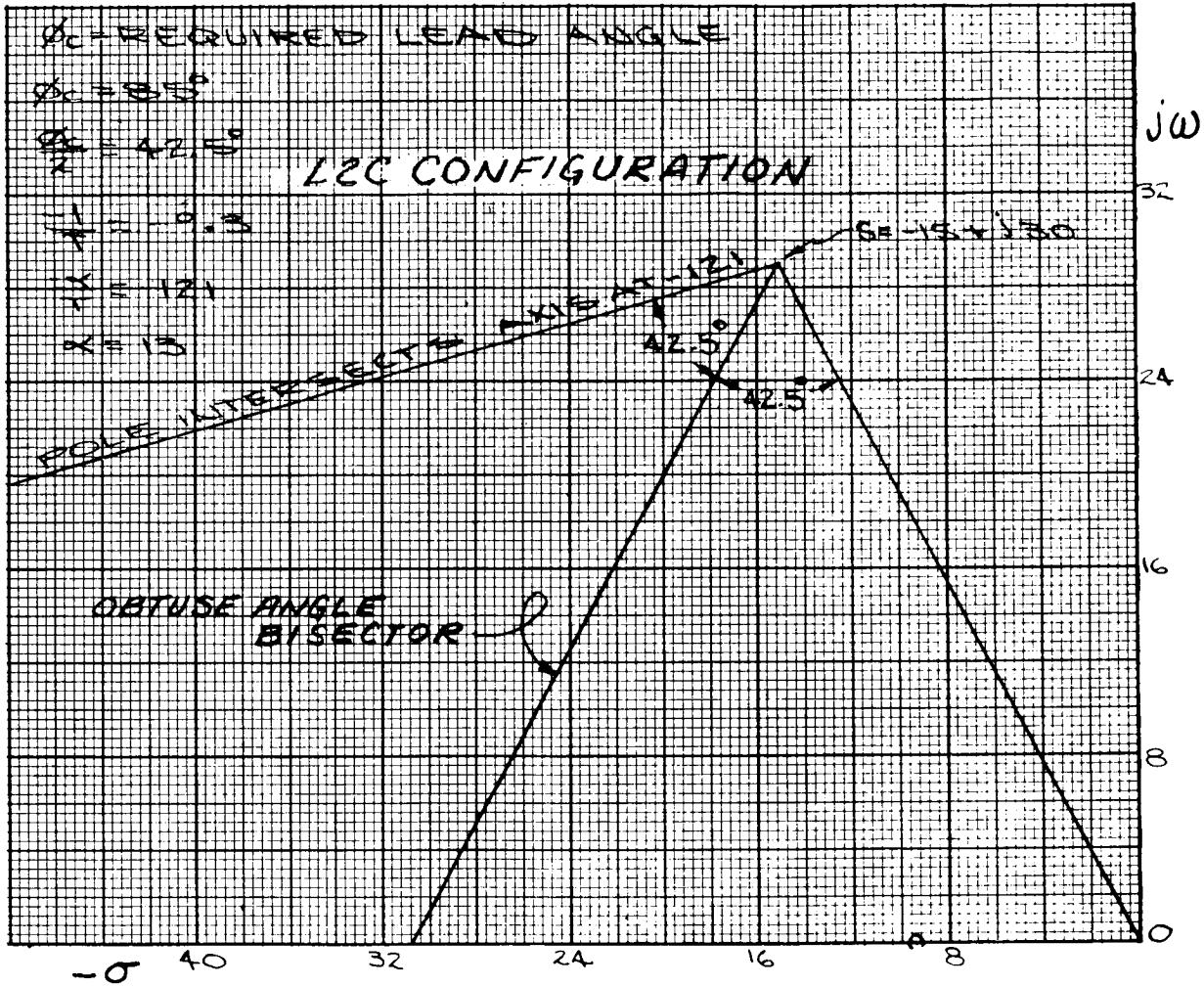


Fig. XI-31. Design of Lead Circuit

~~CONFIDENTIAL~~

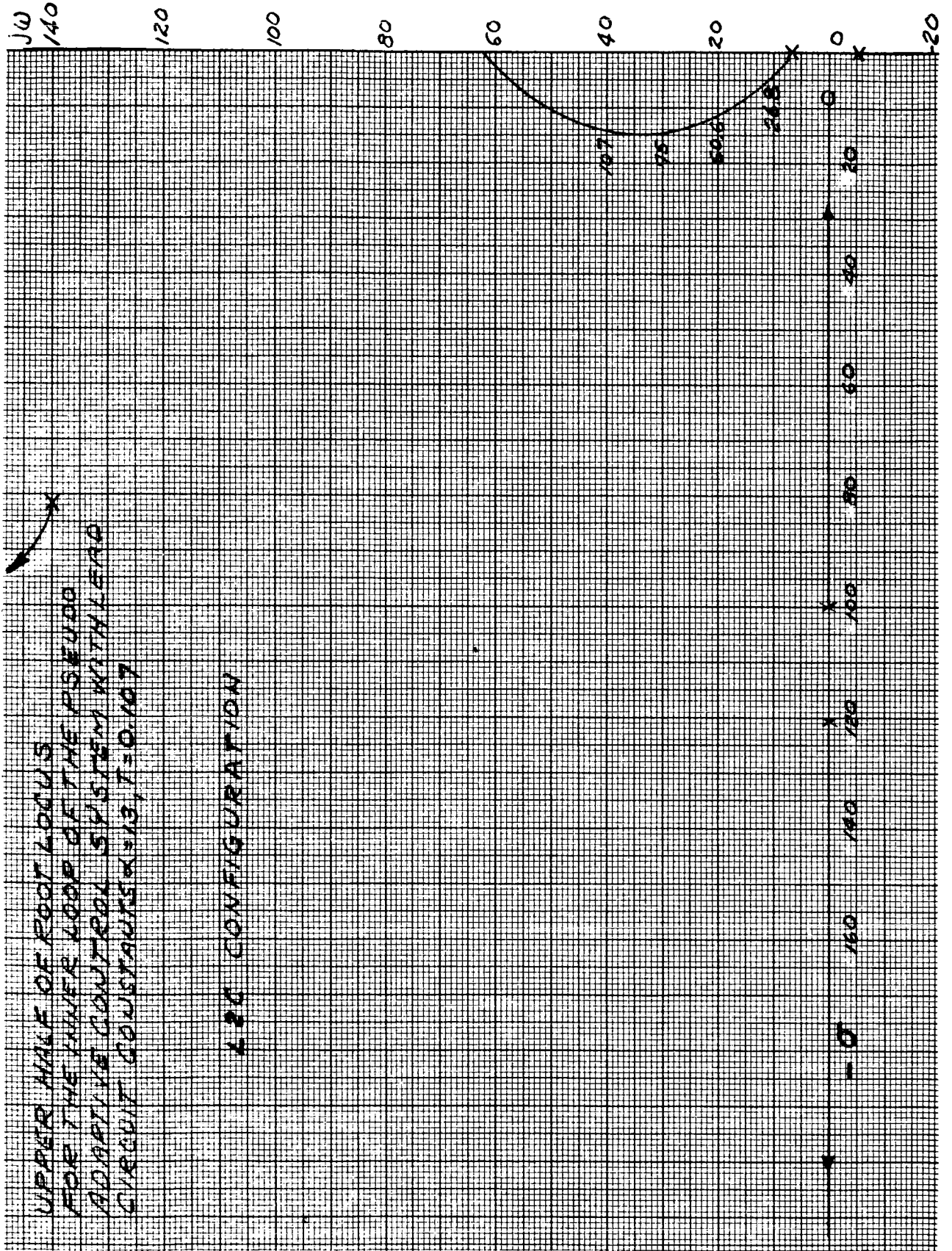


Fig. XI-32. Upper Half of Root Locus for the Inner Loop of the Pseudo Adaptive Control System with Lead Circuit

~~CONFIDENTIAL~~

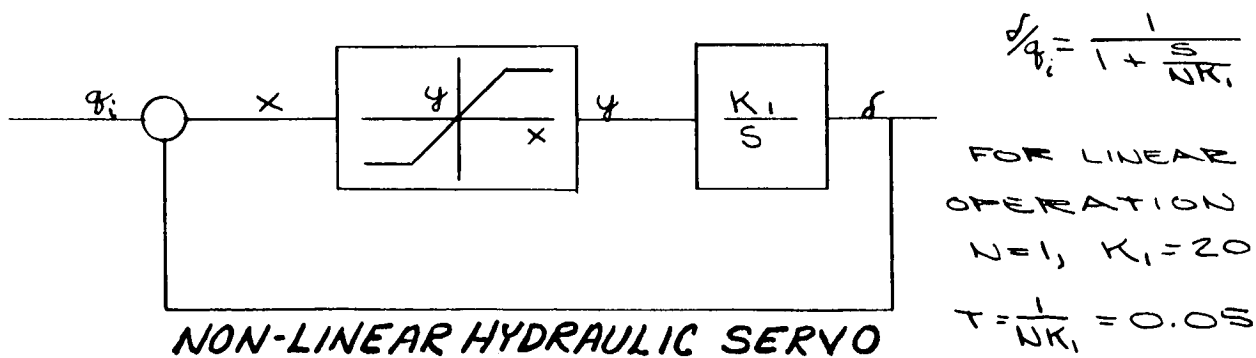
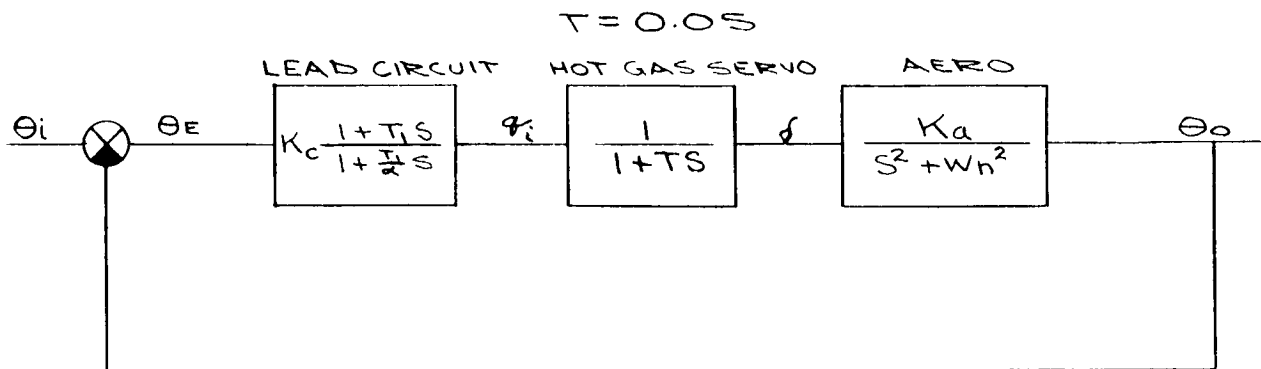
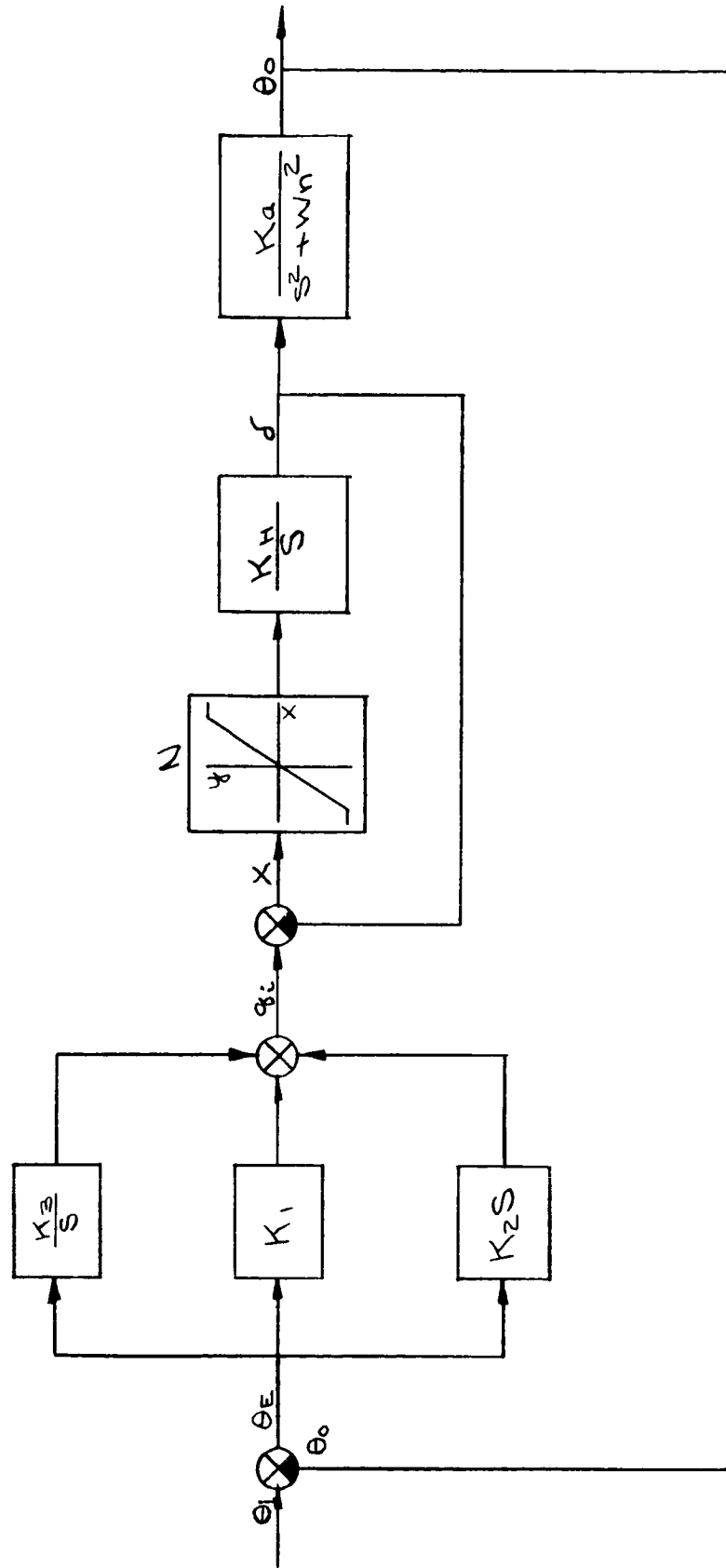


Fig. XI-33. Block Diagram Used to Approximate Rate Saturation



$$\frac{K_a}{K_1} = \frac{K_1}{K_2} = 0.5 W_n$$

Fig. XI-34. Block Diagram of Position-Rate-Integral Control System

CONFIDENTIAL

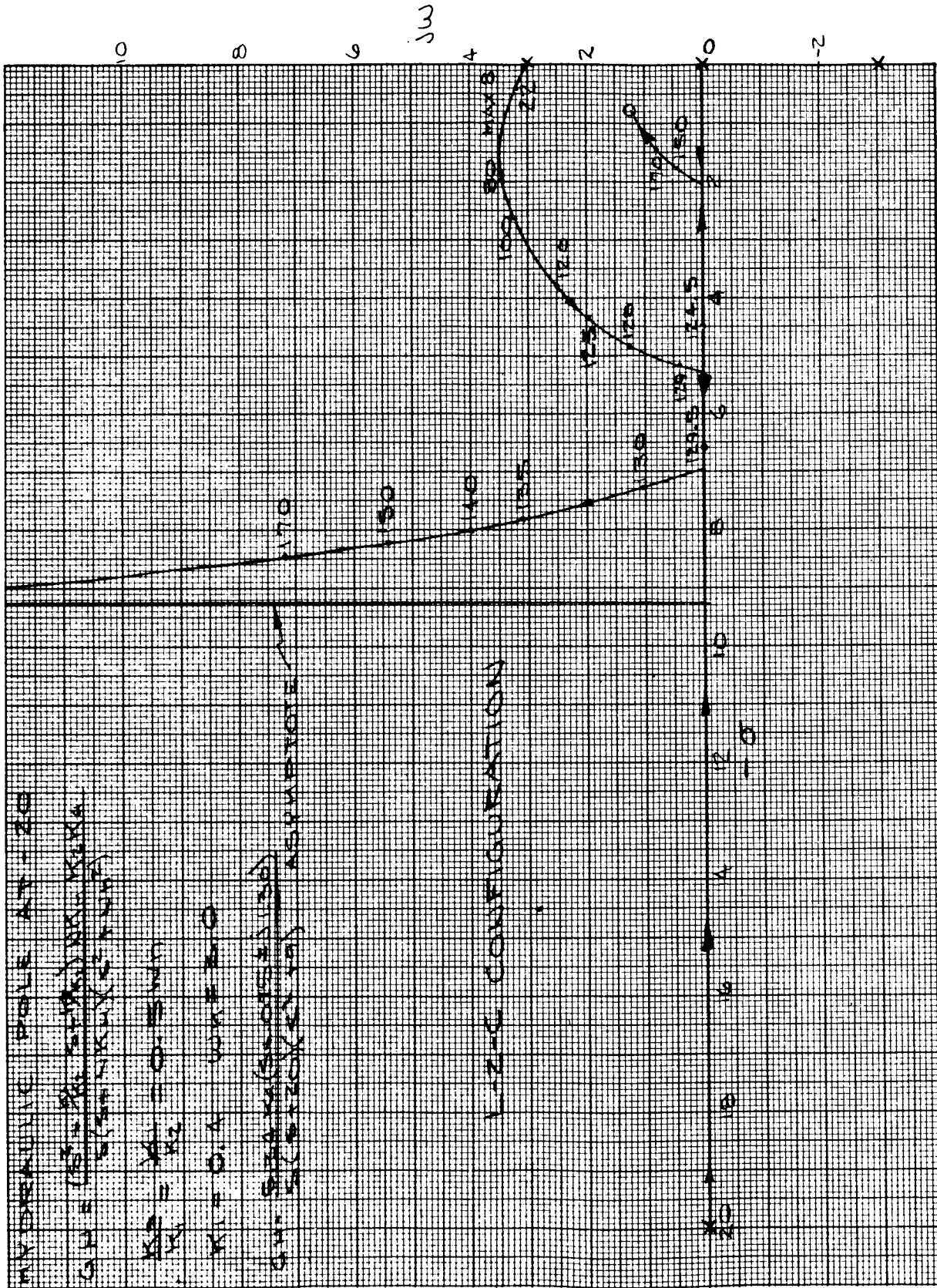


Fig. XI-35. Upper Half of Root Locus for Maximum q Condition with Hydraulic Pole at -20

CONFIDENTIAL

HYDRAULIC POLE AT -10

$$GH = \frac{(s^2 + \frac{K_1}{K_2}s + \frac{K_3}{K_2})NK_H K_2 K_a}{s(s + NK_H)(s^2 + \omega_n^2)}$$

$$\frac{K_3}{K_1} = \frac{K_1}{K_2} = 0.5\omega_n$$

$$K_1 = 0.4 \quad \omega_n = 3.0$$

$$GH = \frac{2.67K_a(s + 0.75 \pm j1.30)}{s(s + 10)(s^2 + 9)}$$

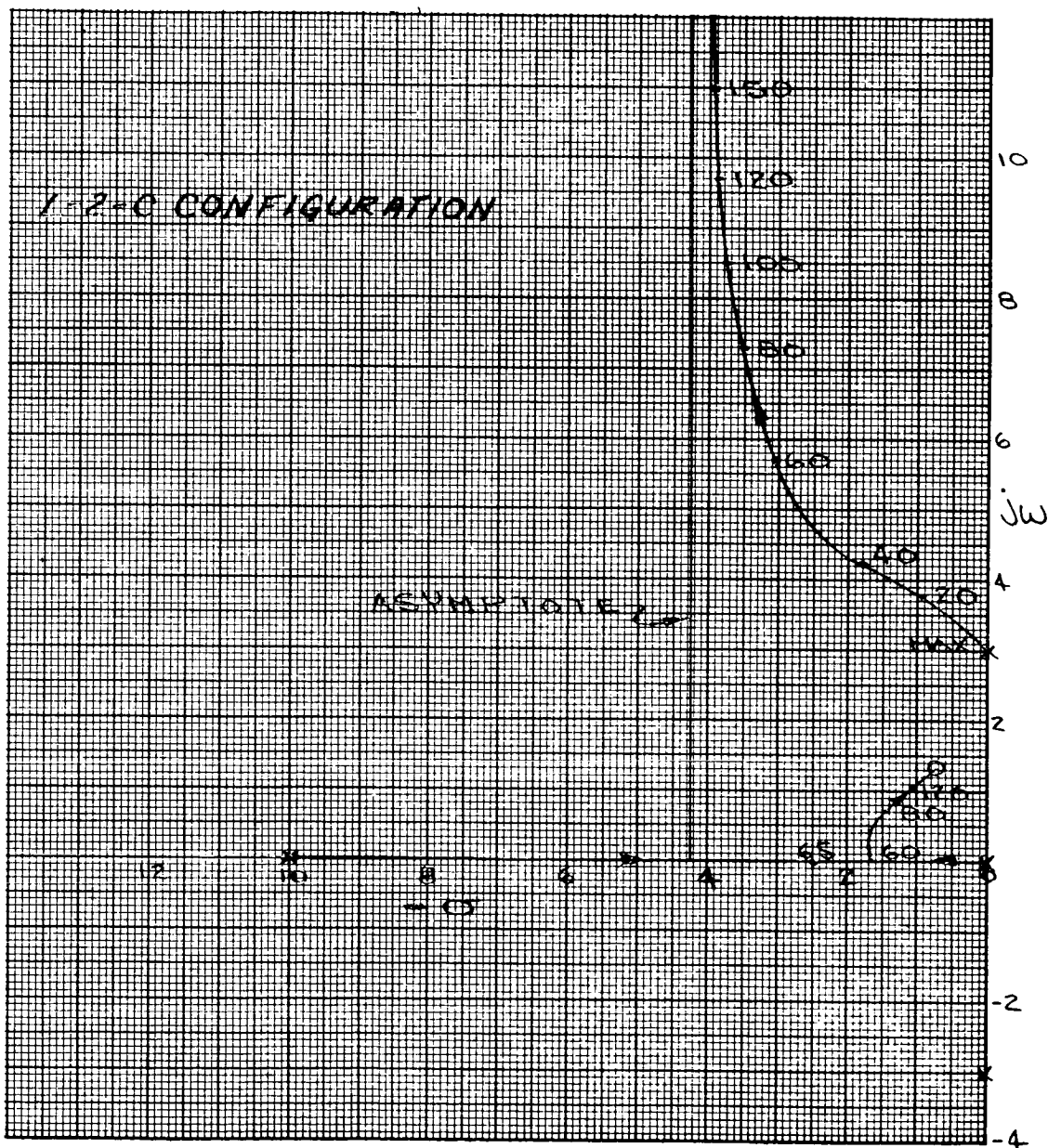


Fig. XI-36. Upper Half of Root Locus for Maximum q Condition with Hydraulic Pole at -10

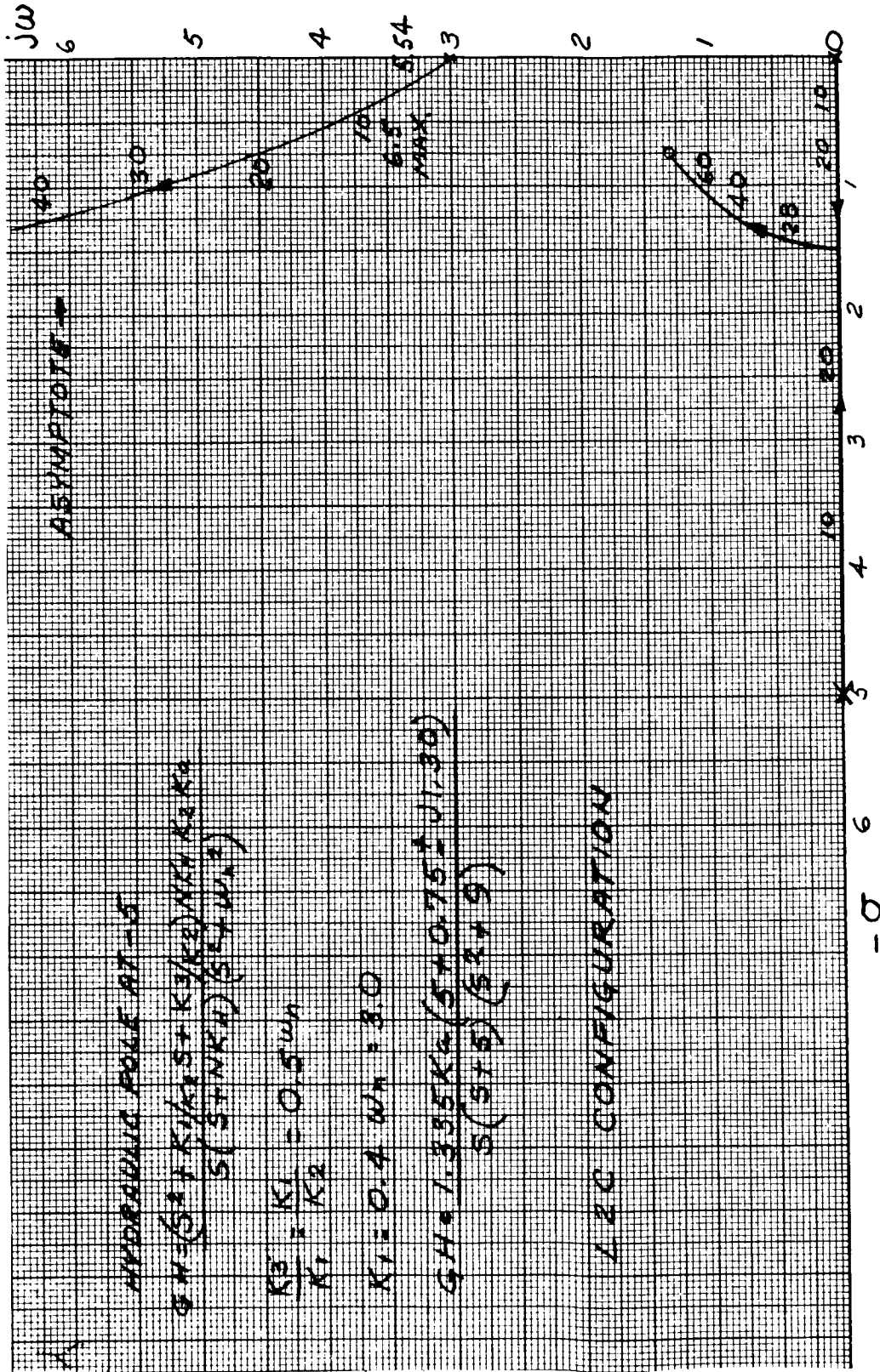


Fig. XI-37. Upper half of Root Locus for Maximum q Condition with Hydraulic Pole at 15

CONFIDENTIAL

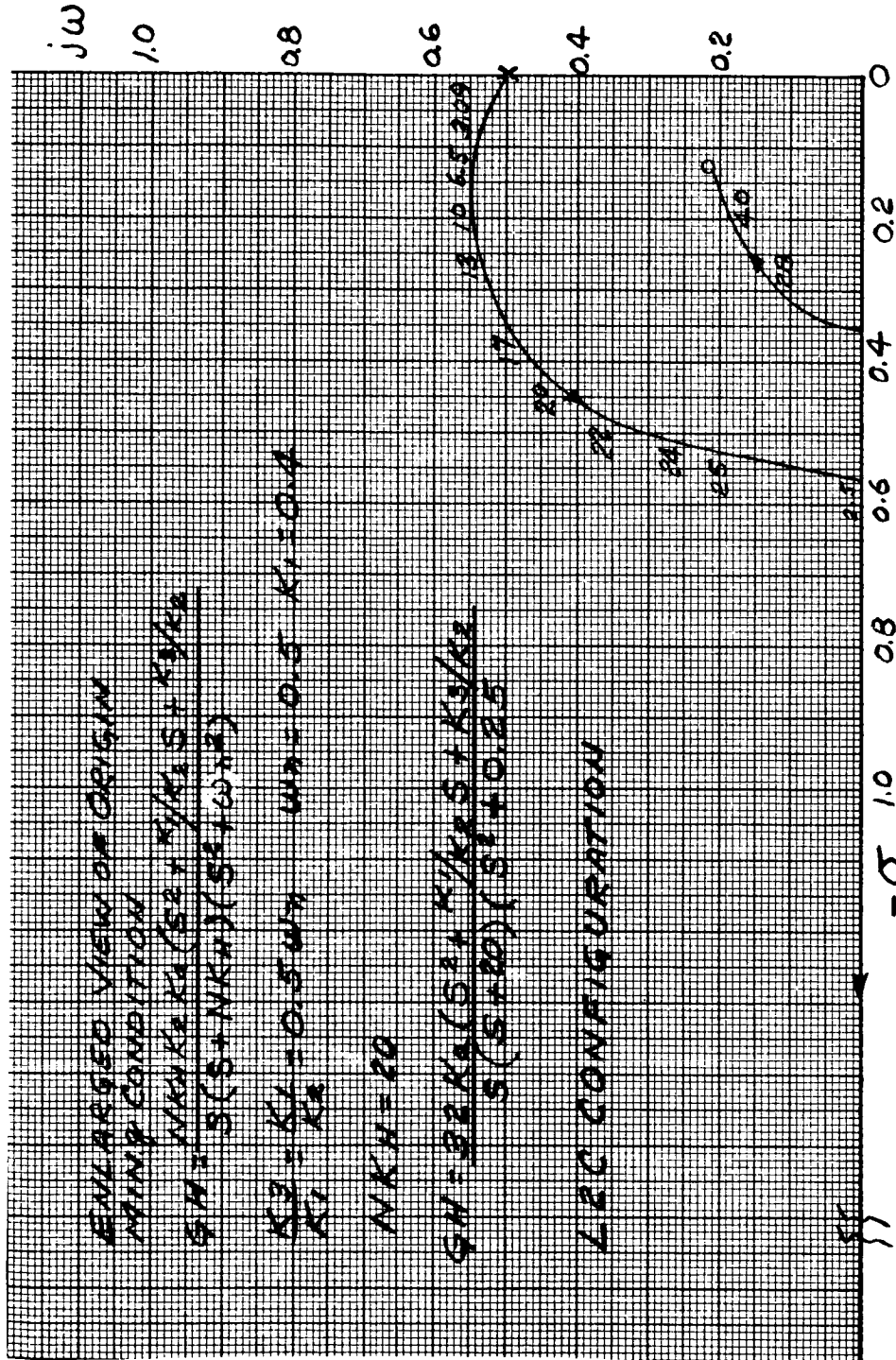


Fig. XI-38. Upper Half of Root Locus, Minimum q Condition with Hydraulic Pole at -20

CONFIDENTIAL

~~CONFIDENTIAL~~

$$GH = \frac{N K_H K_Z K_G (S^2 + K_1/K_2 S + K_3/K_2)}{S(S + N K_H)(S^2 + W_n^2)} \quad \text{MIN } \delta$$

$$\frac{K_3}{K_1} = \frac{K_1}{K_2} = 0.5 W_n \quad W_n = 0.5 \quad K_1 = 0.4$$

$$GH = \frac{32 K_G (S^2 + 0.25S + 0.0625)}{S(S+20)(S^2 + 0.25)}$$

LZC CONFIGURATION

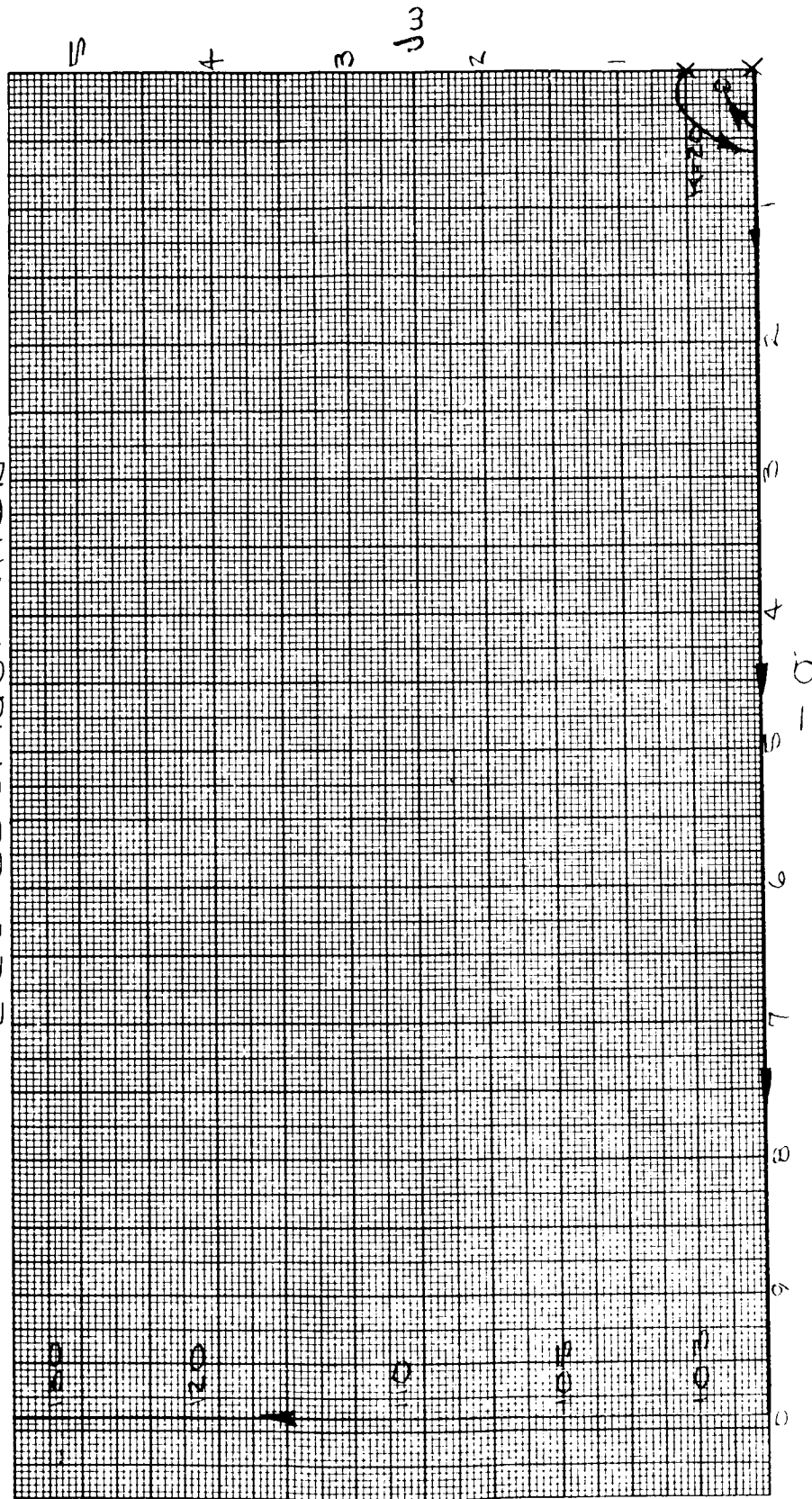


Fig. XI-39. Upper Half of Root Locus for Minimum δ Condition with Hydraulic Pole at -20

~~CONFIDENTIAL~~

$$GH = \frac{NK_H K_2 K_0 (s^2 + \frac{K_1}{K_2} s + \frac{K_3}{K_2})}{s(s + NK_H)(s^2 + \omega_n^2)}$$

$$\frac{K_3}{K_1} = \frac{K_1}{K_2} = 0.5 \omega_n \quad \omega_n = 0.5 \quad K_1 = 0.4$$

$$NK_H = 10$$

$$GH = \frac{16K_0 (s^2 + \frac{K_1}{K_2} s + \frac{K_3}{K_2})}{s(s + 10)(s^2 + 0.25)}$$

L·Z·C CONFIGURATION

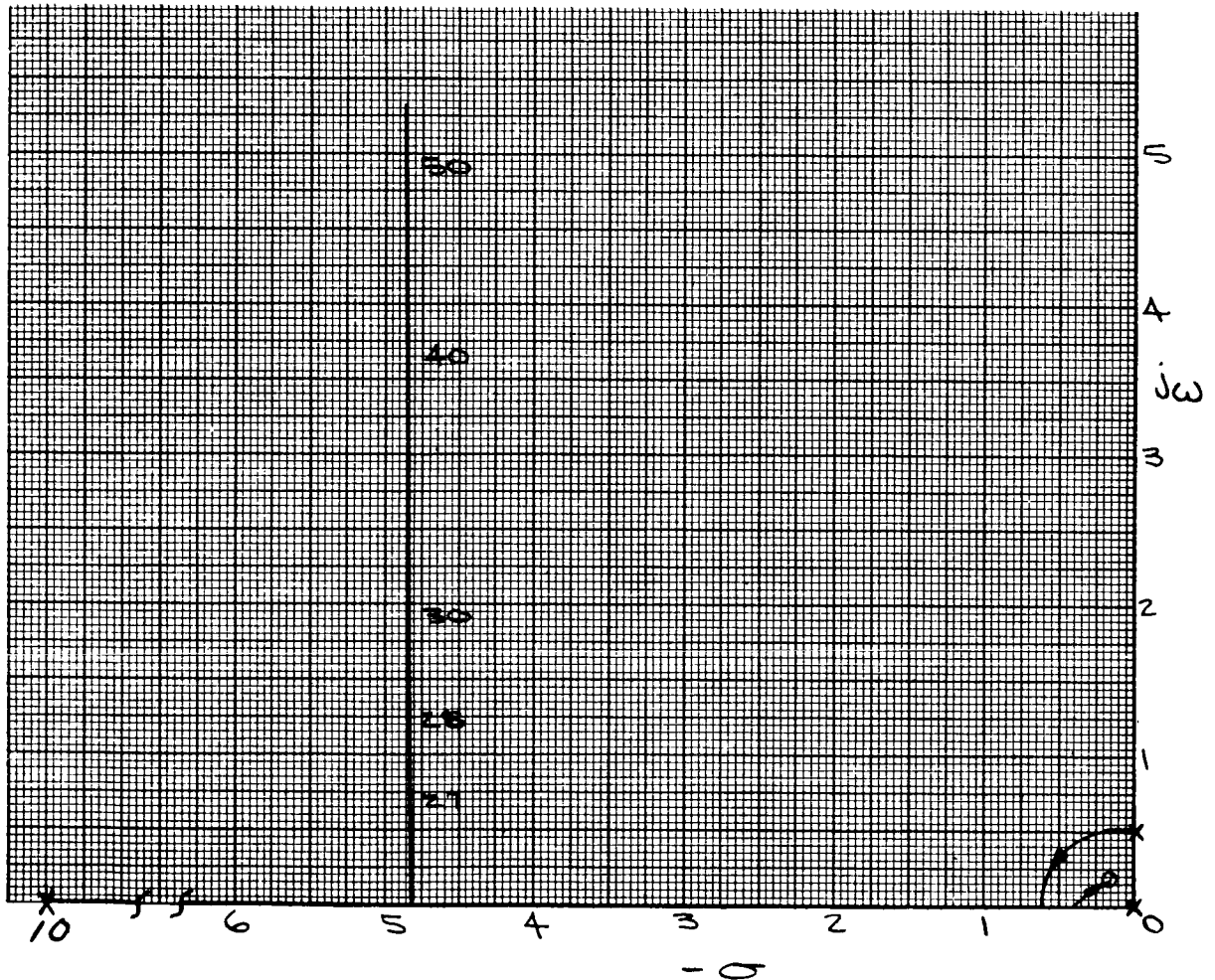


Fig. XI-40. Upper Half of Root Locus for Minimum q Condition with Hydraulic Pole at -10

$$GH = \frac{NK_1 K_2 K_a (s^2 + K_1/K_2 s + K_2/K_2)}{s_1 (s + NK_1) (s^2 + \omega_n^2)}$$

$$\frac{K_2}{K_1} = \frac{K_1}{K_2} = 0.5 \omega_n$$

$$\omega_n = 0.5 \quad K_2 = 0.4 \quad NK_1 = 5$$

$$GH = \frac{8K_a (s^2 + 0.25s + 0.0625)}{s (s + 5) (s^2 + 0.25)}$$

L 2 C CONFIGURATION

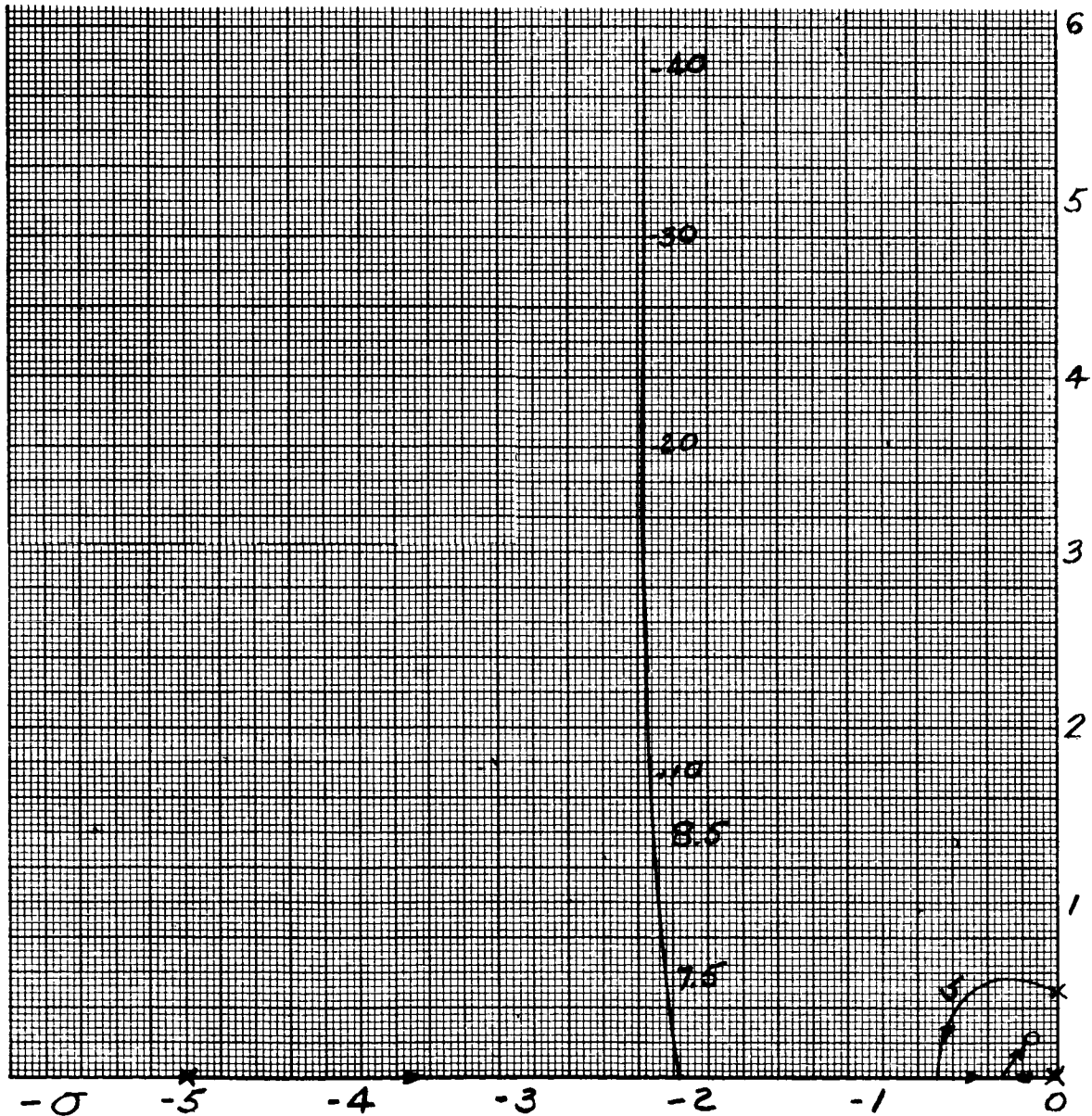


Fig. XI-42. Upper Half of Root Locus for Minimum q Condition with Hydraulic Pole at -5

~~CONFIDENTIAL~~

$$GH = \frac{NK_H K_2 K_3 (S^2 + K_1/K_2 S + K_3/K_2)}{S(S + NK_H)(S^2 + \omega_n^2)}$$

$$\frac{K_3}{K_1} = \frac{K_1}{K_2} = 0.5 \omega_n \quad \omega_n = 0.5 \quad K_1 = 0.4$$

$$NK_H = 5$$

$$GH = \frac{8KA(S^2 + 0.25S + 0.0625)}{S(S + 5)(S^2 + 0.25)}$$

L-2-C CONFIGURATION

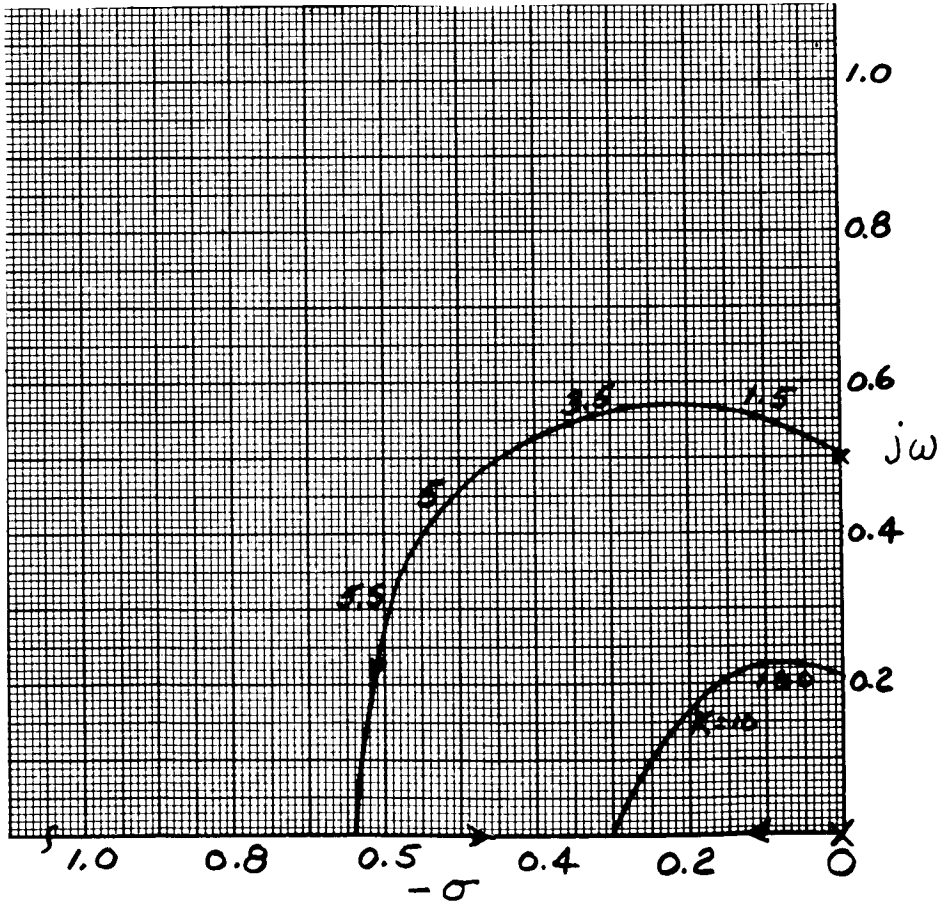


Fig. XI-43. Enlarged View of Origin for Upper Half of Root Locus, Minimum q Condition with Hydraulic Pole at -5

~~CONFIDENTIAL~~

$$GH = \frac{(s^2 + \frac{K_1}{K_2}s + (\frac{K_2}{K_2})NK_H K_2 K_a)}{s(s + NK_H)(s^2 + \omega_n^2)}$$

$$\frac{K_2}{K_1} = \frac{K_1}{K_2} = 0.5 \omega_n \quad K_1 = 0.4 \quad \omega_n = 1.5 \quad NK_H = 20$$

$$GH = \frac{10.66 K_a (s^2 + 0.75s + 0.563)}{s(s + 20)(s^2 + \omega_n^2)}$$

L 2C CONFIGURATION

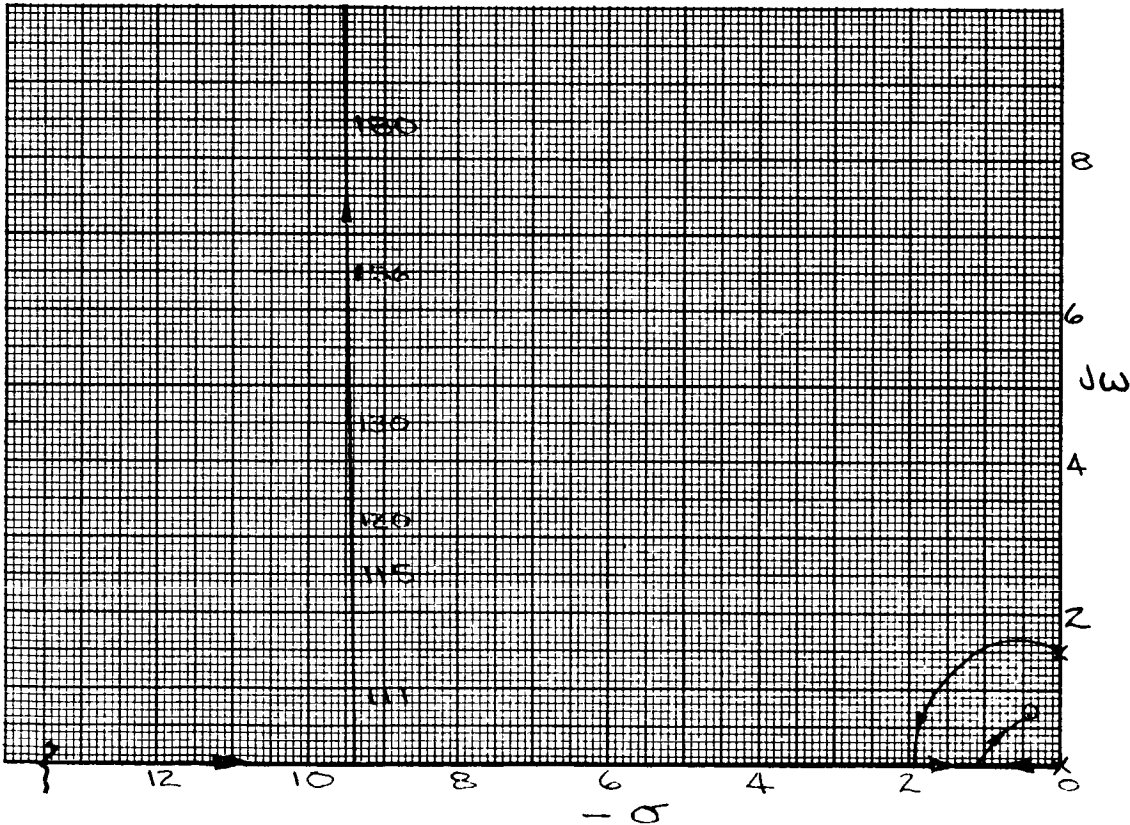


Fig. XI-44. Upper Half of Root Locus for Middle q Condition with Hydraulic Pole at -20

$$GH = \frac{(s^2 + \frac{K_1}{K_2} s + \frac{K_3}{K_2}) NK_H K_2 K_a}{s(s + NK_H)(s^2 + \omega_n^2)}$$

$$\frac{K_3}{K_1} = \frac{K_1}{K_2} = 0.5 \omega_n \quad K = 0.4 \quad \omega_n = 1.5 \quad NK_H = 20$$

$$GH = \frac{10.66 K_a (s^2 + 0.75s + 5.63)}{s(s + 20)(s^2 + \omega_n^2)}$$

L-2-C CONFIGURATION

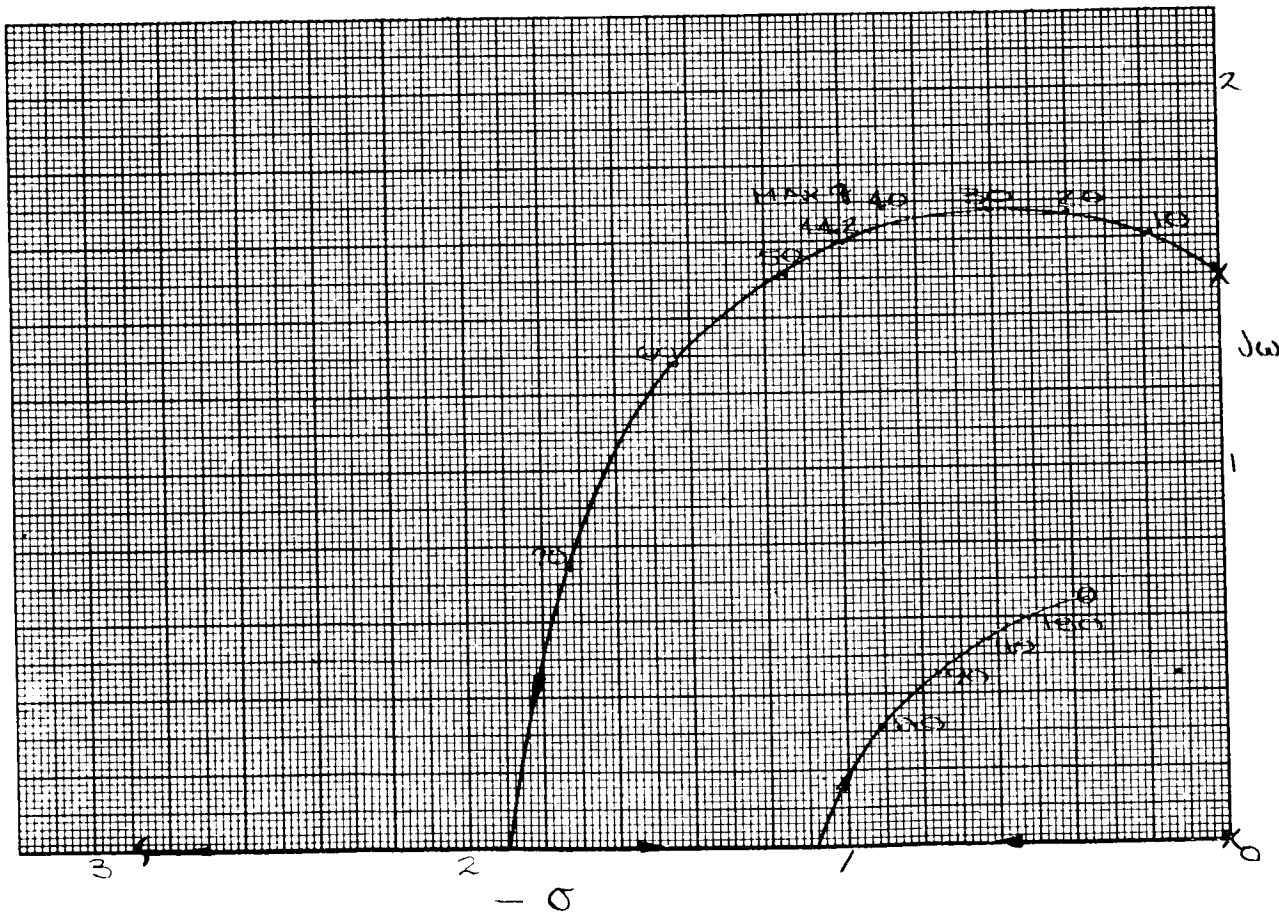


Fig. XI-45. Enlarged View of Origin for Upper Half of Root Locus, Middle q Condition with Hydraulic Pole at -20

~~CONFIDENTIAL~~

$$GH = \frac{(s^2 + K_1/K_2 s + K_3/K_2) NK_H K_2 K_a}{s(s + NK_H)(s^2 + \omega_n^2)}$$

$$\frac{K_3}{K_1} = \frac{K_1}{K_2} = 0.5 \omega_n \quad K_1 = 0.4 \quad \omega_n = 1.5$$

$$NK_H = 10$$

$$GH = \frac{5.33 K_a (s^2 + 0.75s + 0.563)}{s(s + 10)(s^2 + \omega_n^2)}$$

L-2-C CONFIGURATION

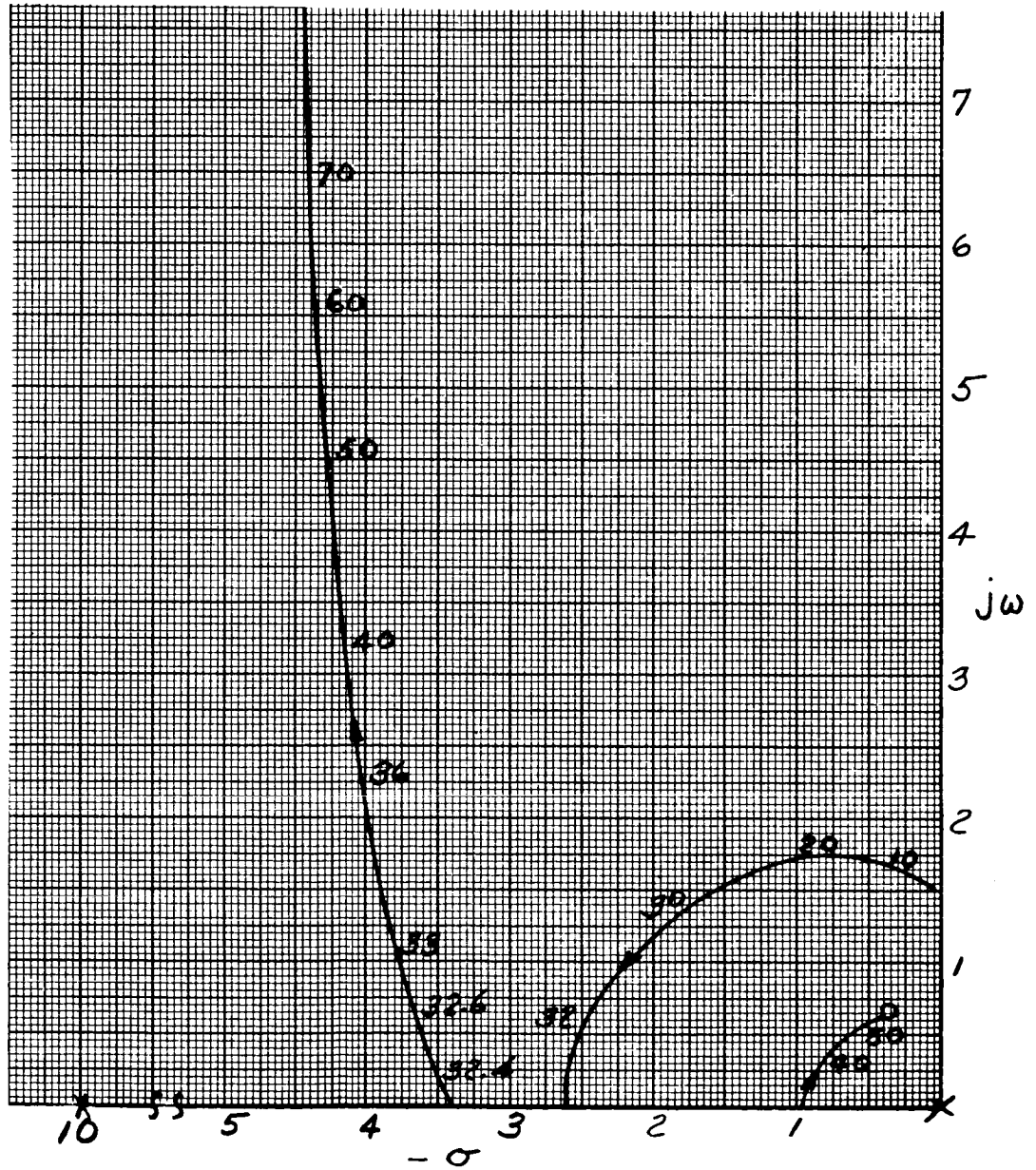


Fig. XI-46. Upper Half of Root Locus for Middle q Condition with Hydraulic Pole at -10

$$GH = \frac{(S^2 + K_1/K_2 S + K_3/K_2) NKH K_2 K_a}{S(S + NKH)(S^2 + \omega_n^2)}$$

$$\frac{K_3}{K_1} = \frac{K_1}{K_2} = 0.5 \omega_n \quad K_1 = 0.4 \quad \omega_n = 1.5 \quad NKH = 10$$

$$GH = \frac{S.33 K_a (S^2 + 0.75S + 0.563)}{S(S + 10)(S^2 + \omega_n^2)}$$

L2C CONFIGURATION

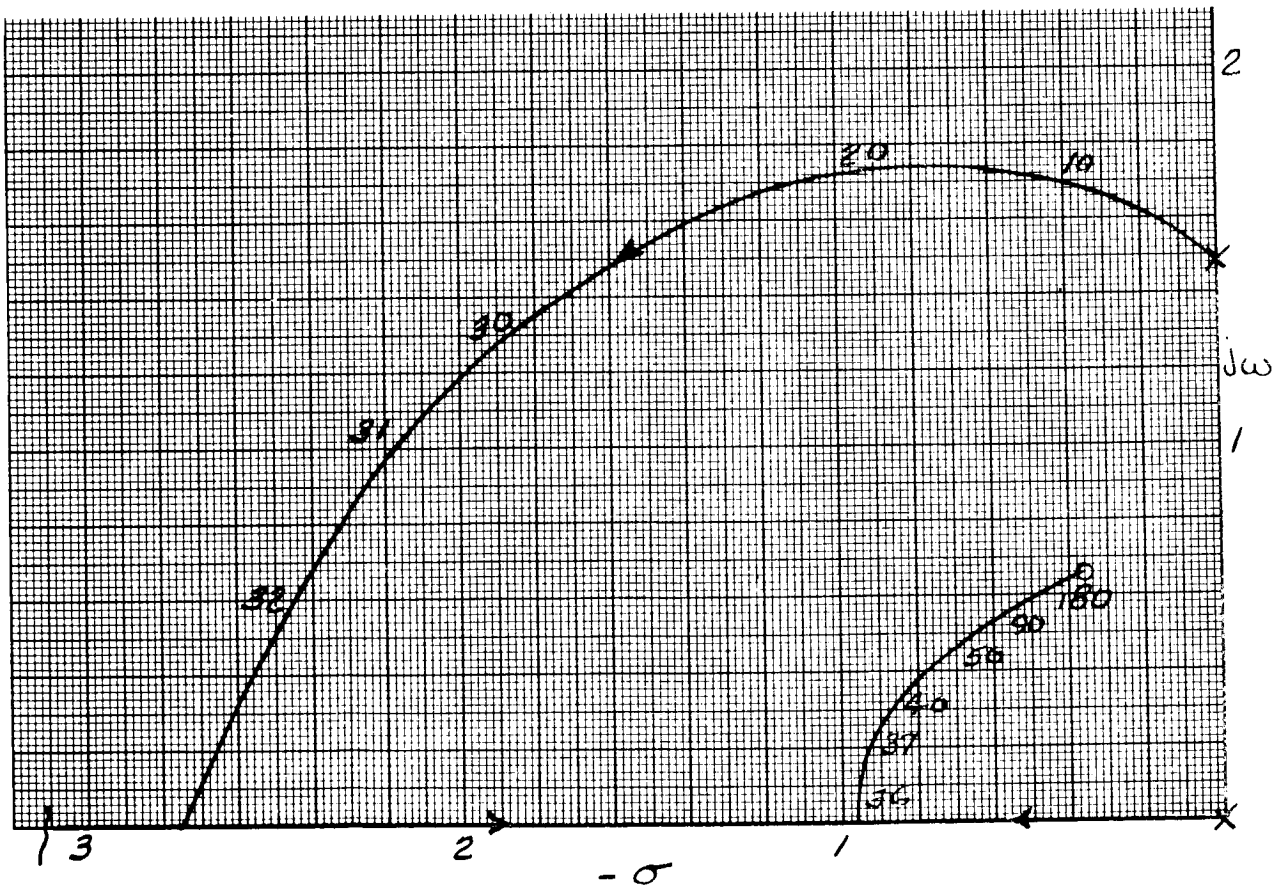


Fig. XI-47. Upper Half of Root Locus for Middle q Condition with Hydraulic Pole at -10

$$GH = \frac{(S^2 + K_1/K_2 S + K_3/F_2) NK_H K_2 K_a}{S(S + NK_H)(S^2 + \omega_n^2)}$$

$$\frac{K_2}{K_1} = \frac{K_1}{K_2} = 0.5 \omega_n$$

$$K_1 = 0.4 \quad \omega_n = 1.5 \quad NK_H = 5$$

$$GH = \frac{2.67 K_a (S^2 + 0.75S + 0.563)}{S(S + 5)(S^2 + 2.25)}$$

L-2-C CONFIGURATION

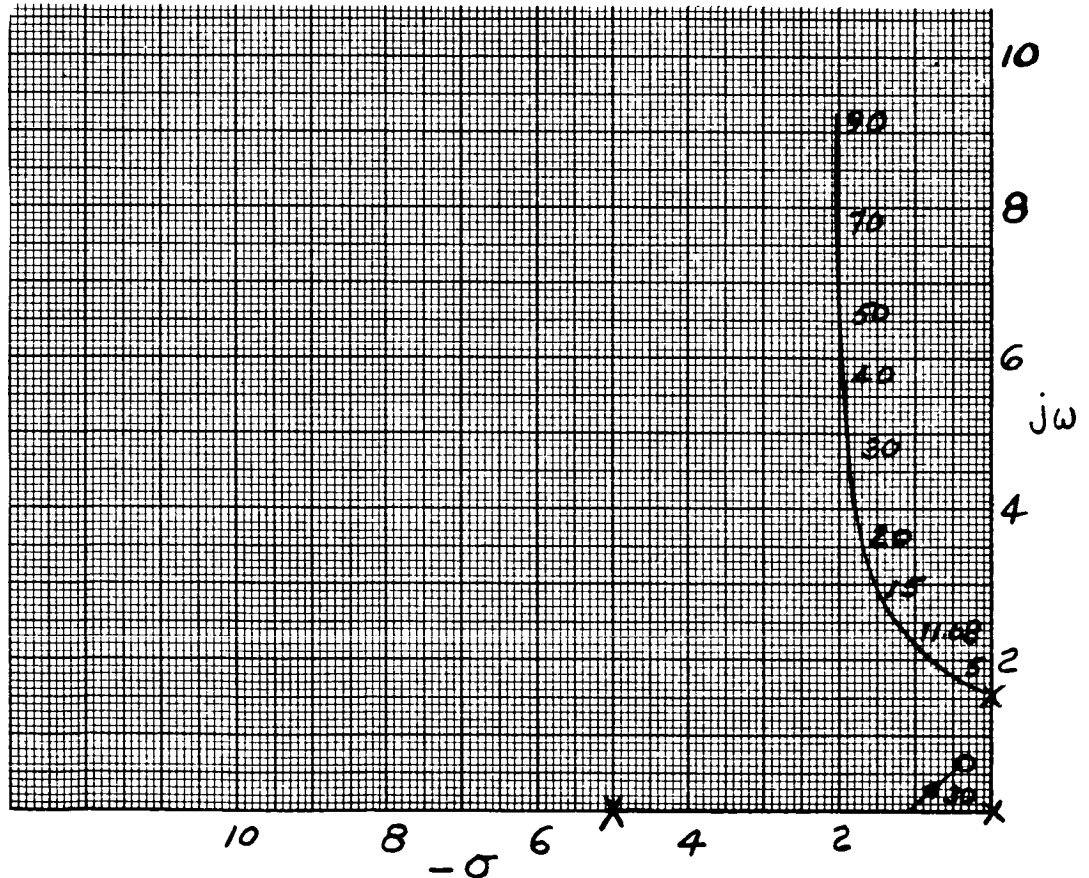


Fig. XI-48. Upper Half of Root Locus for Middle q Condition with Hydraulic Pole at -5

~~CONFIDENTIAL~~

HYDRAULIC POLE AT -20 $\alpha = 15^\circ$
MAX q CONDITION
INTEGRATED W-I CONFIGURATION

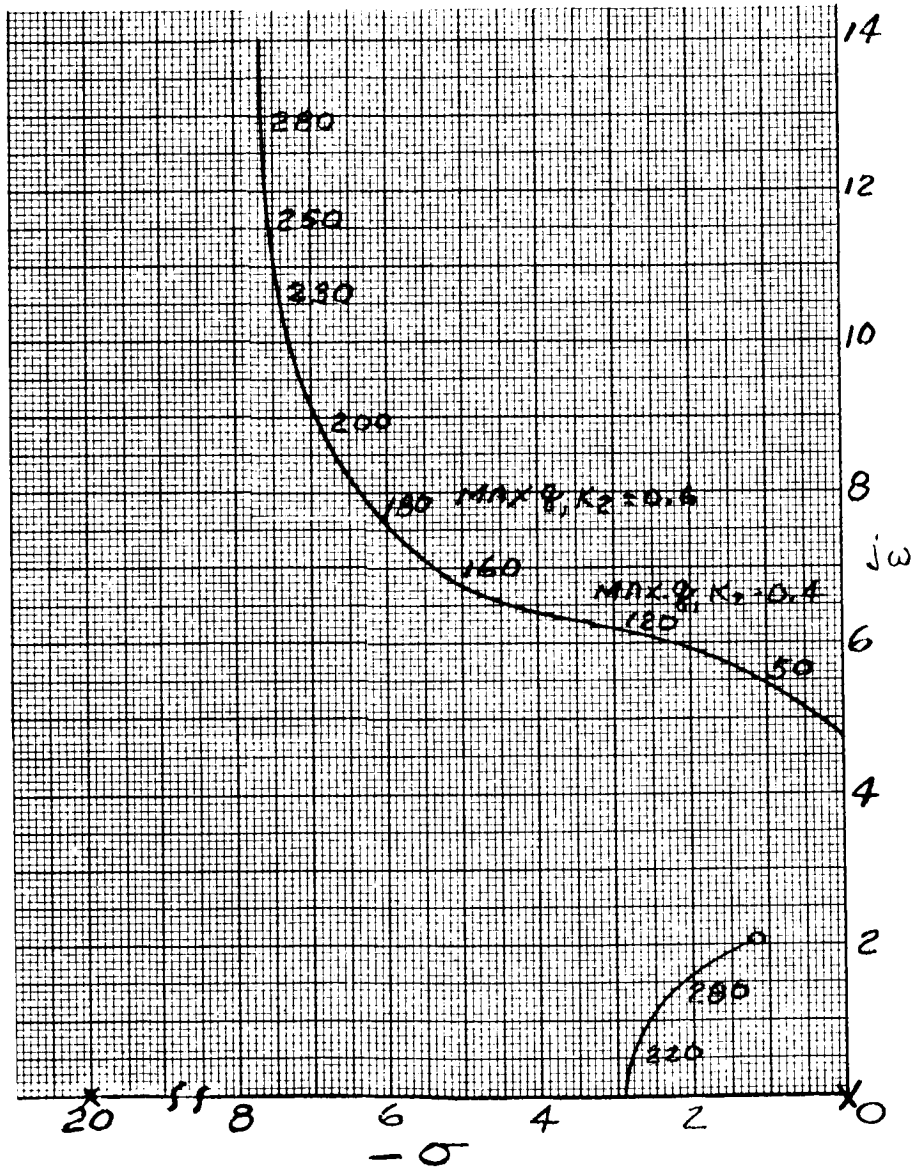


Fig. XI-49. Upper Half of Root Locus for Maximum q Condition with Hydraulic Pole at -20

~~CONFIDENTIAL~~

ENLARGED VIEW OF ORIGIN $\alpha=50^\circ$
HYDRAULIC POLE AT -20
MIN q CONDITION, $\text{MIN } q = 5 \text{ PSI}$
INTEGRATED W-1 CONFIGURATION

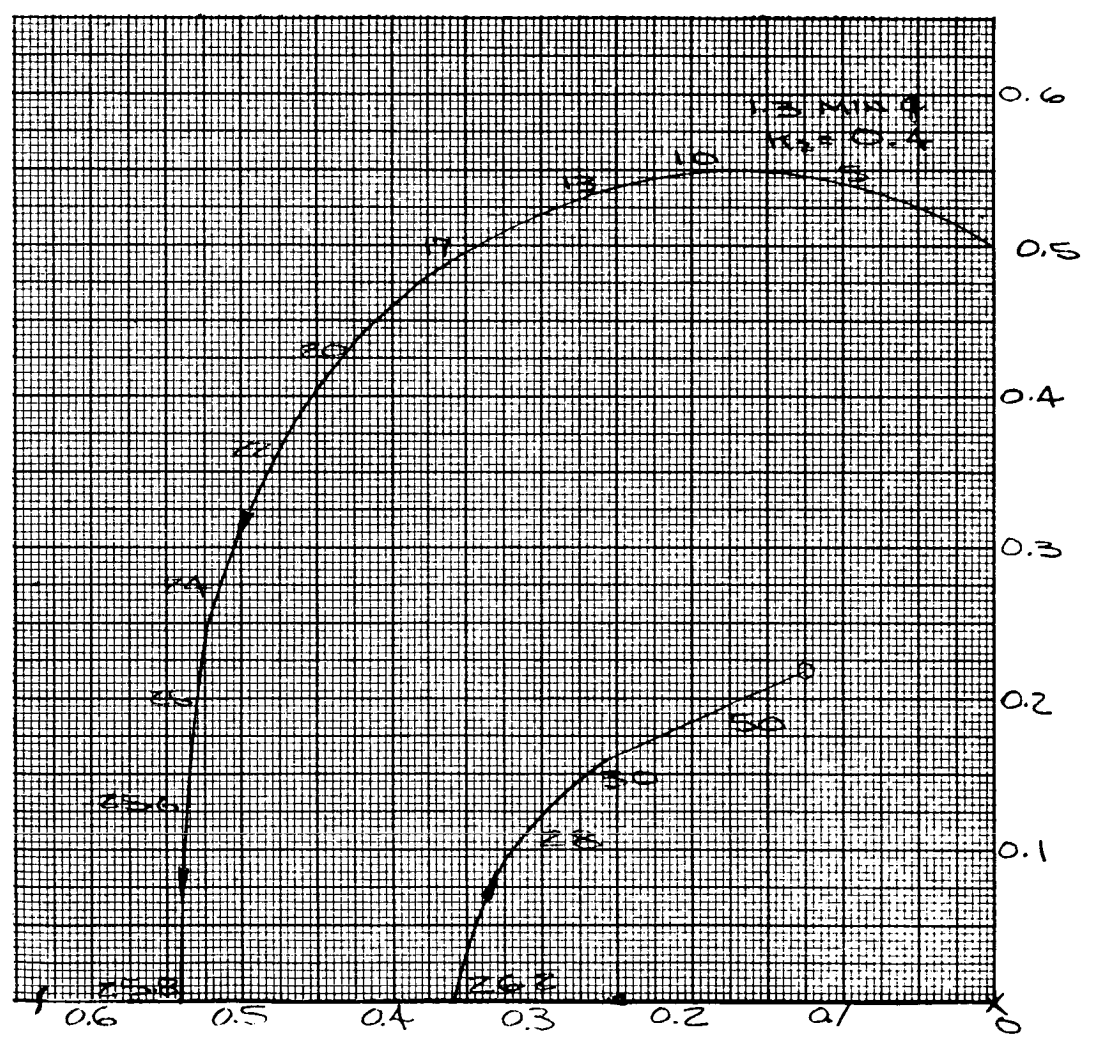


Fig. XI-50. Enlarged View of Origin for Upper Half of Root Locus. Minimum q Condition, Hydraulic Pole at -20

~~CONFIDENTIAL~~

HYDRAULIC POLE AT -20

$L = 50$ $q = 5$ PSF

MIN. q CONDITION

INTEGRATED W-1 CONFIGURATION

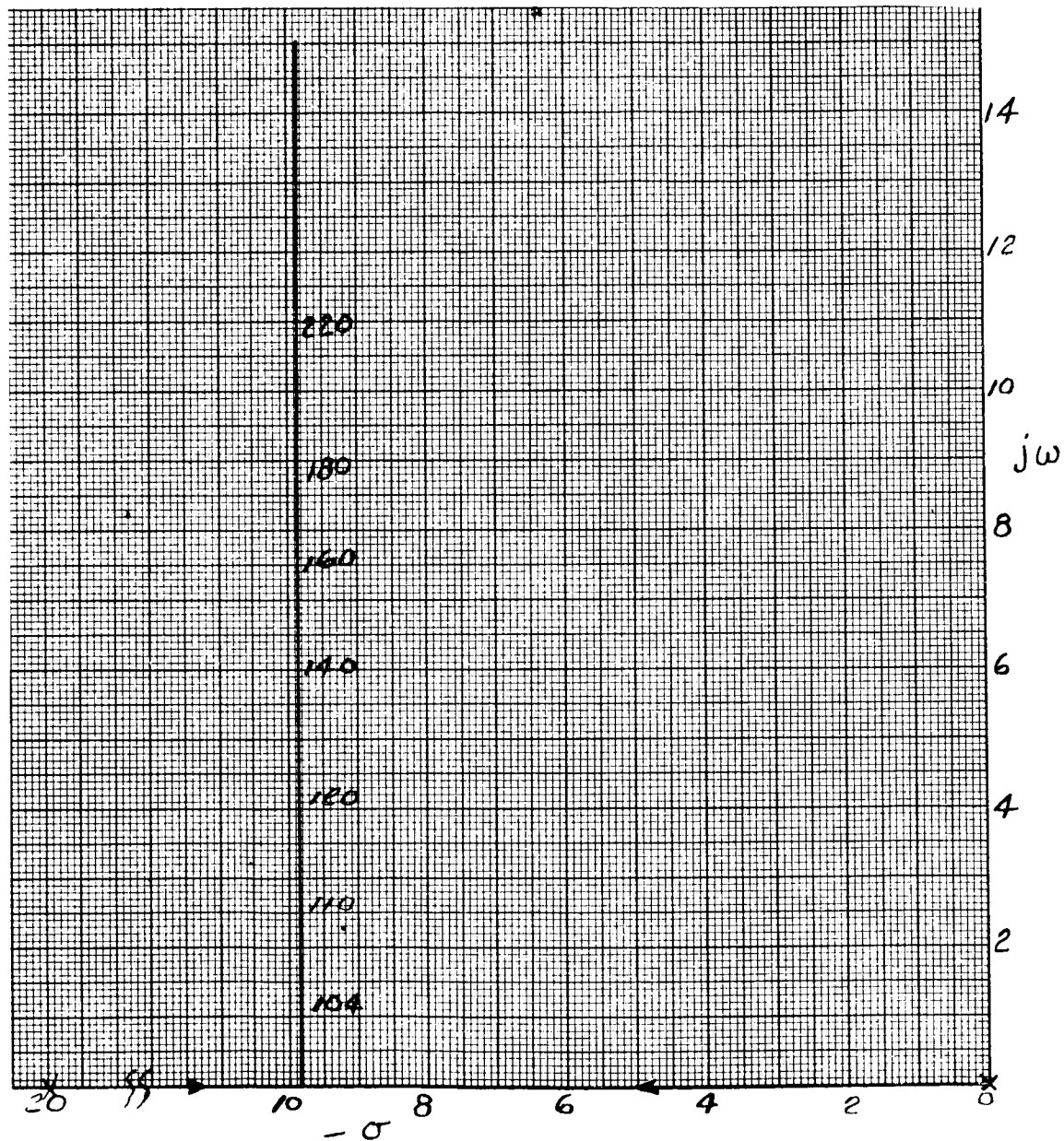


Fig. XI-51. Upper Half of Root Locus for Minimum q Condition, Hydraulic Pole at -20

~~CONFIDENTIAL~~

ENLARGED VIEW OF ORIGINAL $\alpha = 50^\circ$
HYDRAULIC POLE AT -20
MIN. q CONDITION, $q = 20$ P.S.F.
INTEGRATED W-1 CONFIGURATION

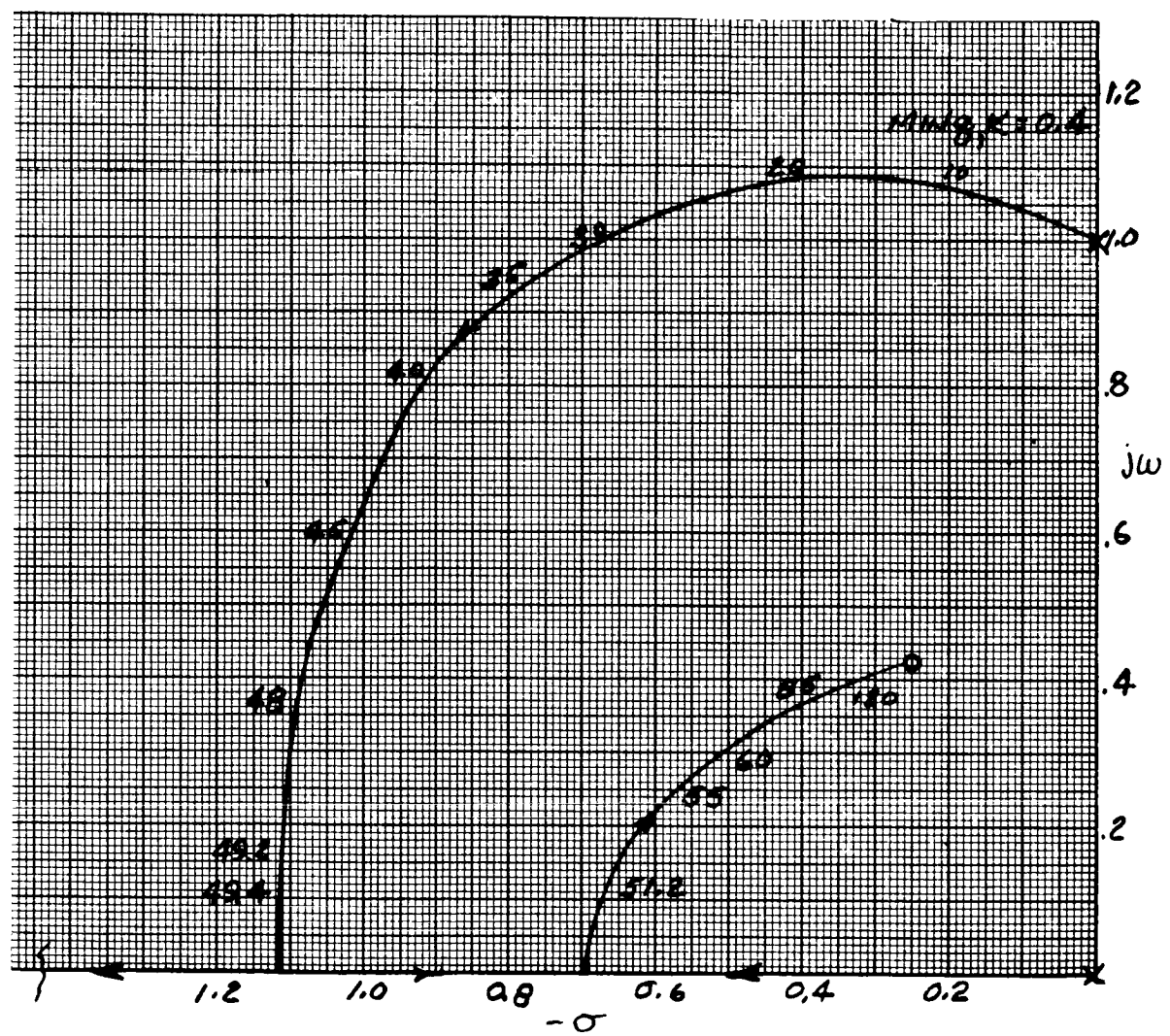


Fig. XI-52. Upper Half of Root Locus, Minimum q Condition with Hydraulic Pole at -20

HYDRAULIC POLE AT -20
 MIN. q CONDITION
 MIN $q = 20 \text{ PSF } L = 50$
 INTEGRATED W-I CONFIGURATION

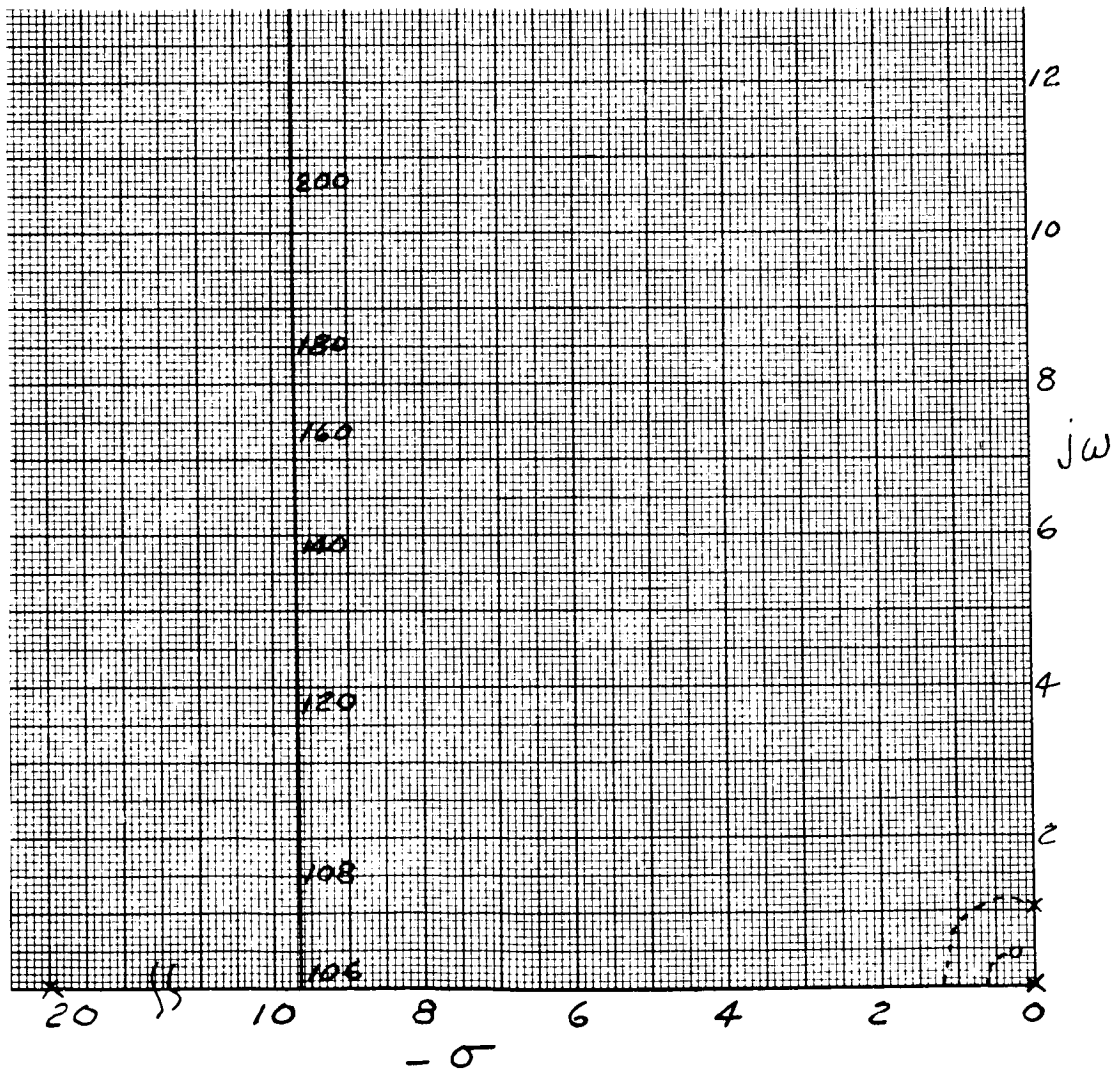


Fig. XI-53. Upper Half of Root Locus for Minimum q Condition, Hydraulic Pole at -20

HYDRAULIC POLE AT -20
MID q CONDITION
 $q = 238$ P.S.F. $\alpha = 50^\circ$
INTEGRATED W1 CONFIGURATION

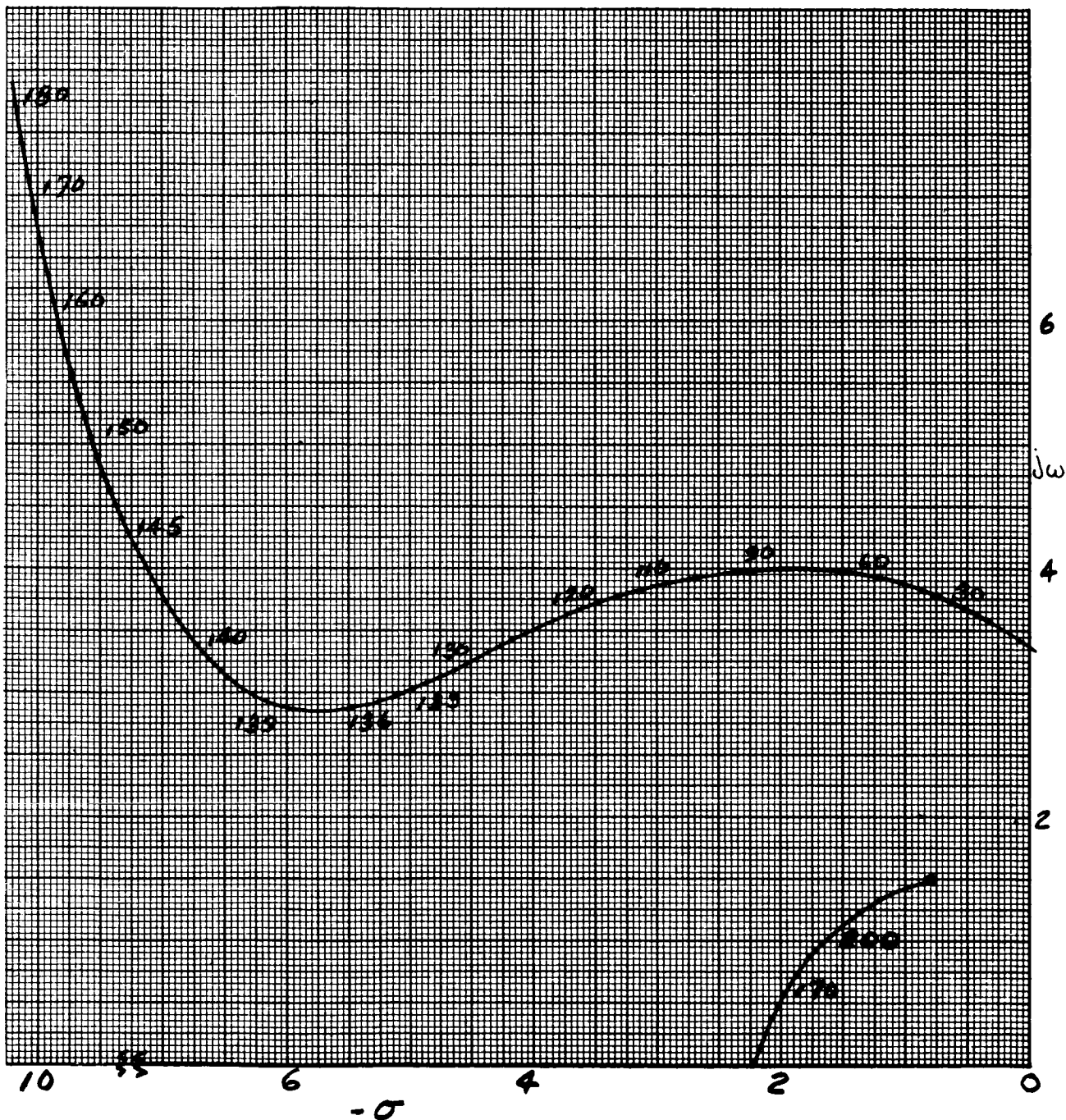


Fig. XI-54. Upper Half of Root Locus for Middle q Condition with Hydraulic Pole at -20

~~CONFIDENTIAL~~

HYDRAULIC POLE AT -10 $\alpha=50^\circ$
 MAX q CONDITION $q=476$ F/SF
 INTEGRATED W-1 CONFIGURATION

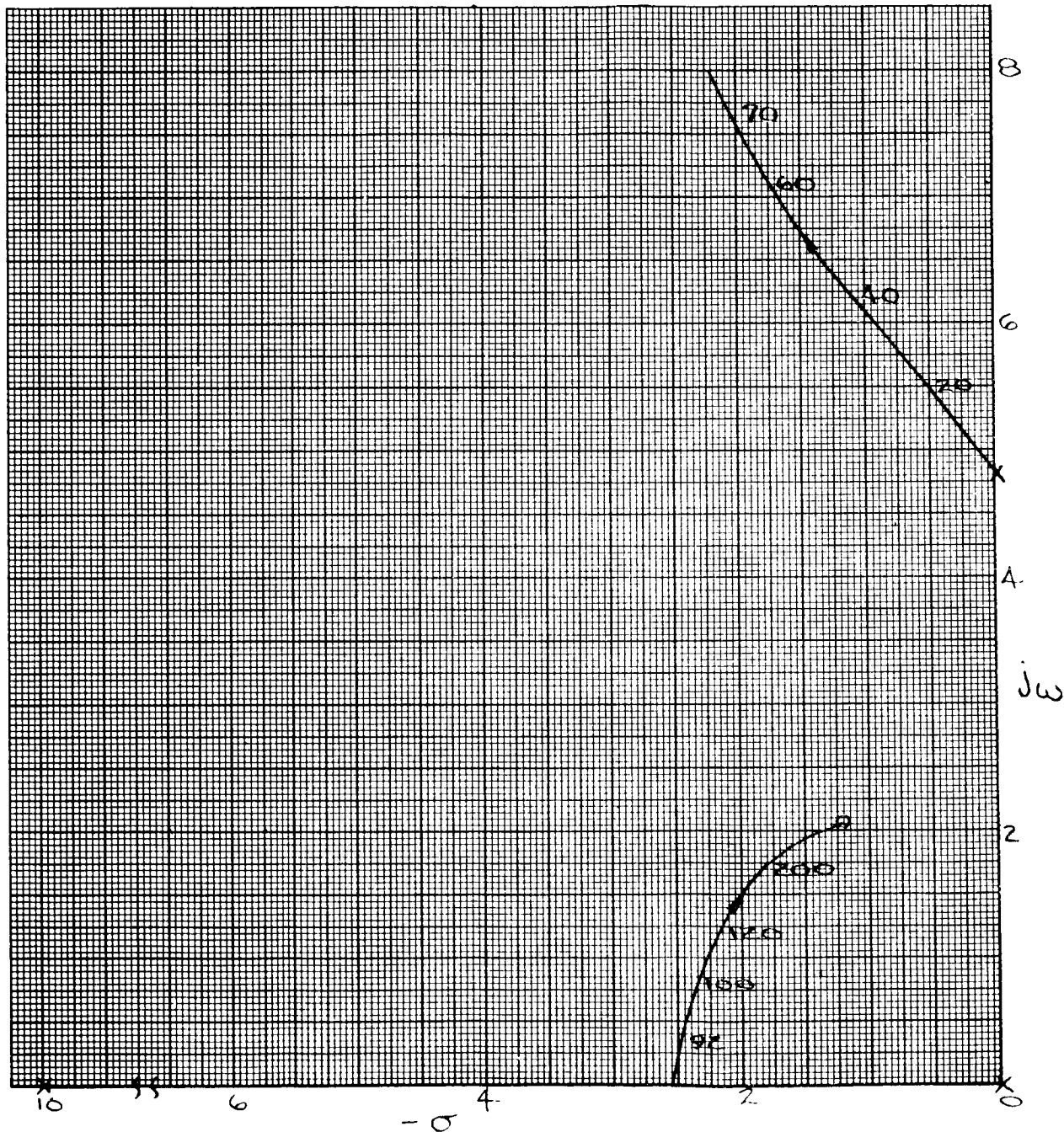


Fig. XI-55. Upper Half of Root Locus for Maximum q Condition, Hydraulic Pole at -10

~~CONFIDENTIAL~~

~~CONFIDENTIAL~~

HYDRAULIC POLE AT -5
MAX. q CONDITION

$L = 50^\circ$ $q = 476$ P.S.F.

INTEGRATED W-1 CONFIGURATION

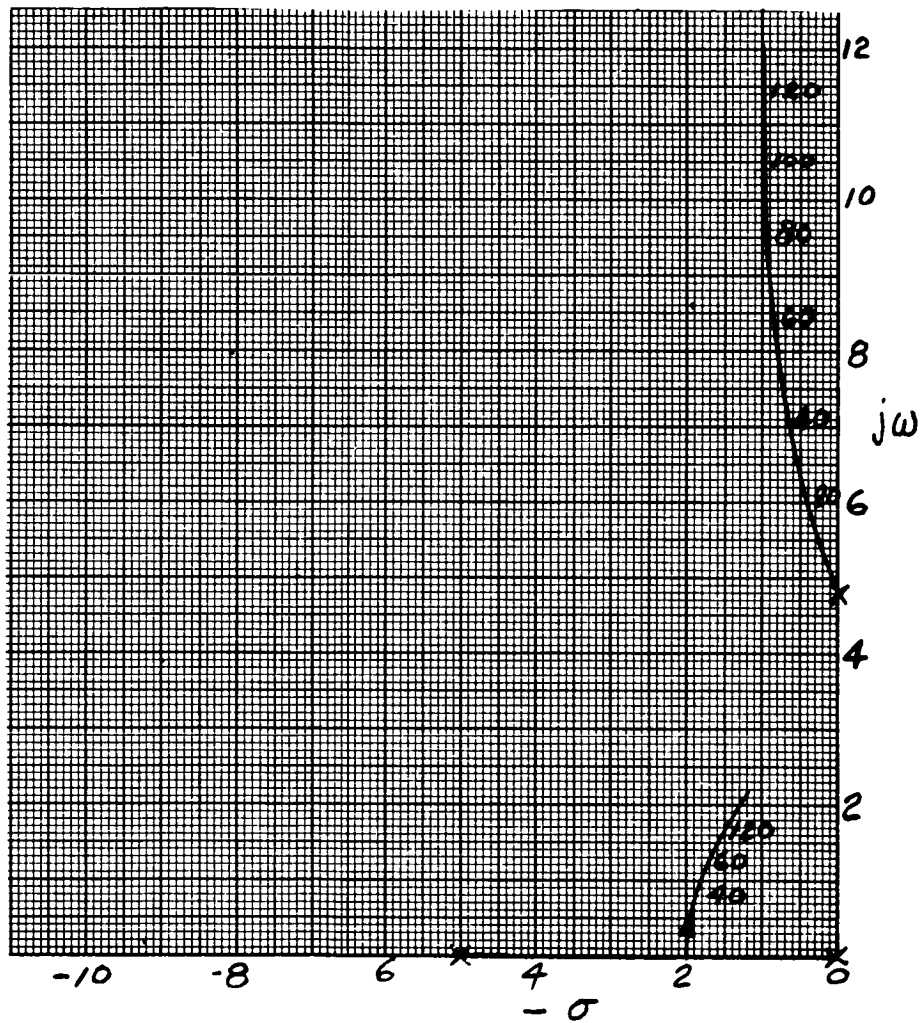


Fig. XI-56. Upper Half of Root Locus for Maximum q Condition, Hydraulic Pole at -5

~~CONFIDENTIAL~~

~~CONFIDENTIAL~~

HYDRAULIC POLE AT $-10 \alpha = 50^\circ$
 MIN q CONDITION, $q = 5 \text{ PSI}$
 INTEGRATED W-1 CONFIGURATION

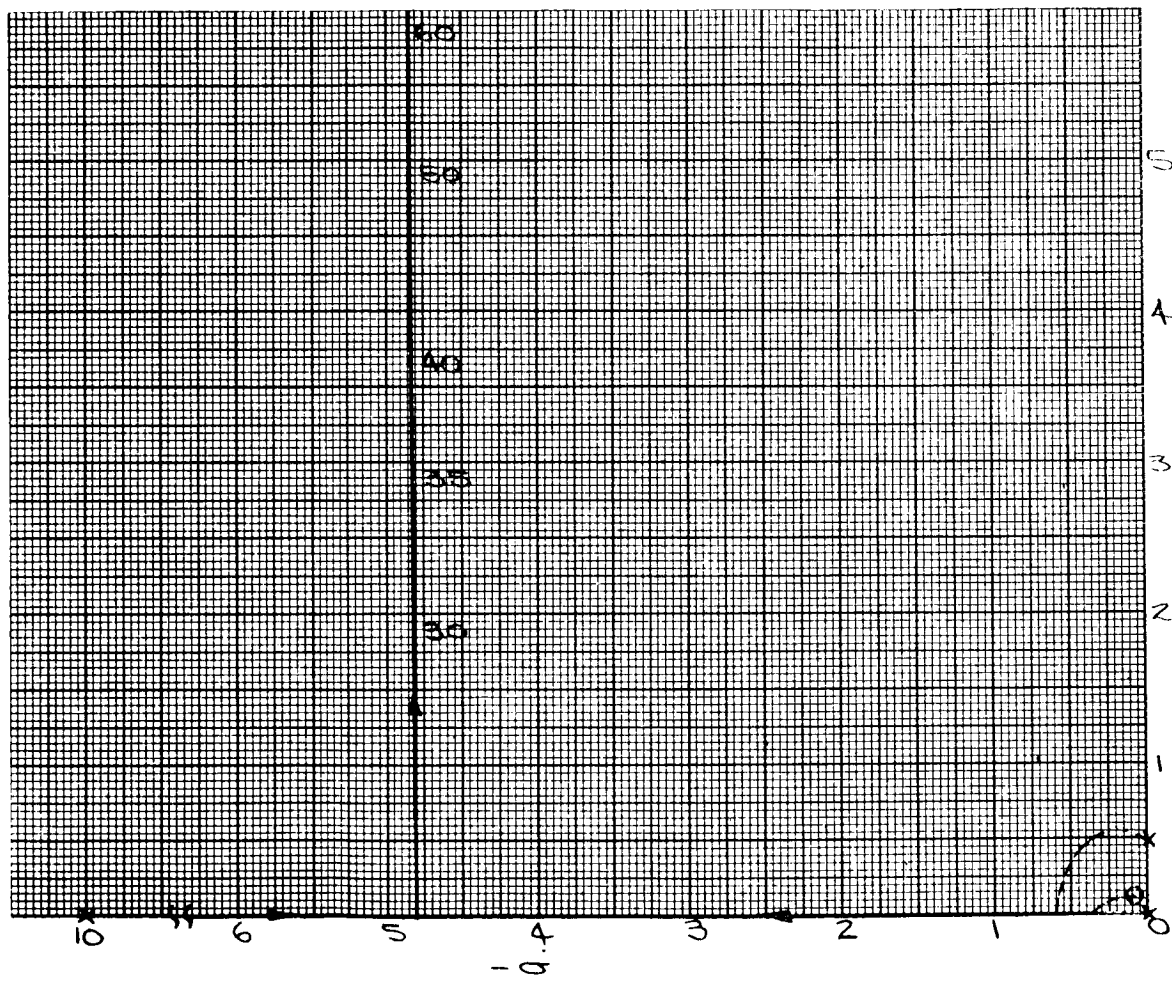


Fig. XI-57. Upper Half of Root Locus for Minimum q Condition, Hydraulic Pole at -10

ENLARGED VIEW OF ORIGIN $\alpha = 50^\circ$
HYDRAULIC POLE AT -10
MIN. q CONDITION, $q = 5$ PSSF
INTEGRATED W-1 CONFIGURATION

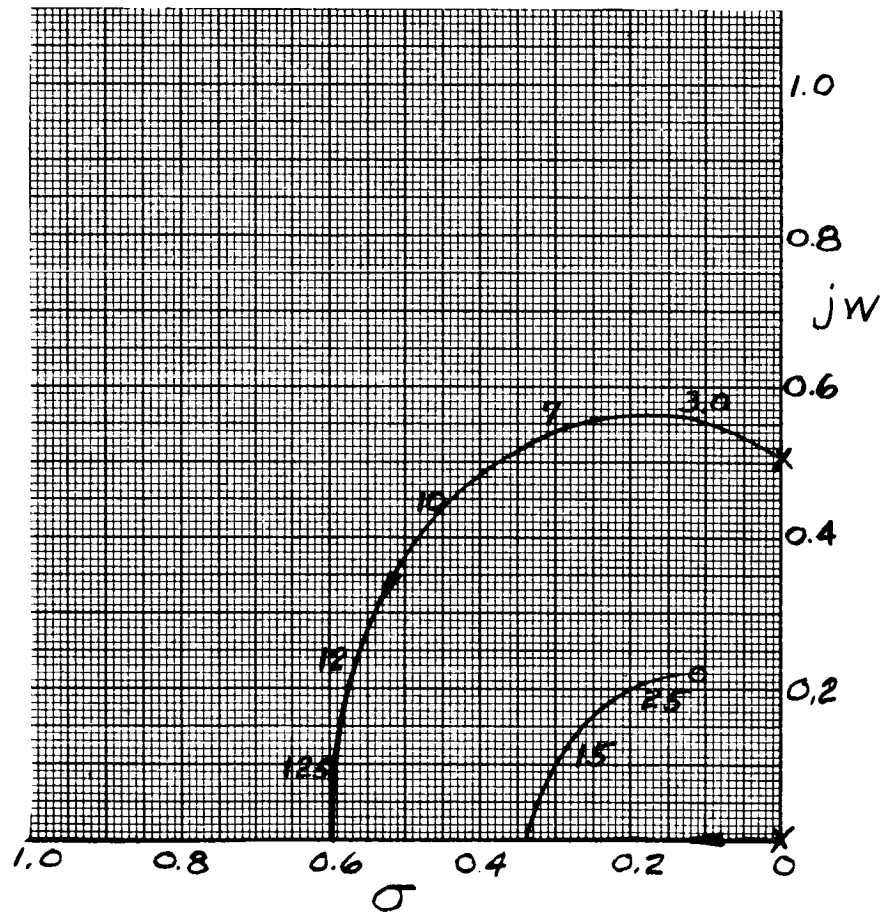


Fig. XI-58. Enlarged View of Origin for Upper Half of Root Locus, Minimum q Condition with Hydraulic Pole at -10

~~CONFIDENTIAL~~

HYDRAULIC POLE AT -5
 MIN. q CONDITION, $q = 5$ PSF
 INTEGRATED W-1 CONFIGURATION

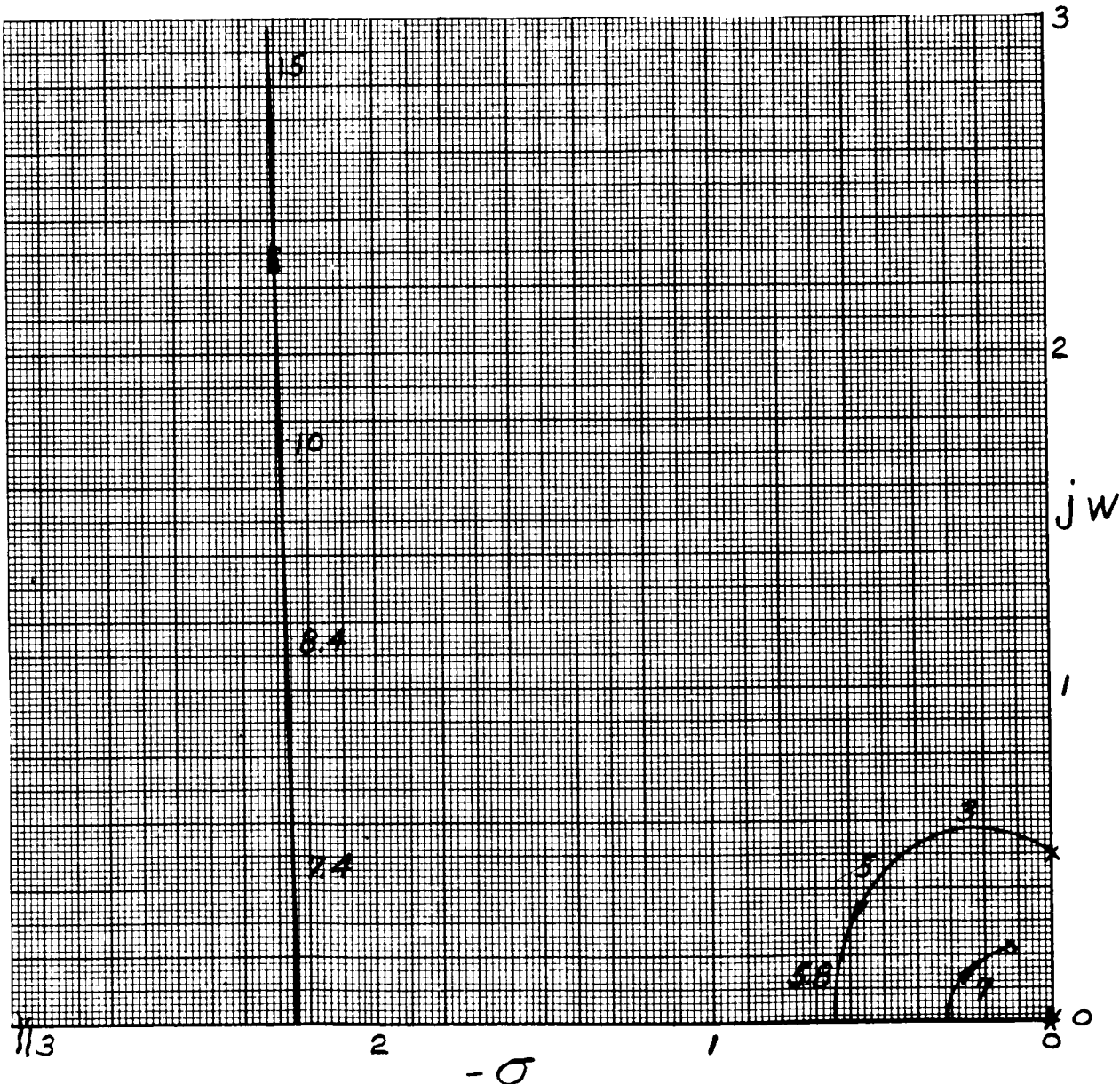


Fig. XI-59. Upper Half of Root Locus for Minimum q Condition with Hydraulic Pole at -5

~~CONFIDENTIAL~~

HYDRAULIC POLE AT -10
MIN. q CONDITION, $q = 20$ P.S.F.
INTEGRATED W1 CONFIGURATION

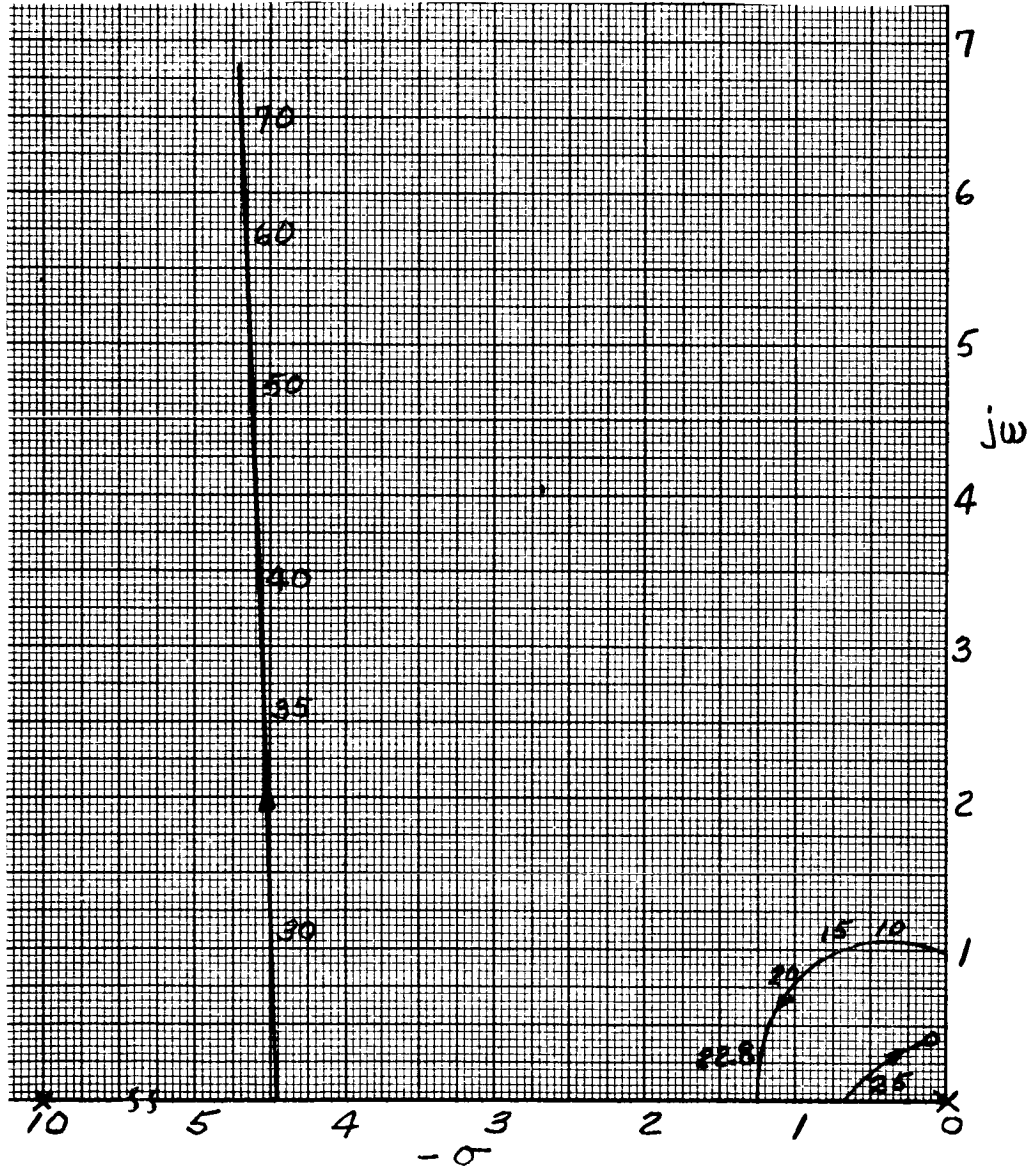


Fig. XI-60. Upper Half of Root Locus for Minimum q Condition with Hydraulic Pole at -10

~~CONFIDENTIAL~~

HYDRAULIC POLE AT -5
 MIN. q CONDITION, $q = 20$ P.S.F.
 INTEGRATED W-1 CONFIGURATION

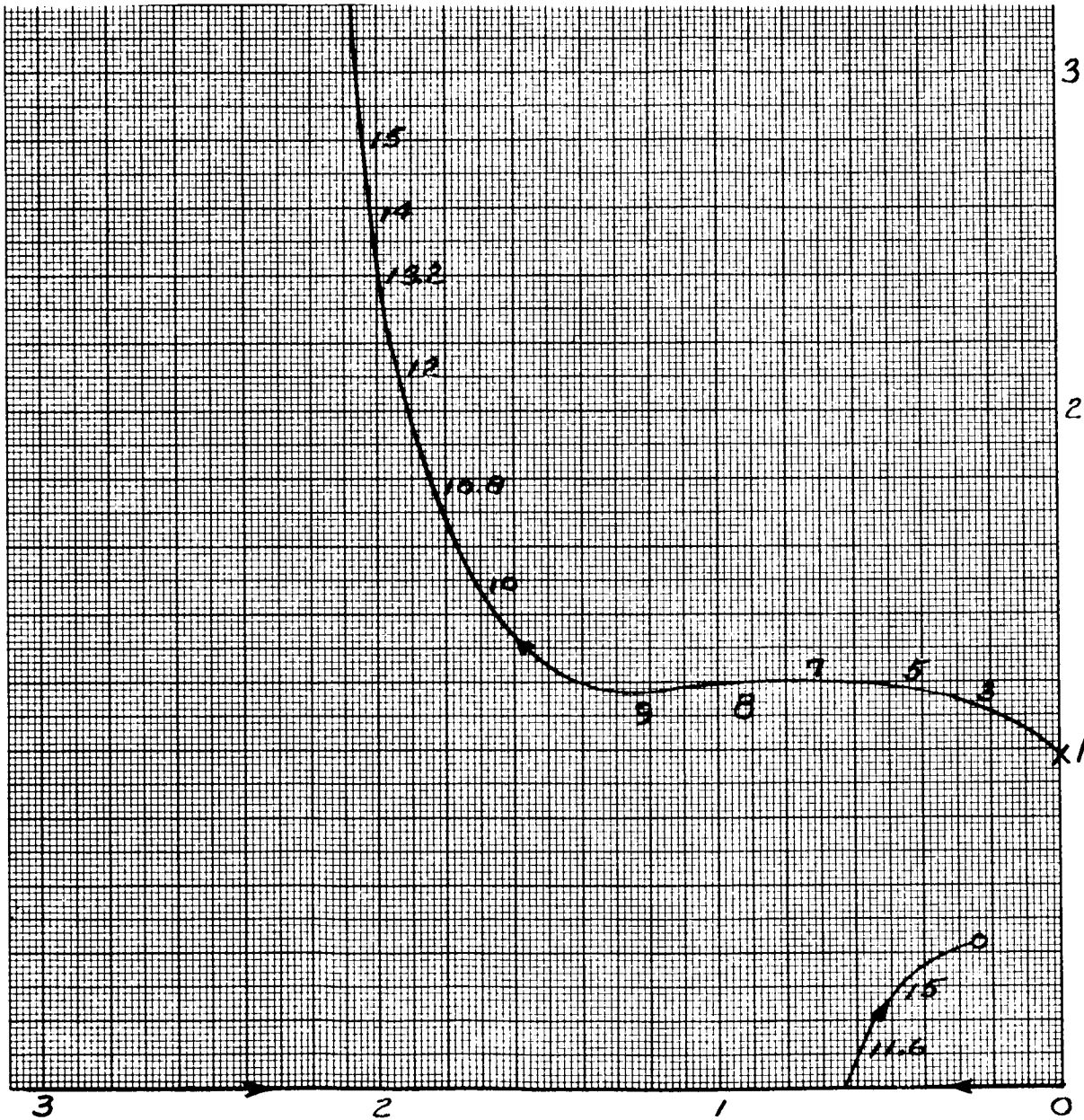


Fig. XI-61. Upper Half of Root Locus for Minimum q Condition with Hydraulic Pole at -5

HYDRAULIC POLE AT -10
MID. q CONDITION, $q = 238$ P.S.F.
INTEGRATED W_1 CONFIGURATION

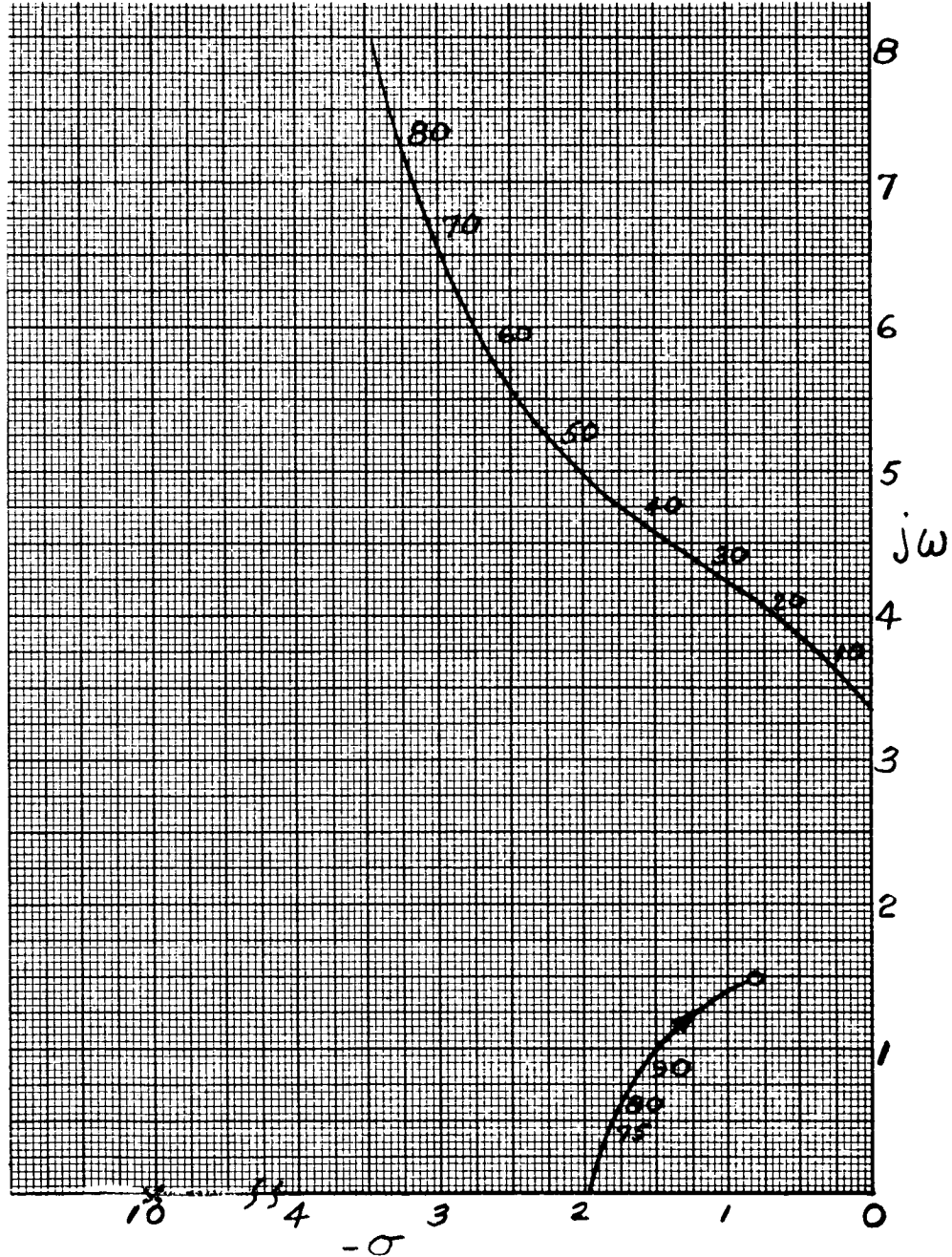


Fig. XI-62. Upper Half of Root Locus for Middle q Condition with Hydraulic Pole at -10

HYDRAULIC POLE AT-5
 MIN. q CONDITION, $q = 238$ P.S.F.
 INTEGRATED W-1 CONFIGURATION

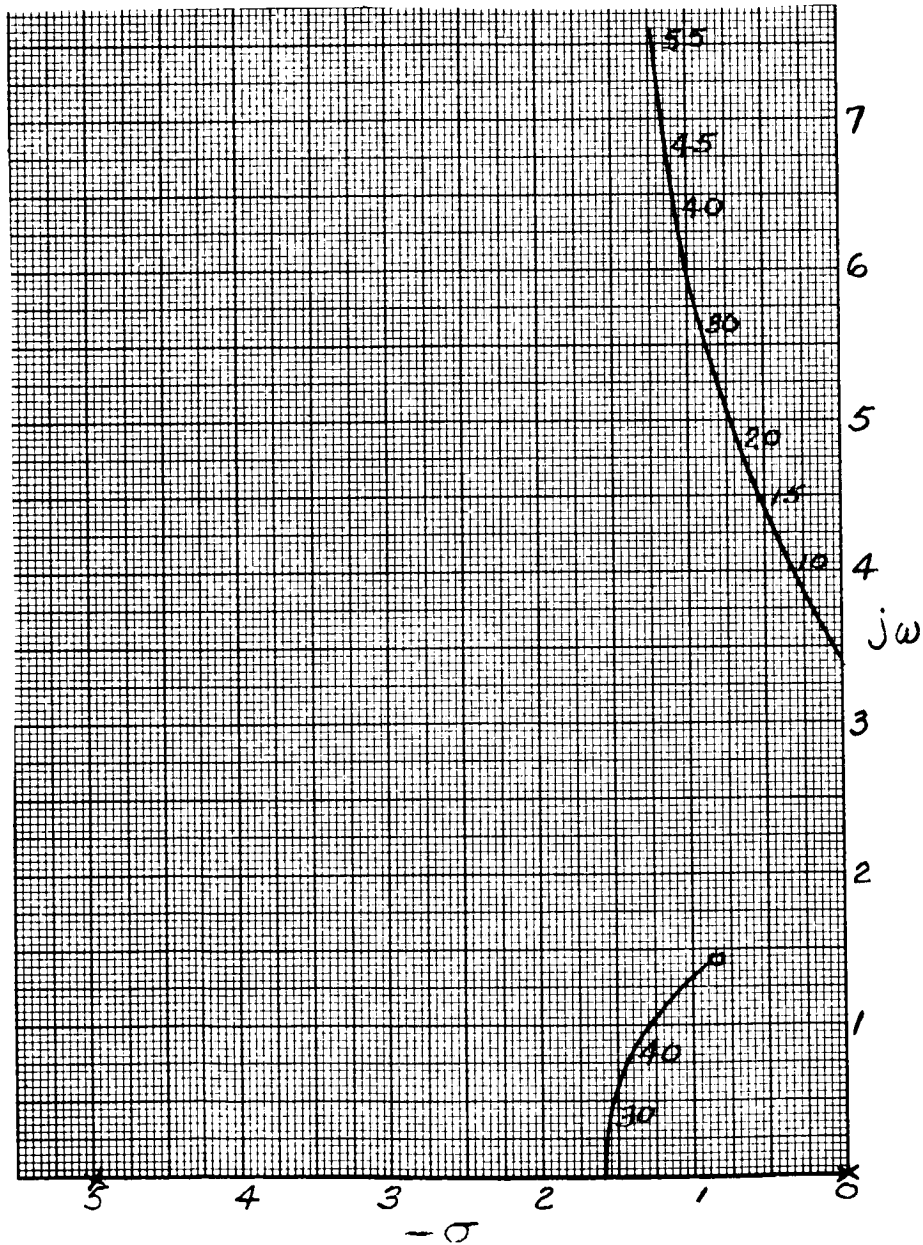


Fig. XI-63. Upper Half of Root Locus for Middle q Condition with Hydraulic Pole

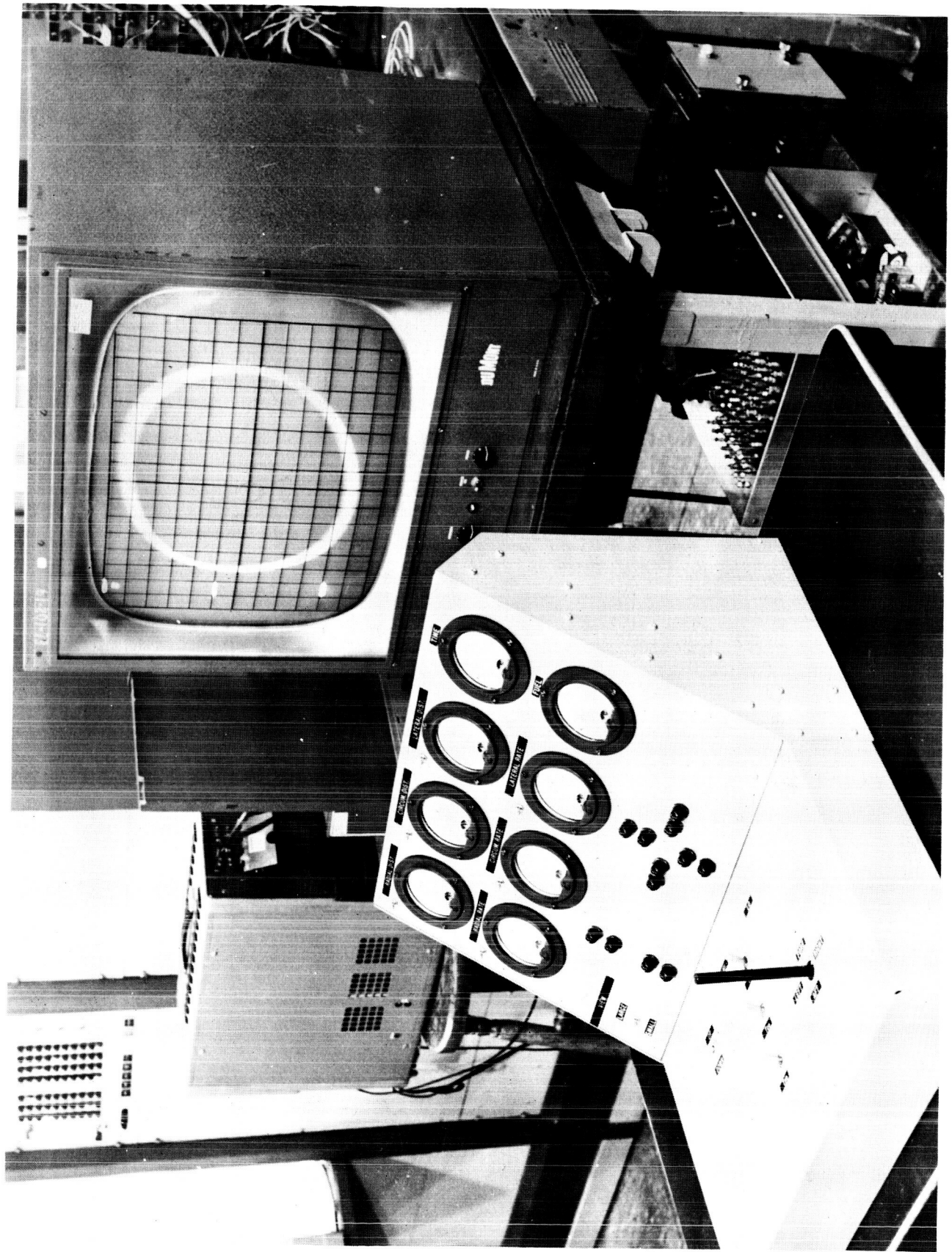


Fig. XII-1. Rendezvous Simulation Control Panel and Scope

~~CONFIDENTIAL~~

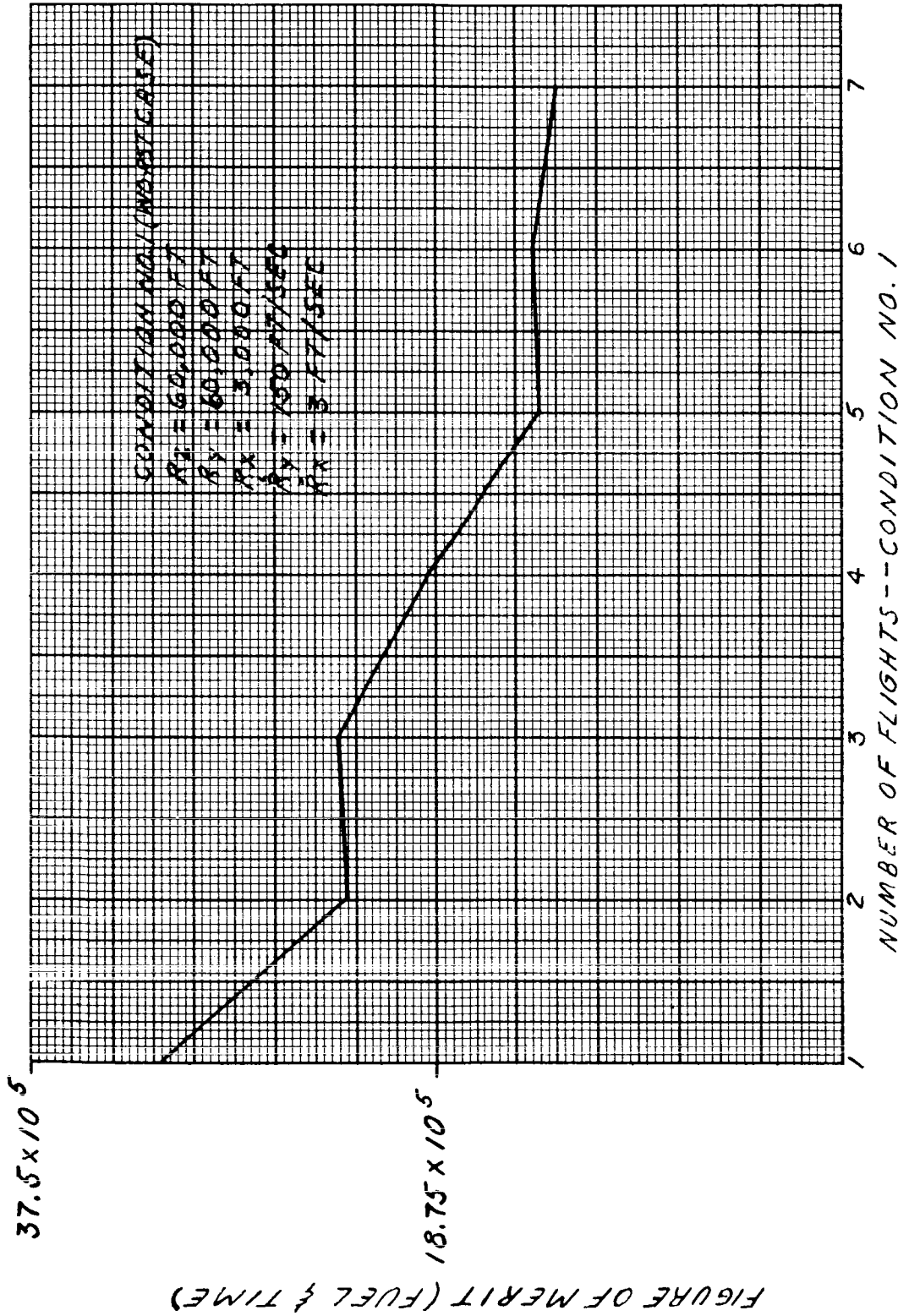


Fig. XII-2. Typical Effect of Training on Figure of Merit

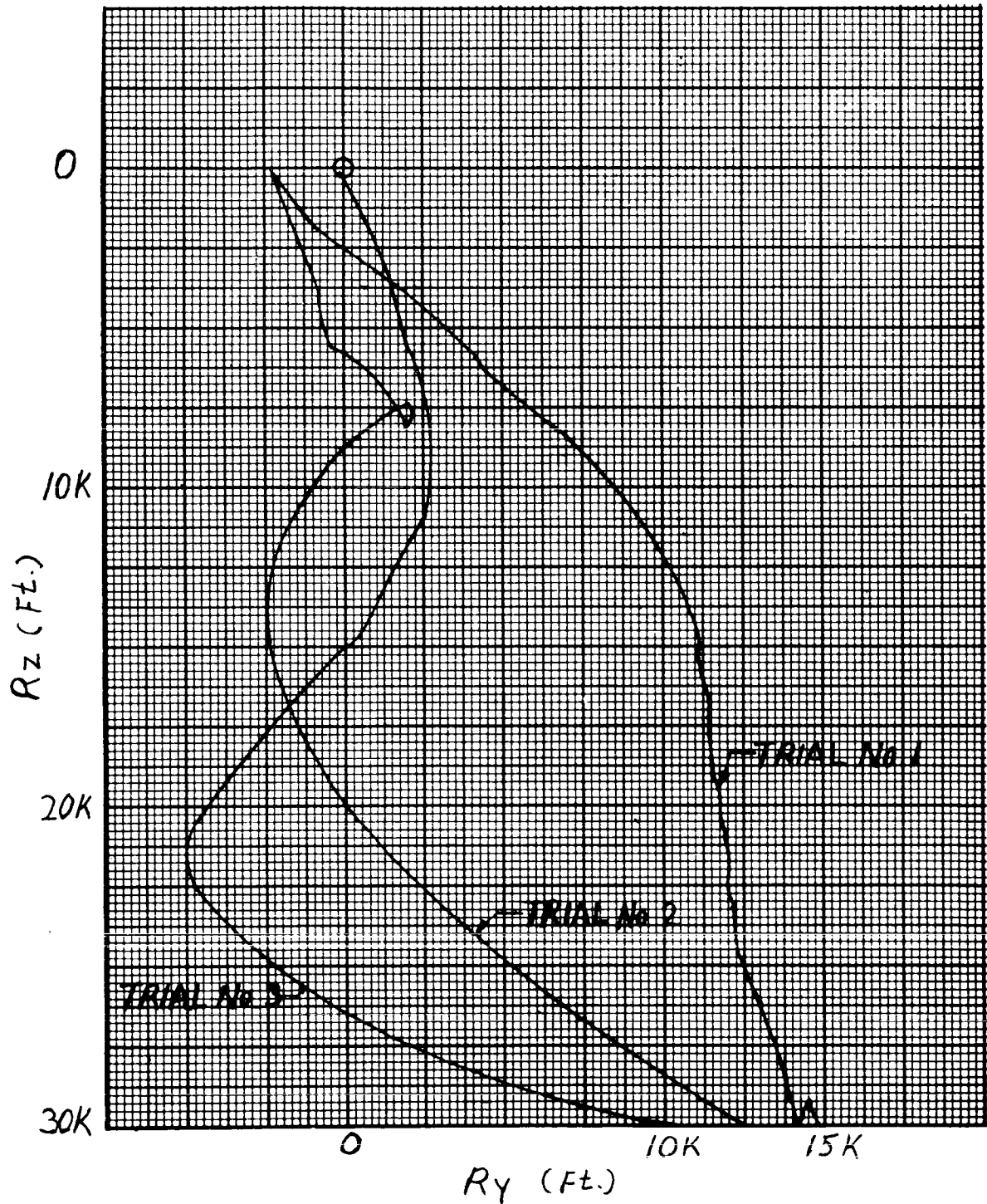


Fig. XII-3. Flight Path (untrained pilot)

~~CONFIDENTIAL~~

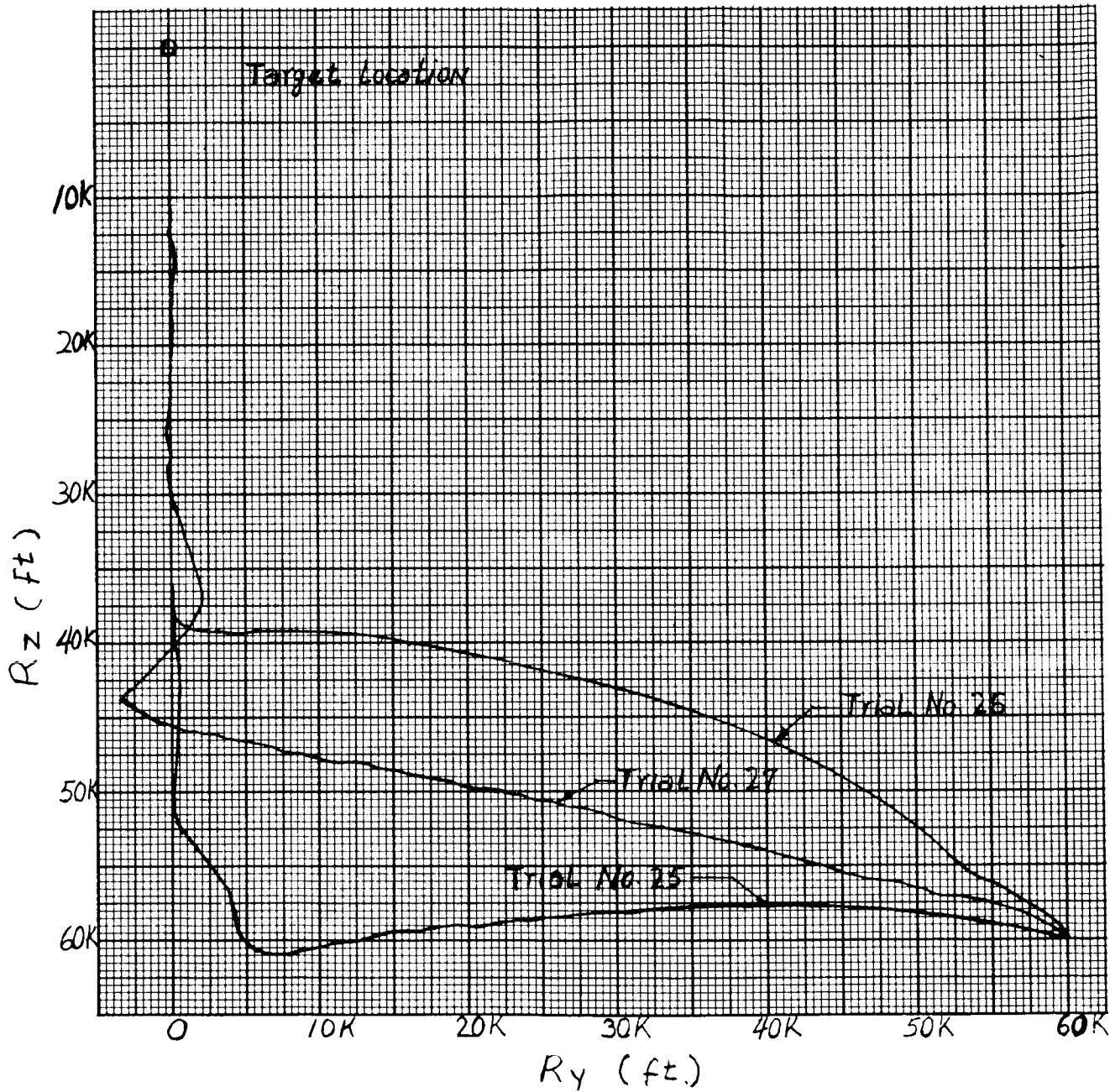
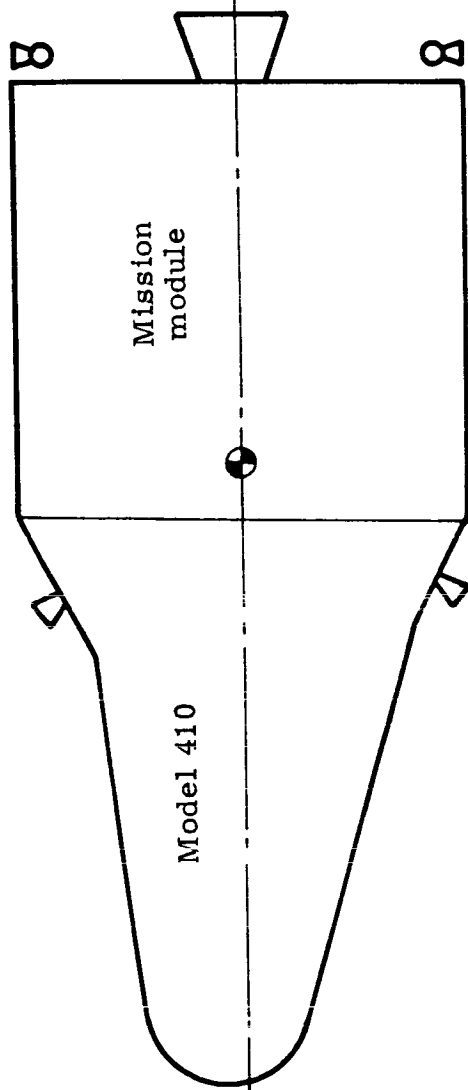
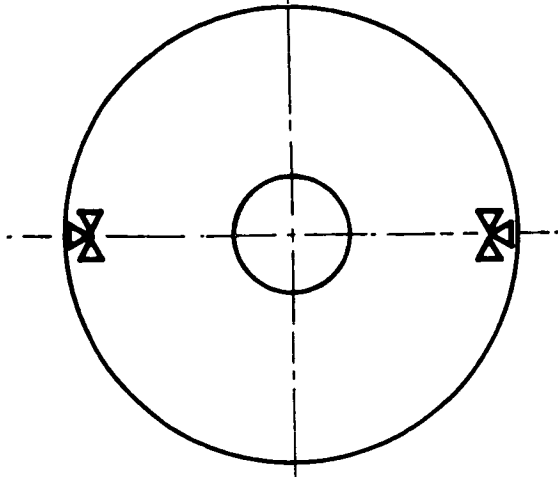


Fig. XII-4. Flight Path (trained pilot)

~~CONFIDENTIAL~~

~~CONFIDENTIAL~~



Translation control jets	3 nozzles
Attitude control jets	<u>12 nozzles (redundant)</u>
Total	15

Fig. XII-5. Single-Axis Translation Control System

~~CONFIDENTIAL~~

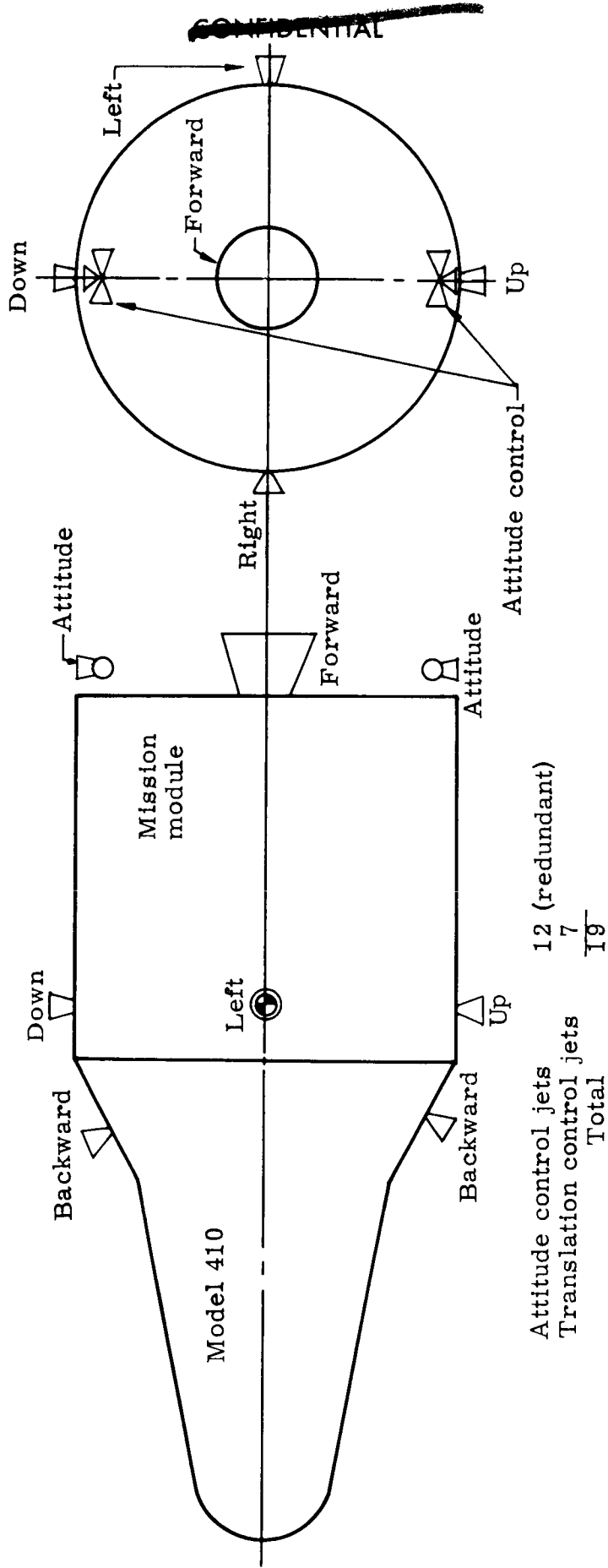
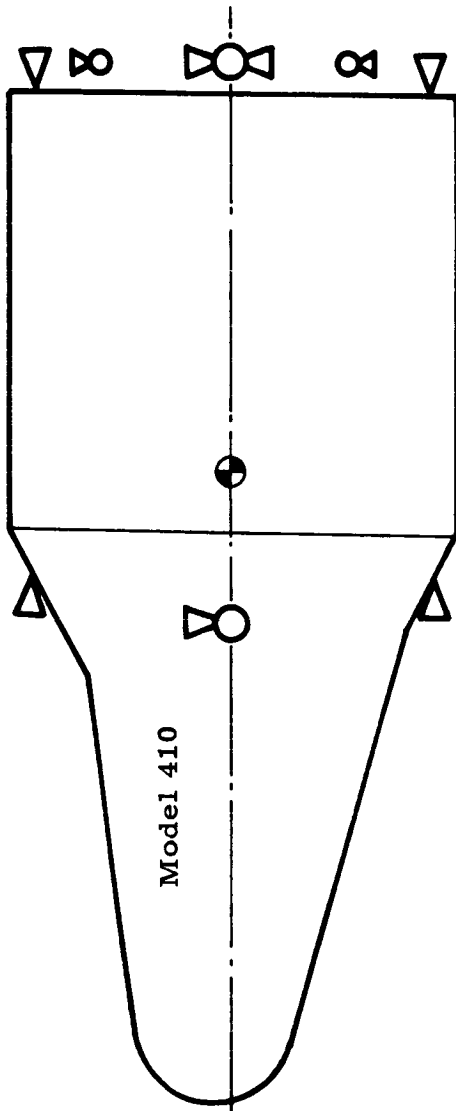
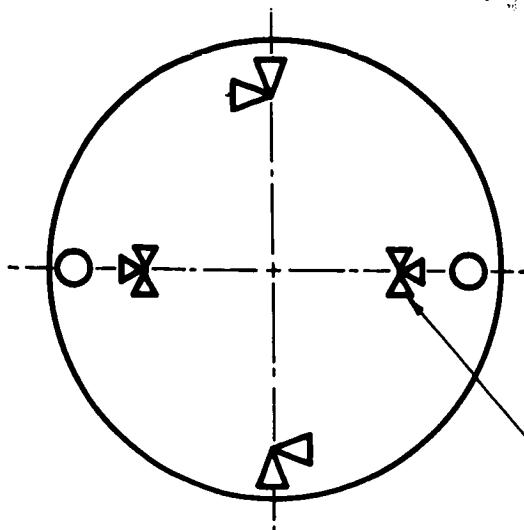


Fig. XII-6. A Three-Axis Translation Plus Attitude Control System



Limit cycle attitude control

Translation and high thrust attitude control	12 nozzles (no redundancy)
Low thrust (limit cycle) attitude control	6
Total	<u>18</u>

Fig. XII-7. A Three-Axis Translation Control Combined with Attitude Control System

~~CONFIDENTIAL~~

~~CONFIDENTIAL~~

THE FINAL REPORT of The Martin Company's Apollo design feasibility study comprises the following publications:

System and Operation	ER 12001
Support	ER 12002
Trajectory Analysis	ER 12003
Configuration	ER 12004
Aerodynamics	ER 12017
Mechanical Systems	ER 12005
Aerodynamic Heating	ER 12006
Guidance and Control	ER 12007
Life Sciences	ER 12008
Onboard Propulsion	ER 12009
Structures and Materials	ER 12010
Instrumentation and Communications	ER 12011
Space Environment Factors	ER 12018
Test Program	ER 12012
Fabrication and Quality Assurance	ER 12013
Program Management	ER 12014
Business Plan	ER 12015
Preliminary Specifications	ER 12016

110949